Phytochemical Investigation and Biological Activities of Moraceae Plants

Kedsaraporn Parndaeng

A Thesis Submitted in Fulfillment of the Requirements for the Degree of Doctor of Philosophy in Pharmaceutical Sciences

Prince of Songkla University

2020

Phytochemical Investigation and Biological Activities of Moraceae Plants

Kedsaraporn Parndaeng

A Thesis Submitted in Fulfillment of the Requirements for the Degree of Doctor of Philosophy in Pharmaceutical Sciences

Prince of Songkla University

2020

Thesis Title	Phytochemical Investigation and Biological Activities of Moraceae Plants
Author	Miss Kedsaraporn Parndaeng
Major Program	Pharmaceutical Sciences

Major Advisor

.....
(Asst. Prof. Dr.Sukanya Dej-adisai)

Co-advisor

.....
(Asst. Prof. Dr.Chatchai Wattanapiromsakul)

Examining Committee:

.....Chairperson
(Asst. Prof. Dr.Lalita Wirasathien)

.....Committee
(Asst. Prof. Dr.Chatchai Wattanapiromsakul)

.....Committee
(Assoc. Prof. Dr. Supinya Tewtrakul)

.....Committee
(Asst. Prof. Dr.Sukanya Dej-adisai)

The Graduate School, Prince of Songkla University, has approved this thesis as fulfillment of the requirements for the Doctor of Philosophy Degree in Pharmaceutical Sciences.

.....
(Prof. Dr. Damrongsak Faroongsarng)
Dean of Graduate School

This is to certify that the work here submitted is the result of the candidate's own investigations. Due acknowledgment has been made of any assistance received.

.....Signature
(Asst. Prof. Dr.Sukanya Dej-adisai)
Major Advisor

.....Signature
(Miss Kedsaraporn Parndaeng)
Candidate

I hereby certify that this work has not been accepted in substance for any degree, and is not being currently submitted in candidature for any degree.

.....Signature
(Miss Kedsaraporn Parndaeng)
Candidate

ชื่อวิทยานิพนธ์ การศึกษาพฤกษเคมีและฤทธิ์ทางชีวภาพของพืชในวงศ์ Moraceae

ผู้เขียน นางสาวเกศราภรณ์ ปานแดง

สาขาวิชา เภสัชศาสตร์

ปีการศึกษา 2562

บทคัดย่อ

จากการศึกษาฤทธิ์ทางชีวภาพของพืชในวงศ์ Moraceae พบว่า สารสกัดหยาบชั้นเอทิลอะซิเตทและเมทานอลของขนุนปาน (*Artocarpus chama*) และข่อยหนาม (*Streblus taxoides*) สามารถยับยั้งเอนไซม์ไทโรซิเนส ได้ดี สารสกัดหยาบชั้นเอทิลอะซิเตทของพืชทั้งสองต้นสามารถลดปริมาณเมลานินในเซลล์ B16F1 melanoma ผ่านการยับยั้งเอนไซม์ไทโรซิเนส และมีฤทธิ์ยับยั้งแบคทีเรียแกรมบวกคือ *Staphylococcus aureus, S. epidermidis, Cutibacterium acnes* และ methicillin-resistant *S. aureus* (MRSA) นอกจากนี้ยังพบว่า สารสกัดหยาบชั้นเอทิลอะซิเตทและเมทานอลของข่อยหนามยังสามารถลดเม็ดสีในปลาม้าลาย (zebrafish)

ผลการแยกสารสำคัญจากพืชทั้ง 2 ต้นโดยใช้เทคนิคคอลัมน์โครมาโตกราฟี พบว่า สารสกัดหยาบชั้นเอทิลอะซิเตทของขนุนปานแยกสารได้ทั้งหมด 8 สารคือ สารใหม่ 3 สารได้แก่ 3´-farnesyl-apigenin; 3-(hydroxyprenyl) isoetin และ 3-prenyl-5, 7, 2´, 5´-tetrahydroxy-4´-methoxyflavone สารที่มีรายงานแล้ว 5 สารได้แก่ homoeriodictyol, isocycloartobiloxanthone, artocarpanone, naringenin และ artocarpin และจากสารสกัดหยาบชั้นเอทิลอะซิเตทและเมทานอลของข่อยหนามสามารถแยกสารได้ทั้งหมด 6 สารคือ สารใหม่ 1 สารได้แก่ ω-hydroxymoracin C, สารที่มีรายงานแล้ว 4 สารได้แก่ moracin M; moracin C; 3, 4, 3´, 5´-tetrahydroxybibenzyl; piceatannol และสารผสมระหว่าง β-sitosterol และ stigmasterol

ในการศึกษาฤทธิ์ทางชีวภาพของสารที่แยกได้พบว่า สาร 8 สารคือ homoeriodictyol; 3´-farnesyl-apigenin; artocarpanone; ω-hydroxymoracin C; moracin M; moracin C; 3, 4, 3´, 5´-tetrahydroxybibenzyl และ piceatannol มีฤทธิ์ยับยั้งเอนไซม์ไทโรซิเนสที่ดี โดยมีค่า IC_{50} เท่ากับ 52.18 135.70 38.78 109.64 47.34 128.67 35.65 และ 149.73 µg/mL ตามลำดับ จากการศึกษาฤทธิ์ยับยั้งเอนไซม์ไทโรซิเนสในเซลล์ B16F1 melanoma และยืนยันผลโดยดูการแสดงออกของโปรตีนที่เกี่ยวข้องกับกระบวนการสังเคราะห์เมลานินโดยวิธี western blot พบว่า สารที่แยกได้ส่งผลต่อปริมาณเมลานินในเซลล์ 2 กลไกคือ artocarpanone; ω-hydroxymoracin C; moracin M และ moracin C สามารถยับยั้งเอนไซม์ไทโรซิเนสได้ดี และช่วยลดการแสดงออกของโปรตีนที่เกี่ยวข้องกับการสร้างเมลานิน จึงส่งผลให้ปริมาณเมลานินในเซลล์ลดลง ตรงกันข้ามกับ naringenin ไม่มีฤทธิ์ยับยั้งเอนไซม์ไทโรซิเนส และยังช่วยเพิ่มการแสดงออกของโปรตีนที่เกี่ยวข้องกับการสร้างเมลานิน จึงส่งผลให้ปริมาณเมลานินในเซลล์เพิ่มขึ้น ในขณะที่ homoeriodictyol; 3´-farnesyl-apigenin; 3, 4, 3´, 5´-tetrahydroxybibenzyl และ piceatannol แม้จะมีฤทธิ์ยับยั้งเอนไซม์ไทโรซิเนสที่ดี แต่ช่วยเพิ่มการแสดงออกของโปรตีนที่เกี่ยวข้องกับการสร้างเมลานิน จึงส่งผลให้เมลานินในเซลล์เพิ่มขึ้น นอกจากนี้ยังพบว่า isocycloartobiloxanthone, 3-(hydroxyprenyl) isoetin, 3-prenyl 5,7,2´,5´ tetrahydroxy-4´-methoxyflavone, artocarpanone และ artocarpin มีฤทธิ์ยับยั้งแบคทีเรีย *S. epidermidis* โดยมีค่า MIC เท่ากับ 4 16 16 64 และ 2 µg/mL ตามลำดับ มีฤทธิ์ยับยั้งแบคทีเรีย *S. aureus* โดยมีค่า MIC เท่ากับ 4 16 4 64 และ 2 µg/mL ตามลำดับ มีฤทธิ์ยับยั้งแบคทีเรีย methicillin-resistant *S. aureus* (MRSA) โดยมีค่า MIC เท่ากับ 16 16 4 128 และ 2 µg/mL ตามลำดับ และมีฤทธิ์ยับยั้งแบคทีเรีย *C. acnes* โดยมีค่า MIC เท่ากับ 256 128 128 32 และ 8 µg/mL ตามลำดับ ในขณะที่ ω-hydroxymoracin C และ moracin C มีฤทธิ์ยับยั้งแบคทีเรีย *S. epidermidis* โดยมีค่า MIC เท่ากับ 16 และ 128 µg/mL ตามลำดับ มีฤทธิ์ยับยั้งแบคทีเรีย *S. aureus* โดยมีค่า MIC เท่ากับ 16 และ 32 µg/mL ตามลำดับ และมีฤทธิ์ยับยั้งแบคทีเรีย MRSA โดยมีค่า MIC เท่ากับ 16 และ 32 µg/mL ตามลำดับ นอกจากนี้ moracin M 3, 4, 3´, 5´-tetrahydroxybibenzyl และ piceatanol มีฤทธิ์ยับยั้งแบคทีเรีย *S. epidermidis* โดยมีค่า MIC เท่ากับ 64 128 และ 64 µg/mL ตามลำดับ และมีฤทธิ์ยับยั้งแบคทีเรีย MRSA โดยมีค่า MIC เท่ากับ 64 64 และ 128 µg/mL ตามลำดับ

การค้นพบสารใหม่คือ 3´-farnesyl-apigenin; 3-(hydroxyprenyl) isoetin 3-prenyl-6, 8, 2´, 5´-tetrahydroxy -4´-methoxyflavone และ ω-hydroxymoracin C โดยเฉพาะ 3´-farnesyl-apigenin ที่มีฤทธิ์ยับยั้งเอนไซม์ไทโรซิเนสที่ดี และ ω-hydroxymoracin C ที่สามารถลดปริมาณเมลานินในเซลล์ B16F1 melanoma และยังมีฤทธิ์ยับยั้งเชื้อแบคทีเรียที่ดี สามารถนำไปใช้เป็นสารต้นแบบในการพัฒนาเป็นเครื่องสำอางหรือยารักษาโรคที่เกี่ยวข้องกับความผิดปกติของเม็ดสี และเป็นยารักษาโรคติดเชื้อแบคทีเรียที่เหมาะสมหรือมีฤทธิ์ที่ดียิ่งขึ้น งานวิจัยนี้เป็นงานวิจัยชิ้นแรกที่รายงานฤทธิ์ทางชีวภาพ และองค์ประกอบทางเคมีของข่อยหนาม พร้อมทั้งการรายงานการค้นพบสารใหม่จากขนุนปานและข่อยหนาม

Thesis Title Phytochemical Investigation and Biological Activities of Moraceae Plants
Author Miss Kedsaraporn Parndaeng
Major Program Pharmaceutical Sciences
Academic 2019

Abstract

In this recent biological study of Moraceae plants, ethyl acetate and methanol extracts from *Artocarpus chama* and *Streblus taxoides* exhibited potent enzymatic antityrosinase activity. The ethyl acetate extracts of both plants were decreased the melanin content by increasing the antityrosinase activity on B16F1 melanoma cells. Moreover, these extracts sufficiently revealed antibacterial against gram-positive bacteria such as *Staphylococcus aureus, Staphylococcus epidermidis, Cutibacterium acnes* and methicillin-resistant *S. aureus* (MRSA). On the other hand, ethyl acetate and methanol extracts from *S. taxoides* were suppressed pigmentation producing on zebrafish assay.

The chemical constituents from both plants were isolated by column chromatography. Eight compounds were isolated from ethyl acetate extract of *A. chama* which are three new compounds as 3´-farnesyl-apigenin; 3-(hydroxyprenyl) isoetin and 3-prenyl-5, 7, 2´, 5´-tetrahydroxy-4´-methoxyflavone; five known compounds as homoeriodictyol; isocycloartobiloxanthone; artocarpanone; naringenin and artocarpin. Six compounds were isolated from ethyl acetate and methanol extracts of *S. taxoides* are composed of one new compound as ω-hydroxymoracin C; four known compounds as moracin M; moracin C; 3, 4, 3´, 5´-tetrahydroxybibenzyl; piceatannol and one mixture of β-sitosterol and stigmasterol.

In determination of biological activities showed that, 8 isolated compounds as known as homoeriodictyol; 3´-farnesyl-apigenin; artocarpanone; ω-hydroxymoracin C; moracin M; moracin C; 3, 4, 3´, 5´-tetrahydroxybibenzyl and piceatannol exhibited enzymatic tyrosinase inhibitory activity. Further, all compounds were affected to intracellular antityrosinase activity on B16F1 melanoma by 2 different mechanisms as western blot confirmation. First, 4 compounds including artocarpanone;

ω-hydroxymoracin C; moracin M and moracin C inhibited enzymatic tyrosinase activity and down-regulated the expression of melanogenic proteins, resulting in decreasing melanin content. Second, one compound which is naringenin was not active as enzymatic tyrosinase inhibitory and up-regulated the expression of melanogenic proteins by increasing melanin content. Moreover, other 4 compounds which are homoeriodictyol; 3´-farnesyl-apigenin; 3, 4, 3´, 5´-tetrahydroxybibenzyl and piceatannol inhibited enzymatic tyrosinase activity but increased melanin production by up-regulated the expression of melanogenic proteins. Additionally, isocycloartobiloxanthone, 3-(hydroxyprenyl) isoetin, 3-prenyl 5,7,2´,5´ tetrahydroxy-4´-methoxyflavone, artocarpanone and artocarpin showed antibacterial effect against *S. epidermidis* with MIC value 4, 16, 16, 64 and 2 μg/mL, respectively, against *S. aureus* with MIC value 4, 16, 4, 64 and 2 μg/mL, respectively, against methicillin-resistant *S. aureus* (MRSA) with MIC value 16, 16, 4, 128 and 2 μg/mL, respectively and against *C. acnes* with MIC value 256, 128, 128, 32 and 8 μg/mL, respectively. While, ω-hydroxymoracin C and moracin C showed antibacterial effect against *S. epidermidis* with MIC value 16 and 128 μg/mL, respectively, against *S. aureus* with MIC value 16 and 32 μg/mL, respectively and against MRSA with MIC value 16 and 32 μg/mL, respectively. Moreover, moracin M, 3, 4, 3´, 5´-tetrahydroxybibenzyl and piceatanol showed antibacterial effect against *S. epidermidis* with MIC value 64, 128 and 64 μg/mL, respectively and against MRSA with MIC value 64, 64 and 128 μg/mL respectively.

The discovery of new compounds (3´-farnesyl-apigenin; 3-(hydroxyprenyl) isoetin; 3-prenyl-5, 7, 2´, 5´-tetrahydroxy -4´-methoxyflavone; ω-hydroxymoracin C) that showed the potential of enzymatic antityrosinase activity and new compound (ω-hydroxymoracin C) which showed the potential of antibacterial activity and decreased melanin content by reducing tyrosinase activity on B16F1 melanoma cells, will be useful to be the lead compound of new medicine development for treatment of hyperpigmentation and infectious diseases. This study is the first report for phytochemical investigation and biological activities of *S. taxoides* which was also for the new isolated compounds from *A. chama* and *S. taxoides*.

ACKNOWLEDGEMENTS

First, I would like to express my deepest appreciation and grateful thank to my advisor, Asst. Prof. Dr. Sukanya Dej-adisai for all her help, guidance and assistance throughout the course of the project. It has been a great pleasure and wonderful learning experience to work under her supervision.

I also would like to express my thesis co-advisor Asst. Prof. Dr. Chatchai Wattanapiromsakul for his helpful advice for the structure elucidation, encouragement and suggestion throughout the course of this work.

I would like to thank to Prof. Dr.Jae Sung Hwang my collaboration Skin Biotechnology center, Department of Genetic engineering, College of Life Sciences, Kyung Hee University, for his kindness and valuable advice in cell culture and western blot practice.

I would like to thank to Prof. Dr.Tong Ho Kang, laboratory of Natural Product, Pharmacology and Hearing Loss, Department of Oriental Medicinal Materials & Processing, College of Life Sciences, Kyung Hee University, for his help to determine pigmentation inhibitory on zebrafish.

I would like to thank to Asst. Prof. Dr.Wandee Udomuksorn, Department of Pharmacology, Prince of Songkla University, for her help and western blot equipment support.

I would like to thank to Faculty of Pharmaceutical Sciences and Graduate School of Prince of Songkla University for the scholarship supporting the research.

I would like to thank to all staffs of Department of Pharmacognosy and Pharmaceutical Botany, Faculty of Pharmaceutical Sciences, Prince of Songkla University for their contribution and friendship.

Finally, I would like to thank to all friends for their encouragement, contribution and friendship. Most important, I would like to thank my family for their support, encouragement, contribution and love.

Kedsaraporn Parndaeng

CONTENTS

LIST OF TABLES

LIST OF FIGURES

LIST OF SCHEMES

LIST OF ABBREVIATIONS AND SYMBOLS

α	alpha
δ	chemical shift in ppm
mg	microgram
ml	microliter
%	percentage
br	broad signals for NMR spectrum
^{o}C	degree Celsius
CFU	colony forming unit
Chloroform-*d*	deuterated chloroform
COSY	correlation spectroscopy
d	doublet (for NMR spectra)
dd	doublet of doublets (for NMR spectra)
DEPT	distortionless enhancement by polarization transfer
DMSO-d_6	deuterated dimethylsulfoxide
EIMS	electron-impact mass spectroscopy
g	gram
HMBC	^{1}H-detected heteronuclear multiple bond coherence
HMQC	^{1}H-detected heteronuclear multiple quantum coherence
hr	hour
hpf	postfertilization
Hz	Hertz
IC_{50}	median inhibitory concentration
IR	infrared
J	coupling constant
kg	kilogram
m	multiplet (for NMR spectra)
mg	milligram
mL	milliliter
mm	millimeter

MS	mass spectroscopy
NaCl	sodium chloride
nm	nanometer
NMR	nuclear magnetic resonance
ppm	part per million
q	quartet (for NMR spectra)
s	singlet (for NMR spectra)
spp.	in the plural in place of the specific epithet
t	triplet (for NMR spectra)
tq	triplet of quartet (for NMR spectra)
TLC	thin layer chromatography
UV-VIS	ultraviolet-visible
v/v	volume by volume
w/w	weight by weight
w/v	weight by volume
ACTH	adrenocorticotropic hormone
DHI	dihydroxyindole
DHICA	dihydroxyindole-2-carboxylic acid
DCT	dopachrome tautomerase
ET-1	endothelin-1
GSK3ß	glycogen synthesis kinase 3ß
L-Dopa	L-dihydroxyphenylalanine
α-MSH	α-melanocyte-stimulating hormone
MITF	microphthalmia-associated transcription factor
MAPK	mitogen-activated protein kinases
NO	nitric oxide
PI3K	phosphatidylinositol 3-kinase
PI3K-Akt	phosphatidylinositol 3-kinase-Protein Kinase B
SCF	stem cell factor
TYR	tyrosinase
TRP1	tyrosinase-related protein 1
TRP2	tyrosinase-related protein 2

CHAPTER 1
INTRODUCTION

1. Background

Nowaday, skin whitening or skin lightening is popular thus, the skin whitening agent has grown up. Melanin is an important factor that determines skin color (Jang and Ahn, 2015). Melanin is a polyphenolic pigment and cause to dark-color. It is produced in the process called melanogenesis (Lopez-Serrano *et al*., 2004). There are two major types of melanins, a black-brown pigment color which known as eumelanin and a yellow-red pigment color which known as pheomelanin (Rozanowska *et al*., 1999; Kim and Uyama, 2005).

In melanogenesis, tyrosinase enzyme is an important enzyme to catalyses L-tyrosine to L-Dopa and to *o*-Dopaquinone-H^+ after that pass the intermediate to final melanins (Garcia-Molina *et al.,* 2005). Tyrosinase (TYR), tyrosinase-related protein 1 (TRP1) and tyrosinase-related protein 2 (TRP2) are the melanocyte-specific enzymes can regulate melanogenesis. In particular, tyrosinase is a key role in the process, which is an attractive target in the search for de-pigmenting agents (Kobayashi *et al*., 1994; Yokoyama *et al*., 1994; Briganti *et al*., 2003).

The melanin major function is to provide protection against ultraviolet (UV) radiation. However, UV may cause of the sunburn reaction within the skin and absorbed by the epidermis and upper dermis to stimulate the melanogenesis (Garland *et al*., 2003; Tengamnuay *et al*., 2006; Costin and Hearing, 2007) involved with inflammatory mediators and hormone (Slominski *et al*., 2004) produce the epidermal pigmentation accumulation with an excessive rate or hyperpigmentation due to uneven of skin color or age spots, darker skin color, melasma and sites of actinic damage (Kim and Uyama, 2005). Moreover, it may cause of lentigo or melasma. Disorders of hyperpigmentation; post melasma and inflammatory hyperpigmentation might be a difficult circumstances for patients that generating a negative effect for their life grade (Woolery-Lloyd and Kammer, 2011).

Tyrosinase is one of the main causes of melanogenesis, then inhibition the activity of tyrosinase can decrease melanogenesis. The most commonly used treatment for all types of hyperpigmentary disorders is topical hydroquinone. It can lead side effect reactions such like skin irritation, dermatitis, melanocyte demolition, ochronosis, post-inflammatory pigmentation, cytotoxicity and skin cancer (Chiari *et al*., 2011).

The infection of pathogenic bacteria for example *Cutibacterium acnes*, *Staphylococcus epidermidis* and *S. aureus* can cause to acne vulgaris or acne inflammation result to post-inflammatory hyperpigmentation (Kumar *et al*., 2007; Athikomkulchai *et al*., 2008).

Postinflammatory hyperpigmentation treatment to help hasten its resolution and management of the initial inflammatory condition (bacteria) should be started early. Moreover, topical tyrosinase inhibitors can effectively lighten areas of hyperpigmentation (Davis and Callender, 2010; Tanghetti, 2013).

Tyrosinase inhibitor agent can develop into new drug to treat hyperpigmentation and useful in cosmetology4. The investigation of tyrosinase inhibitors from natural products has been paid great attention because they are cheap and have little side effect (Kiken and Cohen, 2002; Okunji *et al*., 2007).

Moraceae is the most interesting plant family to study biological activities especially, antityrosinase activity because of many compounds from this family showed inhibitory activity against tyrosinase enzyme. *Artocarpus chama* and *Streblus taxoides* also belong to Moraceae family. According to the screening results they showed the potent antityrosinase activity. Since, they have not been reported on antityrosinase on both intracellular and extracellular enzyme assays, the effect on pigmentation in zebrafish and anti-bacterial activity. So, they were selected for further study on phytochemistry and bioactivities.

2. Objectives

The main objectives in this study are as follows:

1. Preliminary screening of antityrosinase and antibacterial activities of *Artocarpus chama* stem and *Streblus taxoides* wood extracts
2. Isolation and identification of the chemical constituents from these plants
3. Determination of antityrosinase and antibacterial activities of pure compounds from these plants

CHAPTER 2
HISTORICAL

1. Botanical characteristic

1.1. Moraceae

Plants in Moraceae family are usually trees, shrubs, woody climbers or herbs, terrestrial, hemi-epiphytic (or holo-epiphytic). dioecious or monoecious, with milky sap. **Leaves** alternate and spirally arranged or distichous, (sub) opposite or subverticillate; **stipules** fully amplexicaul or semi-amplexicaul and lateral or intrapetiolar, free or connate; lamina basally attached (or peltate), with the margin entire or incised (to seemingly compound), venation pinnate or subpalmate, brochidodromous. **Inflorescences** typically in pairs, unisexual or bisexual, racemose, spicate, globose-capitate, capitate with a discoid to cup-shaped receptacle (and then with or without involucre), or with an urceolate receptacle, multi- to uniflorous, bracteate. **Flowers** unisexual, free or connate (or also adnate to the receptacle). **Staminate flowers**: tepals 2-4 (-7) and free or connate, or perianth lacking; stamiens 1-4(-6), straight or inflexed before anthesis; pistillode present or absent. **Pistillate flowers**: tepals (3-) 4 (-8), free or connate; pistil 1, ovary unilocular, free or adnate to the perianth; stigmas 2 or 1, various in shape, ovule 1, (sub)apically attached, anatropous to campylotropous. **Fruit** an achene or drupaceous (dehiscent or indehiscent), free or adnate to the perianth, often forming a drupaceous whole with the fruiting perianth or also with the (fleshy) receptacle; seed large and without endosperm or small and with endosperm, embryo various. The family comprises 37 genera and 1,070–1,100 species represented by 11 native genera with in total 139 indigenous species recognised; 12 species are introduceed in Thailand. Most species are elements of lowland evergreen forest (Santisuk and Larsen, 2011).

1.2. *Artocarpus chama*

Artocarpus chama Buch.-Ham. (Figure 2-1) has many synonyms such as *A. chaplasha* Roxb., *A. calophyllus* Kurz, *A. asperulus* Gagnep., *A. rigidus* Blume subsp. *Asperulus* Gagnep. and *A. asperulus* Gagnep. var. *hirta* Gagnep. It is a tree 40 m tall. **Leafy twigs** 2-8 mm thick, ± densely brown hirtellous to puberulous or strigillose, ± scabrous, drying brown to dark brown. **Leaves** spirally arranged; lamina coriaceous, entry, elliptic to oblong or to ovate, 10-29 by 5-14 cm, entire, apex short-acuminate, acute,apiculate, rounded or obtuse, base rounded to subcordate, margin entire to repand or denticulate towards the apex; upper surface densely brown puberulous or strigillose on the midrib and/or also on the lateral veins to hispidulous elsewhere, ± scabrous, lower surface brownish strigose, hirtellous, puberulous subtomentose or strigillose on the main veins and puberulous to hispidulous or subtomentose on the smaller veins, ± scabrous or smooth; lateral veins 8-12 pairs,most or some of them branched or forked away from the margin, tertiary venation loosely scalariform, ± prominent; petiole 1-4 cm long, 2-3 mm thick, brown strigose to puberulous, the epidermis persistent or ± flaking off; stipules 1-3 cm, brown strigose caduceus. **Staminate inflorescences** axillary, solitary; peduncle 0.0-0.2 cm or 1.5-5 cm long, brown hispidulous to strigillose, scabrous; head subglobose to ovoid or ellipsoid, 1-1.5 cm diam. or 2-2.5 x 1.5-2 cm; perianth tubular ca. 2 mm long, the apex 2-lobate, minutely puberulous; stamen ca. 2.5 mm long, anther ca. 0.3 mm long; interfloral bracts peltate, apical part ca. 0.4 mm diam., puberulous. **Pistillate inflorescences** axillary, solitary; peduncle 0.0-0.3 cm or 1-5 cm long, brown puberulous, scabridulous; head subglobose; perianth tubular, brown hispidulous, the apex convex; stigma simple; interfloral bracts peltate, apical part 0.2-0.4 mm diam., puberulous. Infructescences subglobose, ca. 4-7 cm diam., covered with 5-10 mm long, cylindrical apices of the perianths; fruits ellipsoid, 1-1.5 cm long. . It is widely distributed in evergreen and mixed deciduous forests, to 750 m, in Thailand and also found in India, Sikkim, Bangladesh (type), Burma, Cambodia and Vietnam. The local names in Thailand are Khanun pan (Surat Thani), Khanun pa (Chachoengsao) (Santisuk and Larsen, 2011).

A. chama has been reported on anti-oxidant and cytotoxic activities (Ahmed *et al*., 2012 and 2013) and chemical constituents as artocarpin, cycloartocarpin A, cudraflavone A, artonin A, E, U, cycloartobiloxanthone, 3′,4′,5,7-tetrahydroxy-8-(methylbut-2-enyl)flavone, artostilbene A-B, artochamin A-K as shown in Figure 2-3, (Wang *et al*., 2004, 2006 and 2007).

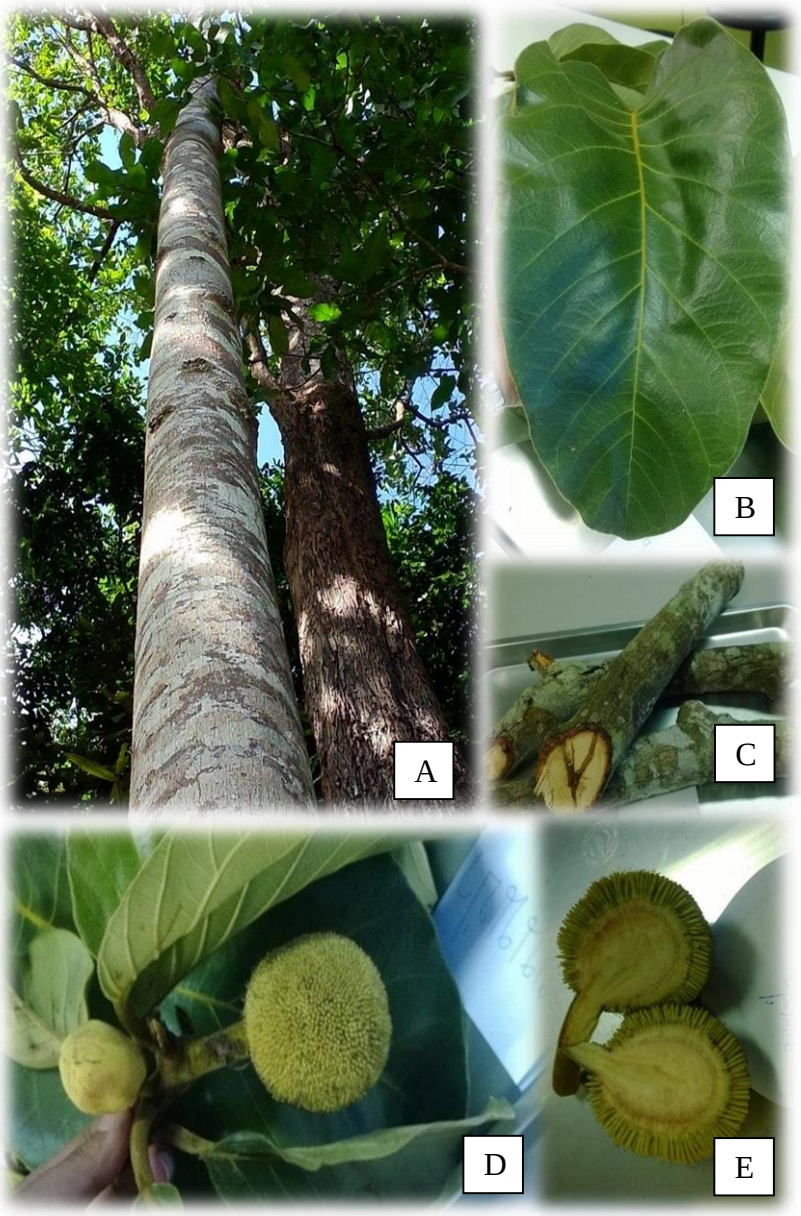

Figure 2-1 *Artocarpus chama* from Southern Literature Botanical Garden, Songkhla (A = Tree, B = Leaf, C = Stem, D-E = Fruit)

1.3. *Streblus taxoides*

Streblus taxoides (Heyne ex Roth) Kurz (Figure 2-2) has many synonyms such as *Trophis taxoides* Heyne ex Roth, *Phyllochlamys taxoides* (Heyne ex Roth) Koord., *Trophis spinosa* Roxb., *Epicarpurus spino*sus (Roxb.) Wight, *Phyllochlamys spinosa* Roxb., *Epicarpurus zeylanicus* Thwaites, *Streblus zeylanicus* (Thwaites) Kurz, *Diplocos zeylanicus* Thwaites, *Streblus microphyllus* Kurz, *Streblus taxoides* (Roth) Kurz var. *microphylla* (Kurz) Kurz, *Phyllochlamys wallichii* King ex Hook.f., *Phyllochlamys tridentate* Gagnep., *Taxotrophis poilanei* Gagnep, *Taxotrophis crenata* Gagnep. and *Streblus crenatus* (Gagnep.) Corner. It is a shrub or treelet 5 m tall, much branched, with thorns to 1.5 cm long, mostly terminating leafy twigs, dioecious; short-shoots often present, bearing leaves and/or inflorescences. **Leafy twigs** 1-2.5 mm thick, brown to whitish puberulous, on one side only or more densely. **Leaves** distichous; lamina oblong, elliptic, lanceolate or obovate 2-10 by 1-4.5 cm, subcoriaceous to coriaceous, apex cuminate to acute, acumen acute to obtuse, base obtuse to rounded, margin dentate todnticulate, mainly in the upper part of the lamina; both surfaces glabrous and smooth; midrib impressed above, lateral veins 6-12 pairs, tertiary venation reticulate; petiole 0.1-0.4 cm long, brown to whitish puberulous, adaxially only; stipules 0.2-0.5 mm long, ciliolate, subpersistent. It is widely distributed in mixed deciduous, dry evergreen and evergreen forests, also on limestone and open at low altitudes, in Thailand and also found in Sri Lanka, India, Bhutan, Burma, China, Vietnam, Laos, Cambodia, Peninsular Malaysia, Indonesia and Philippines.

The local names in Thailand are Katae mai (Pattani), Khoi nam (General), Khi raet, Nam khi raet (Peninsular) (Santisuk and Larsen, 2011).

S. taxoides has not been reported on chemical constituents and biological activities. Therefore, this study would be furture investigated.

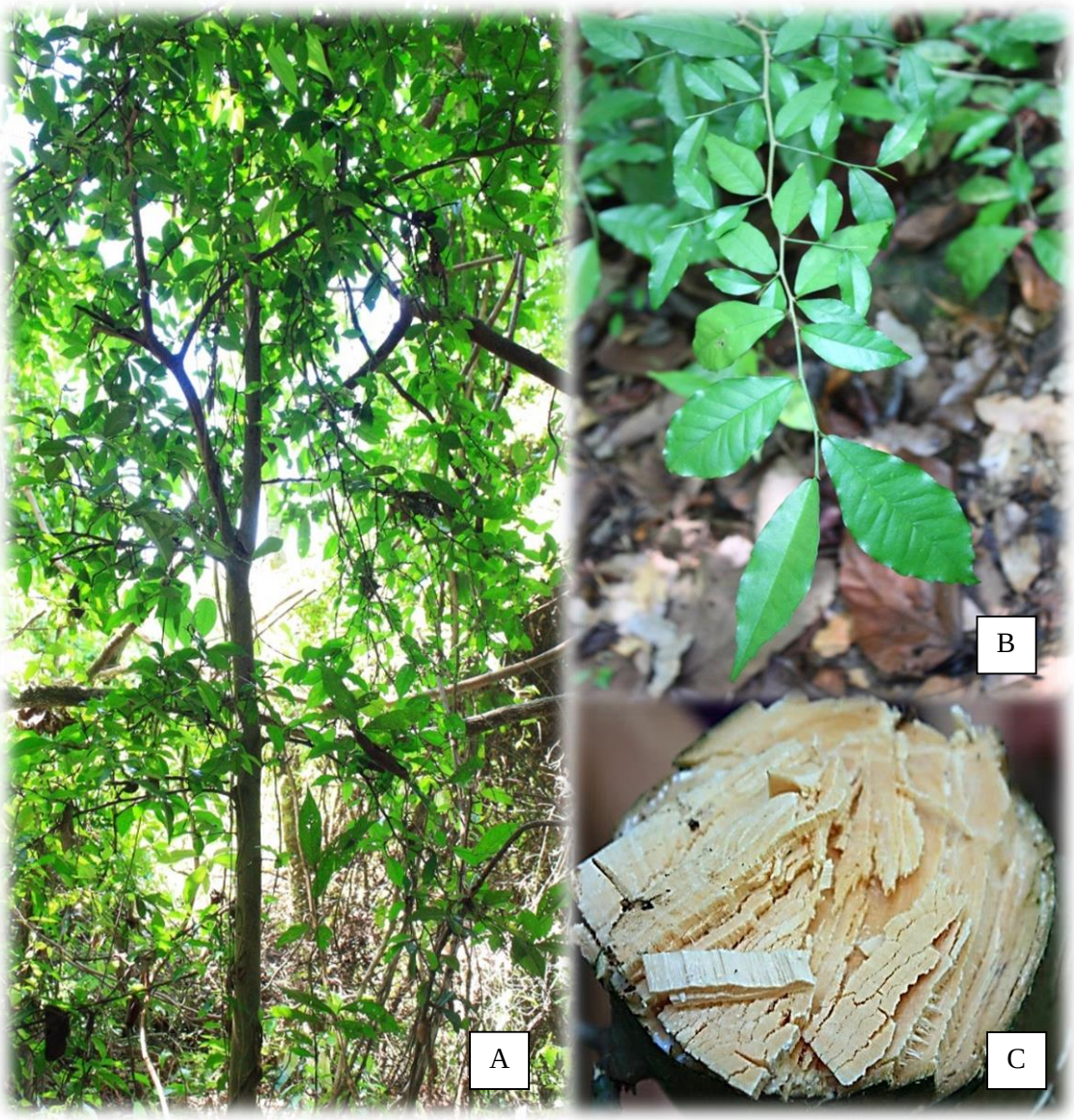

Figure 2-2 *Streblus taxoides* from Rajjaprabha Dam, Surat Thani

(A = Tree, B= Leaf, C = wood)

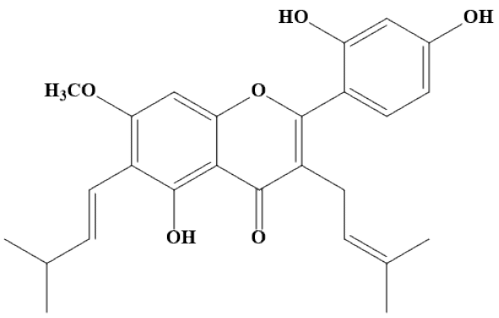

Artocarpin

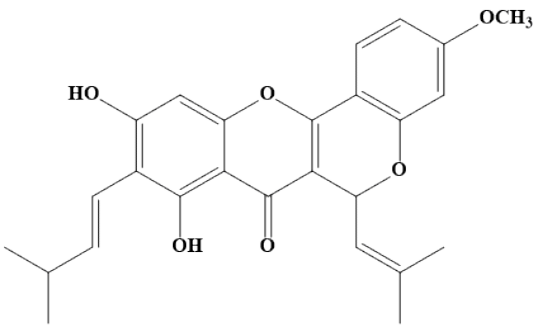

Cycloartocarpin A

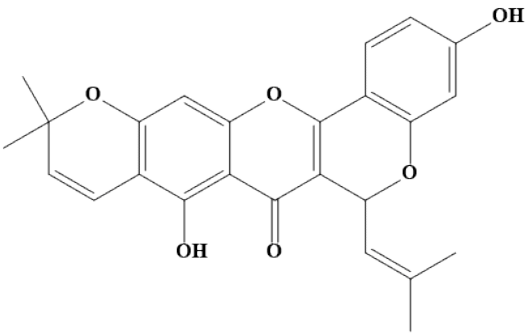

Cudraflavone A

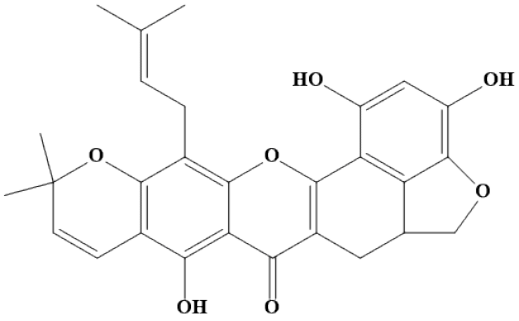

Artonin A

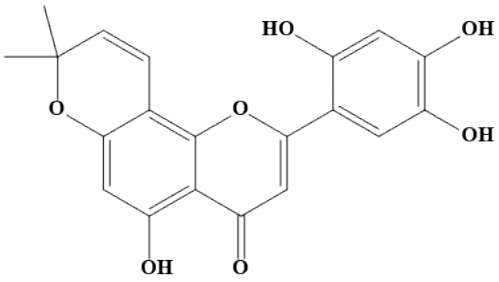

Artonin E

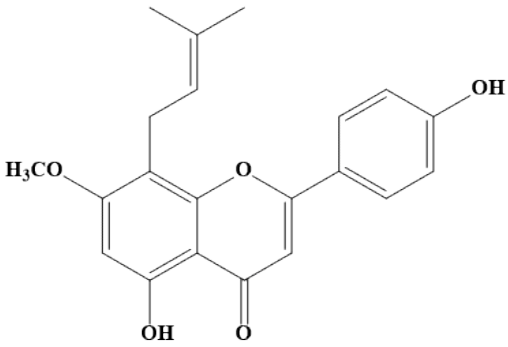

Artonin U

Figure 2-3 Compounds isolated from *A. chama*

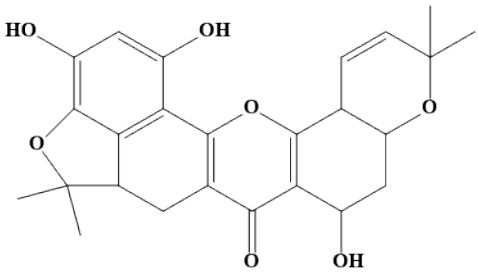

Cycloartobiloxanthon

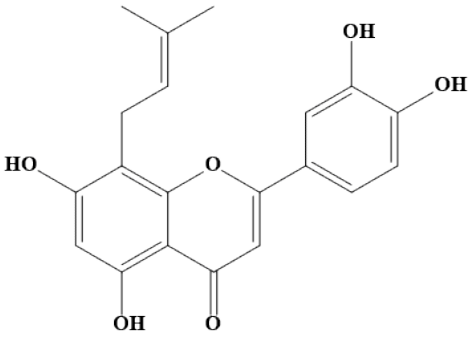

3′,4′,5,7-Tetrahydroxy-8-(methylbut-2-enyl)flavone

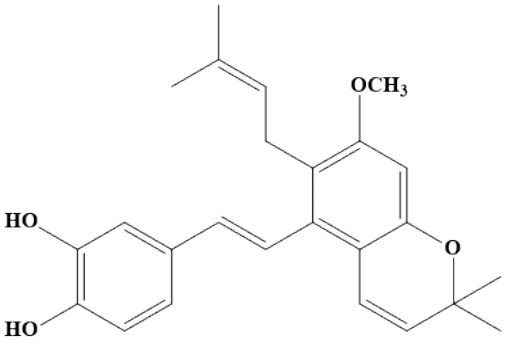

Artostilbene A

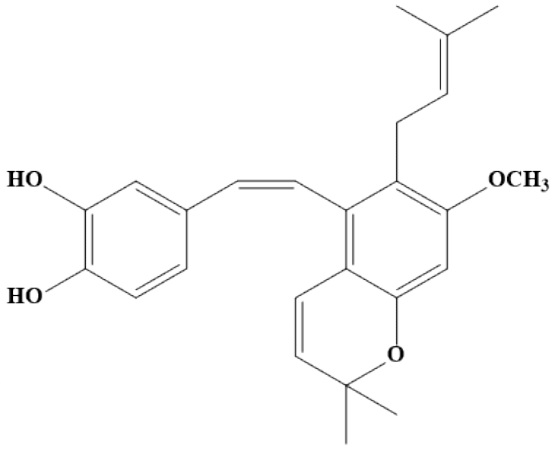

Artostilbene B

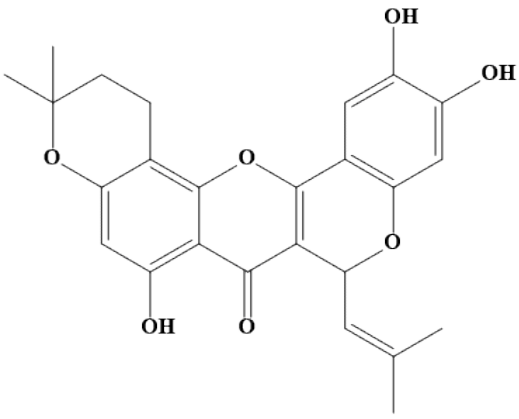

Artochamin A

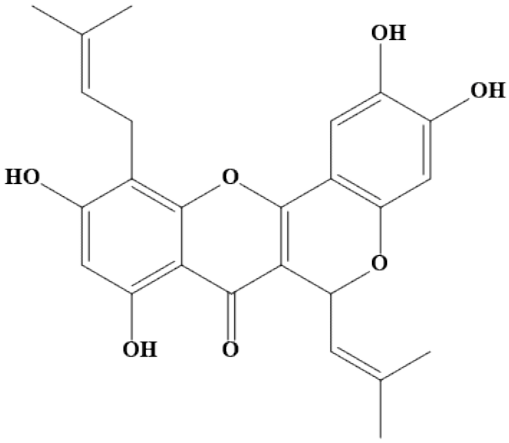

Artochamin B

Figure 2-3 Compounds isolated from *A. chama* (continued)

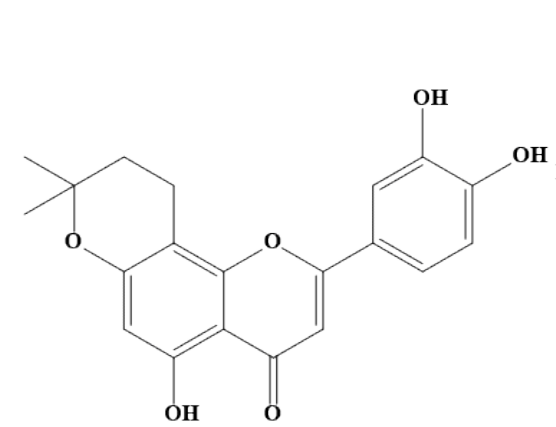

Artochamin C

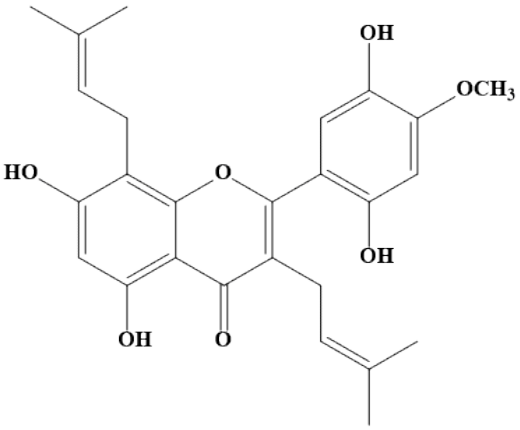

Artochamin D

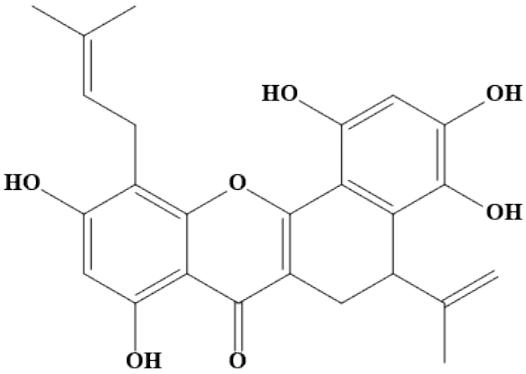

Artochamin E

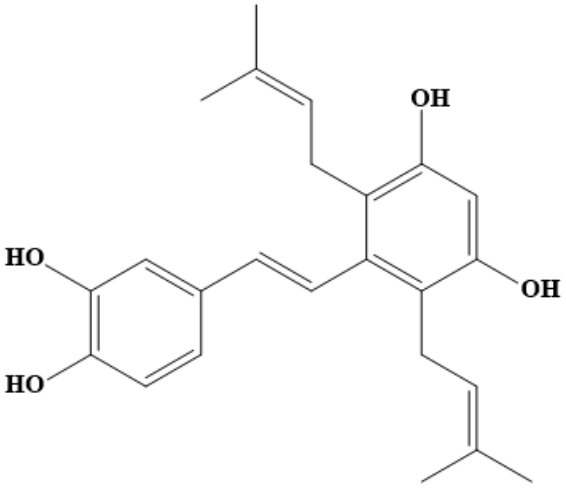

Artochamin F

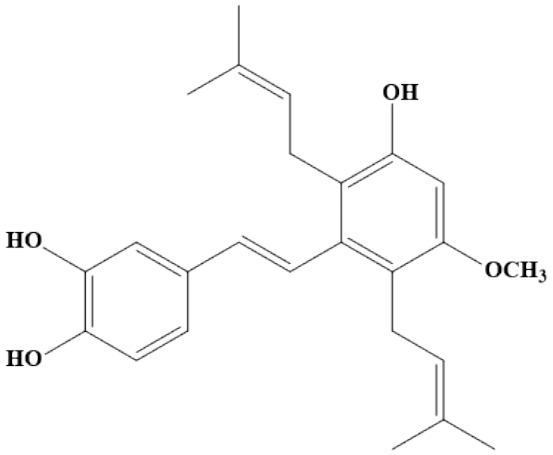

Artochamin G

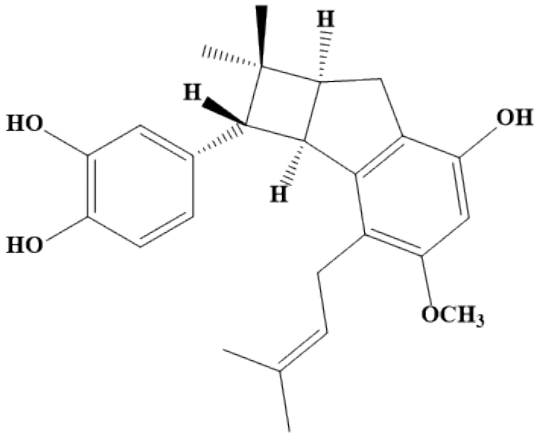

Artochamin H

Figure 2-3 Compounds isolated from *A. chama* (continued)

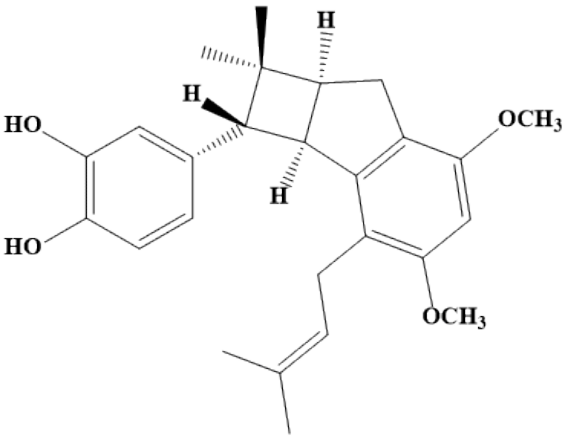

Artochamin I

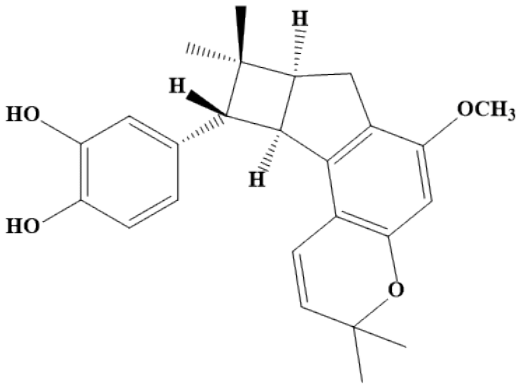

Artochamin J

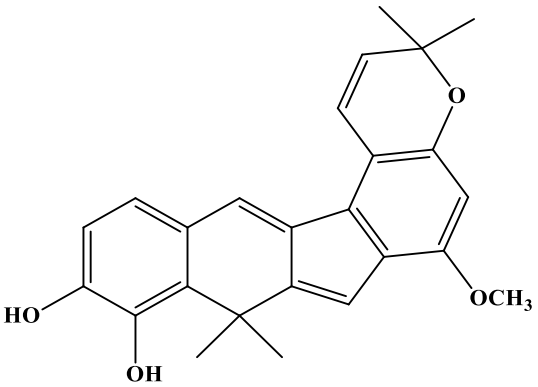

Artochamin K

Figure 2-3 Compounds isolated from *A. chama* (continued)

2. Human skin

The skin is the outer covering of the body. It provides the dynamic interphase between the body and the external environment. It is the largest organ of the body, covering over 7600 sq cm (3000 sq inch) area in an average adult and accounts for approximately 79% of the person's body weight (Lowe and Shaath, 1990; Singh, 2015)

2.1. Skin functions

The skin is a dynamic organ. It is not only protects the body from external environments but it also function in maintaining body homeostasis. The major functions of the skin include; protect the skin from pathogens and external injury, prevents the loss of body fluids, control the regulation of body temperature at 37 °C, plays as sensory reception, synthesis vitamin D with the help of ultraviolet rays, excrete he excess of water, salts and waste products and skin can also communicate emotions (Singh, 2015).

2.2. Skin structure

The skin composed of two principal layers: epidermis is the surface skin epithelium, the keratinized stratified squamous variety and the deeper dermis consists primarily of collagen fibers bundles, blood vessels, elastic tissue, nerve fibers and lymphatics (Figure 2-4) (Costin and Hearing, 2007).

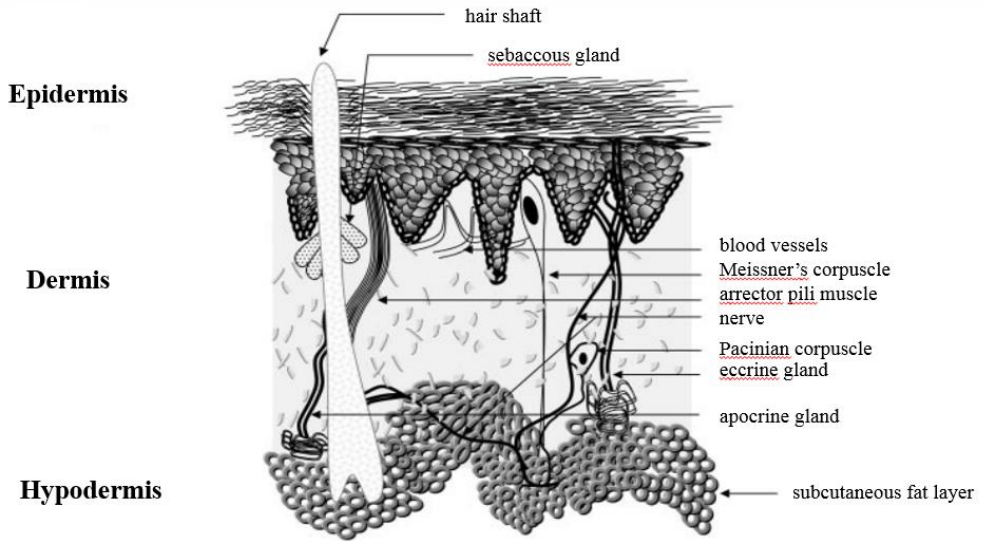

Figure 2-4 Skin structure (Costin and Hearing, 2007)

2.2.1. Epidermis

The epidermis is an external, superficial avascular layer of stratified squamous keratinized epithelium of 5-100 um thickness and derived from surface ectoderm of the body. It arranged in four layers; the deepest epidermis is stratum basale followed by stratum spinosum, stratum granulosum and the most upper layer is stratum corneum (Costin and Hearing, 2007). The epidermis consists of four main types of cells; 1-the main is keratinocyte cells, they protects the skin from environments by produce keratin protein, 2-melanocyte cells, they produce melanin pigments which responsible for determine human skin color geographical variability and protect the skin from ultraviolet light, 3-langerhans cells, they are important in immune response and 4-merkel cells, they contact with sensory neuron and act as receptors (Cichorek *et al*., 2013; Singh, 2015).

2.2.2. Dermis

The dermis is the deep vascular layer, it is a 2-4 mm-thick connective tissue layer and fibroblasts derived from mesoderm. The dermis is usually divided to be two layers; 1-superficial papillary layer, the layer that contact with epidermis. It forms dermal papillae extending into the epidermis and serve to interlock the dermis and the epidermis and 2-deep reticular layer, this layer composed of collagen fibers arranged mostly in parallel bundles (Singh, 2015).

2.2.3. Melanin, melanocytes and melanosomes

Melanin is the main pigment in mammal found in skin, hair and eyes (Jimenez-Cervantes *et al.,* 1995; Kim and Uyama, 2005), melanocytes of mammalian produce two different types of melanin pigments: eumelanin (blackbrown) and pheomelanin (yellow-reddish). It synthesis by complex pathway, melanogenesis in a melanocyte cells in membrane-bound organelles called melanosomes (Costin and Hearing, 2007). Then, melanosome are transferred to the epidermal keratinocytes, via melanocyticdendrite to protect the skin from removing reactive oxygen species (ROS) and UV radiation damage (Hoogduijn *et al.,* 2004; Kim and Uyama, 2005; Singh, 2015).

2.3. Regulation of melanogenesis

Histamine, α-melanocyte-stimulating hormone (α-MSH), endothelin-1 (ET-1), prostaglandins, nitric oxide (NO), stem cell factor (SCF), adrenocorticotropic hormone (ACTH) and thymidine dinucleotide are paracrine cytokines which regulate melanogenesis pathway. Those factors regulate the gene expression of tyrosinase (TYR), tyrosine-related protein 1 (TRP1) and tyrosine-related protein2 (TRP2) which can stimulate the expression and activation of microphthalmia-associated transcription factor (MITF) by binding with the M box of a promoter region leads to induced melanogenesis. The melanogenesis-related enzymes expression can activate or depress by up-down-regulations of MITF activity, so it can be in stimulation or inhibition of melanogenesis as showed in the Figure 2-5, (Costin and Hearing, 2007; Chang, 2012; Niu and Aisa, 2017).

Melanin biosynthesis or melanogenesis start from the hydroxylation and oxidation of L-tyrosine to L-dihydroxyphenylalanine (L-Dopa) and *o*-dopaquinone, catalyzed by tyrosinase enzyme. Two different types of *o*-dopaquinone reactions to produce different types of melanin, eumelanin and pheomelanin (Figure 2-5). First reaction (eumelanogenic pathway) started by the cyclization of *o*-dopaquinone, amino group goes through $1,4$-addition to the benzene ring to leukodopachrome, the intermediate is quickly oxidized to dopachrome. The dopachrome form to synthesis eumelanin by two difference type reactions; (1) dopachrome decarboxylate to 5, 6-dihydroxyindole (DHI), and DHI oxidation to indole-5, 6-quinone (IQ) and (2) enzymatically transformed of dopachrome to $5,6$-dihydroxyindole-2-carboxylic acid (DHICA) by dopachrome tautomerase (DCT) or TRP2 and then, responsible of TRP1, DHICA further oxidized to indole-5, 6-quinone carboxylic acid. Both IQ and indole-5, 6-quinone carboxylic acid are subsequent polymerization to eumelanin (Kim and Uyama, 2005; Slominski *et al.,* 2004). The second reaction (pheomelanogenic pathway) is the attack of sulfhydryl such as cysteine and glutathione nucleophilically compounds with *o*-dopaquinone to produce cysteinyldopa or glutathionyldopa. Then, cyclization and polymerization of cysteinyldopa or glutathionyldopa to pheomelanin (Slominski *et al.,* 2004; Kim and Uyama, 2005; Chang, 2012).

There are three enzymes involved in the melanogenesis pathway (Figure 2-6); tyrosinase (TYR), tyrosinase-related protein 1 (TRP1) and tyrosinase-related protein 2 (TRP2) or DOPAchrome tautomerase (DCT). However, only tyrosinase (TYR) is absolutely necessary for melanogenesis because its key enzyme in the process (Chang, 2012). Tyrosinase (TYR) is responsible for the first steps of melanogenesis (the hydroxylation and oxidation of L-tyrosine to L-Dopa and *o*-dopaquinone). While, TRP1 and DCT or TRP2 are involved in modifying the melanin types, the subsequent step of DOPA and its derivatives by TRP1 and TRP2 or DCT results in the synthesis of eumelanin. Briefly, DOPAchrome decarboxylate to DHI and DHI oxidation to IQ, However, in the presence of TRP2 or DCT, DOPAchrome transformed to 5, 6- DHICA, and responsible of TRP1, DHICA further oxidized to indole-5, 6-quinone carboxylic acid. Then, IQ, indole-5, 6-quinone carboxylic acid and DHICA are subsequent polymerization to eumelanin (Slominski *et al.*, 2004; Kim and Uyama, 2005; Costin and Hearing, 2007; Chang, 2012).

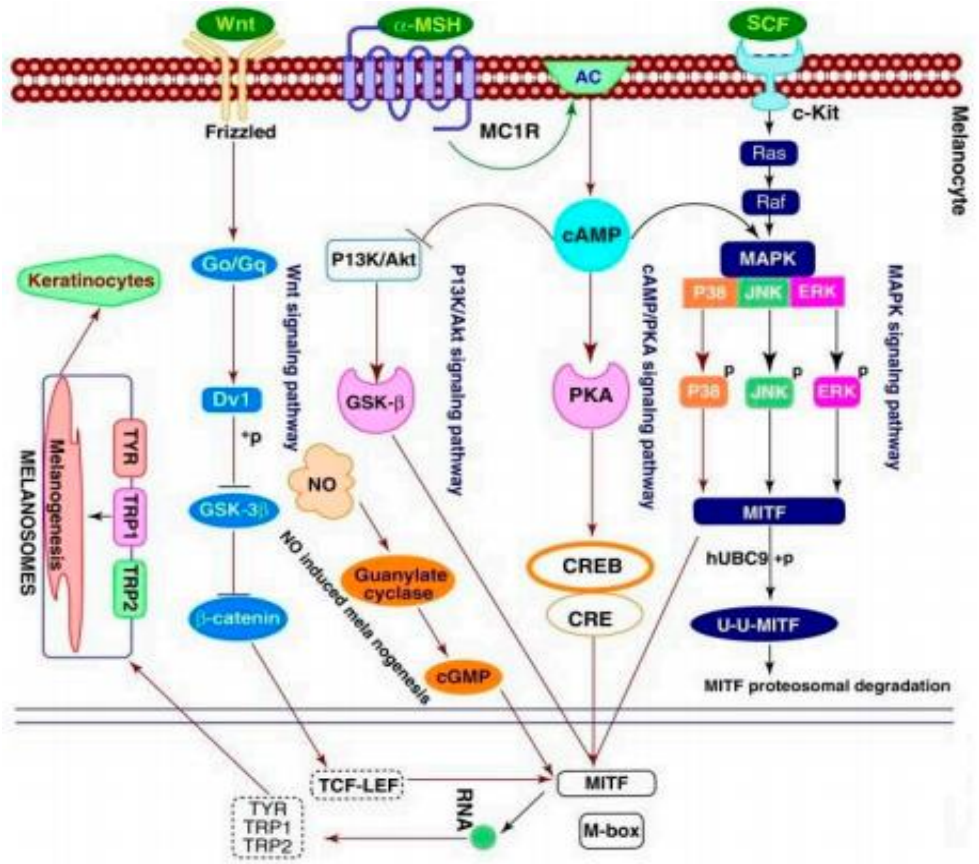

Figure 2-5 Regulation of melanogenesis through different signal pathways

(Niu and Aisa, 2017)

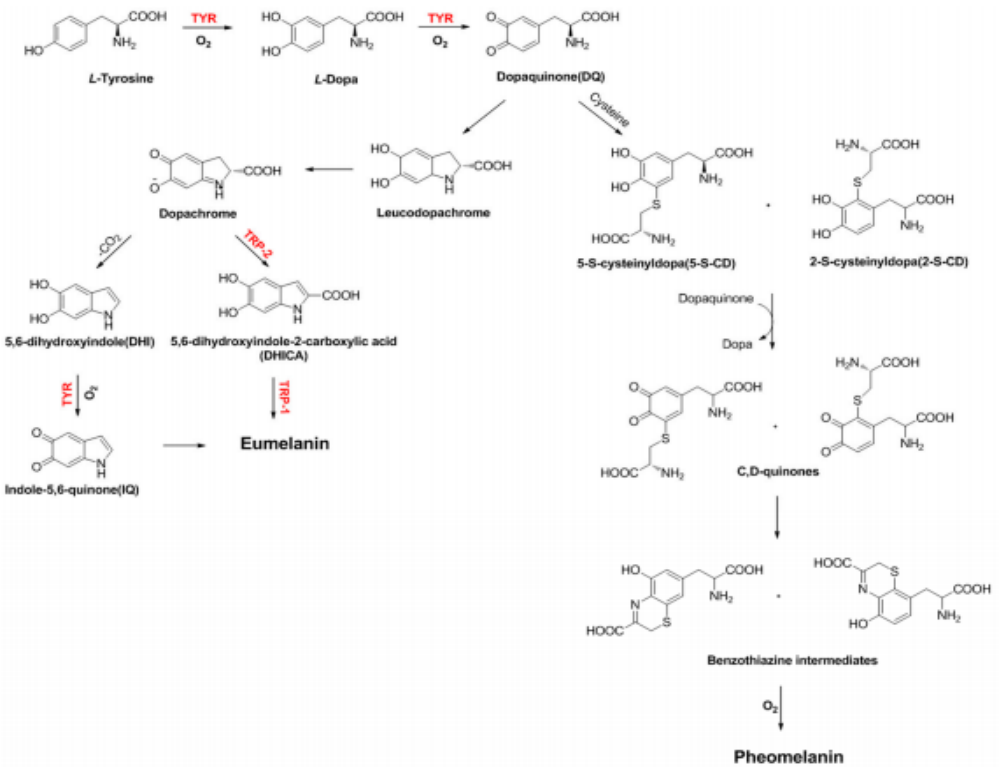

Figure 2-6 Melanogenesis catalyzed by tyrosinase (TYR), tyrosinase-related protein 1 (TRP1) and tyrosinase-related protein 2 (TRP2 or DCT)

(Niu and Aisa, 2017)

2.4. Hyperpigmentation

The melanin has major function to provide protection against radiation of ultraviolet (UV). However, UV may cause the sunburn effect within the skin and absorbed by the epidermis and upper dermis to stimulate the melanogenesis (Garland *et al.*, 2003; Tengamnuay *et al.*, 2006; Costin and Hearing, 2007) involved with inflammatory mediators and hormone (Slominski *et al.*, 2004) result in the epidermal pigmentation accumulation in an excessive level or even highly pigmentation due to deeply dark or uneven of skin color, sites of actinic damage, age spots and melasma (Kim and Uyama, 2005). Moreover, it may cause of lentigo or melasma. Disorders of hyperpigmentation; melisma and post inflammatory hyperpigmentation might be a hard situations for patients generating a negative affect to their quality of life (Woolery-Lloyd and Kammer, 2011). Hydroquinone has been used to treat many forms of epidermal hyperpigmentation but it is harmful to the skin (Hu *et al.*, 2009).

2.5. Tyrosinase enzyme

Tyrosinase or polyphenoloxidase (Peñalver *et al*., 2005) is a copper-containing enzyme (Gasowska *et al*., 2006), that is ubiquitously produced in nature; bacteria, fungi, plant and animal. It is important in melanogenesis catalysis and substitute another procession, such like the browning of vegetables and fruits (Garcia-Molina *et al*., 2005; Claus and Decker, 2006). It catalyzes several processes in the melanin synthesis. Also, catalyzes two different kinds of enzymatic reactions: monophenolase is the hydroxylation of monophenols (tyrosine) and diphenolase is the oxidation of diphenols (3,4-dihydroxyphenylalanine, L-Dopa) to *o*-diquinones (Kim and Uyama, 2005; Claus and Decker, 2006) and subsequent polymerization to melanin (Slominski *et al*., 2004; Kim and Uyama, 2005). In human tyrosinase is a type I of membrane glycoprotein which consist of 529 amino acid, divided into three mature protein domains; a C-terminal cytoplasmic tail, a single transmembrane domain and a N-terminal (Wang and Hebert, 2006).

2.6. Tyrosinase inhibitors

Tyrosinase inhibition by inhibiting tyrosinase activity can decrease melanin produce in melanogenesis pathway (Okunji *et al*., 2007) . Especially, tyrosinase inhibitors from natural might be developing to treat hyperpigmentation disease and useful in cosmetology to find the problem solving which concerns with the presence of the agent that harmful to the skin's health for skin whitening products for example hydroquinone (Kiken and Cohen, 2002; Kim and Uyama, 2005). It has long been a mainstay for the topical treatment of hyperpigmentation (Woolery-Lloyd and Kammer, 2011; Konda *et al.,* 2012). However, some mechanisms of its action include interfering with DNA and RNA synthesis, degrading melanosomes and destroying melanocytes (Woolery-Lloyd and Kammer, 2011) then, concerns regarding ochronosis, allergic and irritant contact dermatitis, melanocyte toxicity and carcinogenicity (Konda *et al.*, 2012).

The discovery of natural tyrosinase inhibitors will be the alternatives way to provide the leads compounds for anti-pigmentation and can be developed for whitening and antibrowning agents. Moraceae is the most interesting plant family to study on antityrosinase activity because of many compounds from this family showed inhibitory *activity against* tyrosinase enzyme. For example, *Artocarpus lakoocha* wood water extract, which is applied for the control and other natural tyrosinase inhibitors of compounds/ extracts of Moraceae plants from previously reports are showed in the Table 2-1.

Table 2-1 Tyrosinase inhibitors from Moraceae plants

Plant	Compound/Extract	Reference
Artocarpus		
A. gomezianus	norartocarpetin resveratrol	Likhitwitayawuid *et al*., 2000
A. heterophyllus	dihydromorin steppogenin	Zheng *et al*., 2008b; Zheng *et al*., 2009
A. heterophyllus	norartocarpetin artocarpanone artocarpesin isoartocarpesin	Zheng *et al*., 2008b; Zheng *et al*., 2009
A. incises	flavonoids stilbenes related 4-substituted resorcinols	Shimizu *et al*., 2000
A. integer	artocarpanone EtOH stem bark extract EtOH wood extract EtOH root bark extract EtOH root extract	Dej-adisai *et al*., 2014

Table 2-1 Tyrosinase inhibitors from Moraceae plants (continued)

Plant	Compound/Extract	Reference
A. lakoocha	oxyresveratrol(*trans*-2,4,3′,5′-tetrahydroxystilbene)	Likhitwitayawuid *et al*., 2006
	trans-2-methoxy-4,3′,5′-trihydroxystilbene	
	trans-2,3′-dimethoxy-4,5′–dihydroxystilbene	
	trans-4,3′-dimethoxy-2,5′–dihydroxystilbene	
	trans-2,4,3′,5′-tetramethoxystilbene	
	cis-2,4,3′,5′-tetramethoxystilbene	
	2,4,3′,5′–tetrahydroxybibenzyl	
	2,4,3′,5′- tetramethoxybibenzyl	
A. lakoocha	water heartwood extract	Sritularak *et al*., 1998; Tengamnuay *et al*., 2006
A. obtusus	pyranocycloartobiloxanthone A	Hashim *et al*., 2012
Broussonetia		
B. kazinoki	kazinol C	Baek *et al*., 2009
	kazinol F	
	broussonin C	
	kazinol S	
B. papyrifera	broussonetone A	Ko *et al*., 2008
	broussonetone B	
	broussonetone C	
	apigenin	

Table 2-1 Tyrosinase inhibitors from Moraceae plants (continued)

Plant	Compound/Extract	Reference
B. papyrifera	3,5,7,4′-tetrahydroxy-3′-(2-hydroxy-3-methylbut-3-enyl) flavone	Zheng *et al*., 2008a
	uralenol	
	quercetin	
	broussoflavonol F	
Cudrania		
C. cochinchinensis	MeOH root extract	Loizzo *et al*., 2012
	MeOH stem extract	
C. javanensis	EtOH wood extract	Dej-adisai *et al*., 2014
C. tricuspidata	Flaniostatin	Kang e*t al*., 2013
C. tricuspidata	*trans*-dihydromorin	Zheng *et al*., 2013
	oxyresveratrol	
	steppogenin	
Ficus		
F. racemosa	EtOH wood extract	Dej-adisai *et al*., 2014
F. virens	condensed tannins from the leaves, fruit, and stem bark	Chen *et al*., 2014
Morus		
M. alba	EtOH twig extract	Chang *et al*., 2011
	maclurin	
	rutin	
	isoquercetrin	

Table 2-1 Tyrosinase inhibitors from Moraceae plants (continued)

Plant	Compound/Extract	Reference
Morus		
M. alba	resveratrol morin	Chang *et al*., 2011
M. bombycis	80% EtOH leaf extract	Moon *et al*., 2010
Streblus		
S. ilicifolius	EtOH wood extract moracin M umbelliferone *trans*-resveratrol	Dej-adisai *et al*., 2016
S. taxoides	EtOH wood extract	

3. Bacterial and skin disease

3.1 Skin disease

Bacteria that cause disease are called pathogenic bacteria. Gram-positive bacteria are the main cause of human skin disease such as *Staphylococcus aureus, S. epidermidis* can be cause of impetigo, folliculitis and furunculosis (Cushnie and Lamb, 2005), *Cutibacterium acnes* can be cause of inflammatory mediators (papules, pustules, etc.) (Drott *et al.*, 2010).

Acne vulgaris or acne inflammation is one of dermal skin infection diseases that trigger social distraction and psychological disruption on sufferers. The infection of *P. acnes, Malassezia furfur, S. epidermidis* and *S. aureus* deu to the acne inflammation (Kumar *et al*., 2007; Athikomkulchai *et al*., 2008), which can stimulate the melanogenesis by several inflammatory mediators like prostaglandin E2 (PGE2) (Petit and Pierard, 2003).

3.2 Antibacteria

Antibiotics were used to treat the skin infections such as β-lactam (penicilins and mecillinams, cephalosporins, clavams, nocardicin, monobactams), tetracycline (tetracyclins, glycylcyclines), glycopeptides (vancomycin, teicoplanin), polyenes (nystatin, amphotericin B). Using antibiotic may cause of drug resistance in pathogens is the result of overuse of drugs (Heinemann *et al.*, 2000).

It has been found alternative microbial inhibitors from natural product. The discovery of microbial inhibition from natural plants is an alternative way to provide the lead compound for treatment of skin disease because of pathogenic bacteria. Antimicrobial activity of compounds/ extracts of Moraceae plants from previously reports are showed in the Table 2-2.

Table 2-2 Antimicrobial compounds/ extracts from Moraceae plants

Plant	Compound/ extract	Microbe*	Reference
Artocarpus			
A. altilis	hexane extract	*B. cereus* *C. albicans*	Kamal *et al.*, 2012
	EtOAc leaf extract MeOH leaf extract	*S. mutans*	Pradhan *et al*., 2012
	petroleum ether leaf extract	*E. faecalis* *S. aureus*	
	MeOH leaf extract	*P. aeruginosa*	

Table 2-2 Antimicrobial compounds/ extracts from Moraceae plants (continued)

Plant	Compound/ extract	Microbe*	Reference
A. anisophyllus *A. lowii*	artocarpin	*S. aureus* *B. cereus* *E. coli* *P. putida* *C. albicans* *C. glabrata*	Jamil *et al*., 2014
	Isobavachalcone	*S. aureus* *B. cereus*	
A. communis	MeOH fruit latex extract	*A. niger* *B. subtilis*	Madhavi *et al*., 2013
	$CHCl_3$ fruit latex extract	*S. aureus*	
A. integer	EtOH root extract	*S. aureus* *S. epidermidis* *P. acnes* *T. mentagrophytes*	Dej-adisai *et al*., 2014
A. lakoocha	aqueous extract	*A.actinomycetemcomitans* *P. gingivalis* *S. mutans* *S. sobrinus*	Teanpaisan *et al*., 2014

Table 2-2 Antimicrobial compounds/ extracts from Moraceae plants (continued)

Plant	Compound/ extract	Microbe*	Reference
A. lakoocha	MeOH bark extract	*S. soneii* *E. coli* *B. pumilus* *P. mirabilis* *B. subtilis* *E. coli*	Pandey and Bhatnagar, 2009
A. obtusus	pyranocycloartobilo-xanthone A	MRSA *B. subtilis*	Hashim *et al*., 2012
Broussonetia			
B. luzonicus	epitaraxerol lupenone betulin aldehyde fatty acid ester	*C. albicans* *A. niger* *S. aureus* *E. coli* *P. aeruginosa* *B. subtilis*	Tsai *et al.*, 2012
B. papyrifera	broussochalcone A papyriflavonol A	*C. albicans* *S. cerevisiae* *E. coli* *S. Typhimurium* *S. epidermidis* *S. aureus*	Sohn *et al*., 2004; Sohn *et al*., 2010;

Table 2-2 Antimicrobial compounds/ extracts from Moraceae plants (continued)

Plant	Compound/ extract	Microbe*	Reference
B. papyrifera	kazinol B	*C. albicans* *S. cerevisiae* *S. epidermidis* *S. aureus*	Sohn *et al*., 2004; Sohn *et al*., 2010;
Ficus			
F. carica	hexane leaf extract hydro-alcoholic leaf extract	*S. aureus*	Weli *et al*., 2015
	EtOAc leaves extract	*S. aureus* *P. aeruginosa*	
F. drupacea	*β*-amyrin *β*-sitosterol-3-*O*- *D*-glucopyranoside 5-*O*-methyllatifolin epilupeol acetate	*A. flavus* *A. versicolor* *A. niger* *A. ochraceus* *C. albicans* *P. funiculosum* *P. ochrochloron* *B. cereus* *L. monocytogenes* *M. flavus* *S. aureus* *S. typhimurium* *P. aeruginosa*	Yessoufou *et al*., 2015

Table 2-2 Antimicrobial compounds/ extracts from Moraceae plants (continued)

Plant	Compound/ extract	Microbe*	Reference
F. drupacea	*β*-amyrin *β*-sitosterol-3-*O*- *D*-glucopyranoside 5-*O*-methyllatifolin	*E. cloacae*	Yessoufou *et al.*, 2015
	oleanolic acid epifriedelanol friedelin	*S. aureus* *E. coli*	
F. pseudopalma	$CHCl_3$ and EtOAc fractions of EtOH leaf extract	*S. aureus* *S. epidermidis* *B. subtilis*	Llagas *et al*., 2014
F. thonningii	taxifolin	*E. coli* *P. vulgaris* *P. stuartii* *S. aureus* *C. albicans*	Fongang *et al.*, 2015
	conrauiflavonol shuterin	*E. coli* *P. vulgaris* *P. aeruginosa* *S. aureus*	

Table 2-2 Antimicrobial compounds/ extracts from Moraceae plants (continued)

Plant	Compound/ extract	Microbe*	Reference
Maclura			
M. cochinchinensis	$CHCl_3$ wood extract	*S. aureus* *S. epidermidis* *B. subtilis* *T. rubrum* *T. mentagrophytes* *M. gypseum*	Kummee and Intaraksa, 2008
	MeOH bark extract	*B. cereus* *S. aureus*	Swargiary and Ronghang, 2013
M. pomifera	osajin	*C. neoformans* MSSA* MRSA* *L. donovani*	Dharmaratne *et al*., 2013
	pomiferin	*S. aureus* MRSA* *L. donovani*	
M. tinctoria	MeOH : water bark extract	*S. mutans*	Lamounier *et al*., 2012
	cyclohexane : EtOH bark extract	*P. nigrescens* *A. naeslundii* *P. gingivalis*	

Table 2-2 Antimicrobial compounds/ extracts from Moraceae plants (continued)

Plant	Compound/ extract	Microbe*	Reference
Morus			
M. lhou	moracins C	MSSA	Fukai *et al*., 2005
M. alba		MRSA	
		M. luteus	
		B. subtilis	
		K. pneumoniae	
	moracins M	MSSA	
	moracins P	MRSA	
	mulberrofurans D	*M. luteus*	
	mulberrofuran F		
	mulberrofurans G		
	mulberrofurans Y		
	chalcomoracin		
	albanol B		
M. mongolica	kuwanon C	*C. albicans*	Sohn *et al*., 2004
		E. coli	
		S. typhimurium	
		S. epidermidis	
		S. aureus	
	sanggenon B	*C. albicans*	
		S. cerevisiae	
		S. epidermidis	
		S. aureus	

Table 2-2 Antimicrobial compounds/ extracts from Moraceae plants (continued)

Plant	Compound/ extract	Microbe*	Reference
M. mongolica	morusin	*C. albicans* *S. epidermidis* *S. aureus*	Sohn *et al*., 2004
	sanggenon D	*C. albicans* *S. cerevisiae* *S. typhimurium* *S. epidermidis* *S. aureus*	
M. alba	mulberrofuran G albanol B	*C. albicans* *S. cerevisiae* *E. coli* *S. typhimurium* *S. epidermidis* *S. aureus*	Fukai *et al*., 2005
Streblus			
S. asper	50% EtOH leaf extract	*S. mutans*	Taweechaisupapong *et al*., 2000; Wongkham *et al*., 2001
	EtOH leaf extract	*C. albicans*	Taweechaisupapong *et al.*, 2005; Taweechaisupapong *et al*., 2006

Table 2-2 Antimicrobial compounds/ extracts from Moraceae plants (continued)

Plant	Compound/ extract	Microbe*	Reference
S. ilicifolius	EtOH wood extract	*S. aureus* *S. epidermidis*	Dej-adisai *et al*., 2016
	2,3-dihydroxy-4-geranyl benzaldehyde moracin M	*S. aureus* *S. epidermidis* MRSA	

**A. actinomycetemcomitans = Aggregatibacter actinomycetemcomitans, A. flavus = Aspergillus flavus, A. naeslundii = Actinomyces naeslundii, A. niger = Aspergillus niger, A. ochraceus = Aspergillus ochraceus, A. versicolor = Avicularia versicolor, B. cereus = Bacillus cereus, B. pumilus = Bacillus pumilus, B. subtilis = Bacillus subtilis, C. albicans = Candida albicans, C. glabrata = Candida glabrata, C. neoformans = Cryptococcus neoformans, E. cloacae = Enterobacter cloacae, E. coli = Escherichia coli, E. faecalis = Enterococcus faecalis, K. pneumonia = Klebsiella pneumonia, L. donovani = Leishmania donovani, L. monocytogenes = Listeria monocytogenes,* MRSA = *Methicillin-resistant Staphylococcus aureus,*MSSA = *Methicillin-susceptible Staphylococcus aureus, M. flavus = Myotis flavus, M. gypseum = Microsporum gypseum, M. luteus = Micrococcus luteus, P. acnes = Cutibacterium acnes, P. aeruginosa = Pseudomonas aeruginosa, P. funiculosum = Penicillium funiculosum, P. gingivalis = Porphyromonas gingivalis, P. mirabilis = Proteus mirabilis, P. nigrescens = Prevotella nigrescens, P. ochrochloron = Penicillium ochrochloron, P. putida = Pseudomonas putida, P. stuartii = Providencia stuartii, P. vulgaris = Proteus vulgaris, S. aureus = Staphylococcus aureus, S. cerevisiae = Saccharomyces cerevisiae, S. epidermidis = Staphylococcus epidermidis, S. mutans = Streptococcus mutans, S. sobrinus = Streptococcus sobrinus, S. sonnei = Shigella sonnei, S. typhimurium = Salmonella typhimurium, T. mentagophytes = Trichophyton mentagrophytes, T. rubrum = Trichophyton rubrum*

CHAPTER 3
EXPERIMENTALS

1. Plant materials

Forty eight Moraceae plant samples were collected from Rajjaprabha Dam, Surat Thani Province, Southern Literature Botanical Garden, Songkhla Province, Botanical Garden, Faculty of Pharmaceutical Sciences, Prince of Songkla University, Songkhla Province and Walailak University, Nakhon Si Thammarat Province. The voucher specimen number of *Artocarpus chama* Buch. and *Streblus taxoides* (Heyne ex Roth) Kurz were SKP 117 01 03 01 and SKP 117 19 20 01, respectively. The herbarium specimen of these plants were kept at Department of Pharmacognosy and Pharmaceutical Botany, Faculty of Pharmaceutical Sciences, Prince of Songkla University. *A. chama* and *S. taxoides* were selected for further study on phytochemistry and bioactivities.

2. Bacteria, cell, media, antibiotic, enzyme antibodies, and chemicals

Table 3-1 Microorganisms, media, antibiotics and chemicals for antimicrobial test and their sources

Microorganisms	Sources
Staphylococcus aureus ATCC 25923	Thailand Institute of Scientific and Technology Research, Bangkok, Thailand.
Staphylococcus epidermidis TISTR 517	Thailand Institute of Scientific and Technology Research, Bangkok, Thailand.
Methicillin-resistant *Staphylococcus aureus* DMST 20654	Department of Pathology, Faculty of Medicine, Prince of Songkla University.

Table 3-1 Microorganisms, media, antibiotics and chemicals for antimicrobial test and their sources (continued)

Microorganisms	**Sources**
Cutibacterium acnes DMST 14916	Department of Medical Science, Ministry of Public Health, Thailand.
Mueller-Hinton Broth (MHB)	Difco, Bacto Dickinson and Company, Spark USA
Brain Heart Infusion Broth (BHIB)	Difco, Bacto Dickinson and Company, Spark USA
Oxacillin paper disc	Oxoid Limited, England
Vancomycin paper disc	Oxoid Limited, England
Oxacillin sodium salt	Fluka, Sigma-Aldrich, China
Vancomycin hydrochloride	Fluka, Sigma-Aldrich, Denmark

Table 3-2 Cell, media and chemicals for intracellular test and their sources

Cell	**Sourses**
Murine melanoma B16-F1 cells (CLS-400122**)**	CLS Cell Lines Service GmbH, Germany
Dulbecco's Modified Eagle Medium (DMEM)	Gibco, England
Arbutin	Sigma, Sigma-Aldrich, Germany

Table 3-3 Enzyme and chemicals for antityrosinase test and their sources

Enzyme	Source
Tyrosinase enzyme	Sigma, Sigma-Aldrich, Germany
$NaH_2PO_2.2H_2O$	MAY & BAKER Limited Dagenham, England
Na_2HPO_4	MAY & BAKER Limited Dagenham, England
Kojic acid	Fluka, Sigma-Aldrich, Germany
Dimethyl sulfoxide (DMSO)	Fluka, Sigma-Aldrich, Germany

Table 3-4 Antibodies and chemicals for western blot test and their sources

Antibodies	Sources
Primary antibodies;	
-beta Actin Loading Control Monoclonal Antibody (BA3R)	ThermoFisher Scientific #MA5-15739, USA
-DCT Polyclonal Antibody	ThermoFisher Scientific #PA5-36485, USA
-MiTF Monoclonal Antibody (21D1418)	ThermoFisher Scientific #MA5-16214, USA
-TRPC1 Polyclonal Antibody	ThermoFisher Scientific #OSR00085W, USA
-Tyrosinase Monoclonal Antibody (T311)	ThermoFisher Scientific #35-6000, USA

Table 3-4 Antibodies and chemicals for western blot test and their sources (continued)

Antibodies	sources
Secondary antibodies;	
-Goat anti-Mouse IgG (H+L) Secondary Antibody, HRP	ThermoFisher Scientific #31430, USA
-Goat anti-Rabbit IgG (H+L) Secondary Antibody, HRP	ThermoFisher Scientific #31460, USA
40% Acrylamide/ Bissolution, 29:1 [Acrylamide:N,Nmethylenbisacrylamide)	InvitrogenThermoFisher Scientific, USA
Ammonium per sulphate(APS)	InvitrogenThermoFisher Scientific, USA
Bromophenol blue	BIO-RAD Laboratories, Austria
Clarity™ Western ECL Substrate	BIO-RAD Laboratories, USA
Glycine from Sigma-Aldrich(St Louis, MO, USA)	BIO-RAD Laboratories, USA
N, N, N', N'-tetramethylenediamine (TEMED)	InvitrogenThermoFisher Scientific, USA
Nitrocellulose membranes 0.45µM	BIO-RAD Laboratories, Germany
2-ß-mercaptoethanol	BIO-RAD Laboratories, China
Sodium dodecyl sulphate (SDS)	BIO-RAD Laboratories**,** Japan
Tris base from Sigma-Aldrich	Sigma-Aldrich ,USA

Table 3-5 Chemicals for extraction and isolation and their sources

Chemicals	Sources
Acetone	Thaioil Co. Ltd., Thailand
Anisaldehyde	Fluka, Sigma-Aldrich, USA
Chloroform	RCI Labscan Limited, Thailand
Dichloromethane	RCI Labscan Limited, Thailand
Ethyl acetate	Thaioil Co. Ltd., Thailand
Glacial acetic acid	RCI Labscan Limited, Thailand
Hexane	Thaioil Co. Ltd., Thailand
Hydrochloric acid (37% w/w)	Fluka, Sigma-Aldrich, USA
Methanol	Thaioil Co. Ltd., Thailand
Petroleum ether	Thaioil Co. Ltd., Thailand
Sephadex LH-20	Merck, Darmstadt, Germany
Silica gel 60	Merck, Darmstadt, Germany
Silica gel 60 RP-18	Merck, Darmstadt, Germany
Sulfuric acid	Fluka, Sigma-Aldrich, USA
TLC plate (Silica gel GF_{254})	Merck, Darmstadt, Germany
TLC plate (Silica gel 60 RP-18)	Merck, Darmstadt, Germany

3. Plant samples extraction

Dried powder of plant materials were extracted by maceration procedure which repeated for 3 times by using ethanol for 3 days at common room temperature. The macerates were grouped continued by evaporation with rotary under pressure below 40 °C to yield the extract of ethanol. All extracts were then kept in 4 °C and ready for the test.

Plants that showed the potent effects on antityrosinase and/or anti-bacterial activities and have not been studied will be selected for this project.

4. General techniques

4.1 Analytical thin-layer chromatography (TLC)

Technique	:	One dimension, ascending
Adsorbent	:	Silica gel 60 F_{254} (E. Merck) precoated plate
Layer thickness	:	0.2 mm
Distance	:	6 cm
Detection	:	1) Visual detection under day light 2) Visual detection under uv light at the wavelengths of 254 and 365 nm

4.2 Column chromatography

4.2.1 Quick column chromatography

Adsorbent	:	Silica gel 60 particle size 0.040-0.063 nm (230-400 mesh ASTM) (Merck, Darmstadt, Germany).

Packing method : Adsorbent was dry-packing. The adsorbent and organic solvent were poured into the column. The solvent was sucked out, and the adsorbent was pressed tightly.

Sample loading : Dry-loading; dissolved the sample with a small volumn of organic solvent, then mixed the sample with silica gel and placed on surface of the adsorbent.

Detection : Fractions were examined by TLC using visual detection under day light and uv light at the wavelengths of 254 and 365 nm.

4.2.2 Flash column chromatography

Adsorbent : Silica gel 60 particle size 0.040-0.063 nm (Merck, Darmstadt, Germany)

Packing method : Adsorbent was wet-packing. The slurry of adsorbent in organic solvent was poured into the column and allowed to be settled tightly.

Sample loading : **Dry-loading**; dissolved the sample in a small volumn of organic solvent, mixed with silica gel and placed gently on surface of the adsorbent.

Wet-loading; dissolved the sample in a small volumn of eluent and then put gently on surface of adsorbent.

Detection : Fractions were examined by TLC using visual detection under day light and ultraviolet light at the wavelengths of 254 and 365 nm.

4.2.3 Gel filtration chromatography

Adsorbent	:	Sephadex LH-20 (Merck, Darmstadt, Germany)
Packing method	:	Suspended the adsorbent in the eluent. Then, the adsorbent was poured into the column and allowed to be settled tightly.
Sample loading	:	Dissolved the sample in a small volumn of eluent and then put gently on the surface of adsorbent in column.
Detection	:	Examined the fractions by TLC using visual detection under day light and ultraviolet light at the wavelengths of 254 and 365 nm.

4.3 Spectroscopy

4.3.1 Ultraviolet (UV) absorption spectra

The UV spectra were obtained on a Spectronic Genesys 6 UV-Visible Spectrophotometer, Thermo Scientific, Thermo Electron Corporation (Department of Pharmacognosy and Pharmaceutical Botany, Faculty of Pharmaceutical Sciences, Prince of Songkla University). The samples were dissolved in methanol or chloroform before measured ultraviolet absorption.

4.3.2 Infrared (IR) absorption spectra

The IR spectra were obtained from a Perkin Elmer FT-IR Spectrum One spectrometer (Department of Pharmaceutical Chemistry, Faculty of Pharmaceutical Sciences, Prince of Songkla University, using potassium bromide disc to determine the spectra.

4.3.3 Mass spectra (MS)

Electron Impact Mass Spectra (EIMS) were measured on a Thermo Finnigan MAT 95 XL mass spectrometer at Scientific Equipment Center, Prince of Songkla University.

4.3.4 Proton-1 and Carbon-13 Nuclear Magnetic Resonance (^{1}H and ^{13}C-NMR) spectra

^{1}H and ^{13}C spectra were obtained from a Fourier Transform NMR Spectrometer (^{1}H-NMR 500 MHz and ^{13}C-NMR 125 MHz), model UNITY INNOVA, Varian at Scientific Equipment Center, Prince of Songkla University.

5. Bioactivities determination

5.1 Antityrosinase activity

5.1.1 Enzymetic antityrosinase activity

Antityrosinase activity was determined by Dopachrome method, L-dopa was use as the substrate. The oxidation of L-Dopa to dopachrome which show the red color and can detect by visible light at 492 nm (Sritularak, 1998; Sritularak *et al.*, 1998).

5.1.1.1 Preparation of 20 mM buffer (pH 6.8)

Na_2HPO_4 (284 mg) and $NaH_2PO_2.2H_2O$ (312 mg) were dissolved with H_2O (100 mL). Then, mix both solution until pH 6.8 reached.

5.1.1.2 Preparation of 0.85 mM L-Dopa

Dissolved L-dopa (0.85 mg) in 5 mL of 20 mM phosphate buffer pH 6.8.

5.1.1.3 Preparation of tyrosinase enzyme (203.3 unit/mL)

Dissolved Tyrosinase enzyme in 20 mM phosphate buffer pH 6.8 to concentration 203.3 unit/mL.

5.2.1.4 Preparation of positive control and sample

Positive control and sample were dissolved and diluted with DMSO until the suitable range of concentration was 200 μg/mL, water extract of *Artocarpus lakoocha* wood and kojic acid were used for positive controls.

5.1.1.5 Determination of antityrosinase activity

The method was tested in 96 well plate. The raction mixture measured in 4 wells; (Control (A), Blank control (B), Test sample (C) and Blank sample (D)) total volumn is 200 μL/well was. In each well contain; phosphate buffer pH 6.8, 20 μL dimethylsulfoxide (for control and blank control); 20 μL sample or standard solution (for test sample and blank sample), 20 μL of 203.3 unit/mL tyrosinase solution (for control and test sample) then, incubated at 25°C for 10 min after that added 20 μL of 0.85 mM L-Dopa and detected the optical density (OD). After incubated at 25°C for 20 min, detected the optical density (OD) again.

5.1.1.6 Calculation of the percent inhibition of tyrosinase enzyme

The percent inhibition of tyrosinase reaction was calculated as follow;

$$\% \text{ Antityrosinase activity} = \left(\frac{(A-B)-(C-D)}{(A-B)} \right) \times 100$$

A, B, C, D : The difference of optical density before and after incubation for 20 min at 25°C with microplate reader.

5.1.1.7 Calculation of the half maximal inhibitory concentration (IC_{50})

Samples and positive controls were dissolved in dimethyl sulfoxide or DMSO and diluted half-fold to give final concentrations ranging from 200-3.12 µg/mL. Then determined and calculated the activity. After the % tyrosinase inhibition of the test samples and positive controls in each concentration was calculated, the curve of each concentration and its % tyrosinase inhibition was plotted. The IC_{50} of each pure compound was then obtained from the graph.

5.1.2 Antityrosinase activity and melanin content in cell line

5.1.2.1 Preparation of 10% fetal bovine serum (FBS) Dulbecco's modified Eagle's medium (DMEM)

DMEM and 3.7g of $NaHCO_3$ were dissolve with 1L of sterile water, adjusted to pH 7.3 after that added 10 mL of antibiotic, steriled by filtration and then add 10% FBS.

5.1.2.2 Preparation of Phosphate-Buffered Saline (DPBS)

8 g of NaCl, 0.2 g of KCl, 1.44 g of Na_2HPO_4 and 0.24 g of $KHPO_4$ were dissolve in 1 L water and steriled by filtration.

5.1.2.3 Cell culture

Murine melanoma B16-F1 cells (CLS-400122) were cultured in DMEM or Dulbecco's modified Eagle's medium containing 10% FBS heat-inactivated fetal bovine serum at 37°C in a humidified atmosphere with 5% CO_2. When cells reach 70-80% confluence cell viability, cellular tyrosinase activity and melanin content were measured (Hunt *et al*., 1994; Skehan *et al*., 1990; Takahashi H and Parsons, 1992; Ye *et al*., 2010).

5.1.2.4 Cell viability assay

Cell viability was determined by Sulphorhodamine B (SRB) assay. $5x10^3$ cells/well were seeded in 96-well plate, incubated for 24 h and treated with test samples, control cells were treated with 0.5% dimethyl sulfoxide or DMSO. After 48 h incubation, fixed cells with 10% TCA or trichloroacetic acid and kept at 4°C, 1 h. After strained with 0.45% SRB added 10 mM Tris base and shaken for dissolved the SRB color. Optical densities were determined at 492 nm. The percent cell viability would be calculated.

5.1.2.5 Intracellular antityrosinase activity and melanin content assays

$3x10^5$ cells/well were seeded in 12 well plates and allowed to adhere at 37 °C for 12 h. Treated cells with test samples and 0.5% dimethyl sulfoxide or DMSO for control cells. After 48 h incubation, cells were lysed with RIPA and centrifuged 14000 rpm for 20 min (4°C) to separate supernatant for measured tyrosinase activity and cell pellet for measured melanin content.

(1) Intracellular antityrosinase activity

Collected the supernatants and determined the protein content by the Bradford method, BSA was use as standard. Added supernatant of lysate cells and 2 mg/mL L-Dopa into 96-well plate. Incubated at 25°C for 1 h, optical densities were determined at 492 nm. Tyrosinase inhibition was then calculated.

(2) Melanin content

Cells pellet were dissolved with 1M NaOH, incubated at 55°C for 1 h. Calculated melanin concentrations by comparison with the standard curve of synthetic melanin at 475 nm.

5.2 Antimicrobial activity

5.2.1 Microorganisms and growth conditions

Microorganisms; *Staphylococcus aureus* (ATTC 25923), *Staphylococcus epidermidis* (TISTR 517), *Cutibacterium acnes* (DMST 14916) and methicillin-resistant *Staphylococcus aureus* (DMST20654) were cultured in different conditions as follow Table 3-6.

Table 3-6 Media and culture condition

Bacteria	Media**	Time (hr.)	Temp (°C)
- *S. aureus*	MHA or MHB	18-24	35-37
- *S. epidermidis*	MHA or MHB	18-24	35-37
- MRSA	MHA or MHB	18-24	35-37
- *C. acnes**	BHIA or BHIB	72	35-37

* = anaerobe condition

**MHA = Mueller Hinton Agar; MHB = Mueller Hinton Broth;
BHIA = Brain Heart Infusion Agar; BHIB = Brain Heart Infusion Broth

5.2.2 Screening of antimicrobial activity

The preliminary screening of antimicrobial activity was used agar disc diffusion method (Lorian, 2005).

5.2.2.1 Preparation of samples and positive controls

The plant extracts were screened for antimicrobial activity. The extracts were dissolved in DMSO and diluted to achieve a concentration 200 mg/mL and then 10 μL of samples were dropped on the sterile paper disc (diameter 6 mm) so that each disc was saturated with 2 mg of the extract. Using DMSO as a negative

control, 1 μg/disc oxacillin as a positive control of *S. aureus*, *S. epidermidis* and *C. acnes* and 30 μg/disc vancomycin as a positive control of MRSA.

5.2.2.2 Preparation of microorganisms

The bacterium was streaked on the medium agar and cultured follow the upper condition. Suspended a colony in 0.85% NaCl solution, the bacterium suspension was diluted to achieve a concentration of approximately to 10^8 colony forming unit (CFU)/mL (OD at 625 nm). The inoculum was swabbed over the surface media, then placed the paper disc of samples, positive control and negative control on the surface of media that inoculated cell and cultured follow the upper condition.

5.2.2.3 Determination of the result

After incubation, measured the inhibition zone or clear zone diameters with venires caliper.

5.2.3 Determination of minimum inhibitory concentration (MIC) and minimum bactericidal concentration (MBC)

5.2.3.1 The minimum inhibitory concentration (MIC)

The samples shown inhibition zone were selected for test the lowest of compound to inhibit the growth of microorganisms or MIC by modified broth microdilution method (CLSI, 2006; Lorian, 2005).

5.2.3.1.1 Preparation of microbial

Prepared and adjusted the bacterium suspension to achieve a concentration of approximately 10^6 CFU/mL, with 0.85% NaCl to match OD with 0.085-0.13 of spectrophotometer at 625 nm. Then diluted 1: 100 in the media to contain 10^6 CFU/mL.

5.2.3.1.2 Preparation of sample and testing

Dissolved the sample with dimethyl sulfoxide or DMSO and diluted halffold with 10% DMSO to give concentrations ranging from 2560 to 1.25 µg/mL. The positive control was prepared same as the sample.

Performed the test in 96-well plate. 20 µL of the samples (dilution series ranging from 2560 to 1.25 µg/mL) were added into well 1 to 12. Then, all well were added 80 µL of media. Next, added 100 µL of the inoculum (concentration 10^6 CFU/mL) into all well. The final concentration of bacterium suspension in each well was 5 x 10^5 CFU/mL. Then, incubated the cultures follow the condition. The positive control and negative control were prepared and incubated under the same conditions.

5.2.3.1.3 Determination of the result

MIC was recorded as the lowest concentration of the bioactive compound that was not permitted for any turbidity of the tested organism, and confirmed with Alamar blue as indicator (colorimetric method). Briefly 5 µL of 1% Alamar blue was added in every well and incubated 5-10 hr. The active sample showed blue color, which indicated no growth of organism. While, the inactive sample showed the pink color, which indicated the growth of organism.

5.2.3.2 Minimum bactericidal concentration (MBC)

The incubation mixture which show positive result of MIC was tested the lowest concentration of compound to kill microorganisms or MBC by streaked on media agar, then incubated follow condition. The lowest concentration that did not show any growth was taken as the MBC

5.3 Western blot

Western blot was used for determination of the effect of isolated compounds on the expression of melanogenic proteins in B16-F10 cells. Cells were treated with 25 µg/mL and 50 µg/mL of isolated compounds. Whole cell lysates were subjected to western blot analysis using specific antibodies against microphthalmia-associated transcription factor (MITF), tyrosinase, tyrosinase-related protein 1 (TRP1) and tyrosinase-related protein 2 (TRP2). The method applied from Western Blot analysis for UGT1A family, Department of Clinical Pharmacology, Flinders Medical Center.

5.3.1 Buffer, chemical substance and gel preparations

- **1.5 M Tris-HCl, pH 8.8:**

27.23 g Tris base, dissolved in 80 mL distilled water, adjusted to pH 8.8 with 1N HCl. Then, made to 150 mL with distilled water and stored at 4°C.

- **0.5 M Tris-HCl, pH 6.8:**

6 g Tris base dissolved in 60 mL distilled water, adjusted to pH 6.8 with 1N HCl. Then, made to 100 mL with distilled water and stored at 4°C.

- **10%(w/v) SDS preparation:**

1 g SDS dissolved in 10 mL distilled water.

- **10%(w/v) APS preparation**:
0.1 g APS dissolved in 1 mL distilled water.

- **Separating gel: (for 2 gels) use;**

1.	Distilled water	4.85 mL
2.	1.5 M Tris-HCl, pH 8.8	2.5 mL
3.	10% (w/v) SDS	100 µL
4.	30% Acrylamide/Bis Solution	2.5 mL

5. 10% (w/v) APS 80 µL
6. TEMED 12.5 µL

- **Stacking gel: (for 2 gels)**

1. Distilled water 3 mL
2. 0.5 M Tris-HCl, pH 6.8 1.25 mL
3. 10% (w/v) SDS 50 µL
4. 30% Acrylamide/Bis Solution 620 µL
5. 10% (w/v) APS 40 µL
6. TEMED 10 µL

- **Running buffer: 5X electrode (Running) buffer, pH 8.3 use;**

1. Tris base 9 g
2. Glycine 43.2 g
3. SDS 3 g

Dissolved in 600 mL with distilled water and stored at 4°C. Warmed to 37°C before use. Diluted 60 mL 5X stock with 240 mL distilled water for one electrophoretic run.

- **Sample buffer: 0.5 M Tris-Base pH 6.8 use;**

1. Distilled water 4.0 mL
2. 0.5 M Tris-base, pH 6.8 1.0 mL
3. Glycerol 2.0 mL
4. 10% (w/v) SDS 1.6 mL
5. 2-ß-mercaptoethanol 0.4 mL
6. 0.1 % (w/v) bromophenol blue 0.2 mL

5.3.2 Protocols of western blot

5.3.2.1 Gel setting

Prepare separating gel and placed into gel setting holder then placed isopropanol on the top layer to get rid of some air bubble. After gel setting (30 min), poured out isopropanol and washed twice with water. Prepared and placed stacking gel into gel setting then placed a comb (10 well) onto the stacking gel and wait for 1 hr for gel setting.

5.3.2.2 Samples preparation and loading

Combined protein 25 μg of protein lysate and water to get the final volume 20 μL and then added the diluted sample loading buffer (diluted 5x) 5 μL in each sample. Denature protein by heating at 95°C in a water bath for 5 min then centrifuged for 2 second.

When stacking gel was set, took the comb off and set the gel set into running cassette then placed in the running bath and poured the running buffer into the bath and load samples 25 μL/well.

Samples were then electrophoresed on running gel at 90 volts when running through stacking gel (15 min) and then 150 volts when running through separating gel, running time about 90 min in running buffer.

5.3.2.3 Transferring protein band from gel to nitrocellulose membrane

- **Materials :**

1. Tris base
2. Glycine
3. Methanol
4. Nitrocellulose membrane

- **Buffer preparations, Transferring buffer, pH 8.3:**

Mixed 3.03 g Tris, 14.4 g glycine 1 L of distilled deionized water and 200 mL of methanol. After that stored at 4°C.

- **Methods:**
  1. Cut 2 pieces of filter papers 6X8 cm for 1 gel.
  2. Cut nitrocellulose membrane 6X8 cm for 1 gel.
  3. Wet filter papers, membrane and sponge brite in transfer buffer.
  4. After finished running samples, washed the gel with transfer buffer for 5 min with shaking.
  5. Packing gel with nitrocellulose membrane follow;
     - Using transfer cassette, placed black site underneath clear site.
     - First layer, placed 2 pieces of sponge brite.
     - Second layer, placed 1 piece of filter paper on top the sponge brite.
     - Third layer, placed gel sheet on top the filter paper.
     - Forth layer, placed nitrocellulose membrane on top the gel.
     - Fifth layer, placed 1 piece of filter paper on top the nitrocellulose membrane.
     - Sixth layer, placed 2 pieces of sponge brite on top the filter paper.
  6. Fitted the cassette with the transfer bath by black site close to black and put stirrer bar into the bath.
  7. Poured transfer buffer and placed ice bar close to transfer cassette.
  8. Placed transfer bath in the tray and put some ice around the bath.
  9. Placed transfer bath on magnetic stirrer in cold room and closed the lid which was connected to the power supply via setup 30 volts (90 mA).
  10. Left transferring overnight.

5.3.2.4 Membrane blocking

- **Materials and methods:**

1. **Tris buffered saline (TBS), pH 7.5**

   50 mM Tris base, 150 mM NaCl

   Dissolved 6.05 g tris base and 8.76 g NaCl in 800 mL distilled water, adjusted to pH 7.5 with HCl and adjusted volume to 1 L with distilled water.

2. **Blocking solution**:

   15% (v/v) non-fat sterile milk in TBS, pH 7.5.

3. **Blocking**

   Block non-specific binding of antibody by incubation the membrane in 15 mL 15% (v/v) non-fat sterile milk in TBS, pH 7.5 for 3.5 hr at 4°C and shaking 30 min at 25°C. After that wash the membrane with TBS 2 times (5 min/ time).

5.3.2.5 Primary & Secondary antibody

- **Materials and methods:**

1. Primary antibodies
2. TBS-Tween-20 (TBST)
   : Diluted 1 mL of Tween 20 in 1 L of TBS to give final concentration 0.1% (v/v).
3. 10% (v/v) non-fat sterile milk in TBS, pH 7.5
   : 100 μL non-fat sterile milk in 9.9 mL TBS (2 tubes).
4. Prepared the dilution of primary antibodies (1:500) :
   20 μL : 10 mL primary antibody : 10% non-fat sterile milk.
5. Incubated the membrane with primary antibodies 2 hr at 25 °C.
6. The membrane was washed with TBST 3 times (4 min/ time).
7. Prepared the dilution of secondary antibodies (1:500) :

20 µL : 10 mL secondary antibody : 10% non-fat sterile milk.

8. Incubated the membrane with secondary antibodies 1 hr at 25 °C.
9. The membrane was washed with TBST 3 times (4 min/ time).
10. The membrane was washed with TBST 3 times (4 min/ time).

5.3.2.6 Detection

- **Clarity™ Western ECL Substrate, Bio-Rad**

1. Mixed substrate kit compound in 9:1 ratio.
2. Incubated the membrane in substrate solution for 5 min.
3. Imaged the membrane with a digital imager (UPV, VisionWork™ LS, Image Acquisition & Analysis Software).

5.4 Pigmentation inhibitory effects on zebrafish

Zebrafish (*Danio rerio*) was used to evaluate pigmentation inhibitory effect. The method was applied and perform by Department of Oriental Medicinal Biotechnology, College of Life Sciences, Kyung Hee University, Republic of Korea.

The method was modified from Le *et al*., 2016. Briefly, placed 20 embryos/well of embryos at 9 hr postfertilization (hpf) individually into 96-well plate filled filled with 0.03 % sea salt solution 100 µl/well and each sample solution. 25 µM 1-phenyl-2-thiourea or PTU was used as positive group and 0.03% sea salt solution was used as normal group. Phenotype-based evaluations of body pigmentation were conducted after embryos hatched (at 72 hpf), put and embedded the larvae on glass slides by using 2% low melting agarose. Photo-captured the zebrafish fry dorsal view and evaluated the black spot size in the head-dorsal region at 81 hpf.

6. Extraction

A. chama and *S. taxoides* were selected for phytochemical investigation. 6.8 kg of *A. chama* stem powder and 18 kg of *S. taxoides* wood powder were macerated repeatedly with petroleum ether for 3 days (3 times). Evaporated the filtrates by rotary evaporator under reduced pressure at below 40 °C temperature to yield a petroleum ether extract. Then the marc was macerated three times with ethyl acetate, methanol for 3 days (3 times, each) and boiled with H_2O, respectively. Removal of organic solvents gave an ethyl acetate extract, methanol extract and H_2O extract. The separation of *A. chama* and *S. taxoides* shown on Scheme 3-1.

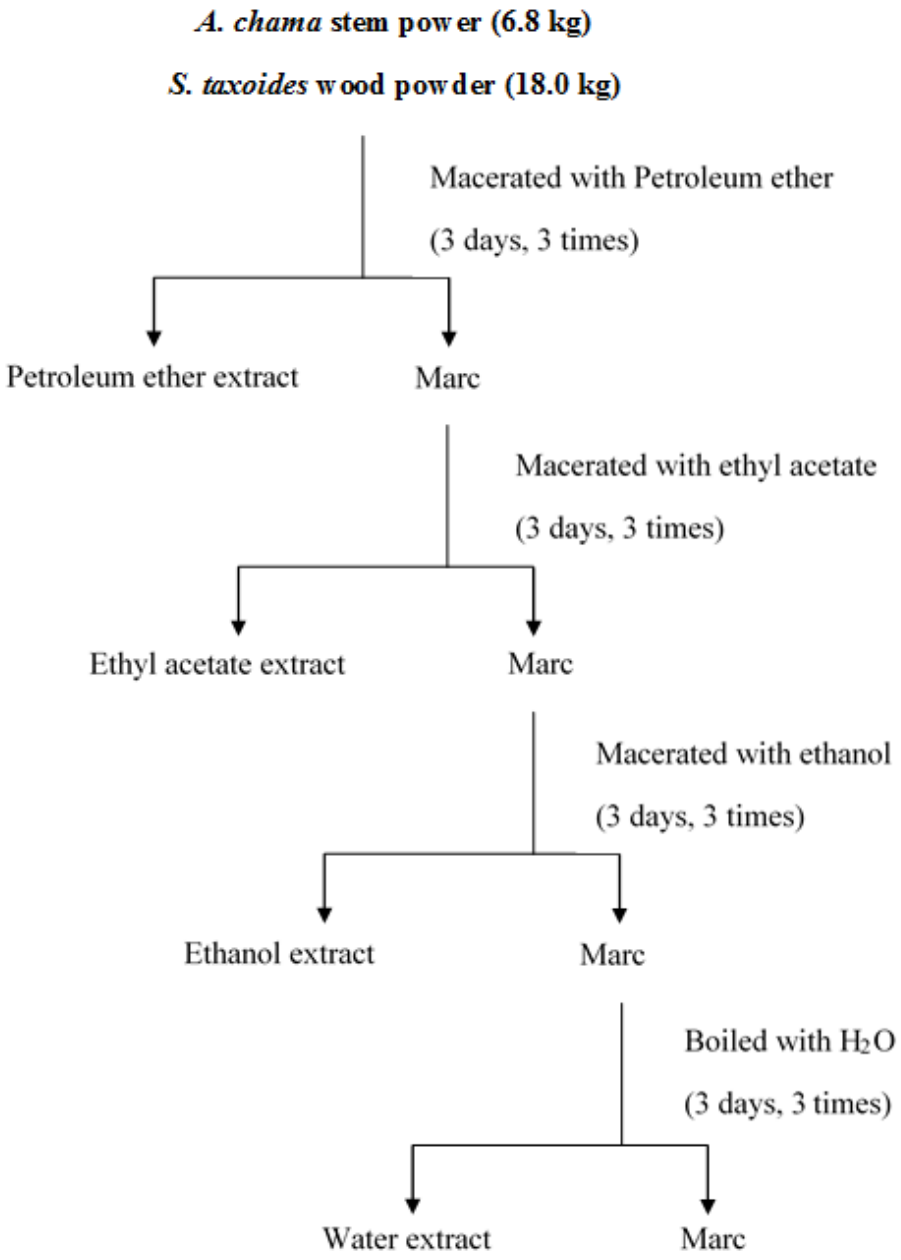

Scheme 3-1 Solvent extraction of *A. chama* stem and *S. taxoides* wood

7. Isolation and purification

The ethyl acetate extract of *A. chama*, ethyl acetate and methanol extract of *S. taxoides* which showed the potent effects on antityrosinase and antimicrobial activities were selected for further phytochemical investigation by using chromatographic techniques.

7.1 Isolation and purification of *A. chama* stem

Eight compounds were successfully isolated from *A. chama* stem (Scheme 3-2). The beginning by the ethyl acetate extract (40 g) was fractionated by quick column chromatography, the eluateds were examined by TLC using gradient of hexane, ethyl acetate and methanol as solvent system. The fraction giving similar chromatographic pattern were combined. The interesting fractions were D, F, G and H were selected to isolate and purify. The step of isolation was exhibited in the Scheem 3-2. Afterward, the isolated compounds were interpreted their chemical structures by using nuclear magnetic resonance (NMR) and other spectroscopic techniques.

7.2 Isolation and purification *S. taxoides* wood

Five compounds and one mixture compound were isolated from *S. taxoides* wood (Schem 3-3). Initially, 22 g of ethyl acetate extract was isolated by quick column chromatography, the gradient of dichloromethane, ethyl acetate and methanol were used as an eluent. The interesting fractions were E, H, J and K. Moreover, fraction C, D, E and F were the interesting fractions which fractionated by quick column chromatography from 50 g of methanol extract, using the gradient of hexane, ethyl acetate and formic acid as an eluent. All interesting fractions were selected to further isolate and purify. However, many isolated compounds from interesting fractions did not stable, they were easy to degrade. The step of isolation were summarized in the Scheem 3-3.

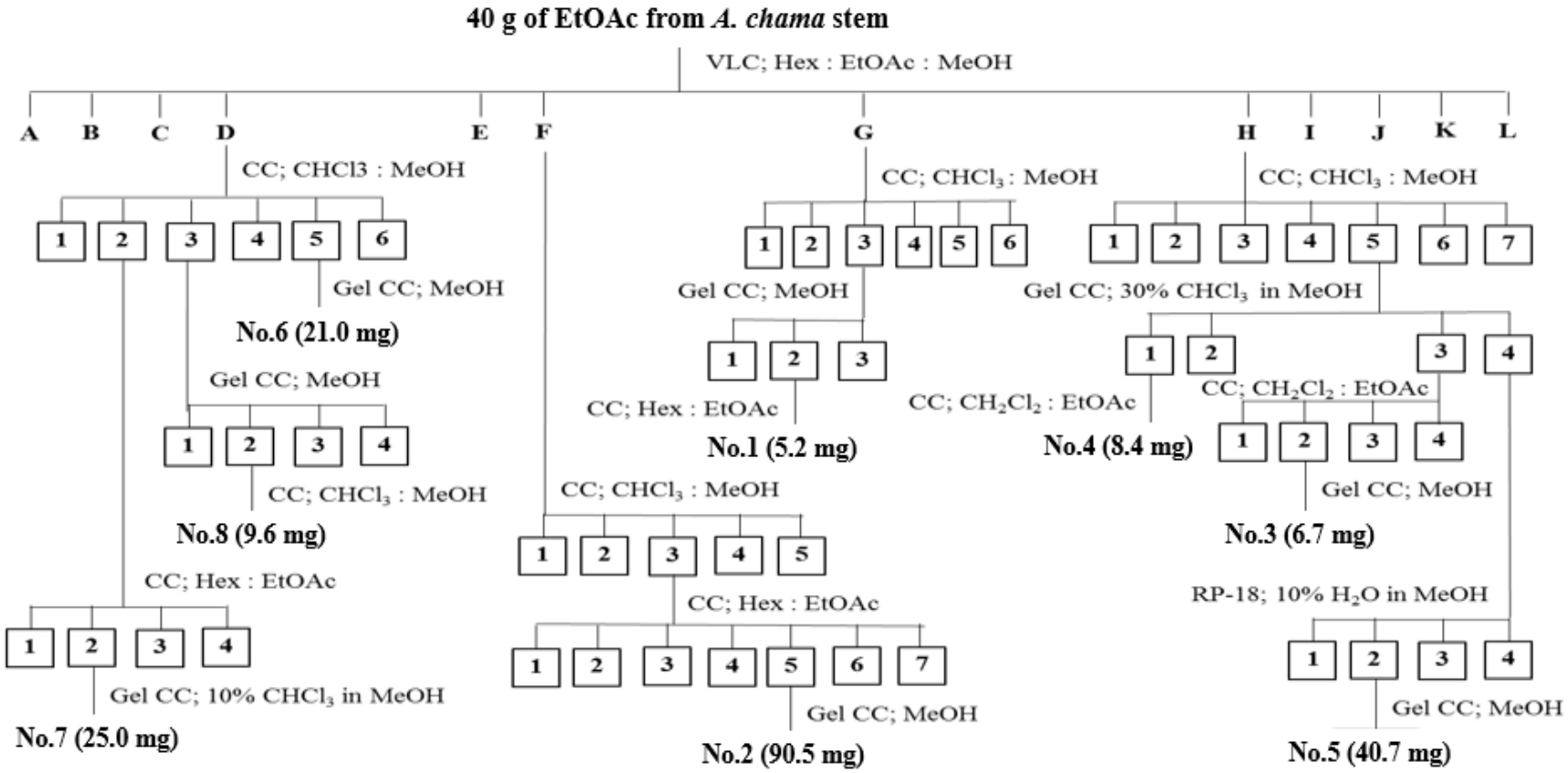

Scheme 3-2 Phytochemical investigation from ethyl acetate extract of *A. chama* stem

VLC= vacuum liquid chromatography; CC= classical column chromatography; Gel CC= sephadex LH-20; FA= formic acid; Hex= Hexane; CH_2Cl_2= dichloromethane; $CHCl_3$= chloroform; EtOAc= ethyl acetate; MeOH= Methanol; H_2O= water

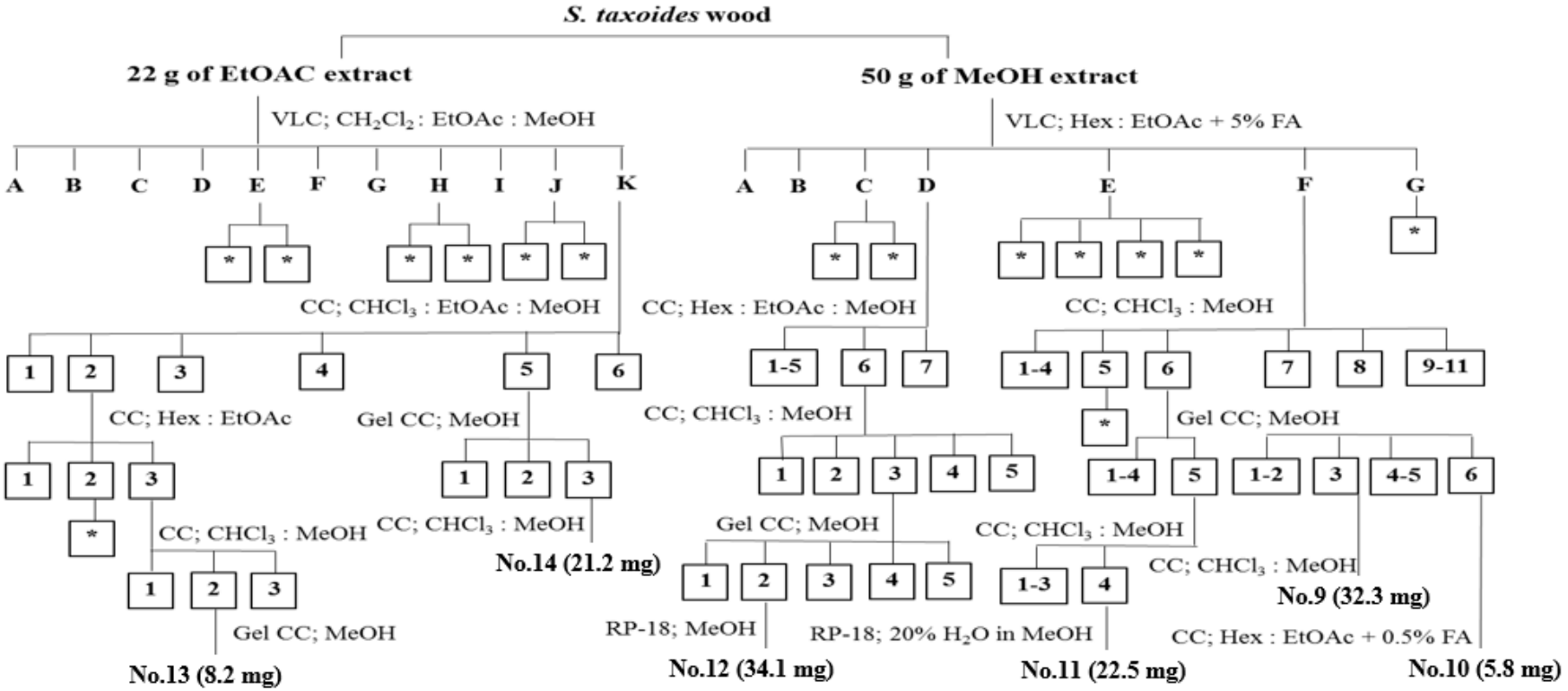

Scheme 3-3 Phytochemical investigation from ethyl acetate and ethanol extracts of *S. taxoides* wood

VLC= vacuum liquid chromatography; CC= classical column chromatography; Gel CC= sephadex LH-20; FA= formic acid; Hex= Hexane; CH_2Cl_2= dichloromethane; $CHCl_3$= chloroform; EtOAc= ethyl acetate; MeOH= Methanol; H_2O= water; *=unstable compoun

CHAPTER 4
RESULTS AND DISCUSSION

1. Screening of enzymetic antityrosinase activity from Moraceae plant extracts

Among 48 samples from 25 Moraceae plant extracts from Rajjaprabha Dam, Surat Thani Province, Southern Literature Botanical Garden, Songkhla Province, Botanical Garden, Faculty of Pharmaceutical Sciences, Prince of Songkla University, Songkhla Province and Walailak University, Nakhon Si Thammarat Province were screened for antityrosinase activity. 12 samples showed inhibitory activity of tyrosinase enzyme at 20 µg/mL >30%, including *Artocarpus altilis* branch, *A. integer* branch, *A. chama* wood, *A. chama* stem, *Ficus benghalensis* branch, *F. benghalensis* wood, *F. foveolata* wood, *F. superba* leaf, *Morus alba* branch, *M. alba* leaf, *Streblus ilicifolius* wood, *S. taxoides* wood (as shown in the Table 4-1). The wood extracts of *S. taxoides* and *S. ilicifolius* showed the highest antityrosinase activity with 58.59% ± 1.90% and 69.05% ± 5.00%, respectively. However, *S. ilicifolius* has been reported in chemical constituents and biological activities; antityrosinase and antimicrobial activities (Dej-adisai *et al*., 2016). Only, the extracts of *S. taxoides* and *A. chama* which showed the potential activity against tyrosinase enzyme were selected for further study.

Table 4-1 Screening of enzymetic antityrosinase activity of 48 Moraceae plant samples at 20 µg/mL

No.	Plant	Part	% Antityrosinase activity
1	*A. altilis*	Branch	48.24±1.10
2	*A. altilis*	Leaf	16.32±1.30
3	*A. integer*	Branch	48.76±2.09
4	*A. integer*	Leaf	23.76±2.48
5	*A. rigidus*	Branch	28.09±5.18

Table 4-1 Screening of enzymetic antityrosinase activity of 48 Moraceae plant samples at 20 µg/mL (continued)

No.	Plant	Part	% Antityrosinase activity
6	*A. rigidus*	Leaf	28.29±6.98
7	*A. chama*	Wood	32.48±5.62
8	*A. chama*	Bark	11.89±1.21
9	*A. chama*	Stem	35.87±3.84
10	*A. chama*	Leaf	14.30±7.00
11	*F. benghalensis*	Branch	32.10±1.66
12	*F. benghalensis*	Leaf	-3.80±2.93
13	*F. benghalensis*	Wood	35.44±7.10
14	*F. benghalensis*	Bark	-13.97±6.76
15	*F. callosa*	Branch	7.81±2.65
16	*F. callosa*	Leaf	1.22±5.86
17	*F. celebensis*	Branch	14.70±1.66
18	*F. celebensis*	Leaf	-0.54±7.14
19	*F. chartacea* var. *torulosa*	Branch	-8.25±2.80
20	*F. chartacea* var. *torulosa*	Leaf	4.73±3.43
21	*F. foveolata*	Wood	38.49±6.45
22	*F. fistolusa*	Branch	-3.18±1.55
23	*F. fistolusa*	Leaf	1.37±2.13
24	*F. hispida*	Branch	-28.47±1.80
25	*F. hispida*	Leaf	-13.45±2.83
26	*F. infectoria*	Wood	12.05±7.65
27	*F. microcarba*	Branch	-0.89±6.21
28	*F. microcarba*	Leaf	0.32±6.42
29	*Ficus* spp.	Wood	-1.46±5.67
30	*Ficus* spp.	Wood	-4.78±1.82
31	*Ficus* spp.	Wood	-0.20±4.30

Table 4-1 Screening of enzymetic antityrosinase activity of 48 Moraceae plant samples at 20 µg/mL (continued)

No.	Plant	Part	% Antityrosinase activity
32	*Ficus* spp.	Wood	2.90±3.95
33	*Ficus* spp.	Branch	-2.62±1.41
34	*Ficus* spp.	Leaf	-2.56±1.74
35	*Ficus* spp.	Branch	15.40±8.95
36	*Ficus* spp.	Leaf	13.64±6.63
37	*F. superba*	Branch	17.40±1.90
38	*F. superba*	Leaf	34.25±2.20
39	*F. rocemosa*	Branch	4.65±4.91
40	*F. rocemosa*	Leaf	18.49±2.45
41	*F. vasculosa*	Wood	-12.90±0.86
42	*F. vasculosa*	Bark	-0.35±3.69
43	*F. vasculosa*	Leaf	0.87±7.18
44	*M. alba*	Branch	47.39±4.82
45	*M. alba*	Leaf	49.09±4.71
46	*S. ilicifolius*	Leaf	18.15±2.28
47	*S. ilicifolius*	Wood	69.05±5.00
48	*S. taxoides*	Wood	58.59±1.90
	A. lakoocha [P]	Wood	90.42±0.50
	Kojic acid [P]	-	81.42±0.34

[P] = Positive control

2. Antibacterial activity from Moraceae plant extracts

From the preliminary screening of antibacterial activity, the ethanol extracts of 48 Moraceae plant samples by using agar disc diffusion method shown an inhibition zone againt *S. aureus*, methicillin-resistant *S. aureus* (MRSA), *S. epidermidis* and *P. acnes* (Table 4-2).

Table 4-2 Screening of antibacterial activity of 48 Moraceae plant samples at 20 µg/disc

No.	Plant	Diameter[a] of inhibition zone (mm.)				
		Part	***S. aureus***	***S. epidermidis***	***P. acnes***	**MRSA**
1	*A. altilis*	Branch	-	-	-	-
2	*A. altilis*	Leaf	8.48±0.16	9.63±0.25	15.15±0.71	7.78±0.46
3	*A. integer*	Branch	-	-	-	-
4	*A. integer*	Leaf	11.20±1.35	-	-	7.78±0.16
5	*A. rigidus*	Branch	10.60±0.62	9.73±0.52	8.80±0.22	6.77±0.25
6	*A. rigidus*	Leaf	-	-	-	-
7	*A. chama*	Wood	-	-	-	-
8	*A. chama*	Bark wood	10.83±0.42	9.75±0.52	9.43±0.15	9.93±0.32
9	*A. chama*	Stem	7.23±0.12	-	7.03±0.10	6.98±0.10

Table 4-2 Screening of antibacterial activity of 48 Moraceae plant samples at 20 µg/disc (continued)

No.	Plant	Diameter[a] of inhibition zone (mm.)				
		Part	***S. aureus***	***S. epidermidis***	***P. acnes***	**MRSA**
10	*A. chama*	Leaf	-	-	9.15±0.43	7.92±0.16
11	*F. benghalensis*	Branch	10.10±0.36	-	-	9.15±0.05
12	*F. benghalensis*	Leaf	-	-	-	-
13	*F. benghalensis*	Wood	-	-	-	-
14	*F. benghalensis*	Bark wood	11.03±0.49	-	-	9.40±0.40
15	*F. callosa*	Branch	10.53±0.60	-	-	8.47±0.31
16	*F. callosa*	Leaf	-	-	-	-
17	*F. celebensis*	Branch	8.57±0.40	-	-	9.57±0.45
18	*F. celebensis*	Leaf	-	-	-	-
19	*F. chartacea* var. *torulosa*	Branch	9.63±0.25	-	-	6.68±0.10

Table 4-2 Screening of antibacterial activity of 48 Moraceae plant samples at 20 µg/disc (continued)

No.	Plant	Diameter[a] of inhibition zone (mm.)				
		Part	***S. aureus***	***S. epidermidis***	***P. acnes***	**MRSA**
20	*F. chartacea* var. *torulosa*	Leaf	-	-	-	-
21	*F. foveolata*	Wood	-	10.78±0.96	15.57±0.81	7.42±0.26
22	*F. fistolusa*	Branch	-	-	-	-
23	*F. fistolusa*	Leaf	-	-	-	-
24	*F. hispida*	Branch	-	-	-	9.50±0.56
25	*F. hispida*	Leaf	-	-	-	
26	*F. infectoria*	Wood	-	-	-	-
27	*F. microcarba*	Branch	-	-	-	8.77±0.85
28	*F. microcarba*	Leaf	-	-	-	-
29	*Ficus* spp.	Wood	-	-	-	-

Table 4-2 Screening of antibacterial activity of 48 Moraceae plant samples at 20 µg/disc (continued)

No.	Plant	Diameter[a] of inhibition zone (mm.)				
		Part	***S. aureus***	***S. epidermidis***	***P. acnes***	**MRSA**
30	*Ficus* spp.	Wood	8.03±0.38	6.83±0.60	-	-
31	*Ficus* spp.	Wood	-	-	-	-
32	*Ficus* spp.	Wood	8.67±0.15	6.83±0.31	-	7.02±0.26
33	*Ficus* spp.	Branch	-	-	-	7.63±0.84
34	*Ficus* spp.	Leaf	-	-	-	-
35	*Ficus* spp.	Branch	8.07±0.40	-	-	-
36	*Ficus* spp.	Leaf	-	-	-	-
37	*F. superba*	Branch	-	-	-	-
38	*F. superba*	Leaf	-	-	-	-
39	*F. rocemosa*	Branch	10.87±0.57	7.27±0.40	-	11.58±0.19

Table 4-2 Screening of antibacterial activity of 48 Moraceae plant samples at 20 µg/disc (continued)

No.	Plant	Diameter[a] of inhibition zone (mm.)				
		Part	***S. aureus***	***S. epidermidis***	***P. acnes***	**MRSA**
40	*F. rocemosa*	Leaf	-	-	-	-
41	*F. vasculosa*	Wood	-	-	-	-
42	*F. vasculosa*	Bark wood	9.03±0.35	8.35±0.23	-	7.28±0.30
43	*F. vasculosa*	Leaf	-	-	-	-
44	*M. alba*	Branch	-	-	-	-
45	*M. alba*	Leaf	-	-	-	-
46	*S. ilicifolius*	Leaf	-	-		-
47	*S. ilicifolius*	Wood	8.47±0.31	9.25±0.56	-	-
48	*S. taxoides*	Wood	6.85±0.67	6.70±0.53	7.50±0.45	nt

Table 4-2 Screening of antibacterial activity of 48 Moraceae plant samples at 20 µg/disc (continued)

No.	Plant	Diameter[a] of inhibition zone (mm.)				
		Part	***S. aureus***	***S. epidermidis***	***P. acnes***	**MRSA**
	Oxacillin[P]		20.93±0.25	21.67±0.61	22.68±0.41	nt
	Vancomycin[P]		Nt	nt	nt	14.57±0.06

nt = not test

(-) = No inhibition zone,

[a] = Includes diameter of disc (6 mm)

[P] = Positive control

3. Extraction of *A. chama* stem and *S. taxoides* wood

The dried wood of *A. chama* (6.8 kg) and stem *S. taxoides* (18 kg) were extracted to give petroleum ether, ethyl acetate, methanol and water extracts. The dry weight, % yield (base on dried wood), are shown in Table 4-3. The highest weight of the extracts in both plants were methanol extract.

Table 4-3 Dry weight and % yield of *A. chama* and *S. taxoides* crude extracts

Plant	Crude extract	Dry weight (g)	% yield
A. chama	Petroleum ether	46.02	0.68
	Ethyl acetate	96.19	1.41
	Methanol	234.46	3.45
	H_2O	126.5	1.86
S. taxoides	Petroleum ether	47.97	0.27
	Ethyl acetate	34.95	0.19
	Methanol	351.49	1.95
	H_2O	285.06	1.58

4. Bioactivities determination of crude extracts

The petroleum ether, ethyl acetate, methanol and water extracts of *A. chama* and *S. taxoides* were studied for biological activities including; enzymetic antityrosinase activity, cell viability, intracellular antityrosinase activity and melanin content, pigmentation inhibitory effects on zebrafish and determination of antimicrobial activity.

4.1 Enzymetic antityrosinase activity

The antityrosinase activity of *A. chama* and *S. taxoides* crude extracts showed that the ethyl acetate and methanol extract of *S. taxoides* wood and *A. chama* stem were the most interesting fraction because they showed the potential effects of antityrosinase activity as shown in Table 4-4.

Table 4-4 Enzymetic antityrosinase activity of petroleum ether, ethyl acetate, methanol and water extracts of *A. chama* stem and *S. taxoides* wood at 20 µg/mL

Plant	Crude extract	% antityrosinase activity
A. chama	Petroleum ether	9.35 ± 5.29
	Ethyl acetate	**77.53 ± 2.17**
	Methanol	**70.29 ± 3.24**
	Water extract	17.35 ± 1.90
S. taxoides	Petroleum ether	7.36 ± 0.66
	Ethyl acetate	**57.15 ± 3.33**
	Methanol	**75.53 ± 0.48**
	Water extract	13.74 ± 5.32
positive control	water extract of *A. lakoocha*	91.96 ± 0.97
	Kojic acid	84.38±1.54

4.2 Cell viability

From the results of enzymetic investigation, several sample extracts from selected plants showed the potent inhibitory effect on tyrosinase activity. Thus, the investigations were extended to cellular experiments. Then, the cell viability was measured first. The results indicate that all sample extracts were not considerable cytotoxic in B16-F1 melanoma cells. Cell viability was still more than 80% at the concentration 100 μg/mL except ethyl acetate extract of *A. chama* and *S. taxoides* cell viability was more than 80% at the concentration 5 and 50 μg/mL, respectively.

4.3 Intracellular antityrosinase activity and melanin content

The effect of the extracts on intracellular antityrosinase activity and melanin content on B16F1 melanoma cells were determined. The sample extracts were prepared at 100 μg/mL except ethyl acetate extract of *A. chama* was prepared at 5 μg/mL and ethyl acetate extract of *S. taxoides* was prepared at 50 μg/mL followed the results of cell viability assay. After 48 h incubation with all sample extracts. The supernatant were measured antityrosinase activity, the results showed that the extracts from *A. chama* and *S. taxoides* exhibited antityrosinase activity especially ethyl acetate extract from both plants which were prepared lower concentration (Figure 4-1A). The ethyl acetate extract of *A. chama* showed 64.41±1.27% at 5 μg/mL while the ethyl acetate extract of *S. taxoides* showed 54.37±1.55% at 50 μg/mL. Moreover the melanin content showed inverse result with antityrosinase activity; the increasing of antityrosinase activity can decrease the amount of melanin content (Figure 4-1B).

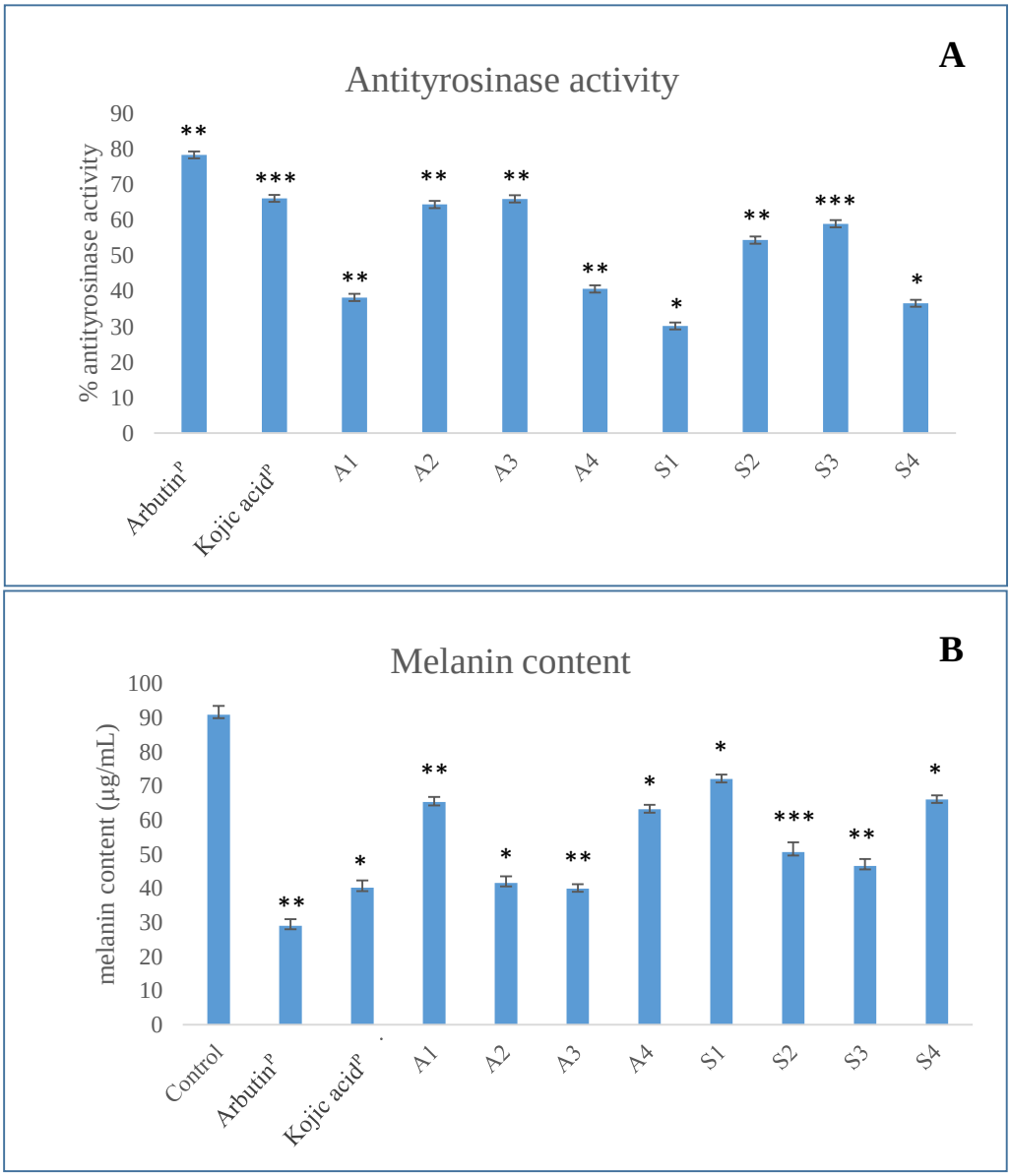

Figure 4-1 Intracellular antityrosinase activity and melanin content

(Figure 4-1A = antityrosinase activity, Figure 4-1B = melanin content**)**

^{P} = positive control

A1, A2, A3 and A4 = petroleum ether, ethyl acetate, methanol, water extracts of *A. chama* stem, respectively.

S1, S2, S3 and S4 = petroleum ether, ethyl acetate, methanol and water extracts of *S. taxoides* wood, respectively.

A1, A3, A4, S1, S3, S4 = 100 ug/mL, A2 = 5 ug/mL, S2 = 50 ug/mL

Data are expressed as mean ± SD from three independent experiments. $^{*}p$ <0.05, $^{**}p$ <0.01 and $^{***}p$ <0.001 indicate a significant difference from control group.

4.4 Pigmentation inhibitory effect on Zebrafish

Screening pigmentation inhibitory effect on zebrafish and measured the size of black spot on the zebrafish found that at the concentration 200 µg/mL (Figure 4-2A) sample extracts could inhibit pigmentation while petroleum ether extracts of *A. chama* stem could stimulate pigmentation. However, ethyl acetate extract of *A. chama* stem, ethyl acetate and methanol extracts of *S. taxoides* wood were toxic to zebrafish. Then the concentrations of ethyl acetate and methanol extracts from *S. taxoides* wood were decreased to 50 µg/mL. The results showed that they could suppress the pigmentation on zebrafish (Figure4-2B).

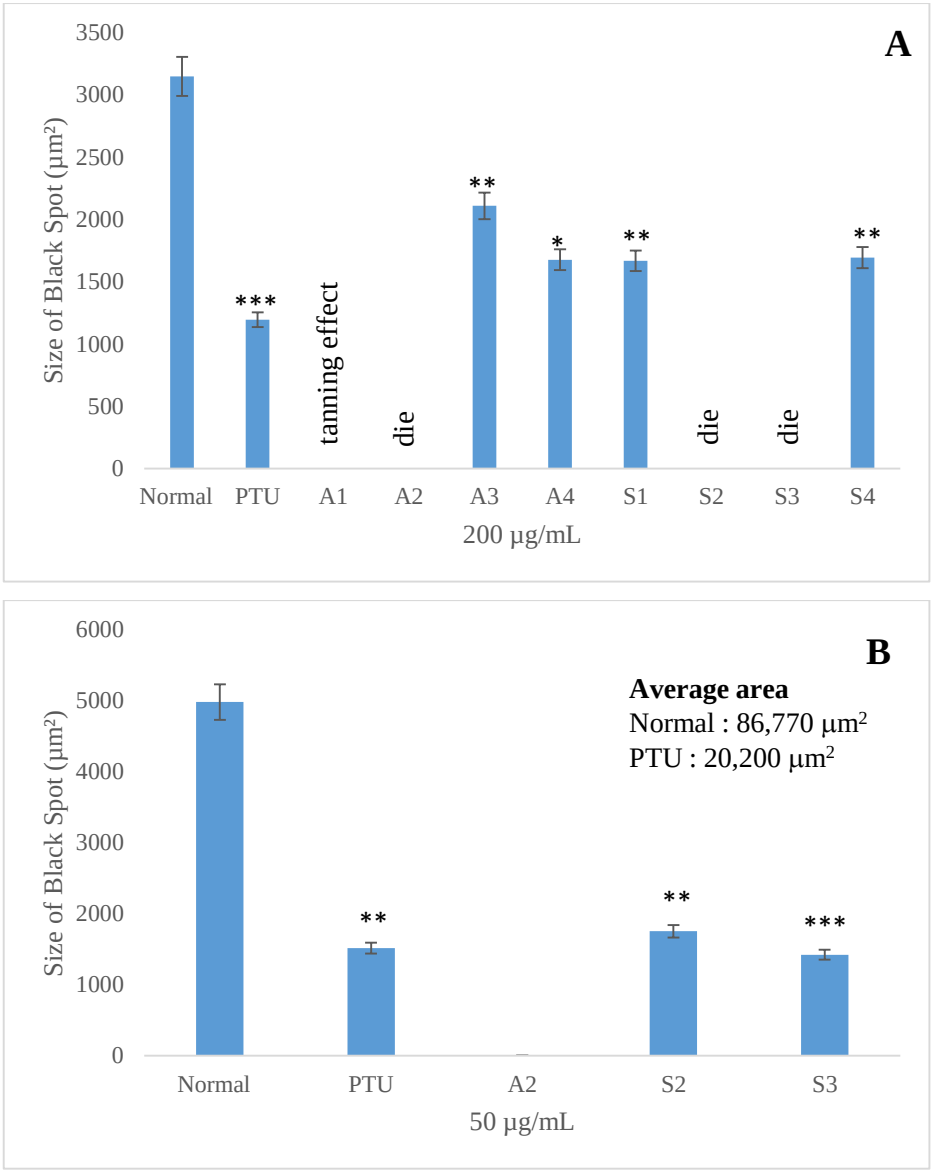

Figure 4-2 Pigmentation inhibitory effect on zebrafish

(Fig 4-2A at concentration 200 µg/mL, Fig 4-2B at concentration 50 µg/mL)

PTU = phenylthiourea; the positive control
A1, A2, A3 and A4 = petroleum ether, ethyl acetate, methanol, water extracts of *A. chama* stem, respectively.
S1, S2, S3 and S4 = petroleum ether, ethyl acetate, methanol and water extracts of *S. taxoides* wood, respectively.

Data are expressed as mean ± SD from three independent experiments. $^{*}p$ <0.05, $^{**}p$ <0.01 and $^{***}p$ <0.001 indicate a significant difference from control group.

4.5 Determination of antimicrobial activity

From the screening test of antimicrobial activity, the ethanol extracts of 48 Moraceae plant samples showed a clear zone against *S. aureus, S. epidermidis, P. acnes* and MRSA as shown in the Table 4-2. Then, for the petroleum ether, ethyl acetate, methanol and water extracts of *S. taxoides* wood and *A. chama* stem investigated the MIC and MBC (half-fold dilution; 15.625 – 2000 μg/mL). The results showed that only the ethyl acetate extract of *A. chama* stem and *S. taxoides* wood against these microbes. MIC and MBC values against *S. aureus, S. epidermidis, P. acnes* and MRSA shown in Table 4-5.

Table 4-5 MIC and MBC of *A. chama* stem and *S. taxoides* wood (15.625 – 2000 μg/mL)

Plant	**Sample extracts**	***S. aureus***		***S. epidermidis***		***P. acnes***		**MRSA**	
		MIC	**MBC**	**MIC**	**MBC**	**MIC**	**MBC**	**MIC**	**MBC**
A. chama	Pet.ether	>2000	>2000	>2000	>2000	500	2000	>2000	>2000
	EtOAc	15.625	125	15.625	62.5	31.25	31.25	15.625	31.25
	MeOH	2000	>2000	>2000	>2000	>2000	>2000	1000	>2000
	Water	>2000	>2000	>2000	>2000	>2000	>2000	>2000	>2000
S. taxoides	Pet.ether	>2000	>2000	>2000	>2000	>2000	>2000	>2000	>2000
	EtOAc	125	1000	1000	>2000	15.625	15.625	31.25	500
	MeOH	>2000	>2000	500	>2000	>2000	>2000	500	>2000
	Water	2000	>2000	>2000	>2000	>2000	>2000	>2000	>2000
Positive control		0.25	0.5	0.5	0.5	0.1	0.2	0.5	1.0

Oxacillin = Positive control for *S. aureus, S. epidermidis* and *P. acnes*

Vancomycin = Positive control for MRSA

5. Structure determination of isolated compounds

Eight pure compounds were isolated from *A. chama* and were identified as homoeriodictyol (No.1), 3´-farnesylapigenin (No.2), isocycloartobiloxanthone (No.3), 3-(hydroxyprenyl) isoetin (No.4), 3-prenyl-5,7,2´,5´-tetrahydroxy-4´-methoxyflavone (No.5), artocarpanone (No.6), naringenin (No.7) and artocarpin (No.8). One mixture compound and five pure compounds were isolated from *S. taxoides* as the identified as the mixture of *β*-sitosterol and stigmasterol (No.9), ω-hydroxymoracin C (No.10), moracin M (No.11), moracin C (No.12), 3, 4, 3´, 5´-tetrahydroxybibenzyl (No.13) and piceatanol (No.14). The structures of these isolated compounds were identified by physical properties and spectroscopic data; UV, IR, NMR and MS data and confirmed by comparison with previous reports.

5.1 Isolated compounds from *A. chama*

5.1.1 Structure determination of compound No.1

The compound No.1 was obtained as a light yellow needles, soluble in chloroform.

The UV spectrum in chloroform (Figure A-1) demonstrated absorption maximum at λ_{max} 287 nm. The IR spectrum (Figure A-2) exhibited maximum absorption bands at 3399, 2948, 1644, 1450, 1416 and 1200 cm^{-1}.

Compound No.1 ($C_{16}H_{14}O_6$) could be assigned as the known compound homoeriodictyol by analysis of its ^1H and ^{13}C-NMR spectra properties. Its ^1H-NMR data have been reported.

From the ^1H-NMR (in $CDCl_3$; 500 MHz) spectrum (Figure A-4), revealed five signals proton of aromatic ring at δ 6.05 (1H, d, *J*=2.4 Hz, H-8) and 6.08 (1H, d, *J*=2.4 Hz, H-6) the coupling constants of the doublets observed indicated meta coupling and at δ 6.43 (1H, dd, *J*=8.3, 2.4 Hz, H-6´) showed ortho coupling with 7.10 (1H, d, *J*=8.3Hz, H-5´) and meta coupling with 6.39 (1H, d, *J*=2.4 Hz, H-2´). Two typical broad hydroxy signals were observed at δ 6.02 (1H, s, 5-OH), 4.91 (1H, s, 4´-OH) as well as at δ 12.03 (1H, s, 5-OH), which occurred as a sharp strong signal indicating an alcoholic proton chelated by a ketone.

The data were consistent with being of the flavanone class. A coupled doublet of doublets pattern of 2.85 (1H, dd, *J*=17.0, 3.1 Hz, H-3α), 3.19 (1H, dd, *J*=17.0, 12.0 Hz, H-3β), and 5.61 (1H, dd, *J*=12.0, 3.1 Hz, H-2) representing the protons at C-2 and C-3. In addition, in the B-ring it could be deduced that C-3′ and C-4′ are substituted with 3.79 (3H, s, 3′-OCH_3) and 4.91 (1H, s, 4′-OH), respectively.

The spectra were compared with previously reports of homoeriodictyol (Fletcher, 2011) as summarized in Table 4-6.

Table 4-6 The ^{1}H- and ^{13}C-NMR data of compound No.1 and homoeriodictyol (Fletcher, 2011)

Position	Compound No.1 (in $CDCl_3$)	Homoeriodictyol (in CD_3COCD_3)
2	5.61 (1H, dd, 12.9, 2.7)	5.43 (1H, dd, 12.9, 2.7)
3	2.85 (1H, dd, 17.1, 3.0),	2.74 (1H, dd, 17.1, 3.0)
	3.19 (1H, dd, 17.1, 12.9)	3.21 (1H, dd, 17.1, 12.9)
4	-	-
4a	-	-
5	12.03 (1H, s)	12.16 (1H, s)
6	6.08 (1H, d, 2.4)	5.98 (1H, s)
7	6.02 (1H, s)	-
8	6.05 (1H, d, 2.4)	5.98 (1H, s)
8a	-	-
1′	-	-
2′	6.39 (1H, d, 2.4)	7.16 (1H, d, 1.2)
3′	-	-
4′	4.91 (1H, s)	-
5′	7.10 (1H, d, 8.3)	6.86 (1H, m)
6′	6.43 (1H, dd, 8.3, 2.4)	6.98 (1H, m)
3′-OCH_3	3.79 (3H, s)	3.89 (3H, s)

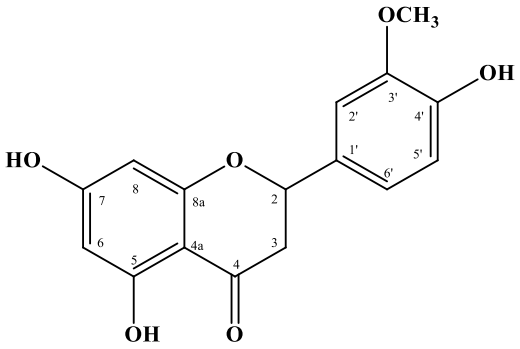

Figure 4-3 The structure of compound No.1 (homoeriodictyol)

5.1.2 Structure determination of compound No.2

The compound No.2 was obtained as a yellow amorphous powder, soluble in methanol.

The UV spectrum in chloroform (Figure B-1) demonstrated absorption maximum at λ_{max} 228, 242, 286 and 396 nm. The IR spectrum (Figure B-2) exhibited maximum absorption bands at 3401, 2923, 2851 and 1622 cm^{-1}. The HR-EIMS which showed a molecular ion peak at m/z 497.2298 calcd. for confirmed a molecular formula of $C_{30}H_{34}O_5$, 497.2298 (Figure B-3).

The ^{1}H and ^{13}C-NMR spectra of No.2, together with 2D-NMR, HMQC and HMBC experiments could be assigned as apigenin derivative, 3´-farnesyl apigenin (Figure 4-4).

The ^{1}H-NMR (Figure B-4) data showed twelve signals at δ 5.34 (1H, td, *J*=7.3, 1.2 Hz, H-2´´), 5.10 (1H, td, *J*=7.0, 1.2 Hz, H-7´´), 4.94 (1H, tt, *J*=7.0, 1.4 Hz, H-12´´), 3.35 (2H, d, *J*=7.3 Hz, H-1´´), 2.14 (2H, dd, *J*=28.7, 6.5 Hz, H-6´´), 2.08 (2H, dd, *J*=28.5, 6.5 Hz, H-5´´), 1.92 (2H, dd, *J*=33.4, 7.0 Hz, H-11´´), 1.85 (2H, dd, *J*=32.7, 7.0 Hz, H-10´´), 1.73 (3H, d, *J*=1.3 Hz, H-4´´), 1.56 (3H, d, *J*=1.4 Hz, H-14´´), 1.54 (3H, d, *J*=1.3 Hz, H-9´´) and 1.48 (3H, d, *J*=1.3 Hz, H-15´´) were identified as a 3,7, 11-trimethyl-2,6,10-dodecatrienyl, the side chain. Six signals of aromatic proton showed at δ 6.49 (1H, s, H-3), 6.18 (1H, d, *J*=2.2 Hz, H-6), 6.39 (1H, d, *J*=2.1 Hz, H-8), 7.63 (1H, d, *J*=2.4 Hz, H-2´), 6.87 (1H, d, *J*=8.2 Hz, H-5´) and 7.62 (1H, dd, *J*=8.2, 2.4 Hz, H-6´).

The ^{13}C-NMR (in $CDCl_3$; 125MHz) spectrum (Figure B-5) showed thirty carbons appeared at δ 183.83 (C-4), 166.57 (C-2), 165.93 (C-7), 163.19 (C-5), 160.50 (C-4′), 159.39 (C-8a), 137.44 (C-3′′), 136.15 (C-8′′), 131.96 (C-13′′), 130.37 (C-3′), 128.92 (C-2′), 126.86 (C-6′), 125.40 (C-12′′), 125.14 (C-7′′), 123.48 (C-2′′), 123.10 (C-1′), 116.25 (C-5′), 105.33 (C-4a), 103.68 (C-3), 100.10 (C-6), 95.05 (C-8), 40.80 (C-10′′), 40.72 (C-5′′), 28.93 (C-1′′), 27.77 (C-11′′), 27.37 (C-6′′), 25.81 (C-14′′), 17.66 (C-15′′), 16.26 (C-4′′) and 16.16 (C-9′′). One of the most downfield carbon signal (183.83) was assigned to the carbonyl carbon at the position C-4. Moreover, at δ 137.44 (C-3′′), 136.15 (C-8′′), 131.96 (C-13′′), 125.40 (C-12′′), 125.14 (C-7′′), 123.48 (C-2′′), 40.80 (C-10′′), 40.72 (C-5′′), 28.93 (C-1′′), 27.77 (C-11′′), 27.37 (C-6′′), 25.81 (C-14′′), 17.66 (C-15′′), 16.26 (C-4′′) and 16.16 (C-9′′) were assigned to a 3,7,11-trimethyl-2,6,10-dodecatrienyl. The ^{1}H and ^{13}C-NMR spectra of No.2, together with 2D-NMR, HMQC and HMBC were assigned in the Table 4-7.

Table 4-7 Carbon-proton correlation of compound No.2 observed in the HMQC and HMBC spectrum

	δ_C (ppm)	**δ_H (ppm) (multiplicity, *J* in Hz)**	**Correlation with proton (HMBC)**
2	166.57	-	H-3, H-2′, H-6′
3	103.68	6.49 (1H, s)	H-3
4	183.83	-	H-3, H-6, H-8
4a	105.33	-	H-3, H-6, H-8
5	163.19	-	H-3, H-6
6	100.10	6.18 (1H, d, 2.2)	H-8
7	165.93	-	H-6, H- 8
8	95.05	6.39 (1H, d, 2.1)	H-6
8a	159.39	-	H-8
1′	123.10	-	H-3, H-5′
2′	128.92	7.63 (1H, d, 2.4)	H-5′, H-6′, H-1′′
3′	130.37	-	H-5′, H-6′, H-1′′,H-2′′, H-4′′
4′	160.50	-	H-2′, H-5′, H-6′, H-1′′

Table 4-7 Carbon-proton correlation of compound No.2 observed in the HMQC and HMBC spectrum (continued)

	δ_C (ppm)	δ_H (ppm) (multiplicity, *J* in Hz)	Correlation with proton (HMBC)
5′	116.25	6.87 (1H, d, 8.2)	H-6′, H-1′′
6′	126.86	7.62 (1H, dd, 8.2, 2.4)	H-2′
1′′	28.93	3.35 (2H, d, 7.3)	H-2′, H-5′, H-1′′, H-2′′
2′′	123.48	5.34 (1H, td, 7.3, 1.2)	H-4′′, H-5′′
3′′	137.44	-	H-1′′, H-4′′, H-5′′, H-6′′
4′′	16.26	1.73 (3H, d, 1.3)	H-1′′, H-2′′
5′′	40.72	2.08 (2H, dd, 28.5, 6.5)	H-1′′, H-2′′, H-4′′, H-6′′
6′′	27.37	2.14 (2H, dd, 28.7, 6.5)	H-1′′, H-2′′, H-5′′, H-7′′
7′′	125.40	5.10 (1H, td, 7.3, 1.2)	H-11′′, H-15′′
8′′	136.15	-	H-6′′, H-9′′, H-10′′, H-11′′
9′′	16.16	1.54 (3H, d, 1.3)	H-7′′, H-10′′
10′′	40.80	1.85 (2H, dd, 32.7, 7.0)	H-7′′, H-11′′, H-12′′
11′′	27.77	1.92 (2H, dd, 33.4, 7.0)	H-10′′, H-12′′
12′′	125.40	4.94 (1H, tt, 7.0, 1.4)	H-11′′, H-15′′
13′′	131.96	-	H-11′′, H-14′′, H-15′′
14′′	25.81	1.56 (3H, d, 1.4)	H-12′′, H-15′′
15′′	17.66	1.48 (3H, d, 1.3)	H-12′′, H-15′′

The HMQC (Figure B-6) revealed correlation between the directly coupled ^{1}H and ^{13}C nuclei. According to the HMQC spectrum suggesting compound No.2 is apigenin derivative (Figure 4-4).

Based on the information obtained from ^{1}H- , ^{13}C-NMR and HMQC spectrum, it could be classified the carbon to four methyl carbons; 25.81 (C-14′′), 17.66 (C-15′′), 16.26 (C-4′′) and 16.16 (C-9′′) attached to proton at 1.56 (3H), 1.48 (3H), 1.73 (3H) and 1.54 (3H), respectively, five methylene carbons; 40.80 (C-10′′), 40.72 (C-5′′), 28.93 (C-1′′), 27.77 (C-11′′) and 27.37 (C-6′′) attached to proton at 1.85 (2H), 2.08 (2H), 3.35 (2H), 1.92 (2H) and 2.14 (2H), respectively, nine olefin or aromatic

carbons at 128.92 (C-2′), 126.86 (C-6′), 125.40 (C-12′′), 125.14 (C-7′′), 123.48 (C-2′′), 116.25 (C-5′), 103.68 (C-3), 100.10 (C-6) and 95.05 (C-8) attached to proton at 7.63 (1H), 7.62 (1H), 4.94 (1H), 5.10 (1H), 5.34 (1H), 6.87 (1H), 6.49 (1H), 6.18 (1H) and 6.39 (1H), respectively, eleven quaternary carbons at 166.57 (C-2), 165.93 (C-7), 163.19 (C-5), 160.50 (C-4′), 159.39 (C-8a), 137.44 (C-3′′), 136.15 (C-8′′), 131.96 (C-13′′), 130.37 (C-3′), 123.10 (C-1′) and 105.33 (C-4a) and the most downfield carbon signal at 183.83 was assigned to be the carbonyl at C-4.

The long-range C-H correlations of compound No.2 could be observed from HMBC spectrum (Figure B-7). 3,7,11-trimethyl-2,6,10-dodecatrienyl or farnesyl side chain suggesting their right position with showed correlations with their neighbor protons; four methyl carbons including the C-4′′ correlations with H-1′′ and H-2′′, C-9′′ correlations with H-7′′ and H-10′′, C-14′′ correlations with H-12′′ and H-15′′ and C-15′′ correlations with H-12′′ and H-15′′), five methylene carbons including the C-1′′ correlations with H-2′, H-5′, H-1′′and H-2′′, C-5′′ correlations with H-1′′, H-2′′, H-4′′and H-6′′ , C-6′′ correlations with H-1′′, H-2′′, H-5′′ and H-7′′ , C-10′′ correlations with H-7′′, H-11′′and H-12′′ and C-11′′ correlations with H-10′′ and H-12′′, three methane carbons including the C-2′′ correlations with H-4′′ and H-5′′ , C-7′′ correlations with H-11′′ and H-15′′ and C-12′′ correlations with H-11′′ and H-15′′ and three quatenary carbon including the C-3′′ correlations with H-1′′, H-4′′, H-5′′and H-6′′, C-8′′ correlations with H-6′′, H-9′′, H-10′′ and H-11′′ and C-13′′ correlations with H-11′′, H-14′′ and H-15′′). In addition, the C-2′ correlations with H-5′, H-6′and H-1′′, C-3′ correlations with H-5′, H-6′, H-1′′,H-2′′, H-4′′, C-4′ correlations with H-2′, H-5′, H-6′, H-1′′ and C-1′′ correlations with H-2′, H-5′ and H-1′′ suggesting the right position of 3,7,11-trimethyl-2,6,10-dodecatrienyl substituted at C-3′. The spectra were compared with previous reports of kuwanone S (Jung *et al*., 2016) and farnesyl phosphosulfate (Gotoh *et al*., 1992) as summarized in Table 4-8 and 4-9.

Table 4-8 The ^{1}H and ^{13}C-NMR data of compound No.2 and kuwanone S (Jung *et al.*, 2016)

	Compound No.2 (in CD_3OD)		**Kuwanone S (in CD_3OD)**	
	δ_C (ppm)	**δ_H (ppm) (multiplicity, *J* in Hz)**	**δ_C (ppm)**	**δ_H (ppm) (multiplicity, *J* in Hz)**
2	166.57	-	166.44	-
3	103.68	6.49 (1H, s)	103.53	6.44 (1H, s)
4	183.83	-	183.72	-
4a	105.33	-	105.21	-
5	163.19	-	163.11	-
6	100.10	6.18 (1H, d, 2.2)	100.11	6.36 (1H, brs)
7	165.93	-	166.03	-
8	95.05	6.39 (1H, d, 2.1)	95.05	6.15 (1H, brs)
8a	159.39	-	159.30	-
1´	123.10	-	-	-
2´	128.92	7.63 (1H, d, 2.4)	-	7.58 (1H, brs)
3´	130.37	-	130.28	-
4´	160.50	-	160.51	-
5´	116.25	6.87 (1H, d, 8.2)	116.17	6.84 (1H, d, 8.8)
6´	126.86	7.62 (1H, dd, 8.2, 2.4)	128.79	7.59 (1H,d 8.8)
1´´	28.93	3.35 (2H, d, 7.3)	28.99	3.31 (2H, d, 7.2)
2´´	123.48	5.34 (1H, td, 7.3, 1.2)	123.26	5.32 (1H, t, 6.8)
3´´	137.44	-	137.64	-
4´´	16.26	1.73 (3H, d, 1.3)	16.36	1.72 (3H, s)
5´´	40.72	2.08 (2H, dd, 28.5, 6.5)	40.86	2.05 (2H, t, 7.2)
6´´	27.37	2.14 (2H, dd, 28.7, 6.5)	27.70	2.11 (2H, dt, 7.2, 6.8)
7´´	125.40	5.10 (1H, td, 7.3, 1.2)	125.37	5.09 (1H, t, 6.8)
8´´	136.15	-	132.11	-
9´´	16.16	1.54 (3H, d, 1.3)	17.79	1.59 (3H, s)
10´´	40.80	1.85 (2H, dd, 32.7, 7.0)	25.85	1.56 (3H, s)

Table 4-8 The ^{1}H and ^{13}C-NMR data of compound No.2 and kuwanone S (Jung *et al*., 2016) (continued)

	Compound No.2 (in CD_3OD)		**Kuwanone S (in CD_3OD)**	
	δ_C (ppm)	**δ_H (ppm) (multiplicity, *J* in Hz)**	**δ_C (ppm)**	**δ_H (ppm) (multiplicity, *J* in Hz)**
11´´	27.77	1.92 (2H, dd, 33.4, 7.0)	-	-
12´´	125.40	4.94 (1H, tt, 7.0, 1.4)	-	-
13´´	131.96	-	-	-
14´´	25.81	1.56 (3H, d, 1.4)	-	-
15´´	17.66	1.48 (3H, d, 1.3)	-	-

Table 4-9 The ^{1}H and ^{13}C-NMR data of compound No.2 and farnesyl phosphosulfate (Gotoh *et al.*,1992)

Position	**Compound No.2 (in $CDCl_3$)**	**Farnesyl phosphosulfate (in D_2O)**
	δ_H (ppm) (multiplicity, *J* in Hz)	**δ_H (ppm) (multiplicity, *J* in Hz)**
1´´	3.35 (2H, d, 7.3)	4.45 (2H, m)
2´´	5.34 (1H, td, 7.3, 1.2)	5.44 (1H, m)
3´´	-	-
4´´	1.73 (3H, d, 1.3)	1.71 (3H, m)
5´´	2.08 (2H, dd, 28.5, 6.5)	2.10 (2H, m)
6´´	2.14 (2H, dd, 28.7, 6.5)	2.10 (2H, m)
7´´	5.10 (1H, td, 7.3, 1.2)	5.18 (1H, m)
8´´	-	-
9´´	1.54 (3H, d, 1.3)	1.71 (3H, m)
10´´	1.85 (2H, dd, 32.7, 7.0)	2.10 (2H, m)
11´´	1.92 (2H, dd, 33.4, 7.0)	2.10 (2H, m)
12´´	4.94 (1H, tt, 7.0, 1.4)	5.18 (1H, m)
13´´	-	-
14´´	1.56 (3H, d, 1.4)	1.65 (3H, m)
15´´	1.48 (3H, d, 1.3)	1.65 (3H, m)

Therefore, on the basis of above evidences, the structure of No.2 was established as 3´-farnesyl apigenin (Figure 4-4), the new compound.

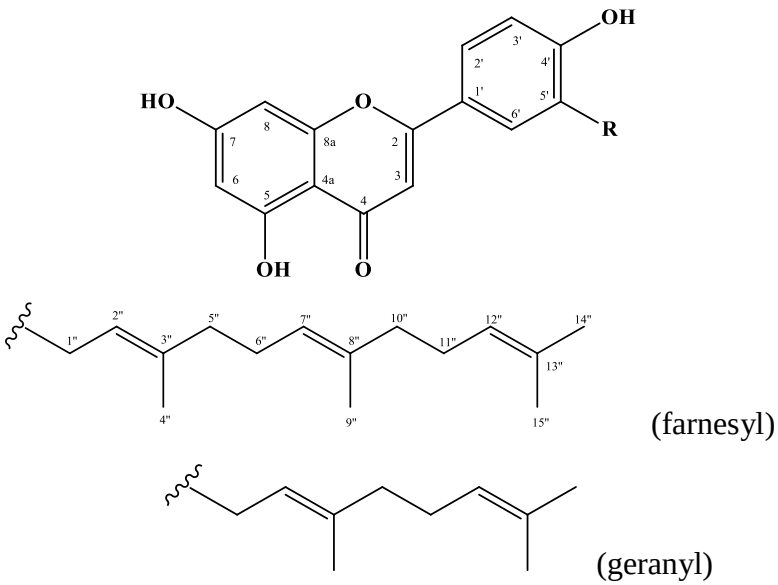

R = H; apigenin

R = geranyl; kuwanone S

R = farnesyl; 3´-farnesyl apigenin

Figure 4-4 The structures of compound No.2 (3´-farnesyl apigenin), apigenin, kuwanone S and 3´-farnesyl apigenin

5.1.3 Structure determination of compound No.3

The compound No.3 was obtained as a yellow amorphous, soluble in methanol.

The UV spectrum in methanol (Figure C-1) showed absorptions at λ_{max} 237, 275 and 292 nm. The IR spectrum (Figure C-2), showed the absorption bands at 3400, 2973, 1649, 1558, 1472, 1351, 1274 and 1152 cm^{-1}.

The HRESIMS (Figure C-3) showed a $[M+Na]^+$ ion peak at m/z 457.1258 correlated with a molecular formula of $C_{25}H_{22}O_7$.

Compound No.3 could be assigned as the known compound isocycloartobiloxanthone (Figure 4-5) by analysis of its ^1H and ^{13}C-NMR spectra properties. Its ^1H-NMR data has been reported (Lan *et al.*, 2013).

The ^1H-NMR spectrum (Figure C-4) showed the presence of a 2, 2-dimethylpyran ring moiety at δ 1.44 (3H, s, H-17) and 1.43 (3H, s, H-18) and two

olefinic protons at δ 5.58 (1H, d, *J*=10.0 Hz, H-15) and 6.86 (1H, dd, *J*=10.0, 0.5 Hz, H-14). In addition, the appearance of methyl group at δ 1.28 (3H, s, H-12) and 1.63 (3H, s, H-13), and ABX type signals at δ 2.32 (1H, t, *J*=15.0 Hz, H-9β), 3.39 (1H, dd, *J*=15.0, 7.0 Hz, H-10), and 3.11 (1H, dd, *J*=15.0, 7.5 Hz, H-9α) suggested a dihydrofuran, may be formed by the oxidative cyclization of the 5´-hydroxy group of the B-ring onto the isoprenyl side chain. It also showed aromatic proton at δ 6.07 (1H, d, *J*=0.5 Hz, H-8) and 6.20 (1H, s, H-3´).

The ^{13}C-NMR spectrum (Figure C-5), showed signals of carbonyl carbon at 181.89 (C-4), fifteen signals of olefin carbon at 162.46 (C-7), 162.36 (C-2), 160.06 (C-5), 152.49 (C-2´), 147.71 (C-4´), 138.00 (C-5´), 133.81 (C-6´), 128.00 (C-15), 116.35 (C-14), 112.60 (C-1´), 105.62 (C-3´), 105.30 (C-4a), 105.00 (C-3), 102.54 (C-6) and 100.38 (C-8), three signals of tertiary carbon at 94.29 (C-11), 79.13 (C-16) and 47.84 (C-10), four signals of methyl carbon at 28.57 (C-13), 28.46 (C-17), 28.26 (C-18) and 22.82 (C-12) and one signals of methylene carbon at 20.72 (C-9).

Based on the information obtained from the HMQC (Figure C-6) and HMBC (Figure C-7) spectra, all protonated carbons and long-range C-H correlations of compound No.3 were assigned, as showed in the Table 4-10.

Table 4-10 Carbon-proton correlation of compound No.3 observed in the HMQC and HMBC spectrum

	δ_C (ppm)	**δ_H (ppm) (multiplicity, *J* in Hz)**	**Correlation with proton (HMBC)**
2	162.36	-	H-9, H-3´
3	105.00	-	H-9, H-10
4	181.89	-	H-9
4a	105.30	-	H-8, H-15
5	160.06	-	H-8, H-14

Table 4-10 Carbon-proton correlation of compound No.3 observed in the HMQC and HMBC spectrum (continued)

	δ_C (ppm)	δ_H (ppm) (multiplicity, *J* in Hz)	Correlation with proton (HMBC)
6	102.54	-	H-8, H-14, H-15
7	162.46	-	H-8
8	100.38	6.07 (1H, d, 0.5)	H-8, H-14
8a	obscure	-	-
9	20.72	2.32 (1H, t, 15.0)	H-10, H-12, H-13
		3.11 (1H, dd, 15.0, 7.5)	-
10	47.84	3.39 (1H, dd, 15.0, 7.0)	H-9, H-13
11	94.29	-	H-9, H-10, H-12, H-13
12	22.82	1.28 (3H, s)	-
13	28.57	1.63 (3H, s)	H-10, H-13
14	116.35	6.86 (1H, dd, 10.0, 0.5)	H-17, H-18
15	128.00	5.58 (1H, d, 10.0)	H-17, H-18
16	79.13	-	H-14, H-15, H-17, H-18
17	28.46	1.44 (3H, s)	H-14, H-15
18	28.26	1.43 (3H, s)	H-14, H-15
1´	112.60	-	H-9
2´	152.49	-	H-10, H-3´
3´	105.62	6.20 (1H, s)	-
4´	147.71	-	H-10, H-3´
5´	138.00	-	H-10, H-3´
6´	133.81	-	H-9, H-10, H-13

The C-5 carbon showed correlation with H-8 and H-14, C-6 showed correlation with H-8, H-14 and H-15 suggested the position of 2, 2-dimethylpyran ring moiety. The C-2 carbon showed correlation with H-9, C-1´ carbon showed correlation with H-9, C-5´ carbon showed correlation with H-10 and H-3´, C-6´carbon showed

correlation with H-9, H-10 and H-13 suggesting the position of a dihydrofuran formed by the oxidative cyclization of the 5´-hydroxy group of the B-ring onto the isoprenyl side chain. The result from HMBC experiment confirmed the structure of compound No.3 was assigned completely. The ^{1}H and ^{13}C-NMR data was compared with those isocycloartobiloxanthone (Lan *et al.*, 2013), as summarized in Table 4-11.

Table 4-11 The ^{1}H and ^{13}C-NMR data of compound No.3 and isocycloartobiloxanthone (Lan *et al.*, 2013)

Position	Compound No.3 (in CD_3OD)		Isocycloartobiloxanthone (in CD_3COCD_3)	
	δ_C (ppm)	δ_H (ppm) (multiplicity, *J* in Hz)	δ_C (ppm)	δ_H (ppm) (multiplicity, *J* in Hz)
2	162.36	-	160.3	-
3	105.00	-	105.2	-
4	181.89	-	182.0	-
4a	105.30	-	106.7	-
5	160.06	-	157.5	-
6	102.54	-	106.1	-
7	162.46	-	162.2	-
8	100.38	6.07 (1H, d, 0.5)	96.3	6.35 (s)
8a	obscure	-	157.9	-
9	20.72	2.32 (1H, t, 15.0) 3.11 (1H, dd, 15.0, 7.5)	21.1	2.36 (t, 15.2), 3.41 (dd, 15.2, 6.8)
10	47.84	3.39 (1H, dd, 15.0, 7.0)	48.1	3.21 (dd, 15.2, 6.8)
11	94.29	-	94.4	-
12	22.82	1.28 (3H, s)	23.5	1.32 (s)
13	28.57	1.63 (3H, s)	29.0	1.66 (s)
14	116.35	6.86 (1H, dd, 10.0, 0.5)	116.6	6.67 (d, 10.0)

Table 4-11 The ^{1}H and ^{13}C-NMR data of compound No.3 and isocycloartobiloxanthone (Lan *et al*., 2013) (continued)

Position	Compound No.3 (in CD_3OD)		Isocycloartobiloxanthone (in CD_3COCD_3)	
	δ_C (ppm)	**δ_H (ppm) (multiplicity, *J* in Hz)**	**δ_C (ppm)**	**δ_H (ppm) (multiplicity, *J* in Hz)**
15	128.00	5.58 (1H, d, 10.0)	129.8	5.75 (d, 10.0)
16	79.13	-	79.2	-
17	28.46	1.44 (3H, s)	29.0	1.45 (d, 1.6)
18	28.26	1.43 (3H, s)	29.1	1.45 (d, 1.6)
1´	112.60	-	113.5	-
2´	152.49	-	151.9	-
3´	105.62	6.20 (1H, s)	106.3	6.45 (s)
4´	147.71	-	147.8	-
5´	138.00	-	138.8	-
6´	133.81	-	134.1	-
5-OH	-	-	-	13.74 (s)

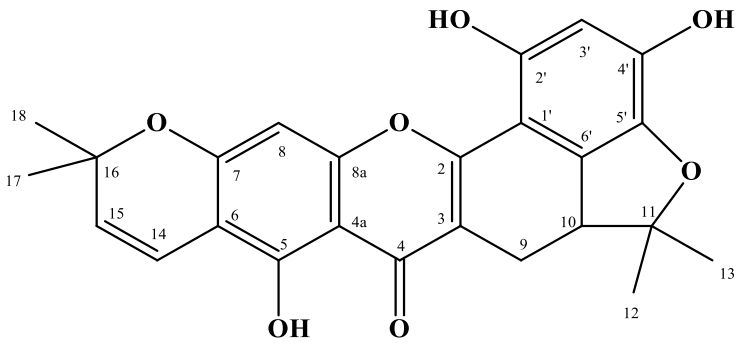

Figure 4-5 The structure of compound No.3 (isocycloartobiloxanthone)

5.1.4 Structure determination of compound No.4

The compound No.4 was obtained as a yellow amorphous, soluble in methanol.

The UV spectrum in methanol (Figure D-1) showed absorptions at λ_{max} 237, 275 and 292 nm. The IR spectrum (Figure D-2), showed the absorption bands at 3435, 1652 and 1550 cm^{-1}.

The ESIMS (Figure D-3) showed a $[M+Na]^+$ ion peak at m/z 409.1618 correlated with a molecular formula of $C_{20}H_{18}O_8$.

Comparison of its ^{1}H- and ^{13}C-NMR spectra with reported data suggested that compound No.4 was identical with 3-(hydroxyprenyl) isoetin (Figure 4-6), the new compound.

^{1}H-NMR spectrum (Figure D-4) indicated resonances corresponding to 1-hydroxy-3,3-dimethylallyl group were at δ 1.68 (3H, d, *J*=0.8 Hz, H-12), 1.92 (3H, d, *J*=1.2 Hz, H-13), 5.42 (1H, dt, *J*=9.2, 1.2 Hz, H-10), and 6.09 (1H, d, *J*=9.2 Hz, H-9). In addition, it showed four aromatic protons at δ 7.13 (1H, s, H-6´), 6.37 (1H, d, *J*=1.7 Hz, H-8), 6.33 (1H, s, H-3´) and 6.16 (1H, d, *J*=1.9, Hz, H-6).

Its ^{13}C-NMR spectrum (Figure B-4), showed signals of carbonyl carbon at 179.52 (C-4), sixteen signals of olefin carbon at 166.40 (C-4´), 165.47 (C-7), 163.31 (C-5), 158.61 (C-8a), 157.61 (C-2), 152.58 (C-2´), 141.95 (C-5´), 139.59 (C-11), 122.45 (C-10), 110.49 (C-1´), 109.94 (C-6´), 107.77 (C-3), 105.64 (C-3´), 105.44 (C-4a), 99.99 (C-6) and 95.01 (C-8), one signals of tertiary carbon at 70.21 (C-9) and two signals of methyl carbon at 25.93 (C-12), 18.66 (C-13).

The information from the HMQC and HMBC spectra of compound No.4 was summarized in Table 4-12.

Table 4-12 Carbon-proton correlation of compound No.4 observed in the HMQC and HMBC spectrum

	δ_C (ppm)	δ_H (ppm) (multiplicity, *J* in Hz)	Correlation with proton (HMBC)
2	157.61	-	H-9, H-3´, H-6´
3	107.77	-	H-3´
4	179.52	-	H-9
4a	105.44	-	H-6, H-8
5	163.31	-	H-6
6	99.99	6.16 (1H, d, 1.9)	H-8
7	165.47	-	H-6, H-8
8	95.01	6.37 (1H, d, 1.7)	H-6
8a	158.61	-	H-9
9	70.21	6.09 (1H, d, 9.2)	-
10	122.45	5.42 (1H, dt, 9.2, 1.2)	H-9, H-12, H-13
11	139.59	-	H-9, H-12, H-13
12	18.66	1.68 (3H, d, 0.9)	H-10, H-13
13	25.93	1.92 (3H, d, 1.2)	H-10, H-12
1´	110.49	-	H-9, H-3
2´	152.58	-	H-9, H-3´, H-6´
3´	105.64	6.33 (1H, s)	-
4´	166.40	-	H-3´, H-6´
5´	141.95	-	H-3´, H-6´
6´	109.94	7.13 (1H, s)	H-9

The data from HMQC (Figure D-6) revealed correlation between the directly coupled ^{1}H and ^{13}C nuclei and the long-range C-H correlations of compound No.4 could be observed from HMBC spectrum (Figure D-7). The C-2 carbon showed correlation with H-9, H-3′ and H-6′ and C-4 carbon showed correlation with H-9 suggesting the right position of 1-hydroxy-3, 3-dimethylallyl group. These findings suggested the structure of compound No.4 is 3-(hydroxyprenyl) isoetin. The ^{1}H and ^{13}C-NMR data was compared with those 8-geranyl-3-(hydroxyprenyl) isoetin (Figure 4-6) (Lan *et al*., 2013), as summarized in Table 4-13.

Table 4-13 The ^{1}H and ^{13}C-NMR data of compound No.4 and 8-geranyl-3-(hydroxyprenyl) isoetin (Lan *et al*., 2013)

	Compound No.4 (in CD_3OD)		**8-geranyl-3-(hydroxyprenyl)isoetin (in CD_3COCD_3)**	
	δ_C (ppm)	**δ_H (ppm) (multiplicity, *J* in Hz)**	**δ_C (ppm)**	**δ_H (ppm) (multiplicity, *J* in Hz)**
2	157.61	-	157.4	-
3	107.77	-	108.3	-
4	179.52	-	180.1	-
4a	105.44	-	106.3	-
5	163.31	-	161.6	-
6	99.99	6.16 (1H, d, 1.9)	100.6	6.32 (s)
7	165.47	-	162.6	-
8	95.01	6.37 (1H, d, 1.7)	108.6	-
8a	158.61	-	156.0	-
9	70.21	6.09 (1H, d, 9.2)	70.6	6.14 (d, 9.6)
10	122.45	5.42 (1H, dt, 9.2, 1.2)	122.8	5.51 (dt, 9.6, 1.2)
11	139.59	-	139.0	-
12	18.66	1.68 (3H, d, 0.9)	19.3	1.67 (d, 1.2)
13	25.93	1.92 (3H, d, 1.2)	26.5	1.93 (d, 1.2)
14	-	-	22.9	3.56 (m)

Table 4-13 The ^{1}H and ^{13}C-NMR data of compound No.4 and 8-geranyl-3-(hydroxyprenyl) isoetin (Lan *et al*., 2013) (continued)

	Compound No.4 (in CD_3OD)		**8-geranyl-3-(hydroxyprenyl)isoetin (in CD_3COCD_3)**	
	δ_C (ppm)	**δ_H (ppm) (multiplicity, *J* in Hz)**	**δ_C (ppm)**	**δ_H (ppm) (multiplicity, *J* in Hz)**
15	-	-	124.0	5.35 (t, 7.0)
16	-	-	136.5	-
17	-	-	17.3	1.49 (s)
18	-	-	27.9	2.05 (m)
19	-	-	41.0	2.05 (m)
20	-	-	125.7	5.03 (t, 6.8)
21	-	-	132.3	-
22	-	-	18.3	1.54 (d, 0.8)
23	-	-	26.4	1.86 (d, 0.8)
1´	110.49	-	110.6	-
2´	152.58	-	152.7	-
3´	105.64	6.33 (1H, s)	106.0	6.47 (s)
4´	166.40	-	153.0	-
5´	141.95	-	142.1	-
6´	109.94	7.13 (1H, s)	110.8	7.32 (s)
5-OH	-	-	-	12.86 (s)

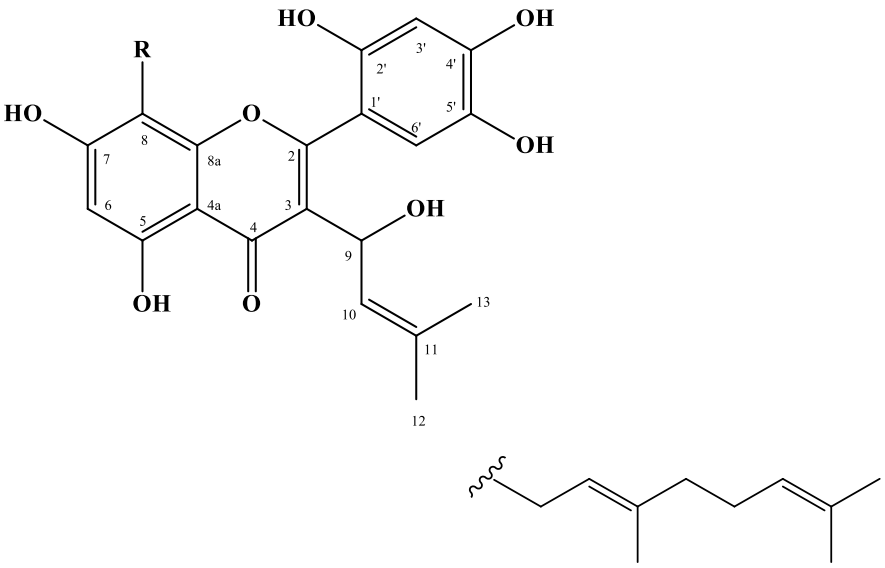

(geranyl)

R = H; 3-(hydroxyprenyl) isoetin

R = geranyl; 8-geranyl-3-(hydroxyprenyl) isoetin

Figure 4-6 The structures of compound No.4 (3-(hydroxyprenyl) isoetin) and 8-geranyl-3-(hydroxyprenyl) isoetin

5.1.5 Structure determination of compound No.5

The compound No.5 was obtained as a yellow amorphous powder, soluble in methanol.

The UV spectrum in methanol (Figure E-1) showed absorptions at λ_{max} 205, 253 and 331 nm. The IR spectrum (Figure E-2), showed the absorption bands at 3412, 1652, 1615, 1512, 1448, 1430, 1359, 1297 and 1166 cm^{-1}.

The HRESIMS (Figure E-3) showed a $[M+Na]^+$ ion peak at m/z 407.1101 correlated with a molecular formula of $C_{21}H_{20}O_7$.

Comparison of its ^{1}H- and ^{13}C-NMR spectra with reported data suggested that compound No.5 was identified as 3-prenyl-5,7,2´,5´-tetrahydroxy-4´ -methoxyflavone (Figure 4-7), the new compound.

The ^{1}H-NMR spectrum (Figure E-4) revealed the presence of methoxy group at δ 3.71 (3H, s, 4´-OCH_3), 3-methyl-2-butenyl group were at δ 5.05 (1H, m, H-10), 3.01 (2H, d, *J*=7.0 Hz, H-9), 1.58 (3H, d, *J*=0.5 Hz, H-12) and 1.36 (3H, d, *J*=0.5 Hz, H-13) and four signals of aromatic proton at δ 6.71 (1H, s, H-6´), 6.59 (1H, s, H-3´), 6.23 (1H, d, *J*=2.0 Hz, H-8) and 6.17 (1H, d, *J*=2.0 Hz, H-6).

Its ^{13}C-NMR spectrum (Figure E-5), showed signals of carbonyl carbon at 183.53 (C-4), fourteen signals of aromatic carbon at 165.57 (C-7), 163.24 (C-5), 162.97 (C-2), 159.73 (C-8a), 152.53 (C-4´), 149.69 (C-2´), 139.93 (C-5´), 121.85 (C-3), 117.83 (C-6´), 113.71 (C-1´), 105.31 (C-4a), 101.43 (C-3´), 99.57 (C-6), 94.46 (C-8) and one signals of methoxy carbon at 56.71 (4´-OCH_3) in aromatic ring. Moreover, it showed two signals of olefinic carbon at 132.68 (C-11) and 122.67 (C-10), one signal of methylene carbon at 24.85 (C-9) and two signals of methyl carbon at 17.56 (C-13), 25.82 (C-12) in 3-methyl-2-butenyl group, side chain.

The assumption was verified by the HMQC and HMBC experiments. The information from the HMQC (Figure E-6), and HMBC (Figure E-7) spectra of compound No.5 is summarized in Table 4-14.

Table 4-14 Carbon-proton correlation of compound No.5 observed in the HMQC and HMBC spectrum

Position	δ_C (ppm)	δ_H (ppm) (multiplicity, *J* in Hz)	Correlation with proton (HMBC)
2	162.97	-	H-9, H-3´, H-6´
3	121.85	-	H-9, H-10
4	183.53	-	H-8, H-9
4a	105.31	-	H-6, H-8
5	163.24	-	H-6
6	99.57	6.17 (1H, d, 2.0)	H-8
7	165.57	-	H-8
8	94.46	6.23 (1H, d, 2.0)	H-6
8a	159.73	-	H-8
9	24.85	3.01 (2H, d, 7.0)	H-9
10	122.67	5.05 (1H, m)	H-12, H-13
11	132.68	-	H-9, H-12, H-13
12	25.82	1.58 (3H, d, 0.5)	H-9, H-12, H-13
13	17.56	1.36 (3H, d, 0.5)	H-9, H-10, H-12
1´	113.71	-	H-3´
2´	149.69	-	H-3´, H-6´
3´	101.43	6.59 (1H, s)	H-6´
4´	152.53	-	H-3´, H-6´, 4´-OCH_3
5´	139.93	-	H-3´, H-6´
6´	117.83	6.71 (1H, s)	H-3´
4´-OCH_3	56.71	3.71 (3H, s)	4´-OCH_3

The methoxy group suggested its position by correlation with C-4´ carbon. In addition, the C-2 carbon showed correlation with H-9, H-3´, H-6´, C-3 carbon showed correlation with H-9, H-10 and C-4 carbon showed correlation with H-8, H-9 suggesting the right position of 3-methyl-2-butenyl group at C-3 carbon. The ^{1}H and

^{13}C-NMR data was compared with artochamin D (Figure 4-6) (Wang *et al*., 2004), as summarized in Table 4-15.

Table 4-15 The ^{1}H and ^{13}C-NMR data of compound No.5 and artochamin D (Wang *et al*., 2004)

Position	Compound No.5 (in CD_3OD)		Artochamin D (in CD_3COCD_3)	
	δ_C (ppm)	δ_H (ppm) (multiplicity, *J* in Hz)	δ_C (ppm)	δ_H (ppm) (multiplicity, *J* in Hz)
2	162.97	-	162.5	-
3	121.85	-	121.4	-
4	183.53	-	183.6	-
4a 10	105.31	-	105.6	-
5	163.24	-	161.2	-
6	99.57	6.17 (1H, d, 2.0)	99.2	6.32 (1H, s)
7	165.57	-	162.1	-
8	94.46	6.23 (1H, d, 2.0)	107.1	-
8a	159.73	-	156.8	-
9	24.85	3.01 (2H, d, 7.0)	25.0	3.05 (2H, brd, 7.0)
10	122.67	5.05 (1H, m)	123.1	5.10 (1H, brt, 7.0)
11	132.68	-	132.3	-
12	25.82	1.58 (3H, d, 0.5)	26.2	1.57 (3H, brs)
13	17.56	1.36 (3H, d, 0.5)	18.0	1.42 (3H, brs)
14	-	-	22.4	3.34 (2H, brd, 7.3)
15	-	-	123.5	5.18 (1H, brs)
16	-	-	132.0	-
17	-	-	26.2	1.59 (3H, brs)
18	-	-	18.0	1.57 (3H, brs)
1´	113.71	-	113.8	-
2´	149.69	-	149.5	-
3´	101.43	6.59 (1H, s)	101.4	6.71 (1H, s)

Table 4-15 The ^{1}H and ^{13}C-NMR data of compound No.5 and artochamin D (Wang *et al*., 2004) (continued)

Position	Compound No.5 (in CD_3OD)		Artochamin D (in CD_3COCD_3)	
	δ_C (ppm)	δ_H (ppm) (multiplicity, *J* in Hz)	δ_C (ppm)	δ_H (ppm) (multiplicity, *J* in Hz)
4´	152.53	-	152.7	-
5´	139.93	-	139.6	-
6´	117.83	6.71 (1H, s)	118.1	6.91 (1H, s)
5´-OH	-	-	-	13.08 (1H s)
4´-OCH_3	56.71	3.71 (3H, s)	56.8	3.76 (3H, s)
2´, 5´, 7´-OH	-	-	-	8.63 (3H, brs)

Therefore, on the basis of above evidences, the structure of No.5 was established as 3-prenyl-6, 8, 2´, 5´-tetrahydroxy-4´ -methoxyflavone (Figure 4-7), the new compound.

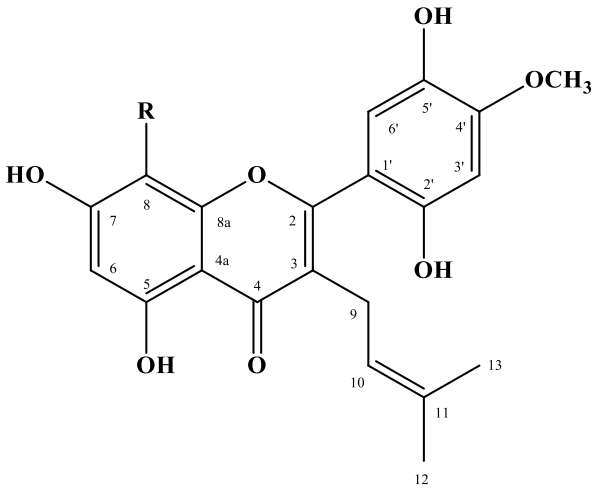

R = H; (3-prenyl-5, 7, 2´, 5´-tetrahydroxy-4´ -methoxyflavone)

R = geranyl; artochamin D

Figure 4-7 The structures of compound No.5 (3-prenyl-5, 7, 2´, 5´-tetrahydroxy-4´-methoxyflavone) and artochamin D

5.1.6 Structure determination of compound No.6

The compound No.6 was obtained as a white crystal, soluble in methanol.

The UV spectrum in methanol (Figure F-1) showed absorptions at λ_{max} 205 and 287 nm. The IR spectrum (Figure F-2), showed the absorption bands at 3435, 1642, 1613, 1456, 1437, 1305, 1193 and 1158 cm^{-1}.

Comparison of its ^{1}H-NMR spectrum with reported data suggested that compound No.6 ($C_{16}H_{14}O_6$) was identical with artocarpanone (Figure 4-8).

The ^{1}H-NMR spectrum of compound No.6 (Figure F-7), showed one signals of methoxy group at δ 3.80 (3H, s) could be assigned to 7-OCH_3, five signals of olefin proton at δ 7.23 (1H, d, *J*=8.0), 6.34 (1H, dd, *J*=8.0, 2.5), 6.31 (1H, d, *J*=2.5), 6.05 (1H, d, *J*=2.5), 6.02 (1H, d, *J*=2.5) could be assigned to H-6´, H-5´, H-3´, H-8 and H-6, respectively. Three more signals showed at δ 5.64 (1H, dd, *J*=13.0, 3.0), 3.13 (1H, dd, *J*=17.5, 13.0) and 2.74 (1H, dd, *J*=17.5, 3.0) could be assigned to H-2, H-3α and H-3β, respectively.

Based on the information obtained from the ^{1}H-NMR spectrum, the splitting patterns and the coupling constants were indicated three proton signals of a flavanone at δ 5.64 (1H, dd, *J*=13.0, 3.0, H-2), 3.13 (1H, dd, *J*=13.0, 17.5, 3-Hα) and 2.74 (1H, dd, *J*=17.5, 3.0, H-3β). The presence of five olefin protons, devided into two rings, the proton at δ 6.34 (1H, dd, *J*=8.0, 2.5 Hz, H-5´) showed *ortho* coupling with 7.23 (1H, d, *J*=8.0 Hz, H-6´) *meta* coupling with 6.31 (1H, d, *J*=2.5, H-3´) on B-ring, 6.05 (1H, d, *J*=2.5 Hz, H-8) showed *meta* coupling with 6.02 (1H, d, *J*=2.5 Hz, H-6) on A-ring. The ^{1}H-NMR data of No.6 were compared with those of artocarpanone (Dejadisai *et al*., 2014), as summarized in Table 4-16.

Table 4-16 The ^{1}H-NMR data of compound No.6 and artocarpanone, (Dej-adisai *et al.*, 2014)

Position	Compound No.6 (in CD_3OD)	Artocarpanone (in CD_3OD)
	δ_H (ppm) (multiplicity, *J* in Hz)	δ_H (ppm) (multiplicity, *J* in Hz)
2	5.64 (1H, dd, 13.0, 3.0)	5.62 (1H, dd, 13.0, 2.9)
3	3.13 (1H, dd, 17.5, 13.0)	3.09 (1H, dd, 17.1, 13.0)
	2.74 (1H, dd, 17.5, 3.0)	2.77 (1H, dd, 17.1, 2.5)
4	-	-
4a	-	-
5	-	-
6	6.02 (1H, d, 2.5)	6.01 (1H, d, *J*=2.2)
7	-	-
8	6.05 (1H, d, 2.5)	6.04 (1H, d, 2.2)
8a	-	-
1´	-	-
2´	-	-
3´	6.31 (1H, d, 2.5)	6.33 (1H, d, 2.2)
4´	-	-
5´	6.34 (1H, dd, 8.0, 2.5)	6.32 (1H, dd, 8.2, 2.2)
6´	7.23 (1H, d, 8.0)	7.22 (1H, d, 8.0)
7-OCH_3	3.80 (3H, s)	3.79 (3H, s)

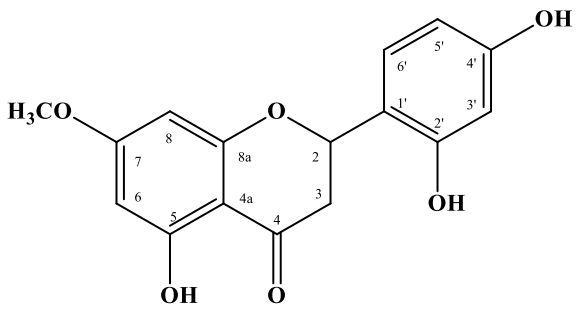

Figure 4-8 The structure of compound No.6 (artocarpanone)

5.1.7 Structure determination of compound No.7

The compound No.7 was obtained as a cream needles, soluble in methanol.

The UV spectrum in methanol (Figure G-1) showed absorptions at λ_{max} 205, 226 and 287 nm. The IR spectrum (Figure G-2), showed the absorption bands at 3412, 1635, 1520, 1457, 1343, 1313, 1250, 1158, 1085 and 1605 cm^{-1}.

Comparison of its ^{1}H-NMR spectrum with previous reported data suggested that compound No.7 ($C_{15}H_{12}O_5$) was identical with naringenin (Figure 4-9).

The ^{1}H-NMR (Figure G-4) spectrum of compound No.7, showed four signals of olefin proton at δ 7.30 (2H, d, *J*=8.5 Hz) , 6.81 (2H, d, *J*=8.5 Hz) , 5.88 (1H, d, *J*=2.1 Hz) and 5.87 (1H, d, *J*=2.1 Hz) could be assigned to H-2´/ H-6´, H-3´/ H-5´, H-6 and H-8, respectively and three signals at δ 5.32 (1H, dd, *J*=12.9, 3.1 Hz), 3.10 (1H, dd, *J*=17.0, 12.9 Hz) and 2.68 (1H, dd, *J*=17.0, 2.9 Hz) could be assigned to H-2, H-3α and H-3β, respectively.

The result obtained from the ^{1}H-NMR spectrum, suggest the signals of a flavanone which the splitting patterns and the coupling constants at δ 5.32 (1H, dd, *J*=12.9, 3.1 Hz, H-2), 3.10 (1H, dd, *J*=17.0, 12.9 Hz, H-3α) and 2.68 (1H, dd, *J*=17.0, 2.9 Hz, H-3β). In addition, the splitting patterns and the coupling constants could predict δ 7.30 (2H, d, *J*=8.5 Hz, H-2´/ H-6´) showed ortho coupling with 6.81 (2H, d, *J*=8.5 Hz, H-3´/ H-5´) both δ 7.30 and 6.81 were integrated into two proton, it meant they were symmetric on B-ring. Due to four proton of δ 7.30 and 6.81 were symmetric on B-ring, suggested the right position of δ 5.88 (1H, d, *J*=2.1 Hz, H-6) showed *meta* coupling with 5.87 (1H, d, *J*=2.1 Hz, H-8) on A-ring. The ^{1}H-NMR data of No.7 were compared with those of naringenin (Dávila *et al*., 2013), as summarized in Table 4-17.

Table 4-17 The ^{1}H-NMR data of compound No.7 and naringenin, (Dávila *et al*., 2013)

Position	Compound No.7 (in CD_3OD)	Naringenin (in CD_3OD)
	δ_H (ppm) (multiplicity, *J* in Hz)	**δ_H (ppm) (multiplicity, *J* in Hz)**
2	5.32 (1H, dd, 12.9, 3.1)	5.34 (1H, dd, 12.9, 2.6)
3	3.10 (1H, dd, 17.0, 12.9)	3.11 (1H, dd, 17.1, 12.9)
	2.68 (1H, dd, 17.8, 2.9)	2.69 (1H, dd, 17.1, 2.8)
4	-	-
4a	-	-
5	-	-
6	5.88 (1H, d, 2.1)	5.90 (1H, brs)
7	-	-
8	5.87 (1H, d, 2.1)	5.89 (1H, brs)
8a	-	-
1´	-	-
2´, 6´	7.30 (2H, d, 8.5)	7.32 (2H, d, 8.4)
3´, 5´	6.81 (2H, d, 8.5)	6.82 (2H, d, 8.4)
4´	-	-

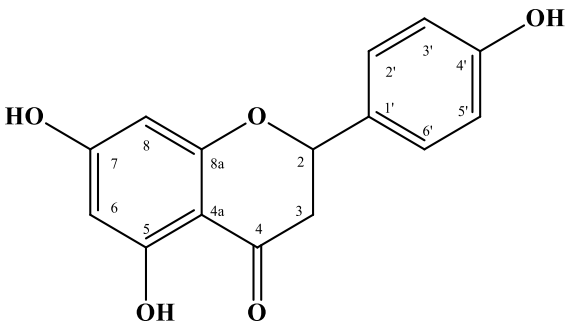

Figure 4-9 The structure of compound No.7 (naringenin)

5.1.8 Structure determination of compound No.8

The compound No.8 was obtained as a yellow powders, soluble in methanol.

The UV spectrum in methanol (Figure H-1) showed absorptions at λ_{max} 205, 279 and 323 nm. The IR spectrum (Figure H-2), showed the absorption bands at 3434, 1647, 1625, 1479, 1450, 1351, 1206 and 1017 cm^{-1}.

Comparison of its ^{1}H- and ^{13}C-NMR spectra with reported data suggested that compound No.8 ($C_{26}H_{28}O_6$) was identical with artocarpin (Figure 4-10).

The ^{1}H-NMR spectrum (Figure H-4) showed thirteen signals, twenty-five protons, including four signals of aromatic proton at δ 6.38 (1H, dd, *J*=8.0, 2.2 Hz) showed *ortho* coupling with 7.06 (1H, d, *J*=8.0 Hz) and showed *meta* coupling with 6.40 (1H, d, *J*=2.4 Hz) and 6.51 (1H, s) could be assigned to H-5´, H-6´ and H-8, respectively, three signals of olefin proton at δ 6.64 (1H, dd, *J*= 23.4, 7.0 Hz) showed *trans* coupling with 6.53 (1H, dd, *J*=16.1, 1.2 Hz) and 5.08 (1H, m) could be assigned to H-15, H-14 and H-10, respectively, three signals of methyl proton at δ 1.57 (3H, d, *J*= 0.98 Hz), 1.09 (6H, s) and 1.07 (3H, s) could be assigned to H-13, H-17/ H-18 and H-12, respectively, one signals of methylene proton at δ 3.09 (2H, d, *J*=6.84 Hz) could be assigned to H-9, one signals of methine proton at δ 2.41 (1H, m) could be assigned to H-16 and one signals of methoxy proton at δ 3.89 (3H, s) could be assigned to 7-OCH_3.

The ^{13}C-NMR spectrum (Figure H-5) showed twenty-five signals, twenty-six carbons, including one signals of carbonyl carbon at δ 183.93 could be assigned to C-4, eighteen signals of aromatic and olefin carbon at δ 164.37, 163.61, 161.94, 159.73, 157.99, 157.78, 142.85, 132.76, 132.39, 122.78, 122.24, 117.23, 113.30, 110.45, 107.98, 105.98, 103.78 and 90.75 could be assigned to C-7, C-2, C-4´, C-5, C-2´, C-8a, C-15, C-3, C-6´, C-10, C-11, C-14, C-1´, C-6, C-3´, C-4a, C-5´and C-8, respectively, one signals of methylene carbon at δ 24.92, one signals of methine carbon at δ 34.43, three signals of methyl carbon at δ 25.83, 23.21 (x2) and 17.64, one signal of methoxyl carbon at δ 56.56 could be assigned to C-9, C-16, C-13, C-17/ C-18, C-12 and 7-OCH_3, respectively. . The ^{1}H and ^{13}C NMR spectra of No.8, together with 2D-NMR, HMQC and HMBC were assigned in the Table 4-18.

Table 4-18 Carbon-proton correlation of compound No.8 observed in the HMQC

Position	δ_C (ppm)	δ_H (ppm) (multiplicity, *J* in Hz)	Correlation with proton (HMBC)
2	163.61	-	H-9, H-6´
3	122.24	-	H-9
4	183.93	-	H-8, H-9
4a	105.98	-	H-8
5	159.73	-	H-14
6	110.45	-	H-8, H-15
7	164.37	-	H-8, 7- OCH_3
8	90.75	6.51 (1H, s)	H-14, H-5´
8a	157.78	-	H-8
9	24.92	3.09 (2H, d, 6.84)	H-9
10	122.78	5.08 (1H, m)	H-13
11	132.76	-	H-9, H-13
12	17.64	1.07 (3H, s)	H-10, H-13
13	25.83	1.57 (3H, d, 0.98)	H-10, H-13
14	117.23	6.53 (1H, dd, 16.1, 1.2)	H-15
15	142.85	6.64 (1H, dd, 23.4,7.0)	H-14, H-15, H-18
16	34.43	2.41 (1H, m)	H-8, H-18
17,18	23.21	1.09 (6H, s)	H-14, 16, 17, 18
1´	113.30	-	H-5´
2´	157.99	-	H-6´
3´	107.98	6.40 (1H, d, 2.4)	H-3´
4´	161.94	-	H-3´, H-6´
5´	103.78	6.38 (1H, dd, 8.0, 2.2)	H-5´,H-6´
6´	132.39	7.06 (1H, d, 8.0)	H-9, H-6´
5-OH	-	-	H-14
7-OCH_3	56.56	3.89 (3H, s)	7-OCH_3

The result obtained from HMBC spectra examination suggesting the right position of two prenyl chains, that connected with C-6 on A-ring (The C-5 and C-8 showed correlation with H-14 and C-6 showed correlation with H-15) and C-3 on C-ring (The C-2, C-3 and C-4 showed correlation with H-9). Moreover, the C-7 carbon showed correlation with -OCH_3 suggesting its position at 7-OCH_3. The spectra were compared with previous reports of artocarpin (Dej-adisai *et al*., 2014) as summarized in Table 4-19.

Table 4-19 The ^{1}H and ^{13}C-NMR data of compound No.8 and artocarpin, (Dej-adisai *et al*., 2014)

Position	Compound No.8 (in CD_3OD)		Artocarpin (in $CDCl_3$)	
	δ_C (ppm)	δ_H (ppm) (multiplicity, *J* in Hz)	δ_C (ppm)	δ_H (ppm) (multiplicity, *J* in Hz)
2	163.61	-	159.3	-
3	122.24	-	120.8	-
4	183.93	-	182.2	-
4a	105.98	-	104.9	-
5	159.73	-	158.6	-
6	110.45	-	109.7	-
7	164.37	-	162.9	-
8	90.75	6.51 (1H, s)	89.4	6.33 (s)
8a	157.78	-	156.0	-
9	24.92	3.09 (2H, d, 6.84)	24.3	3.11 (d, 6.59)
10	122.78	5.08 (1H, m)	121.5	5.14 (t)
11	132.76	-	133.3	-
12	17.64	1.07 (3H, s)	17.6	1.44 (s)
13	25.83	1.57 (3H, d, 0.98)	25.6	1.62 (s)
14	117.23	6.53 (1H, dd, 16.1, 1.2)	115.5	6.55 (dd, 1.22, 16.25)
15	142.85	6.64 (1H, dd, 23.4,7.0)	142.6	6.69 (dd, 7.07, 16.23)
16	34.43	2.41 (1H, m)	33.0	2.46 (m)

Table 4-19 The ^{1}H and ^{13}C-NMR data of compound No.8 and artocarpin, (Dejadisai *et al*., 2014) (continued)

Position	Compound No.8 (in CD_3OD)		Artocarpin (in CD_3OD)	
	δ_C (ppm)	δ_H (ppm) (multiplicity, *J* in Hz)	δ_C (ppm)	δ_H (ppm) (multiplicity, *J* in Hz)
17, 18	23.21	1.09 (6H, s)	22.6	1.09 (d, 6.84)
1´	113.30	-	112.5	-
2´	157.99	-	155.1	-
3´	107.98	6.40 (1H, d, 2.4)	103.8	6.48 (s)
4´	161.94	-	158.9	-
5´	103.78	6.38 (1H, dd, 8.0, 2.2)	108.3	6.50 (d, 2.2)
6´	132.39	7.06 (1H, d, 8.0)	131.5	7.19 (d, 9.03)
5-OH	-	-	-	13.50 (s)
7-OCH_3	56.56	3.89 (3H, s)	55.9	3.86 (s)

Therefore, on the basis above evidences, the structure of No.8 was established as artocarpin (Figure 4-10)

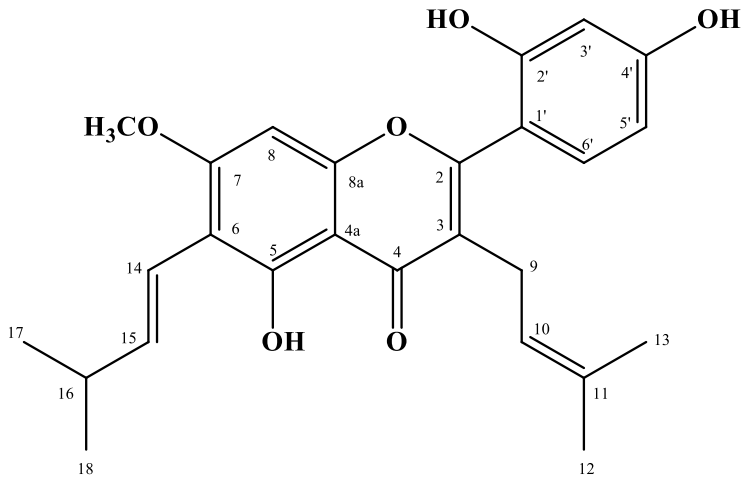

Figure 4-10 The structure of compound No.8 (artocarpin)

5.2 Isolated compounds from *Streblus taxoides*

5.2.1 Structure determination of compound No.9

The compound No.9 was obtained as a colorless needles, soluble in chloroform.

The UV spectrum in chloroform (Figure I-1) demonstrated absorption maximum at λ_{max} 216 and 226 nm. The IR spectrum (Figure I-2) exhibited maximum absorption bands at 3435, 2936 and 2858 cm^{-1}.

Comparison of its ^{1}H-NMR spectra with reported data suggested that compound No.9 was identical with mixture of *β*-sitosterol and stigmasterol (Figure 4-11).

The ^{1}H-NMR (Figure I-4) showed three signals olefin proton at δ 5.32 (m), 5.12 (dd, *J*=15.0, 8.6 Hz) and 4.99 (dd, *J*=15.0, 8.6 Hz), methine proton at δ 3.50 (m), methane and methyl protons (the remaining proton signals appeared at δ 0.65-2.23). The spectra were compared with previous reports of mixture of β-sitosterol and stigmasterol (Dej-adisai *et al*., 2014) as summarized in Table 4-20.

Table 4-20 The ^{1}H and ^{13}C-NMR data of compound No.9 and Mixture of *β*-sitosterol and stigmasterol (Dej-adisai *et al*., 2014)

Position	**Compound No.9 (in $CDCl_3$)**	**Mixture of *β*-sitosterol and stigmasterol (in $CDCl_3$)**
	δ_H (ppm) (multiplicity, *J* in Hz)	**δ_H (ppm) (multiplicity, *J* in Hz)**
3	3.50 (m)	3.54 (m)
5	5.32 (m)	5.36 (d)
18	0.65, 0.67 (s)	0.70, 0.71 (s)
19	0.98 (s)	1.02 (s)
21	0.82, 0.99 (d)	0.93, 1.09 (d)
22	4.99 (dd)	5.02 (dd)

Table 4-20 The ^{1}H and ^{13}C-NMR data of compound No.9 and Mixture of *β*-sitosterol and stigmasterol (Dej-adisai *et al.*, 2014) (continued)

Position	Compound No.9 (in $CDCl_3$)	Mixture of *β*-sitosterol and stigmasterol (in $CDCl_3$)
	δ_H (ppm) (multiplicity, *J* in Hz)	δ_H (ppm) (multiplicity, *J* in Hz)
23	5.12 (dd)	5.17 (dd)
26	0.89, 0.78 (d)	0.94, 0.79 (d)
27	0.89, 0.79 (d)	0.94, 0.81(d)
29	0.81 (dd), 0.80 (t)	0.83 (dd), 0.80 (t)

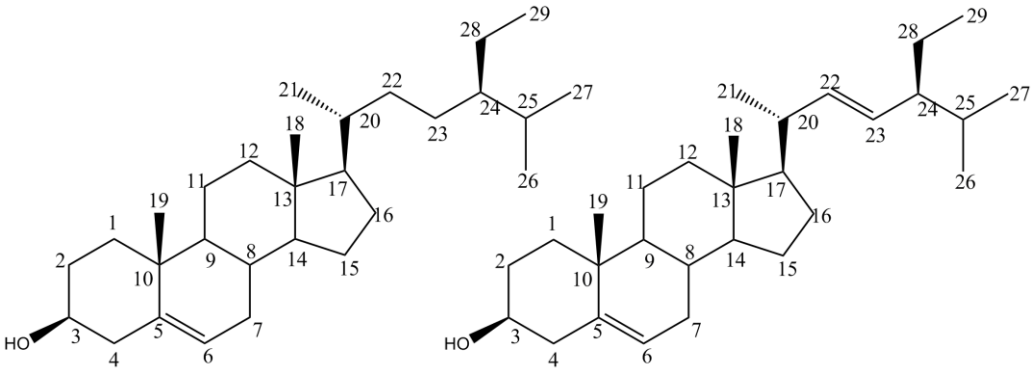

β-sitosterol stigmasterol

Figure 4-11 The structures of compound No.9 (Mixture of *β*-sitosterol and stigmasterol)

5.2.2 Structure determination of compound No.10

The compound No.10 was obtained as a brown amorphous powder, soluble in methanol.

The UV spectrum in methanol (Figure J-1) showed absorptions at λ_{max} 317 and 329 nm. The IR spectrum (Figure J-2), showed the absorption bands at 3216, 1620, 1489, 1444, 1351, 1308, 1150, 1002 and 825 cm^{-1}.

Compound No.10 gave a molecular ion at 326 *m/z* in the EIMS (Figure J-3), corresponding to $C_{19}H_{18}O_5$.

Comparison of its ^{1}H- and ^{13}C-NMR spectra with reported data suggested that compound No.10 was identical with ω-hydroxymoracin C (Figure 4-12), the new compound.

The ^{1}H-NMR spectrum of compound No.10 (Figure J-4), showed five signals in the aromatic region. These aromatic signals appeared δ 7.32 (1H, d, *J*=8.3 Hz, H-4), 6.87 1H, d, *J*=2.2 Hz, H-7), 6.82 (1H, d, *J*=0.97 Hz, H-3), 6.76 (2H, s, H-2´/ H-6´) and 6.72 (1H, dd, *J*=8.3, 2.2 Hz, H-5) were identified as a main structure of moracin C (Figure 4-10**)** compared with previous reported (Kim *et al*., 2012) as showed in the Table 4-21.

The ^{1}H-NMR at δ 1.81 (3H, s, H-4´´), 3.38 (2H, d, *J*=7.3 Hz, H-1´´), 3.90 (2H, s, H-5´´) and 5.55 (1H, dt, *J*=7.3, 1.2 Hz, H-2´´) were identified as a hydroxy prenyl group compared with previous reported, ω-Hydroxymoracin N (Figure 4-12**)** (Matsuyama *et al*., 1991) as shown in the Table 4-22.

Table 4-21 The ^{1}H-NMR (500 MHz) data of compound No.10 and the main structure of moracin C (Kim *et al*., 2012)

Position	Compound No.10 (in CD_3OD)		The main structure of moracin C (in CD_3OD)	
	δ_C (ppm)	δ_H (ppm) (multiplicity, *J* in Hz)	δ_C (ppm)	δ_H (ppm) (multiplicity, *J* in Hz)
2	156.46	-	156.6	-
3	101.33	6.82 (1H, d, 0.9)	101.3	6.82 (1H, d, 0.9)
3a	123.19	-	123.4	-
4	121.77	7.32 (1H, d, 8.3)	121.9	7.32 (1H, d, 8.4)
5	113.12	6.72 (1H, dd, 8.3, 2.2)	113.2	6.72 (1H, dd, 8.4, 2.1)
6-OH	157.17	-	157.3	-
7	98.45	6.87 (1H, d, 2.2)	98.6	6.88 (1H, brd, 2.1)
7a	156.64	-	156.8	-
1´	130.45	-	130.4	-
2´,6´	103.81	6.76 (2H, d, s)	103.8	6.78 (2H, s)
3´,5´-OH	157.61	-	157.7	-
4´	116.26	-	117.0	-

Table 4-22 The ^{1}H-NMR (500 MHz) data of hydroxy prenyl group of compound No.10 (in CH_3OD) and hydroxy prenyl group of ω-Hydroxymoracin N, (Matsuyama *et al*., 1991)

Position	Compound No.10 (in CD_3OD)	Hydroxy prenyl group of ω-Hydroxymoracin N (in CD_3COCD_3)
	δ_H (ppm) (multiplicity, *J* in Hz)	δ_H (ppm) (multiplicity, *J* in Hz)
1´´	3.38 (2H, d, 7.3)	3.44 (2H, d, 7.4)
2´´	5.55 (1H, dt, 7.3, 1.2)	5.66 (lH, t, 6.8)
4´´	1.81 (3H, s)	1.76 (3H, s)
5´´	3.90 (2H, s, H-5")	3.98 (2H, d, 6.0)

The ^{13}C-NMR spectrum (Figure J-5), showed seventeen signals appeared δ 157.61 (x2), (C-3′ ,5′-OH), 157.17 (C-6-OH), 156.64 (C-7a), 156.46 (C-2), 135.07 (C-3′′), 130.45 (C-1′), 125.89 (C-2′′), 123.19 (C-3a), 121.77 (C-4), 116.27 (C-4′), 113.12 (C-5), 103.81 (x2), (C-2′, 6′), 101.33 (C-3), 98.45 (C-7), 69.32 (C-5′′), 22.95 (C-1′′) and 13.83 (C-4′′).

The HMQC (Figure J-6) revealed the correction between the directly coupled ^{1}H and ^{13}C nuclei and HMBC (Figure J-7) revealed the long-range C-H correlation of compound No.10 are summarized in Table 4-23.

Table 4-23 Carbon-proton correlation of compound No.10 observed in the HMQC and HMBC spectrum

Position	δ_C (ppm)	δ_H (ppm) (multiplicity, *J* in Hz)	Correlation with proton (HMBC)
2	156.46	-	H-2′/ 6′
3	101.33	6.82 (1H, d, 0.9)	H-4
3a	123.19	-	H-3, H-5, H-7
4	121.77	7.32 (1H, d, 8.3)	-
5	113.12	6.72 (1H, dd, 8.3, 2.2)	H-7
6	157.17	-	H-4, H-5
7	98.45	6.87 (1H, d, 2.2)	H-5
7a	156.64	-	H-3, H-4
1′	130.45	-	-
2′, 6′	103.81	6.78 (2H, s)	H-2′/ 6′
3′, 5′	157.61	-	H-2′/ 6′
4′	116.26	-	H-2′/ 6′, H-1′′, H-2′′
1′′	22.95	3.38 (2H, brd, 7.32)	H-1′′, H-2′′
2′′	125.89	5.55 (1H, m)	H-1′′, H-4′′, H-5′′
3′′	135.07	-	H-1′′, H-4′′, H-5′′
4′′	13.83	1.81 (3H, s)	H-2′′, H-5′′
5′′	69.32	3.90 (2H, s)	H-1′′, H-2′′, H-4′′

Based on the information obtained from the HMQC and HMBC spectrum could observed the long-range C-H correlations of compound No.10. The C-6 carbon suggested its position with showed correlation with H-5 and H-4. The C-3a carbon showed correlation with H-3, H-5 and H-7. The C-7a carbon showed correlation with H-3 and H-4. The C-2 carbon suggested its position that showed correlation with H-3 and H-6′ on B-ring. The C-3′′ carbon showed correlation with H-1′′, H-4′′ and H-5′′ and the C-2′′ carbon showed correlation with H-1′′ and H-2′′ suggested the right position of olefin carbon at C-2′′ and C3′′ in hydroxy prenyl group. In addition, the C-4′ carbon showed correlation with H-2′, H-6′, H-1′′ and H-2′′ suggested the right position of hydroxy prenyl group at C-4′.

Therefore, on the basis above evidences, the structure of No.10 was established as ω-hydroxymoracin C (Figure 4-12), the new compound.

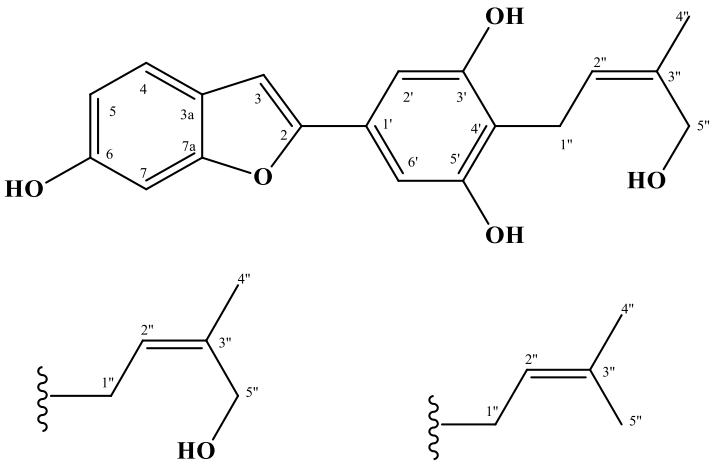

(ω-hydroxy prenyl) (prenyl)

R = H, R′ = H; Moracin M

R = H, R′ = prenyl; Moracin C

R = ω-hydroxy prenyl, R′ = H; ω-hydroxymoracin N

R = H, R′ = ω-hydroxy prenyl; ω-hydroxymoracin C

Figure 4-12 Structures of compound No.10 (ω-hydroxymoracin C), ω-hydroxymoracin N, Moracin M and Moracin C

5.2.3 Structure determination of compound No.11

The compound No.11 was obtained as a cream needles, soluble in methanol and dimethyl sulfoxide.

The UV spectrum in methanol (Figure K-1) showed absorptions at λ_{max} 317 and 329 nm. The IR spectrum (Figure K-2), showed the absorption bands at 3246, 2925, 1613, 1489, 1292 and 1149 cm^{-1}.

Comparison of its ^{1}H- and ^{13}C-NMR spectra with reported data suggested that compound No.11 ($C_{14}H_{10}O_4$) was identical with moracin M (Figure 4-13).

The ^{1}H-NMR spectrum of compound No.11 (Figure K-4), showed the signals at δ 9.53 (1H, brs) and 9.38 (2H, brs) could be assigned to 6-OH and 3′/5′-OH, respectively. Moreover, it showed six aromatic signals appeared at δ 7.38 (1H, d, *J*=8.5 Hz), 7.06 (1H, d, *J*=0.98 Hz), 6.91 (1H, dd, *J*=2.2, 0.97 Hz), 6.72 (1H, dd, *J*=8.5, 2.2 Hz), 6.67 (2H, d, *J*=1.9 Hz) and 6.20 (1H, t, *J*=2.2 Hz) could be assigned at H-4, H-3, H-7, H-5, H-2′/ H-6′ and H-4′, respectively.

The ^{13}C-NMR spectrum (Figure K-5), showed twelve signals appeared at δ 158.94 (×2), 155.87, 155.42, 154.12, 131.82, 121.25, 120.94, 112.61, 102.80, 102.47 (×2), 101.69 and 97.62.

Based on the information obtained from the ^{1}H-NMR spectrum, the splitting patterns and the coupling constants could predict the benzofuran ring and aromatic ring. 1 proton of the H-4′ showed triplet pattern with coupling constant 2.1 Hz matching with 2 proton of the H-2′, H-6′ showed doublet pattern with coupling constant 1.9 Hz could be B-ring. The H-5 showed doublet of doublet pattern with coupling constant 8.5 and 2.2 Hz (*ortho* and *meta*) correspond with the the H-4 (1H, d, *J*=8.5Hz) and H-7 (1H, dd, *J*=2.2, 0.97 Hz). Moreover, the H-3 showed doublet pattern and long-range coupling with H-7, those were the pattern of benzofuran ring. The ^{1}H and ^{13}C-NMR data of No.11 were compared with those of moracin M (Dej-adisai *et al*., 2016), as summarized in Table 4-24.

Table 4-24 The ^{1}H- and ^{13}C-NMR data of compound No.11 and moracin M, (Dejadisai *et al.*, 2016)

Position	Compound No.11 in DMSO-d6		Moracin M in DMSO-d6	
	δ_C (ppm)	δ_H (ppm) (multiplicity, *J* in Hz)	δ_C (ppm)	δ_H (ppm) (multiplicity, *J* in Hz)
2	154.12	-	154.13	-
3	101.69	7.06 (1H, d, 0.9)	101.69	7.05 (1H, d, 0.9)
3a	120.94	-	120.94	-
4	121.25	7.38 (1H, d, 8.5)	121.26	7.37 (1H, d, 8.2)
5	112.61	6.72 (1H, dd, 8.5, 2.2)	112.61	6.72 (1H, dd, 8.4, 2.0)
6-OH	155.87	9.53 (1H, brs)	155.88	9.95 (1H, brs)
7	97.62	6.91 (1H, dd, 2.2, 0.7)	97.62	6.91 (1H, ddd, 2.0, 0.9)
7a	155.42	-	155.42	-
1´	131.82	-	131.82	-
2´,6´	102.47	6.67 (2H, d, 1.9)	102.47	6.67 (1H, d, 2.0)
3´,5´-OH	158.94	9.38 (2H, brs)	158.94	9.39 (2H, brs)
4´	102.80	6.20 (1H, t, 2.2)	102.81	6.20 (1H, t, 2.0)

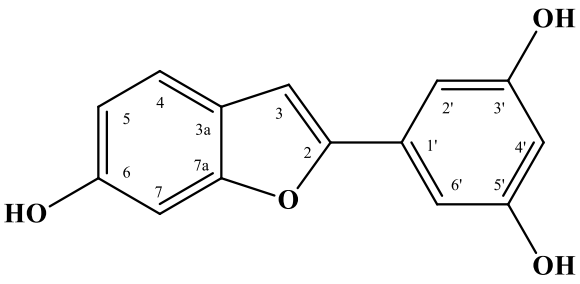

Figure 4-13 Structure of compound No.11 (moracin M)

5.2.4 Structure determination of compound No.12

The compound No.12 was obtained as a brown amorphous powder, soluble in methanol.

The UV spectrum in methanol (Figure L-1) showed absorptions at λ_{max} 317 and 329 nm. The IR spectrum (Figure L-2), showed the absorption bands at 3216, 2693, 1606, 1489, 1357 and 1150 cm^{-1}.

Comparison of its ^{1}H- and ^{13}C-NMR spectra with reported data suggested that compound No.12 ($C_{19}H_{18}O_4$) was identical with moracin C (Figure 4-14).

The ^{1}H-NMR spectrum of compound No.12 (Figure L4), showed the signals at δ 9.51 (1H, s) and 9.28 (2H, s) could be assigned to 6-OH and 3′/5′-OH, respectively. Moreover, it showed five aromatic signals appeared at δ 7.37 (1H, d, *J*=8.2 Hz), 6.90 (1H, brd, *J*=1.9 Hz), 6.89 (1H, d, *J*=0.7 Hz), 6.73 (1H, s) and 6.71 (1H, dd, *J*=8.3, 1.9 Hz) could be assigned at H-4, H-7, H-3, H-2′/ H-6′ and H-5, respectively.

Based on the information obtained from the ^{1}H -NMR spectrum, the splitting patterns and the coupling constants could predict the benzofuran ring, aromatic ring and prenyl group. The H-5 showed doublet of doublet pattern with coupling constant 8.3 and 1.9 Hz (ortho and meta) correspond with the the H-4 (1H, d, *J*=8.2 Hz) and H-7 (1H, brd, *J*=1.9 Hz), the H-3 showed doublet pattern and long-range coupling with coupling constant 0.7 Hz, those are the pattern of benzofuran ring. In addition, the H-2′ and H-6′ showed singlet pattern at δ_H 6.73 (2H, s), it meant they were symmetric proton in B-ring. Moreover, it showed the pattern of prenyl group, 1 proton of the H-5′′ showed multiplet pattern with 2 proton of methelene proton at H-1′′, δ 3.19 (2H, brd, *J*=6.8Hz) and 2 methyl protons, δ 1.60 (3H, brs) and 1.70 (3H, brs). The ^{1}H and ^{13}C-NMR data of No.12 was compared with those of moracin C (Kim *et al*., 2012) as summarized in Table 4-25.

The ^{13}C-NMR spectrum (Figure L-5), showed seventeen signals appeared δ 156.39 (×2), 155.69, 155.30, 154.34, 129.75, 128.14, 123.31, 121.09, 120.99, 115.09 112.48, 102.43 (×2), 100.65, 97.55, 25.64, 22.21, and 17.84.

Table 4-25 The ^{1}H- and ^{13}C-NMR data of compound No.12 and moracin M, (Kim *et al*., 2012)

	Compound No.12 in DMSO-d6		**Moracin C in CH_3OD**	
	δ_C (ppm)	**δ_H (ppm) (multiplicity, *J* in Hz)**	**δ_C (ppm)**	**δ_H (ppm) (multiplicity, *J* in Hz)**
2	154.34	-	156.6	-
3	100.65	6.89 (1H, d, 0.7)	101.3	6.82 (1H, d, 0.9)
3a	121.09	-	123.4	-
4	120.99	7.37 (1H, d, 8.2)	121.9	7.32 (1H, d, 8.4)
5	112.48	6.71 (1H, dd, 8.3, 1.9)	113.2	6.72 (1H, dd, 8.4, 2.0)
6	155.69	9.51 (1H, OH)	157.3	-
7	97.55	6.90 (1H, brd, 1.9)	98.6	6.88 (1H, brd, 2.1)
7a	155.30	-	156.8	-
1′	128.14	-	130.4	-
2′, 6′	102.43	6.73 (2H, s)	103.9	6.78 (2H, s)
3′, 5′	156.39	9.29 (2H, OH)	157.7	-
4′	115.09	-	117.0	-
1′′	22.21	3.19 (2H, brd, 6.8)	23.4	3.32 (2H, brd, 6.9)
2′′	123.31	5.17 (1H, m)	124.5	5.26 (1H, brt, 6.9)
3′′	129.75	-	131.5	-
4′′	25.64	1.70 (3H, brs)	26.2	1.78 (3H, s)
5′′	17.84	1.60 (3H, brs)	18.5	1.66 (3H, s)

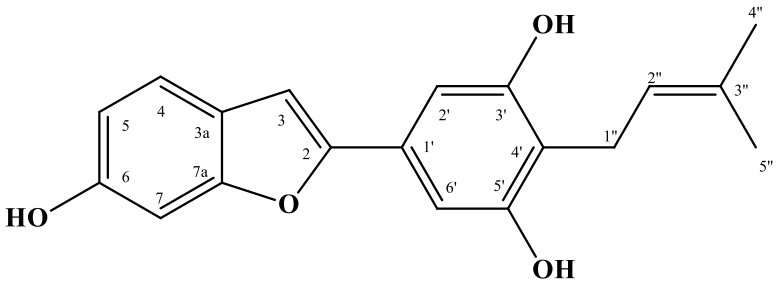

Figure 4-14 Structure of compound No.12 (moracin C)

5.2.5 Structure determination of compound No.13

The compound No.13 was obtained as a brown amorphous powder, soluble in methanol.

The UV spectrum in methanol (Figure M-1) showed absorptions at λ_{max} 205, 208 and 276 nm. The IR spectrum (Figure M-2), showed the absorption bands at 3435, 1616, 1521, 1468, 1285 and 1160 cm^{-1}.

Through comparison with earlier reported ^{1}H- and ^{13}C-NMR data, compound No.13 ($C_{14}H_{14}O_4$) was identified as 3, 4, 3′, 5′- tetrahydroxy-bibenzyl (Figure 4-15).

From the ^{1}H-NMR spectrum (Figure M-4), the presence of the following features was indicated there are six olefin protons, devided into two rings, the proton at δ 6.48 (1H, dd, *J*=8.0, 2.2 Hz) were assignable to H-6, which coupling with H-5 (δ 6.64, 1H, d, *J*=8.0 Hz) and H-2 (δ 6.60, 1H, d, *J*=1.9 Hz) with *ortho* and *meta* coupling, respectively. Moreover, it showed one signal of four methylene protons at δ 2.67 (4H, m) were assignable to H-α and H-α′.

Examination of the ^{13}C-NMR spectrum (Figure M-5), showed twelve signals appeared at δ 159.29 (x2), 146.01, 145.70, 144.26, 135.00, 120.70, 116.24, 108.04 (x2), 101.15, 39.51 and 38.28.

All protonated carbons were assigned by analysis of the HMQC spectrum (Figure M-6) and the long-range C-H correlations of compound No.13 could be observed from HMBC spectrum (Figure M-8), The information from the HMQC and HMBC spectra of compound No.13 were assigned is showed in the Table 4-26.

Table 4-26 Carbon-proton correlation of compound No.13 observed in the HMQC and HMBC spectrum

	δ_C (ppm)	δ_H (ppm) (multiplicity, *J* in Hz)	Correlation with proton (HMBC)
1	135.00	-	H-5, H-α
2	116.24	6.60 (1H, d, 1.9)	H-6, H-α
3	146.01	-	H-2, H-6
4	145.70	-	H-2, H-5, H-6
5	116.60	6.64 (1H, d, 8.0)	H-6
6	120.70	6.48 (1H, dd, 8.0, 2.2)	H-2, H-6, H-α
α	38.28	2.66 (1H, 2, m)	H-2, H-6, H-α´
α´	39.51	2.67 (1H, 2, m)	H-2, H-2´/ 6´, H-α
1´	144.26	-	H-α´
2´, 6´	108.04	6.12 (2H, d, 2.4)	H-4´, H-2´/ 6´
3´, 5´	159.29	-	H-4´, H-2´/ 6´
4´	101.15	6.07 (1H, t, 2.2)	H-2´/ 6´

The result obtained from HMBC spectra examination suggested that the assignments of C-α and C-α´, C-1 and C-1´. All result from experiment confirmed the structure of compound No.13 was 3, 4, 3´, 5´- tetrahydroxy-bibenzyl. The ^{13}C-NMR data were compared with those 3, 4, 3´, 5´- tetrahydroxy-bibenzyl (Mannila *et al*., 1993), as summarized in Table 4-27.

Table 4-27 The ^{1}H- and ^{13}C-NMR data of compound No.13 and 3, 4, 3´, 5´-tetrahydroxy-bibenzyl (Mannila *et al*., 1993)

Position	Compound No.13 in DMSO-d6 δ_C (ppm)	3, 4, 3´, 5´- tetrahydroxy-bibenzyl in $(CD_3)_2CO$ δ_C (ppm)
1	135.00	134.9
2	116.24	116.3
3	146.01	146.2
4	145.70	145.6
5	116.60	116.7
6	120.70	120.8
α	38.28	38.1
α´	39.51	39.3
1´	144.26	144.3
2´, 6´	108.04	108.1
3´, 5´	159.29	159.6
4´	101.15	101.5

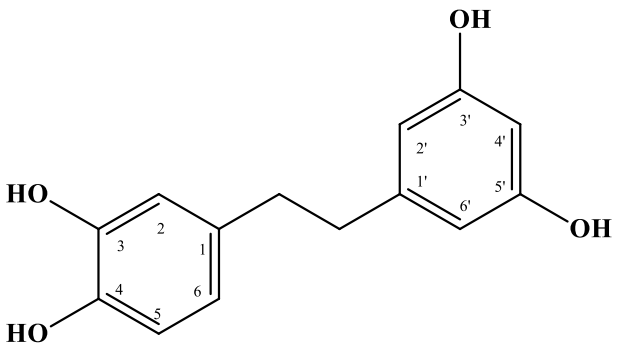

Figure 4-15 Structure of compound No.13 (3, 4, 3´, 5´-tetrahydroxybibenzyl)

5.2.6 Structure determination of compound No.14

The compound No.14 was obtained as a brown needle, soluble in methanol.

The UV spectrum in methanol (Figure N-1) showed absorptions at λ_{max} 202, 220, 305 and 325 nm. The IR spectrum (Figure N-2), showed the absorption bands at 3368, 1600, 1520, 1444, 1285 and 1160 cm^{-1}.

Comparison of its ^{1}H-NMR spectrum with reported data suggested that compound No.14 ($C_{14}H_{12}O_4$) was identical with piceatannol (Figure 4-16).

The information obtained from the ^{1}H-NMR spectrum, the splitting patterns and the coupling constants could predict in to two aromatic rings. On A-ring, the H-6 showed doublet of doublet pattern with coupling constant 8.3 and 1.9 Hz (*ortho* and *meta*) correspond with the H-5 (1H, d, *J*=8.3 Hz) and H-2 (1H, brd, *J*=1.9 Hz) and on B-ring, , the H-4´ showed triplet pattern at δ 6.15 (2H, t, *J*=2.2 Hz) with the H-2´ and H-6´ with showed doublet pattern at δ 6.42 (2H, d, *J*=2.2 Hz), it meant they were symmetric. Moreover, those two rings connected with olefin proton, the H-α showed doublet pattern with coupling constant 16.1 Hz correspond with the the H-α´, that is the trans coupling. The ^{1}H-NMR data of No.14 were compared with those piceatannol (Thakkar, *et al*. 1993) as summarized in Table 4-28.

Table 4-28 The ^{1}H- and ^{13}C-NMR data of compound No.14 and piceatanonl (Thakkar, *et al*. 1993).

Compound No.14 (in DMSO) **δ_H (ppm)** **(multiplicity, *J* in Hz)**	**Piceatannol (in $(CD_3)_2CO$)** **δ_H (ppm)** **(multiplicity, *J* in Hz)**
6.15 (1H, t, 2.2)	6.25 (1H, dd, 2.1, 1.0)
6.42 (2H, d, 2.2)	6.52 (2H, d, 2.1, 1.0)
6.72 (1H, d, 8.3)	6.80 (1H, d, 8.1)
6.73 (1H, d, 16.1)	6.82 (1H, d, 16.1)
6.82 (1H, dd, 8.3, 1.9)	6.90 (1H, dd, 8.1, 2.1)
6.87 (1H, d, 16.1)	6.95 (1H, d, 16.1)
6.96 (1H, d, 1.9)	7.07 (1H, d, 2.1)

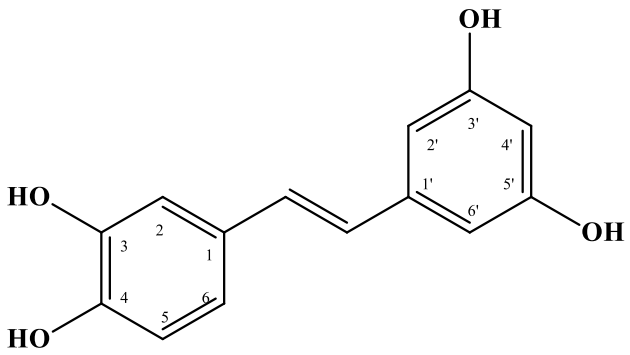

Figure 4-16 Structure of compound No.14 (piceatannol)

6. Bioactivities determination of isolated compounds

6.1 Enzymetic antityrosinase activity

Tyrosinase inhibitory activity of isolated compounds from *A. chama* and *S. taxoides* were determined by Dopachrom method. 3, 4, 3′, 5′-tetrahydroxybibenzyl (No.13) showed highest activity against tyrosinase enzyme with IC_{50} 35.65 μg/mL followed by artocarpanone (No.6), moracin M (No.11) and homoeriodictyol (No.1) with IC_{50} 38.78, 47.34 and 52.18 μg/mL, respectively. While, 3′-farnesyl-apigenin (No.2), ω-hydroxymoracin C (No.10), moracin C (No.12) and piceatannol (No.14) against moderate tyrosinase activity with IC_{50} 135.70, 109.64, 128.67 and 149.73 μg/mL, respectively. Six isolated compounds; isocycloartobiloxanthone (No.3), 3-(hydroxyprenyl) isoetin (No.4), 3-prenyl-6,8,2′,5′-tetrahydroxy-4′-methoxyflavone (No.5), naringenin (No.7), artocarpin (No.8) and mixture of *β*-sitosterol and stigmasterol (No.9) showed IC_{50} higher than 200 μg/mL. The result showed in Table 4-29.

Table 4-29 IC_{50} of isolated compounds from *A. chama* and *S. taxoides* on tyrosinase inhibitory activity

Compound	IC_{50} (μg/mL)
homoeriodictyol (No.1)	52.18
3′-farnesyl-apigenin (No.2)	135.70
isocycloartobiloxanthone (No.3)	>200
3-(hydroxyprenyl) isoetin (No.4)	>200
3-prenyl-6,8,2′,5′-tetrahydroxy-4′-methoxyflavone (No.5)	>200
artocarpanone (No.6)	38.78
naringenin (No.7)	>200
artocarpin (No.8)	>200
Mixture of *β*-sitosterol and stigmasterol (No.9)	>200
ω-hydroxymoracin C (No.10)	109.64

Table 4-29 IC_{50} of isolated compounds from *A. chama* and *S. taxoides* on tyrosinase inhibitory activity (continued)

Compound	IC_{50} (µg/mL)
moracin M (No.11)	47.34
moracin C (No.12)	128.67
3, 4, 3´, 5´-tetrahydroxybibenzyl (No.13)	35.65
piceatannol (No.14)	149.73
Kojic acid[P]	38.67
Water extract of *A. lakoocha*[P] wood	8.73

[P] = positive control

6.2 Cell viability

The initial purpose was to test whether sample extracts inhibited melanogenesis in cultured melanocytes without affecting cell growth. Then, the cell viability was measured first. The results indicated that all sample extracts were not considerable cytotoxic in B16-F1 melanoma cells. Cell viability was still more than 80% at the highest concentration 50 µg/mL. The result showed in Figure 4-17.

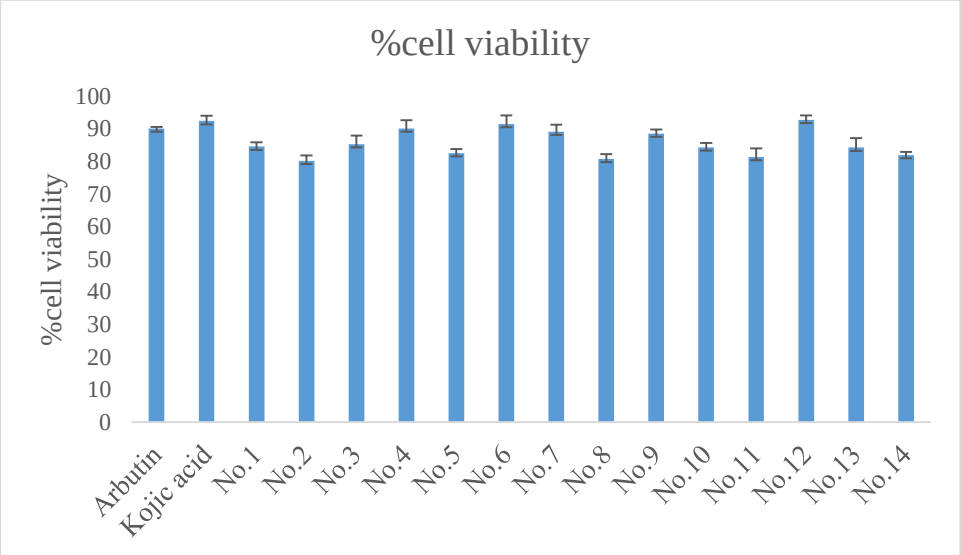

Figure 4-17 Cell viability of isolated compounds at the concentration 50 µg/mL

6.3 Intracellular antityrosinase activity and melanin content

The isolated compounds at concentration as 50 μg/mL were study on the effect of intracellular antityrosinase activity and melanin content on B16F1 melanoma cells. The supernatant were measured antityrosinase activity, the result showed that No.6 (artocarpanone), No.10 (ω-hydroxymoracin C), No.11 (moracin M) and No.12 (moracin C) exhibited antityrosinase activity (Figure 4-18A). Moreover the melanin content showed inverse result with antityrosinase activity; the increasing of antityrosinase activity can decrease the amount of melanin content (Figure 4-18B).

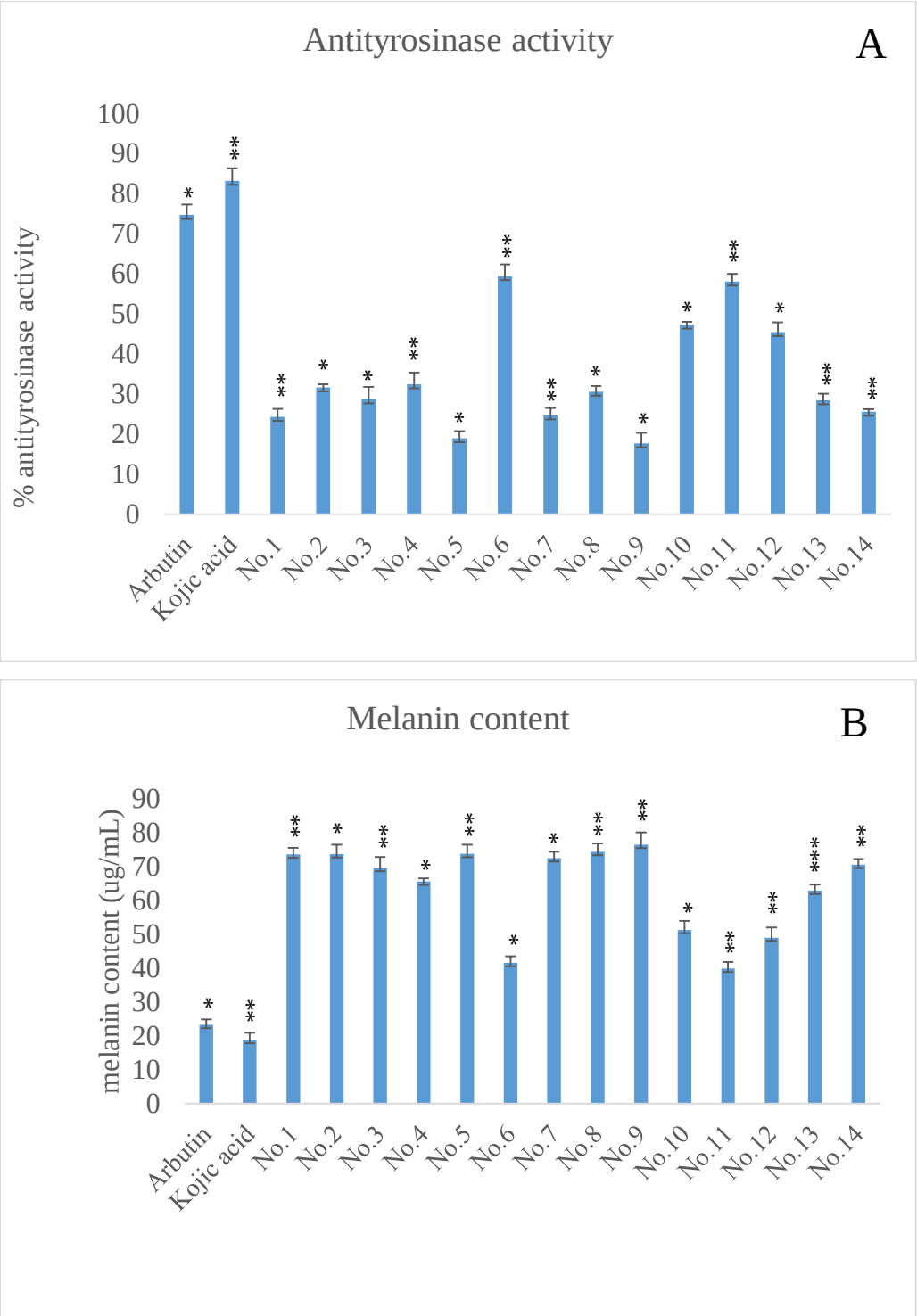

Figure 4-18 Intracellular antityrosinase activity and melanin content

Data are expressed as mean ± SD from three independent experiments. $^{*}p$ <0.05, $^{**}p$ <0.01 and $^{***}p$ <0.001 indicate a significant difference from positive control group. Positive control = rbutin and kojic acid

Homoeriodictyol (No.1), artocarpanone (No.6) and naringenin(No.7) were flavanone group (Figure 4-19), while, isocycloartobiloxanthone (No.3), 3´-farnesyl-apigenin (No.2), 3-(hydroxylprenyl) isoetin (No.4), 3-prenyl-5,7,2´,5´-tetrahydroxy-4´-methoxyflavone (No.5) and artocarpin (No.8) were flavone group (Figure 4-20). Homoeriodictyol (No.1), artocarpanone (No.6) and 3´-farnesyl-apigenin (No.2) showed activity against directly tyrosinase enzyme. The related 4-substituted resorcinols, suggested that compounds with the 4-substituted resorcinol skeleton have potent tyrosinase inhibitory activity (Kim and Uyama, 2005). The additional group, farnesyl at C-3´ position not affect compared with the activity value of apigenin (without farnesyl at C-3´ position) (Ye *et al*., 2010). While, the presence or absence of substituent at C-3 appears to be critical for the tyrosinase inhibitory activity of favone group (Likhitwitayawuid *et al*., 2000). Thus, 3-(hydroxyprenyl) isoetin, 3-prenyl-5,7,2´,5´-tetrahydroxy-4´-methoxyflavone and artocarpin which were substituted with prenyl and isocycloartobiloxanthone which was substituted with cyclohexane at C-3 position showed inactive for antityrosinase activity.

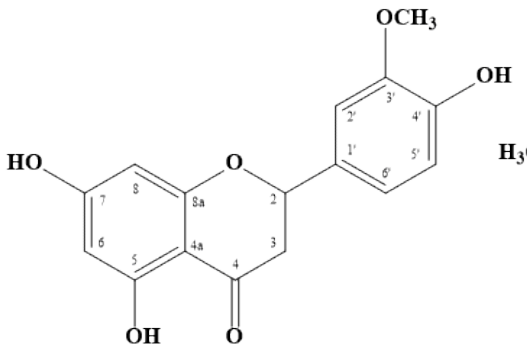

Homoeriodictyol

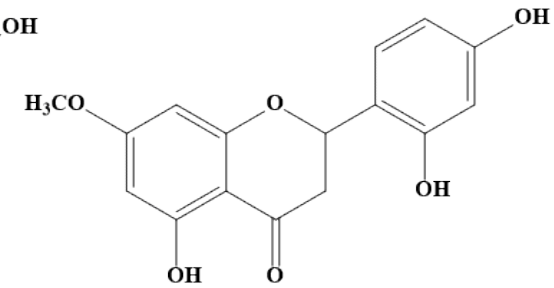

Artocarpanone

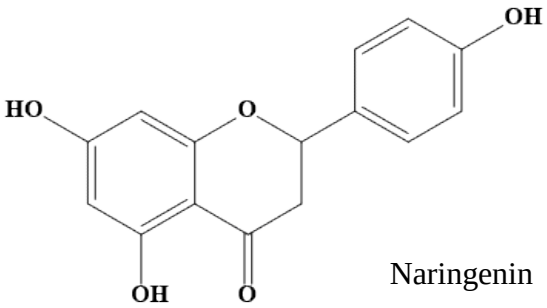

Naringenin

Figure 4-19 Structures of flavanone group

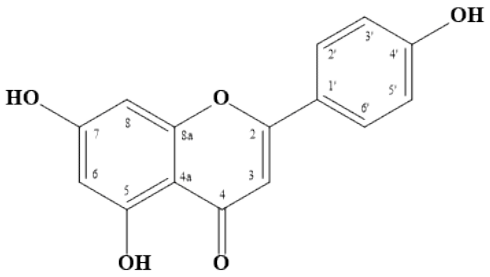

Apigenin

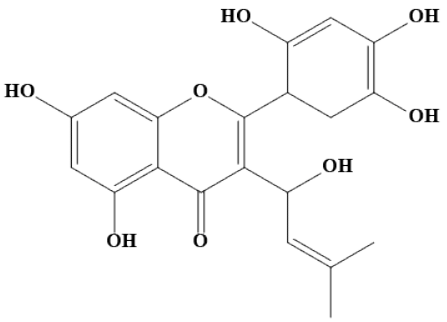

3-(Hydroxyprenyl) isoetin

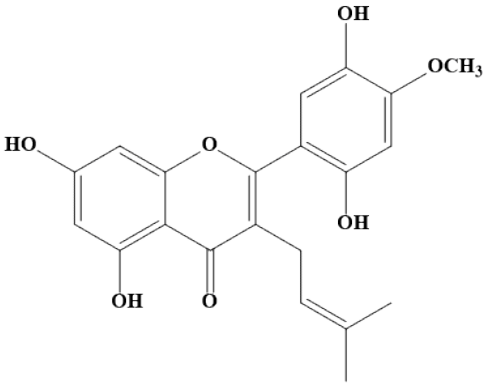

3-Prenyl-5,7,2´,5´tetrahydroxy-4´-methoxyflavone

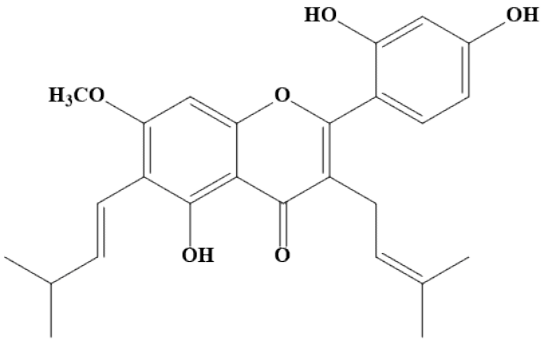

Artocarpin

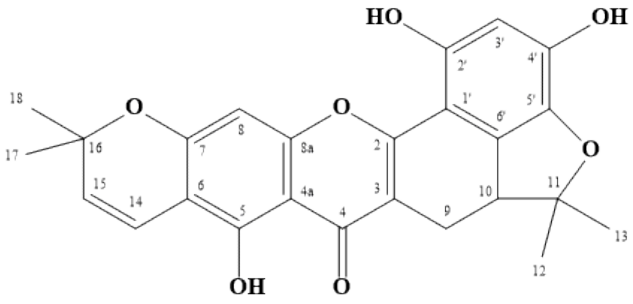

Isocycloartobiloxanthone

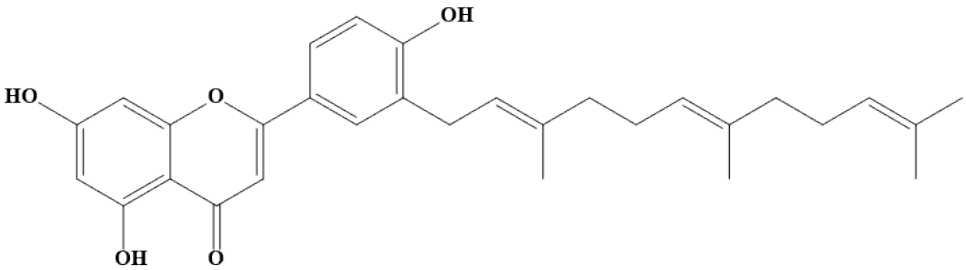

3´-Farnesyl-apigenin

Figure 4-20 Structures of flavone group

3, 4, 3´, 5´-Tetrahydroxybibenzyl (No.13) and piceatannol (No.14) are stilbene group (Figure 4-21). Stilbene group showed inhibitory against tyrosinase enzyme because it was substituted with polyhydroxy group, expectially substituent at C-2, C-4, C-3´ and C-5´ and 4-substituted resorcinol structure is important for the tyrosinase inhibitory activity of several stilbenes (Likhitwitayawuid, 2008). Due to oxyresveratrol consist with 4-substituted resorcinol structure and substituent with hydroxy group at C-2, C-4, C-3´ and C-5´ while piceatannol was substituted with hydroxy group at C-3, C-4, C-3´ and C-5´. So oxyresveratrol showed antityrosinase activity higher than piceatannol (Deguchi *et al*., 2019). Moreover, Likhitwitayawuid *et al*., (2006) rerevealed that the bibenzyl structure, 2, 4, 3´, 5´-tetrahydroxybibenzyl which can be obtained from oxyresveratrol through a single-step reduction reaction showed inhibitory effect against tyrosinase activity higher than oxyresveratrol same with 3, 4, 3´, 5´-tetrahydroxybibenzyl showed activity higher than piceatannol.

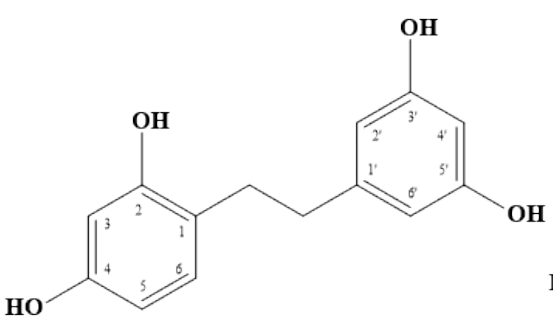

2,4,3´,5´-Tetrahydroxybibenzyl

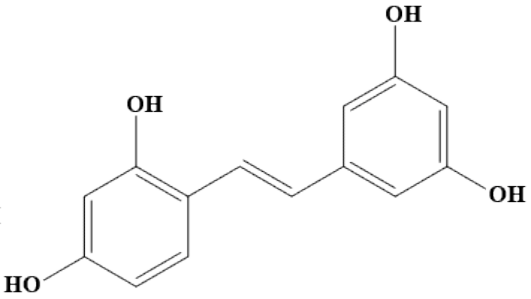

Oxyresveratrol

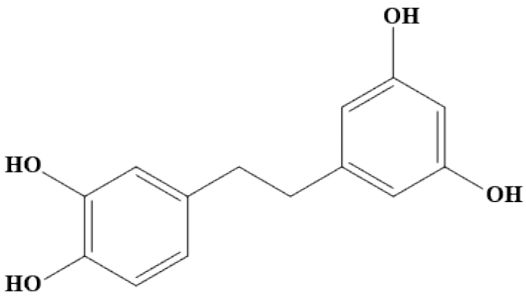

3, 4, 3´, 5´-Tetrahydroxybibenzyl

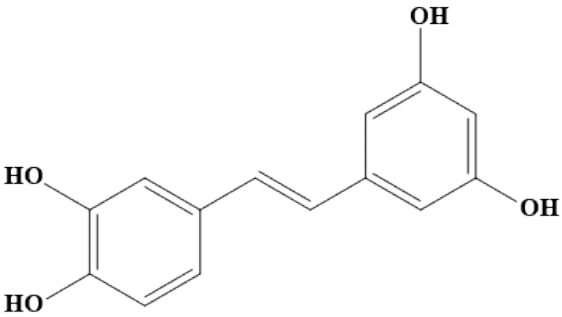

Piceatannol

Figure 4-21 Structures of stilbene group

ω-Hydroxymoracin C (No.10), moracin M (No.11) and moracin C (No.12) are the 2-arylbenzofuran (Figure 4-22) showed activity against directly tyrosinase enzyme. The hydroxyl or methoxy group at the C-6 position might mediate the inhibitory activity compared with other 2-arylbenzofurans; moracin B, moracin J, moracin N and moracin VN (Figure 4-21) (Zheng *et al*., 2010; Zhang *et al*., 2016; Le *et al*., 2017; Jeon and Choi, 2019). Moreover, the hydroxyl group at the C-3′ and C-5′ position might important for the tyrosinase inhibitory activity of several 2-arylbenzofuran compared with moracin D which isoprenyl group forms a six-membered ring with hydroxyl group at C-3′. So moracin D was inactive on antityrosinase activity (Zhang *et al*., 2016). While, the presence or absence of substituent at C-4′ was not affect to the tyrosinase inhibitory activity of 2-arylbenzofuran group so ω-hydroxymoracin C and moracin C which substituted with hydroprenyl and prenyl group, respectively compared with moracin VN which substituent with dihydroxymethylbutyl (Le *et al*., 2017).

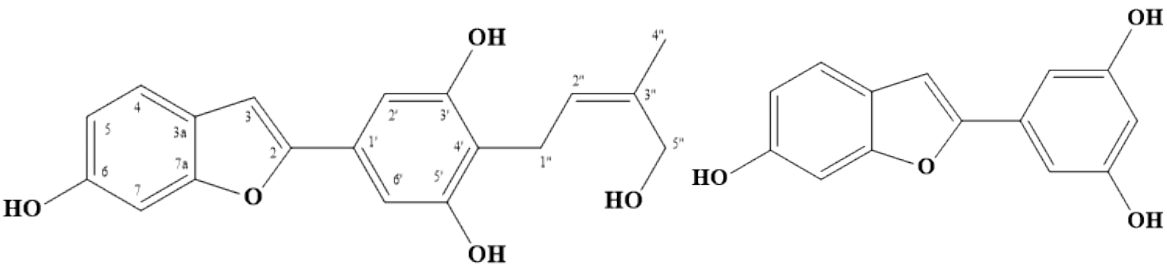

ω-Hydroxymoracin C

Moracin M

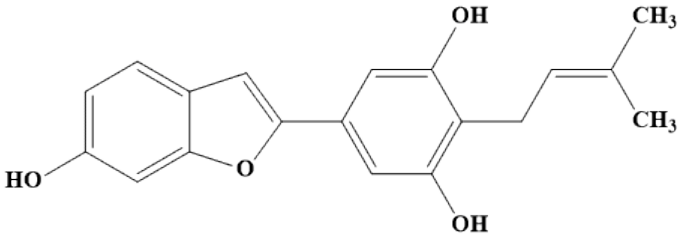

Moracin C

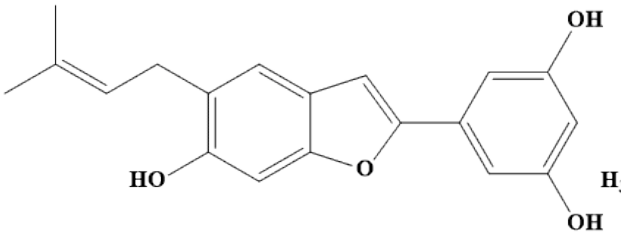

Moracin N

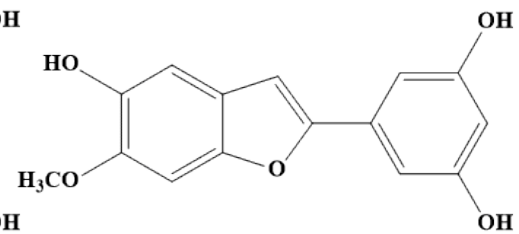

Moracin J

Figure 4-22 Structures of 2-arylbenzofuran

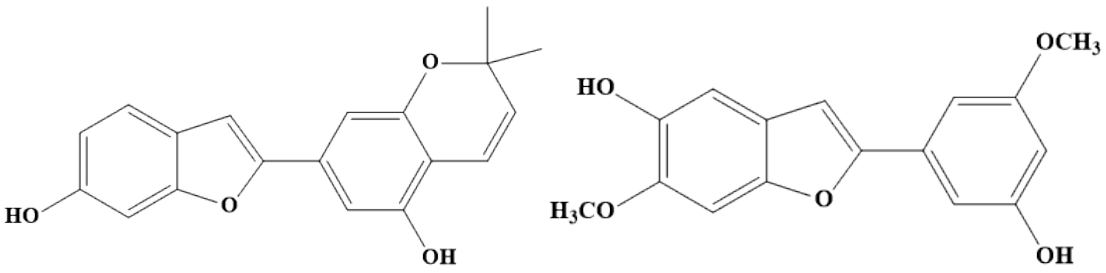

Moracin D Moracin B

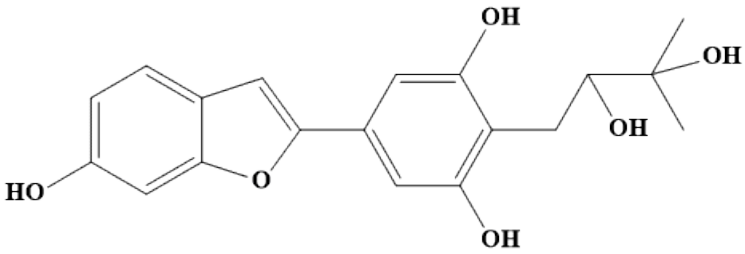

Moracin VN

Figure 4-22 Structures of 2-arylbenzofuran (continued)

6.4 Western blot

The selected compounds from *A. chama* and *S.taxoides* which showed the potential of enzymatic antityrosinase activity and the amount of compound was sufficient to do the test were studied on the expression of melanogenic proteins in B16F1 cells and relative protein expression value. The results of isolated compounds from *A. chama*; artocarpanone (No.6), naringenin (No.7), homoeriodictyol (No.1) and 3´-farnesyl-apigenin (No.2) showed in the Figure 4-23 and 4-24. While, the results of ω-hydroxymoracin C (No.10), moracin M (No.11), moracin C (No.12), 3, 4, 3´, 5´-tetrahydroxybibenzyl (No.13) and piceatannol (No.14) from *S.taxoides* showed in the Figure 4-25 and 4-26.

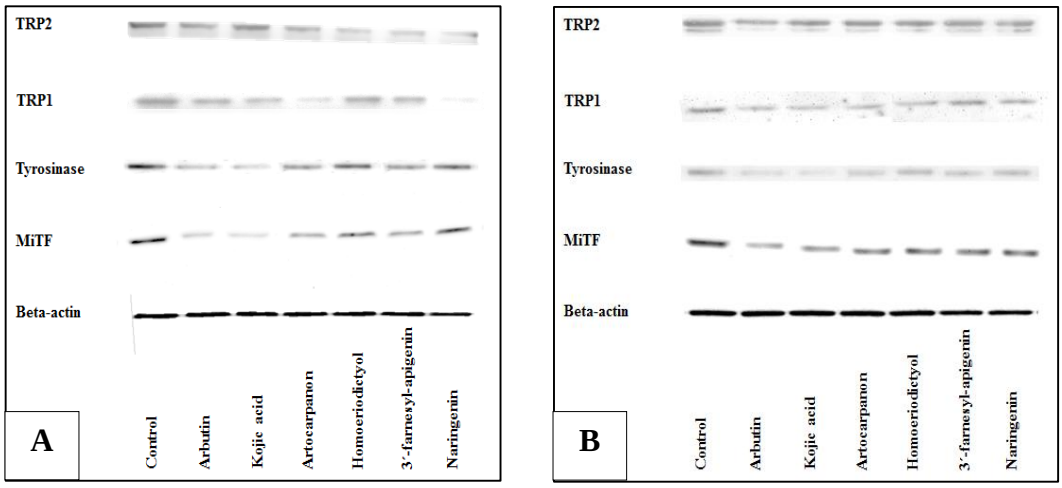

Figure 4-23 Effect of isolated compounds from *A. chama* on the expression of melanogenic proteins in B16F1 cells. Cells were treated with 25 µg/mL (A) and 50 µg/mL (B) of isolated compounds. Whole cell lysates were subjected to Western blot analysis using specific antibodies against MITF, tyrosinase, TRP1 and TRP2.

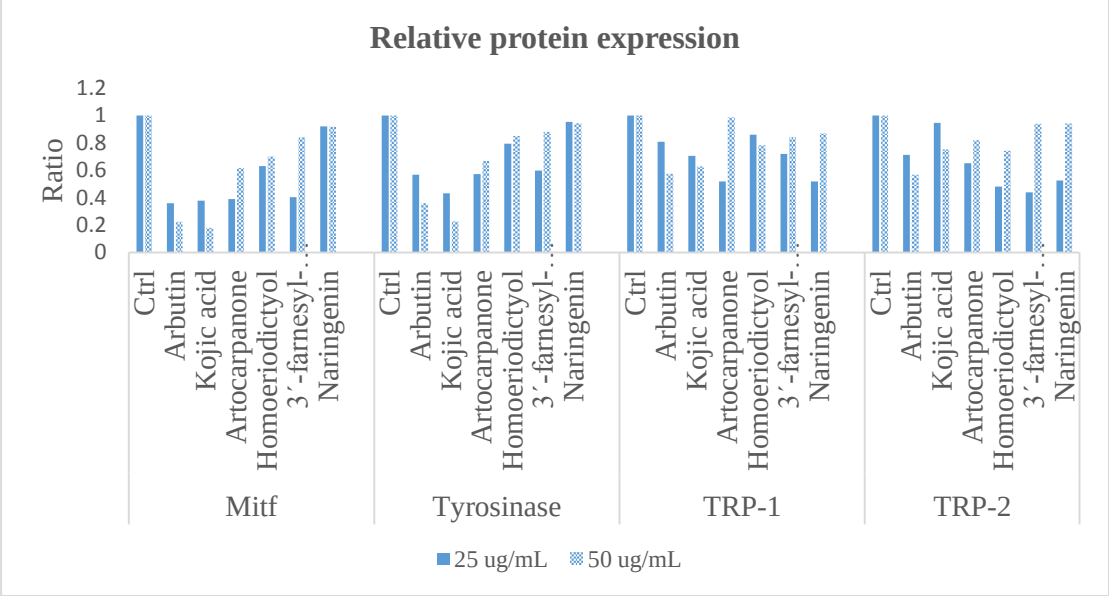

Figure 4-24 Relative protein expression value of isolated compounds from *A. chama* on the expression of melanogenic proteins in B16F1 cells. Cells were treated with 25 µg/mL and 50 µg/mL of isolated compounds. Whole cell lysates were subjected to Western blot analysis using specific antibodies against MITF, tyrosinase, TRP1 and TRP.

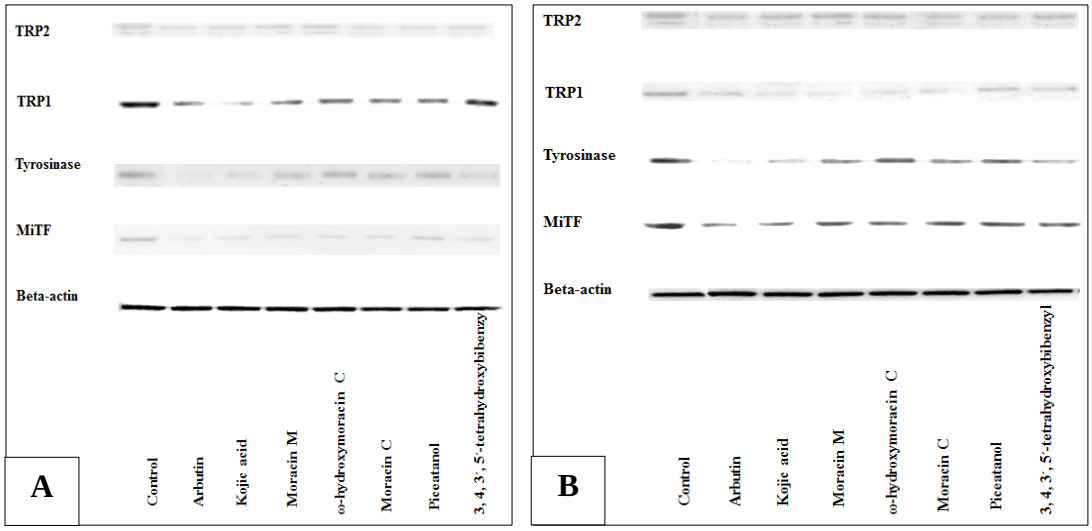

Figure 4-25 Effect of isolated compounds from *S. taxoides* on the expression of melanogenic proteins in B16F1 cells. Cells were treated with 25 μg/mL (A) and 50 μg/mL (B) of isolated compounds. Whole cell lysates were subjected to Western blot analysis using specific antibodies against MITF, tyrosinase, TRP1 and TRP2.

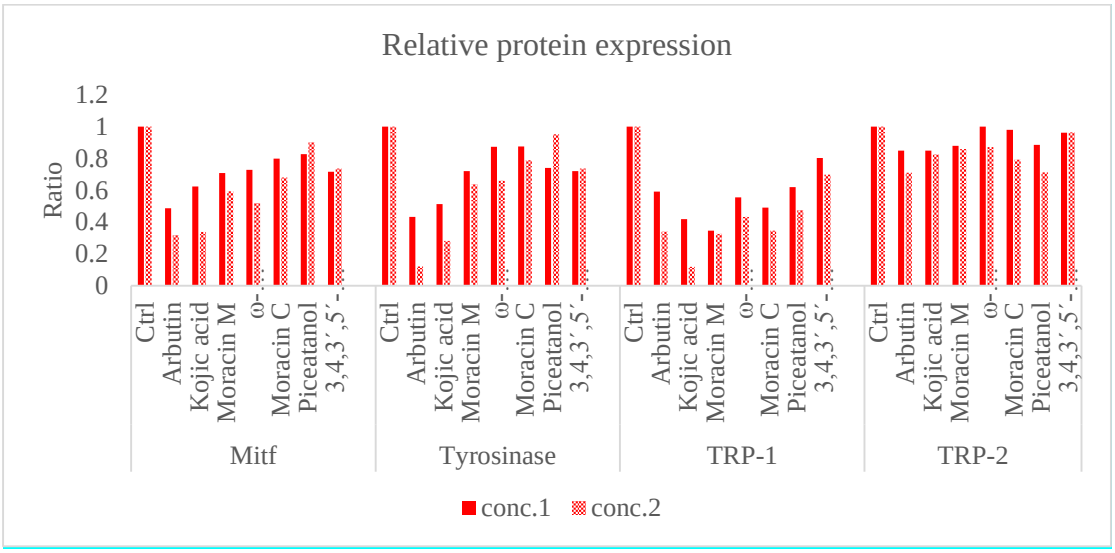

Figure 4-26 Relative protein expression value of isolated compounds from *S. taxoides* on the expression of melanogenic proteins in B16F1 cells. Cells were treated with 25 μg/mL and 50 μg/mL of isolated compounds. Whole cell lysates were subjected to Western blot analysis using specific antibodies against MITF, tyrosinase, TRP1 and TRP2.

The expression of melanogenic proteins showed that only artocarpanone (No.6) could decrease melanin content by decreasing of tyrosinase (TYR) and microphthalmia-associated transcription factor (MITF). While, naringenin (No.7), homoeriodictyol (No.1) and 3´-farnesyl-apigenin (No.2) could not decrease melanin content. Niu and Aisa (2017) reported that, naringenin induced melanogenesis by inactivated the kinase activity of glycogen synthesis kinase 3ß (GSK3ß), resulting in the elevation of intracellular ß-catenin levels (Chang *et at.*, 2012). ß-Catenin promotes melanogenesis by up-regulating the melanocyte differentiation-related proteins, such as microphthalmia-associated transcription factor (MITF) and tyrosinase (TYR) through the Wnt-β-catenin-signalling pathway as showed in Figure 4-27 (Huang *et al*., 2012). Moreover, it can up-regulating of microphthalmia-associated transcription factor (MITF) via phosphatidylinositol 3-kinase (PI3K) pathway (Ohguchi *et al*., 2006). While, hesperetin increase melanogenesis via all pathways; Wnt-β-catenin-signalling pathway, phosphatidylinositol 3-kinase-Protein Kinase B or PI3K-Akt signalling pathway, cAMP/PKA signalling pathway and mitogen-activated protein kinases or MAPK signalling pathway (Huang *et al*., 2012). Due to, homoeriodictyol (No.1) is a group of flavanone, its structure is similar with naringenin (No.7) and hesperetin so it may be affect to some protein signalling pathway. 3´-Farnesyl-apigenin (No.2) may induce melanogenesis by MAPK signalling pathway as same as its main structure, apigenin (Ye *et al*., 2011).

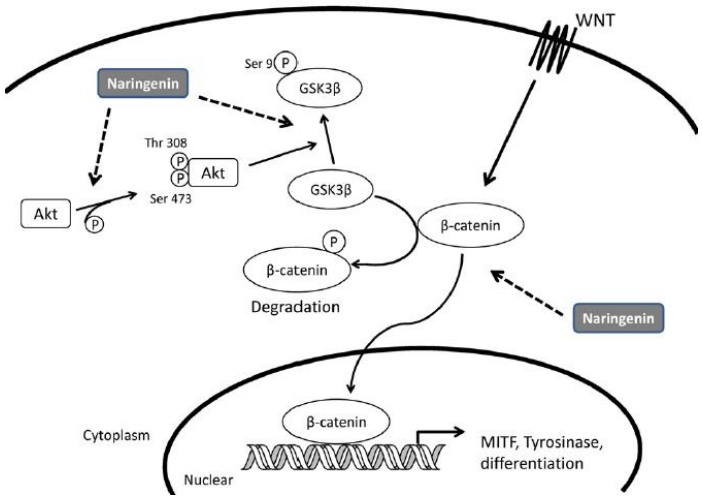

Figure 4-27 Model of signalling pathways involved in naringenin-induced melanogenesis (Huang *et al*., 2012)

The inhibition of melanogenic proteins which related to Wnt-β-catenin-signalling pathway, phosphatidylinositol 3-kinase-Protein Kinase B or PI3K-Akt signalling pathway, cAMP/PKA signalling pathway and mitogen-activated protein kinases or MAPK signalling pathway could be decreasing of melanogenesis. However, the expression of melanogenic proteins of 2-arylbenzofuran group was not clear. Due to the result from western blot analysis revealed that moracin M (No.11), ω-hydroxymoracin C (No.10) and moracin C (No.12) seemed to decrease melanin content by decreasing of microphthalmia-associated transcription factor (MITF), tyrosinase (TYR), tyrosinase-related protein 1 (TRP1) and tyrosinase-related protein 2 (TRP2). While, piceatannol (No.14) and 3, 4, 3´, 5´-tetrahydroxybibenzyl (No.13), stilbene compound increased melanin production by increasing of microphthalmia-associated transcription factor (MITF) and tyrosinase (TYR) when confirmed with previous reports as piceatannol exerted its stimulatory effect on melanogenesis by MAP kinase activation and MITF induction of tyrosinase (Deguchi *et al.*, 2019; Niu and Aisa, 2017).

The compounds which exhibited enzymatic tyrosinase inhibitory activity consist 2 different mechanisms in B16F1 cell as western blot confirmation. Artocarpanone; ω-hydroxymoracin C; moracin M and moracin C showed potential activity with enzymetic antityrosinase and can decrease melanin content by down-regulated the expression of melanogenic proteins in western blot test. While, homoeriodictyol; 3´-farnesyl-apigenin; 3, 4, 3´, 5´-tetrahydroxybibenzyl and piceatannol showed potential activity with enzymetic antityrosinase but increase melanin content by up-regulated the expression of melanogenic proteins in western blot test.

7. Antimicrobial activity of isolated compounds

From the screening of Antimicrobial activity, the ethyl acetate extracts of *A. chama* and *S. taxoides* showed the potential effects against *S. epidermidis, S. aureus,* MRSA and *P. acnes.* Thus, the ethyl acetate extracts of these plants were selected for further isolation of active compounds and then, the isolated compounds were

investigated of the MIC and MBC for *S. epidermidis, S. aureus,* MRSA and *P. acnes.* The MIC and MBC values of isolated compounds were showed in Table 4-30.

Table 4-30 MIC and MBC of pure compounds against *S. epidermidis, S. aureus* MRSA and *P. acnes*

	S. epidermidis		***S. aureus***		**MRSA**		***P. acnes***	
	MIC	**MBC**	**MIC**	**MBC**	**MIC**	**MBC**	**MIC**	**MBC**
No.1	128	256	256	>256	>256	>256	>256	>256
No.2	256	>256	256	>256	>256	>256	>256	>256
No.3	4	8	4	8	16	64	256	>256
No.4	16	32	16	32	16	64	128	>256
No.5	16	64	4	16	4	32	128	>256
No.6	64	128	64	256	128	>256	32	64
No.7	256	>256	>256	>256	>256	>256	>256	>256
No.8	2	32	2	4	2	2	8	32
No.9	>256	>256	>256	>256	>256	>256	>256	>256
No.10	16	32	16	32	16	>256	128	>256
No.11	64	>256	256	>256	64	>256	>256	>256
No.12	128	>256	32	64	32	64	128	>256
No.13	128	>256	128	256	64	256	>256	>256
No.14	64	128	>256	>256	128	>256	>256	>256
Oxa[P]	0.5	0.5	0.125	0.125	NT	NT	0.5	0.5
Van[P]	NT	NT	NT	NT	NT	0.5	NT	NT

[P]= positive control; Oxa = Oxacillin; Van = Vancomycin

ω-hydroxymoracin C (No.10), moracin M (No.11) and moracin C (No.12) were the arylbenzofuran group (Figure 4-28). 3-(Hydroxyprenyl) isoetin (No.9); 3-prenyl-5,7,2´,5´-tetrahydroxy-4´-methoxyflavone (No.5); isocycloartobiloxanthone (No.3); artocarpanone (No.6) and artocarpin (No.8) were the flavonoid group.

Moracin M showed weak inhibitory effect against, *S. epidermidis, S. aureus* and MRSA. While, moracin M derivative as ω-hydroxymoracin C and moracin C and flavonoid group as 3-(Hydroxyprenyl) isoetin; 3-prenyl-5,7,2´,5´-tetrahydroxy-4´-methoxyflavone; isocycloartobiloxanthone; artocarpanone and artocarpin showed stronger inhibitory effect against *S. epidermidis, S. aureus*, MRSA and *P. acnes*.

Moracin M is the arylbenzofuran while moracin C and ω-hydroxymoracin C are the moracin M derivatives which connect with prenyl and hydroxyprenyl, respectively. Kuetu *et al*. (2009) reported that non-prenylated arylbenzofurans; moracin M and moracin Q exhibited Antimicrobial weaker than prenylated arylbenzofurans; moracin T and moracin C because prenyl group increases the antimicrobial activity of arylbenzofurans. Moreover, Matsuyama *et al*. (1991) reported that moracin C against *S. aureus* by protein biosynthesis inhibition.

3-(Hydroxyprenyl)isoetin; 3-prenyl-5,7,2´,5´-tetrahydroxy-4´-methoxyflavone; isocycloartobiloxanthone; artocarpanone and artocarpin exhibited potential activity of antibacterial against Gram-positive bacteria; *S. epidermidis*, *S. aureus*, MRSA and *C. acnes* because of the substituents and positions of hydroxyl and isoprenyl groups. The saturation of the C2=C3 double bond[28] and the present of hydroxyl groups at the C-5 or C-6 or C-7 especially at C-5 and C-7of A-ring (Xie *et al*., 2015; Adamczak *et al*., 2020) and another position such as C-2´ and C-4´ of B-ring improve the antibacterial effect (Cushnie and Lamb, 2005). Moreover, increase of hydrophobicity by prenylation enhanced the antibacterial activity, especially the substituents with isoprenyl at C-6 or C-8 (Cushnie and Lamb, 2005). Furthermore, Xie *et al*. (2015) reported that diprenylated more effective against the Gram positive bacteria than monoprenylated.

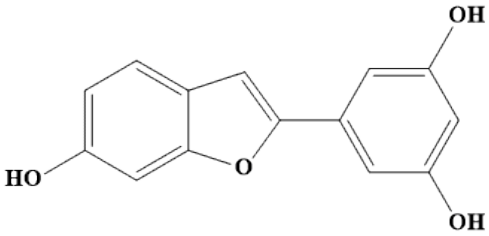

Moracin M

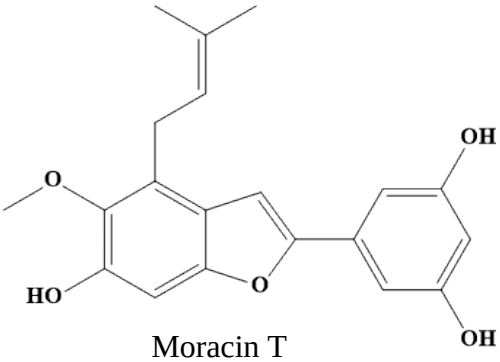

Moracin T

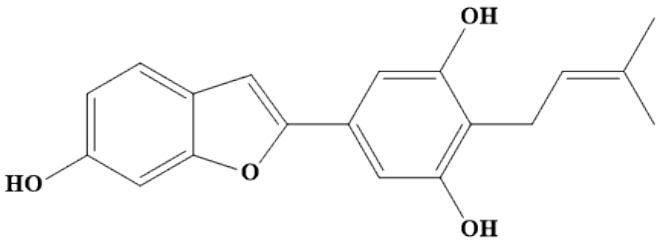

Moracin C

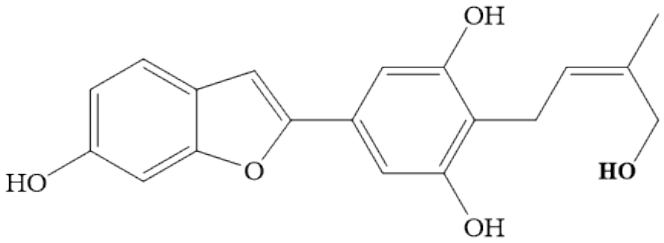

ω-Hydroxymoracin C

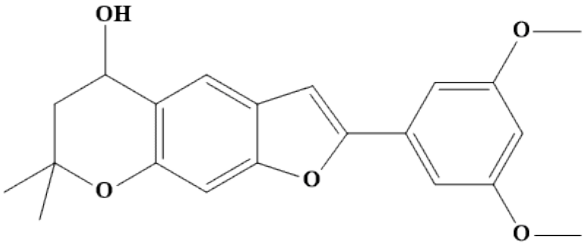

Moracin Q

Figure 4-28 The arylbenzofuran group

CHAPTER 5
CONCLUSION

Forty-eight Moraceae plant samples were screened on antityrosinase and antimicrobial activities. The stem extract of *A. chama* and the wood extract of *S. taxoides* which showed the good bioactivities were selected for further investigation on phytochemical investigation and biological activities.

The ethyl acetate extract of *A. chama* and ethyl acetate and methanol extracts of *S. taxoides* were the most interesting fractions because they showed the potential effects for enzymetic antityrosinase activity. The ethyl acetate extract from both plants could decrease the melanin content by increasing of antityrosinase activity on B16F1 melanoma cells. Moreover, the ethyl acetate and methanol extracts of *S. taxoides* suppressed the pigmentation on zebrafish. In addition, the ethyl acetate extract of both plants showed the antimicrobial activity on *S. aureus, S. epidermidis, P. acnes* and MRSA. Then, ethyl acetate extract of *A. chama*, ethyl acetate and methanol extracts of *S. taxoides* were selected for further investigation of the chemical constituents and their bioactivities.

Eight pure compounds were isolated from the *A. chama,* three new compounds as 3´-farnesyl-apigenin; 3-(hydroxyprenyl) isoetin and 3-prenyl-5, 7, 2´, 5´-tetrahydroxy-4´-methoxyflavone and five known compounds as homoeriodictyol; isocycloartobiloxanthone; artocarpanone; naringenin and artocarpin. Six compounds were isolated from *S. taxoides*, one new compound as ω-hydroxymoracin C, four known compounds as moracin M; moracin C; 3, 4, 3´, 5´-tetrahydroxybibenzyl; piceatannol and one mixture of β-sitosterol and stigmasterol.

Homoeriodictyol (No.1), 3´-farnesyl-apigenin (No.2), artocarpanone (No.6), ω-hydroxymoracin C (No.10), moracin M (No.11), moracin C (No.12), 3, 4, 3´, 5´-tetrahydroxybibenzyl (No.13) and piceatannol (No.14) showed the potential effect of enzymetic antityrosinase activity while, artocarpanone (No.6), ω-hydroxymoracin C (No.10), moracin M (No.11) and moracin C (No.12) could decrease melanin content by increasing antityrosinase activity on B16F1 melanoma cells via different pathway.

From the expression of melanogenic proteins showed that artocarpin (No.8), ω-hydroxymoracin C (No.10), moracin M (No.11) and moracin C (No.12) could decrease melanin content by inhibition the melanogenesis pathway while, homoeriodictyol (No.1), 3´-farnesyl-apigenin (No.2) and naringenin (No.7) could increase melanin production by increasing the melanogenesis. Moreover, ω-hydroxymoracin C (No.10), moracin M (No.11) and moracin C (No.12) showed inhibitory effect against *S. epidermidis, S. aureus* and MRSA.

This study is the first report on the antityrosinase activity of these plants and it is the first report on phytochemical investigation of *S. taxoides*. Also, the new compounds, 3´-farnesyl-apigenin (No.2); 3-(hydroxyprenyl) isoetin (No.4); 3-prenyl-5, 7, 2´, 5´-tetrahydroxy-4´-methoxyflavone (No.5) and ω-hydroxymoracin C (No.10) were investigated. Some isolated compounds showed the effect on biological activities which can be further studied on *in vivo* and clinical trials in order to use for the treatment of hyperpigmentation and/or infectious disease caused by microorganisms. In addition, this study will be the database of *S. taxoides* and *A. chama* for chemical constituents and biological activities.

REFERENCES

Adamczak, A., O˙zarowski M. and Karpi´nski T. M. 2020. Antibacterial activity of some flavonoids and organic acids widely distributed in plants. *Journal of Clinical Medicine*, 9 (109): 2-17.

Ahmed T., Uddin M. N., Ahmed S. F., Saha A., Farhana K. and Rana M. S. 2012. *In vitro* evaluation of antioxidant potential of *Artocarpus chama* Buch. fruits. *Journal of Applied Pharmaceutical Science*, 2 (10): 75-80.

Ahmed T., Uddin M. N., Hossain M. K., Hasan N. and Rana M. S. 2013. Evaluation of antioxidant and cytotoxic potential of *Artocarpus chama* Buch. seed using *in vitro* models. *International Journal of Pharmacy and Pharmaceutical Sciences*, 5 (1): 283-289.

Athikomkulchai S., Watthanachaiyingcharoen R., Tunvichien S., Vayumhasuwan P., Karnsomkiet P., Sae-Jong P. and Ruangrungsi N. 2008. The development of anti-acne products from *Eucalyptus globulus* and *Psidium guajava* oil. *Journal of Health Research*, 22 (3):109-113.

Baek Y.S., Ryu Y.B., Curtis-Long M.J., Ha T.J., Rengasamy R., Yang M.S. and Park K.H. 2009. Tyrosinase inhibitory effects of 1,3-diphenylpropanes from *Broussonetia kazinoki*. *Bioorganic* & *Medicinal Chemistry*, 17 (1):35-41.

Briganti S., Camera E. and Picardo M. 2003. Chemical and instrumental approaches to treat hyperpigmentation. *Pigment Cell & Melanoma Research*, 16 (2):101-110.

Chang L.W., Juang L.J., Wang B.S., Wang M.Y., Tai H.M., Hung W.J., Chen Y.J. and Huang M.H. 2011. Antioxidant and antityrosinase activity of mulberry (*Morus alba* L.) twigs and root bark. *Food and Chemical Toxicology*, 49 (4):785-790.

Chang T.-S. 2012. Natural melanogenesis inhibitors acting through the down-regulation of tyrosinase activity. *Materials* 5 (9):1661–1685.

Chen X.X., Shi Y., Chai W.M., Feng H.L., Zhuang J.X. and Chen Q.X. 2014. Condensed tannins from *Ficus virens* as tyrosinase inhibitors: structure, inhibitory activity and molecular mechanism. *PLoS One*, 9 (3):1-12.

Chiari M.E., Vera D.M.A., Palacios S.M. and Carpinella M.C. 2011. Tyrosinase inhibitory activity of a 6-isoprenoid-substituted flavanone isolated from *Dalea elegans*. *Bioorganic & Medicinal Chemistry*, 19 (11):3474-3482.

Cichorek M., Stasiewicz M. W. and Tymińska A. 2013. Skin melanocytes: biology and development. *Advances in Dermatology and Allergology*, 30 (1):30-41.

Claus H. and Decker H. 2006. Bacterial tyrosinases. *Systematic and Applied Microbiology*, 29 (1):3-14.

Clinical and Laboratory Standards Institute (CLSI). 2006. *Methods for dilution antimicrobial susceptibility testes for bacterial that grow aerobically; approved standards*. 7ed. USA: Clinical and Laboratory Standards Institute, Wayne, Pennsylvania.

Costin G.E. and Hearing V.J. 2007. Human skin pigmentation: melanocytes modulate skin color in response to stress. *The FASEB Journal*, 21 (4):976-994.

Cushnie T. P. T. and Lamb A. J. 2005. Antimicrobial activity of flavonoids. *International Journal of Antimicrobial Agents* 26 (5):343-356.

Dávila M., Sterner O. and Hinojosa N. 2013. Flavonoids from *Baccharis polycephala* Weddell. *Bolivian Journal of Chemistry* 30(2):137-141.

Davis E.C. and Callender V.D. 2010. Postinflammatory hyperpigmentation: a review of the epidemiology, clinical features, and treatment options in skin of color. *Journal of Clinical and Aesthetic Dermatology*, 3 (7):20-31.

Deguchi T., Tamai A., Asahara K., Miyamoto K., Miyamoto A., Nomura M., Kawata-T. T., Yoshioka Y. and Murata K. 2019. Anti-tyrosinase and anti-oxidative activities by asana: the heartwood of *Pterocarpus marsupium. Natural Product Communications*, 14 (10):1-9.

Dej-adisai S., Meechai I., Puripattanavong J. and Kummee S. 2014. Antityrosinase and antimicrobial activities from Thai medicinal plants. *Archives of Pharmacal Research*, 37 (4):473-483.

Dej-adisai S., Parndaeng K. and Wattanapiromsakul C. 2016. Determination of phytochemical compounds, and tyrosinase inhibitory and antimicrobial activities of bioactive compounds from *Streblus ilicifolius* (S Vidal) Corner. *Tropical Journal of Pharmaceutical Research*, 15 (3):497-506.

Dharmaratne H.R.W., Jacob M., Tekwani B.L. and Nanayakkara N.P.D. 2013. Antimicrobial and antileishmanial compounds from *Maclura pomifera* fruits. *Planta Medica*, 79 (10).

Drott J. B., Alexeyev O., Bergstrom P., Elgh F., and Olsson J. 2010. *Propionibacterium acnes* infection induces upregulation of inflammatory genes and cytokine secretion in prostate epithelial cells. *BMC Microbiology*, 10:126.

Fletcher J. N. 2011. Isolation, identification, and biological evaluation of potential flavor modulatory flavonoids from *Eriodictyon californicum*. Degree of Doctor of Philosophy Graduate School of The Ohio State University.

Fongang Y.S.F., Bankeu J.J.K., Ali M.S., Awantu A.F., Zeeshan A., Assob C.N., Mehreen L., Lenta B.N., Ngouela S.A. and Tsamo E. 2015. Flavonoids and other bioactive constituents from *Ficus thonningii* Blume (Moraceae). *Phytochemistry Letters*, 11:139-145.

Fukai T., Kaitou K. and Terada S. 2005. Antimicrobial activity of 2-arylbenzofurans from *Morus* species against methicillin-resistant *Staphylococcus aureus*. *Fitoterapia*, 76 (7-8):708-711.

Garcia-Molina F., Fenoll L.G., Morote J.C., Garcia-Ruiz P.A., Rodriguez-Lopez J.N., Garcia-Canovas F. and Tudela J. 2005. Opposite effects of peroxidase in the initial stages of tyrosinase-catalysed melanin biosynthesis. *The International Journal of Biochemistry & Cell Biology*, 37 (6):1179-1196.

Garland C.F., Garland F.C. and Gorham E.D. 2003. Epidemiologic evidence for different roles of ultraviolet A and B radiation in melanoma mortality rates. *Annals of Epidemiology*, 13 (6):395-404.

Gasowska B., Frackowiak B. and Wojtasek H. 2006. Indirect oxidation of amino acid phenylhydrazides by mushroom tyrosinase. *Biochimica et Biophysica Acta*, 1760 (9):1373-1379.

Gotoh T., Koyama T. and Ogura K. 1992. Farnesyl diphosphate synthase and solanesyl diphosphate synthase reactions of diphosphate-modified allylic analogs: the significance of the diphosphate linkage involved in the allylic substrates for prenyltransferase. *The Journal of Biochemistry*, 112:20-27.

Hashim N.M., Rahmani M., Ee G.C., Sukari M.A., Yahayu M., Amin M.A., Ali A.M. and Go R. 2012. Antioxidant, antimicrobial and tyrosinase inhibitory activities of xanthones isolated from *Artocarpus obtusus* F.M. Jarrett. *Molecules*, 17 (5):6071-6082.

Heinemann J. A., Ankenbauer R. G., and Amabile-Cuevas C. F. 2000. Do antibiotics maintain antibiotic resistance? *Drug Discovery Today*, 5 (5):195-204.

Hoogduijn M. J., Cemeli E., Ross K., Anderson D., Thody A. J., and Wood J. M. 2004. Melanin protects melanocytes and keratinocytes against H_2O_2-induced DNA strand breaks through its ability to bind $Ca2^+$. *Experimental Cell Research*, 294 (1):60-67.

Hu Z.-M., Zhou Q., Lei T.-C., Ding S.-F., and Xu S.-Z. 2009. Effects of hydroquinone and its glucoside derivatives on melanogenesis and antioxidation: Biosafety as skin whitening agents. *Journal of Dermatological Science*, 55 (3):179-184.

Huang Y. C., Liu K. C. and Chiou Y. L. 2012. Melanogenesis of murine melanoma cells induced by hesperetin, a Citrus hydrolysate-derived flavonoid. *Food and Chemical Toxicology*, 50 (3-4):653-659.

Hunt G., Todd C., Cresswell J. E. and Thody A. J. 1994. Alpha-melanocyte stimulating hormone and its analogue Nle4DPhe7 alpha-MSH affectmorphology, tyrosinase activity and melanogenesis in cultured human melanocytes. *Journal of Cell Science*, 107 (1):205-11.

Jang M.H. and Ahn T.W. 2015. Inhibitory effects of *Taraxacum mongolicum* with phreatic water on melanin synthesis. *Integrative Medicine Research*, 4 (2):76-93.

Jamil S., Lathiff S.M.A., Abdullah S.A., Jemaon N. and Sirat H.M. 2014. Antimicrobial flavonoids from *Artocarpus anisophyllus* Miq. and *Artocarpus lowii* King. *Journal Teknologi*, 71 (1):95-99.

Jeon Y. H. and Choi S. W. 2019. Isolation, identification, and quantification of tyrosinase and alpha-glucosidase inhibitors from UVC-Irradiated mulberry (*Morus alba* L.) Leaves. *Preventive Nutrition and Food Science*, 24 (1):84-94.

Jimenez-Cervantes C., Garcia-Borron J. C., Lozano J. A., and Solano F. 1995. Effect of detergents and endogenous lipids on the activity and properties of tyrosinase and its related proteins. *Biochimica et Biophysica Acta (BBA,)* 1243 (3):421-430.

Jung J. W., Park J. H., Lee Y. G., Seo K. H., Oh E. J., Lee D. Y., Lim D. W., Han D. and Baek N. I. 2016. Three new isoprenylated flavonoids from the root bark of *Morus alba*. *Molecules*, 21 (9):1112.

Kamal T., Muzammil A. and Omar M.N. 2012. Evaluation of antimicrobial activity of *Artocarpus altilis* on pathogenic microorganisms. *Science Series Data Report*, 4 (9) :41-48.

Kang Y., Choi J.-U., Lee E.-A. and Park H.-R. 2013. Flaniostatin, a new isoflavonoid glycoside isolated from the leaves of *Cudrania tricuspidata* as a tyrosinase inhibitor. *Food Science and Biotechnology*, 22 (5):1-4.

Kiken D.A. and Cohen D.E. 2002. Contact dermatitis to botanical extracts. *American Journal of Contact Dermatitis*, 13 (3):148-152.

Kim Y.J. and Uyama H. 2005. Tyrosinase inhibitors from natural and synthetic sources: structure, inhibition mechanism and perspective for the future. *Cellular and Molecular Life Sciences*, 62 (15):1707-1723.

Kim Y. J., Sohn M. J. and Kim W. G. 2012. Chalcomoracin and moracin C, new inhibitors of *Staphylococcus aureus* enoyl-acyl carrier protein reductase from *Morus alba*. *Biological and Pharmaceutical Bulletin*, 35 (5):791-795.

Ko H.H., Chang W.L. and Lu T.M. 2008. Antityrosinase and antioxidant effects of ent-kaurane diterpenes from leaves of *Broussonetia papyrifera*. *Journal of Natural Products*, 71 (11):1930-1933.

Kobayashi T., Urabe K., Winder A., Jimenez-Cervantes C., Imokawa G., Brewington T., Solano F., Garcia-Borron J.C. and Hearing V.J. 1994. Tyrosinase related protein 1 (TRP1) functions as a DHICA oxidase in melanin biosynthesis. *The EMBO Journal*, 13 (24):5818-5825.

Konda S., Geria A. N. and Halder R. M. 2012. New horizons in treating disorders of hyperpigmentation in skin of color. *Seminars in Cutaneous Medicine and Surgery* 31 (2):133-139.

Kuete V., Fozing D. C., Kapche W. F., Mbaveng A. T., Kuiate J. R., Ngadjui B. T., and Abegaz B. M. 2009. Antimicrobial activity of the methanolic extract and compounds from *Morus mesozygia* stem bark. *Journal of Ethnopharmacology*, 124 (3):551-555.

Kumar G.S., Jayaveera K.N., Kumar C.K.A., Sanjay U.P., Swamy B.M.V.. and Kumar D.V.K. 2007. Antimicrobial effects of Indian medicinal plants against acne-inducing bacteria. *Journal of Pharmaceutical Research*, 6 (2):717-723.

Kummee S. and Intaraksa N. 2008. Antimicrobial activity of *Desmos chinensis* leaf and *Maclura cochinchinensis* wood extracts. *Songklanakarin Journal of Science and Technology*, 30 (5):635-639.

Lamounier K.C., Cunha L.C., de Morais S.A., de Aquino F.J., Chang R., de Nascimento E.A., de Souza M.G., Martins C.H. and Cunha W.R. 2012. Chemical analysis and study of phenolics, antioxidant activity, and antibacterial effect of the wood and bark of *Maclura tinctoria* (L.) D. Don ex Steud. *Evidence-Based Complementary and Alternative Medicine*, 2012:1-8.

Lan, W. C., Tzeng C. W., Lin C. C., Yen F. L. and Ko H. H. 2013. Prenylated flavonoids from *Artocarpus altilis*: antioxidant activities and inhibitory effects on melanin production. *Phytochemistry*, 89:78-88.

Le H.T., Hong B.N., Lee Y.R., Cheon J.H., Kang T.H., Kim T.W. 2016. Regulatory effect of hydroquinone-tetraethylene glycol conjugates on zebrafish pigmentation. *Bioorganic & Medicinal Chemistry Letters*, 26 (2):699-705.

Le, T. H., Nguyen H. X., Do T. V. N., Dang P. H., Nguye N. T. n and M. Nguyena T. T. 2017. Moracin VN, a new tyrosinase and xanthine oxidase inhibitor from the woods of *Artocarpus heterophyllus*. *Natural Product Communications*, 12 (6):925-927.

Likhitwitayawuid, K. 2008. Stilbenes with tyrosinase inhibitory activity. *Current Science*, 94 (1):44-52.

Likhitwitayawuid K., Sritularak B. and De-Eknamkul W. 2000. Tyrosinase inhibitors from *Artocarpus gomezianus*. *Planta Medica*, 66 (3):275-277.

Likhitwitayawuid K., Sornsute A., Sritularak B. and Ploypradith P. 2006. Chemical transformations of oxyresveratrol (*trans*-2,4,3',5'-tetrahydroxystilbene) into a potent tyrosinase inhibitor and a strong cytotoxic agent. *Bioorganic & Medicinal Chemistry Letters*, 16 (21):5650-5653.

Llagas M.C.D.L., Santiago L. and Ramos J.D. 2014. Antibacterial activity of crude ethanolic extract and solvent fractions of *Ficus pseudopalma* Blanco leaves. *Asian Pacific Journal of Tropical Disease*, 4 (5):367-371.

Loizzo M.R., Tundis R. and Menichini F. 2012. Natural and synthetic tyrosinase inhibitors as antibrowning agents: an update. *Comprehensive Reviews in Food Science and Food Safety*, 11 (4):378-398.

Lopez-Serrano D., Solano F. and Sanchez-Amat A. 2004. Identification of an operon involved in tyrosinase activity and melanin synthesis in *Marinomonas mediterranea*. *Gene,* 342 (1):179-187.

Lorian V. 2005. *Antibiotics in laboratory medicine*. 5 ed. USA: Lippincott Williams & Wilkins.

Lowe N. J. and Shaath N. A. 1990. *Sunscreens*. New York and Basel: Mercel Dekker.

Madhavi Y., Rao D.B. and Rao T.R. 2013. Studies on phytochemical analysis and antimicrobial activity of *Artocarpus communis* fruit latex against selected pathogenic microorganisms. *Indo American Journal of Pharmaceutical Research*, 3 (1):1458-1468.

Mannila, E., Talvitie A. and Kolehmainen E. 1993. Anti-leukaemic compounds derived from stibenes in *Picea abies* bark. *Phytochemistry,* 33 (4):813-816.

Matsuyama S., Y. Kuwahara and Suzuki T. 1991. A New 2-arylbenzofuran, ω -hydroxy moracin N, from mulberry leaves. *Agricultural and Biological Chemistry,* 55 (5):1409-1410.

Moon J.Y., Yim E.Y., Song G., Lee N.H. and Hyun C. G. 2010. Screening of elastase and tyrosinase inhibitory activity from Jeju island plants. *EurAsian Journal of BioSciences*, 4:41-53.

Niu, C. and H. A. Aisa 2017. Upregulation of melanogenesis and tyrosinase activity: potential agents for vitiligo. *Molecules*, 22 (8).

Ohguchi, K., Ahao Y. and Nozawa Y. 2006. Stimulation of melanogenesis by the citrus flavonoid naringenin in mouse B16 melanoma cells. *Bioscience, Biotechnology, and Biochemistry,* 70 (6):1499-1501.

Okunji C., Komarnytsky S., Fear G., Poulev A., Ribnicky D.M., Awachie P.I., Ito Y. and Raskin I. 2007. Preparative isolation and identification of tyrosinase inhibitors from the seeds of *Garcinia kola* by high-speed counter-current chromatography. *Journal of Chromatography A*, 1151 (1-2):45-50.

Pandey A. and Bhatnagar S.P. 2009. Preliminary phytochemical screening and antimicrobial studies on *Artocarpus lakoocha* Roxb. *Ancient Science of Life*, 28 (4):21-24.

Peñalver M.J., Fenoll L.G., Rodríguez-López J.N., García-Ruiz P.A., García-Molina F., Varón R., García-Cánovas F. and Tudela J. 2005. Reaction mechanism to explain the high kinetic autoactivation of tyrosinase. *Journal of Molecular Catalysis B: Enzymatic*, 33 (1-2):35-42.

Petit L., and Piérard G. E. 2003. Skin-lightening products revisited. *International Journal of Cosmetic Science,* 25 (4):169-181.

Pradhan C., Mohanty M. and Rout A. 2012. Phytochemical screening and comparative bioefficacy assessment of *Artocarpus altilis* leaf extracts for antimicrobial activity. *Frontiers in Life Science*, 6 (3-4):71-76.

Rozanowska M., Sarna T., Land E. J. and Truscott T. G. 1999. Free radical scavenging properties of melanin interaction of eu- and pheo-melanin models with reducing and oxidising radicals. *Free Radical Biology and Medicine*, 26 (5-6):518-525.

Santisuk T. and Larsen K. 2011. *Flora of Thailand.* Vol. 4. Original edition, Prachachon, Bangkok: 493, 673-674.

Shimizu K., Kondo R. and Sakai K. 2000. Inhibition of tyrosinase by flavonoids, stilbenes and related 4-substituted resorcinols: structure-activity investigations. *Planta Medica*, 66 (1):11-15.

Singh, V. 2015. *General anatomy with; systemic anatomy, radiological anatomy, medical genetic.* 2 nded. New Delhi, Reed Elsevier India Pvt. Ltd.: 49-58.

Skehan P, Storeng R, Scudiero D, Monks A, McMahon J, Vistica D. 1990. New colorimetric cytotoxicity assay for anticancer-drug screening. *Journal of the National Cancer Institute*, 82 (13):1107-12.

Slominski A., Tobin D.J., Shibahara S. and Wortsman J. 2004. Melanin pigmentation in mammalian skin and its hormonal regulation. *Physiological Reviews*, 84 (4):1155-1228.

Sohn H.Y., Kwon C.S. and Son K.H. 2010. Fungicidal effect of prenylated flavonol, papyriflavonol A, isolated from *Broussonetia papyrifera* (L.) Vent. against *Candida albicans*. *Journal of Microbiology and Biotechnology*, 20 (10):1397-1402.

Sohn H.Y., Son K.H., Kwon C.S., Kwon G.S. and Kang S.S. 2004. Antimicrobial and cytotoxic activity of 18 prenylated flavonoids isolated from medicinal plants: *Morus alba* L., *Morus mongolica* Schneider, *Broussnetia papyrifera* (L.) Vent., *Sophora flavescens* Ait. and *Echinosophora koreensis* Nakai. *Phytomedicine*, 11 (7-8):666-672.

Sritularak B. 1998. *Chemical constituents of Artocarpus lakoocha and A. gomezianus*, Master of Pharmacy in Pharmaceutical Sciences, Chulalongkorn University, Bangkok, Thailand.

Sritularak B., De-Eknamkul W. and Likhitwitayawuid K. 1998. Tyrosinase inhibitors from *Artocarpus lakoocha*. *The Thai Journal of Pharmaceutical Sciences*, 22:149-155.

Swargiary A. and Ronghang B. 2013. Screening of phytochemicals constituents, antioxidannt and antibacterial properties of methanolic bark extracts of *Maclura cochinchinensis* (Lour.) Corner. *International Journal of Pharma and Bio Sciences*, 4 (4):449-459.

Takahashi H. and Parsons P.G. 1992. Rapid and reversible inhibition of tyrosinase activity by glucosidase inhibitors in human melanoma cells. *Journal of Investigative Dermatology*, 98 (4):481-487.

Tanghetti E.A. 2013. The role of inflammation in the pathology of acne. *The Journal of Clinical and Aesthetic Dermatology*, 6 (9):27-35.

Taweechaisupapong S., Choopan T., Singhara S., Chatrchaiwiwatana S. and Wongkham S. 2005. *In vitro* inhibitory effect of *Streblus asper* leaf-extract on adhesion of *Candida albicans* to human buccal epithelial cells. *Journal of Ethnopharmacology*, 96 (1-2):221-226.

Taweechaisupapong S., Klanrit P., Singhara S., Pitiphat W. and Wongkham S. 2006. Inhibitory effect of *Streblus asper* leaf-extract on adhesion of *Candida albicans* to denture acrylic. *Journal of Ethnopharmacology*, 106 (3):414-417.

Taweechaisupapong S., Wongkham S., Chareonsuk S., Suparee S., Srilalai P. and Chaiyarak S. 2000. Selective activity of *Streblus asper* on *Mutans streptococci*. *Journal of Ethnopharmacology*, 70 (1):73-79.

Teanpaisan R., Senapong S. and Puripattanavong J. 2014. *In vitro* antimicrobial and activity of *Artocarpus lakoocha* (Moraceae) extract against some oral pathogens. *Tropical Journal of Pharmaceutical Research*, 13 (7):1149-1155.

Tengamnuay P., Pengrungruangwong K., Pheansri I. and Likhitwitayawuid K. 2006. *Artocarpus lakoocha* heartwood extract as a novel cosmetic ingredient: evaluation of the *in vitro* anti-tyrosinase and *in vivo* skin whitening activities. *International Journal of Cosmetic Science*, 28 (4):269-276.

Thakkar K., Geahlen R. L. and Cushman M. 1993. Synthesis and protein-tyrosine kinase inhibitory activity of polyhydroxylated stilbene analogues of piceatannol. *Journal of Medicinal Chemistry*, 36 (20):2950-2955.

Tsai P.W., de Castro-Cruz K.A., Shen C.-C. and Ragasa C.Y. 2012. Chemical constituents of *Broussonetia luzonicus*. *Pharmacognosy Journal*, 4 (31):1-4.

Wang K. H., Lin R. D., Hsu F. L., Huang Y. H., Chang H. C., Huang C. Y. and Lee M. H. 2006. Cosmetic applications of selected traditional Chinese herbal medicines. *Journal of Ethnopharmacology*, 106 (3):353-359.

Wang N. and Hebert D. N. 2006. Tyrosinase maturation through the mammalian secretory pathway: bringing color to life. *Pigment Cell Research*, 19 (1):3-18.

Wang Y. H., Hou A. J. and Chen D. F. 2007. Two new isoprenylated stilbenes from *Artocarpus chama*. *Journal of Integrative Plant Biology*, 49 (5):605−608.

Wang Y. H., Hou A. J., Chen L., Chen D. F., Sun H. D., Zhao Q. S., Bastow K. F., Nakanish Y., Wang X. H. and Lee K. H. 2004. New isoprenylated flavones, artochamins A--E, and cytotoxic principles from *Artocarpus chama*. *Journal of Natural Products*, 67 (5):757-761.

Weli A. M., Al-Blushi A. A. M. and Hossain M. A. 2015. Evaluation of antioxidant and antimicrobial potential of different leaves crude extracts of Omani *Ficus carica* against food borne pathogenic bacteria. *Asian Pacific Journal of Tropical Disease*, 5 (1):13-16.

Wongkham S., Laupattarakasaem P., Pienthaweechai K., Areejitranusorn P., Wongkham C. and Techanitiswad T. 2001. Antimicrobial activity of *Streblus asper* leaf extract. *Phytotherapy Research*, 15 (2):119-121.

Xie, Y., Yang W., Tang F., Chen X. Ren and L. 2015. Antibacterial activities of flavonoids: structure-activity relationship and mechanism. *Current Medicinal Chemistry*, 22 (1): 132-149.

Woolery-Lloyd H. and Kammer J. 2011. Treatment of hyperpigmentation. *Seminars in Cutaneous Medicine and Surgery Journal*, 30 (3):171-175.

Ye Y., Chou G.X., Mu D.D., Wang H, Chu J.H., Leung A.K., 2010. Screening of Chinese herbal medicines for antityrosinase activity in a cell free system and B16 cells. *Journal of Ethnopharmacology* 129 (3):387-90.

Ye Y., Wang H., Chu J. H., Chou G. X. and Yu Z. L. 2011. Activation of p38 MAPK pathway contributes to the melanogenic property of apigenin in B16 cells. *Experimental Dermatology*, 20 (9):755-757.

Yessoufou K., Elansary H.O., Mahmoud E.A. and Skalicka-Woźniak K. 2015. Antifungal, antibacterial and anticancer activities of *Ficus drupacea* L. stem bark extract and biologically active isolated compounds. *Industrial Crops and Products*, 74:752-758.

Yokoyama K., Suzuki H., Yasumoto K., Tomita Y. and Shibahara S. 1994. Molecular cloning and functional analysis of a cDNA coding for human DOPAchrome tautomerase/tyrosinase-related protein-2. *Biochimica et Biophysica Acta*, 1217 (3):317-321.

Zhang L., Tao G., Chen J. and Zheng Z. P. 2016. Characterization of a newf lavone and tyrosinase inhibition constituents from the twigs of *Morus alba* L. *Molecules*, 21 (9).

Zheng Z.P., Cheng K.W., Chao J., Wu J. and Wang M. 2008a. Tyrosinase inhibitors from paper mulberry (*Broussonetia papyrifera*). *Food Chemistry*, 106 (2):529-535.

Zheng Z.P., Cheng K.W., To J.T., Li H. and Wang M. 2008b. Isolation of tyrosinase inhibitors from *Artocarpus heterophyllus* and use of its extract as antibrowning agent. *Molecular Nutrition & Food Research*, 52 (12):1530-1538.

Zheng Z. P., Cheng K. W., Zhu Q., Wang X. C., Lin Z. X. and Wang M. 2010. Tyrosinase inhibitory constituents from the roots of *Morus nigra*: a structure-activity relationship study. *Journal of Agricultural and Food Chemistry*, 58 (9):5368-5373.

Zheng Z.P., Chen S., Wang S., Wang X.C., Cheng K.W., Wu J.J., Yang D. and Wang M. 2009. Chemical components and tyrosinase inhibitors from the twigs of *Artocarpus heterophyllus*. *Journal of Agricultural and Food Chemistry*, 57 (15):6649-6655.

Zheng Z.P., Tan H.Y., Chen J. and Wang M. 2013. Characterization of tyrosinase inhibitors in the twigs of *Cudrania tricuspidata* and their structure-activity relationship study. *Fitoterapia*, 84:242-247.

APPENDIX

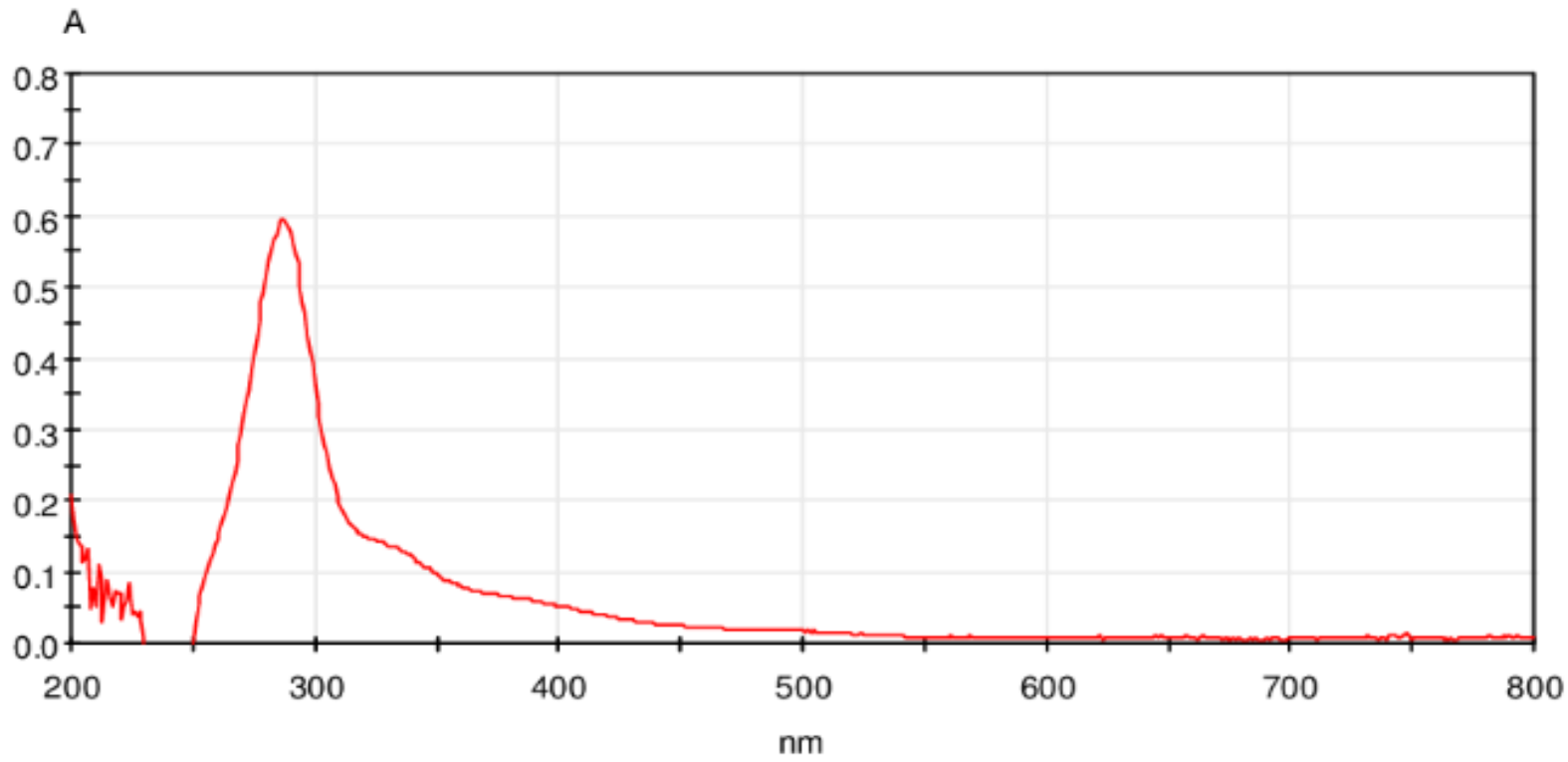

Figure A-1 UV-Visible spectrum of homoeriodictyol (No.1)

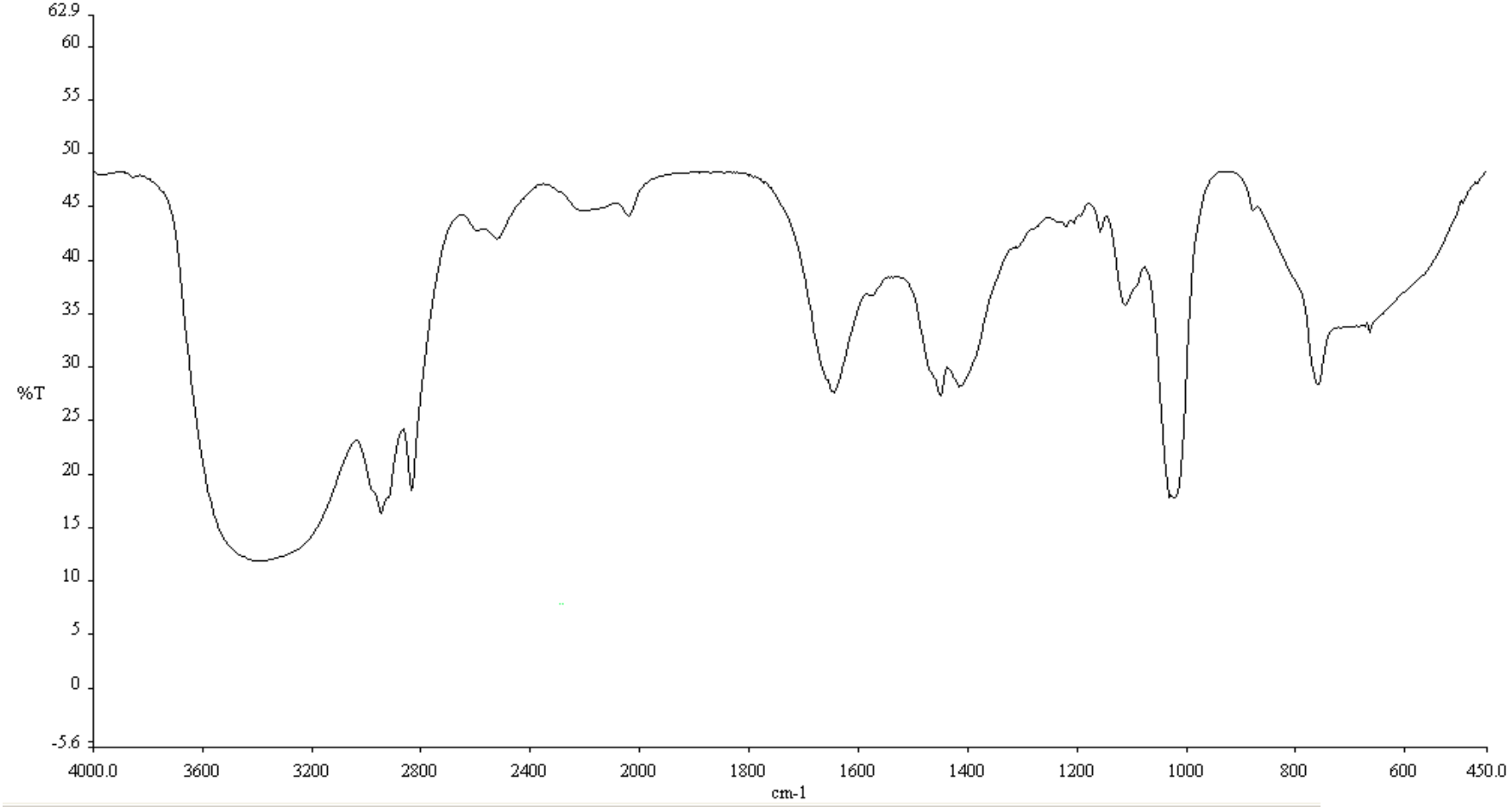

Figure A-2 IR spectrum of homoeriodictyol (KBr disc) (No.1)

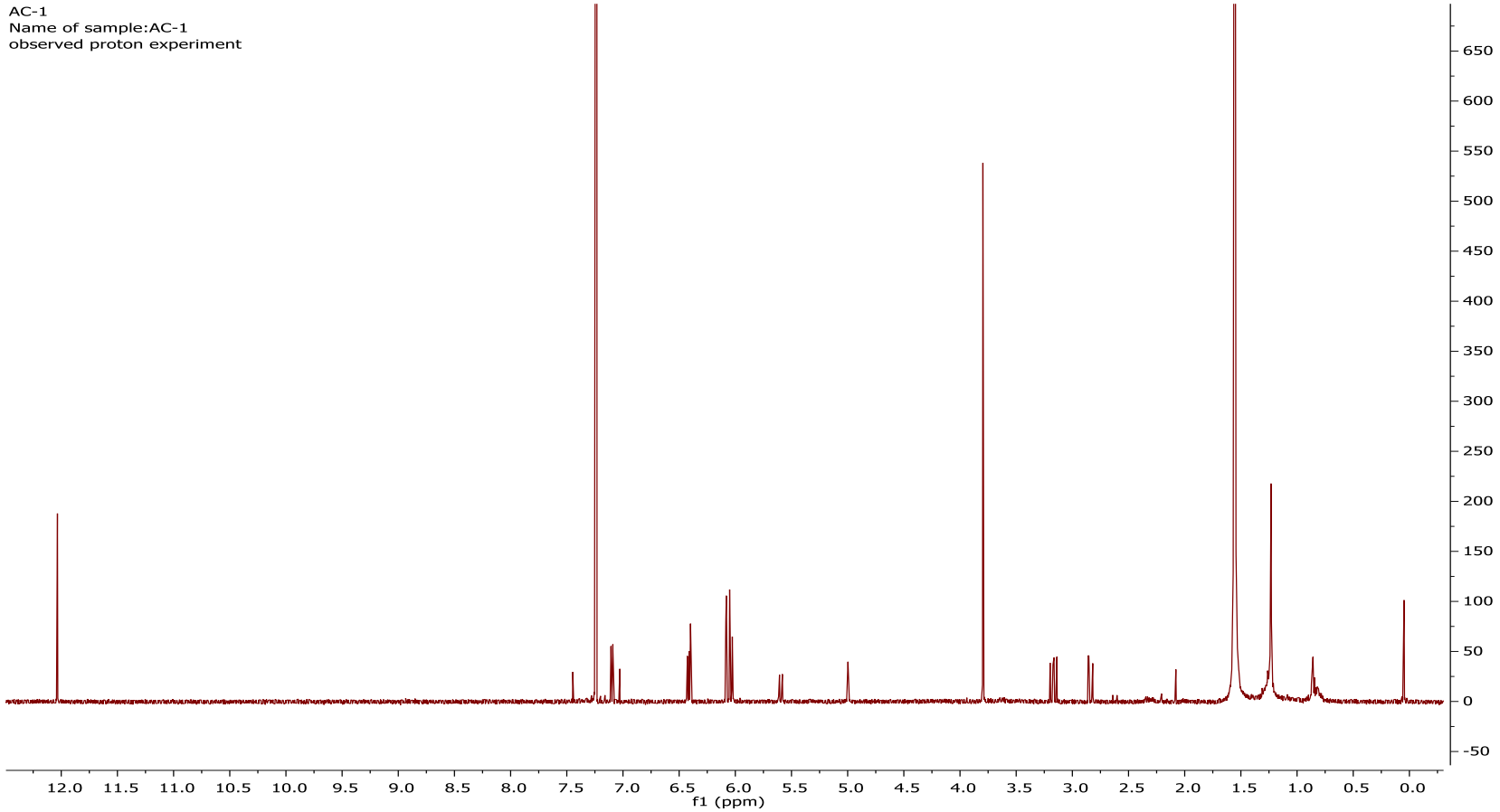

Figure A-4 ^{1}H NMR spectrum of homoeriodictyol (No.1)

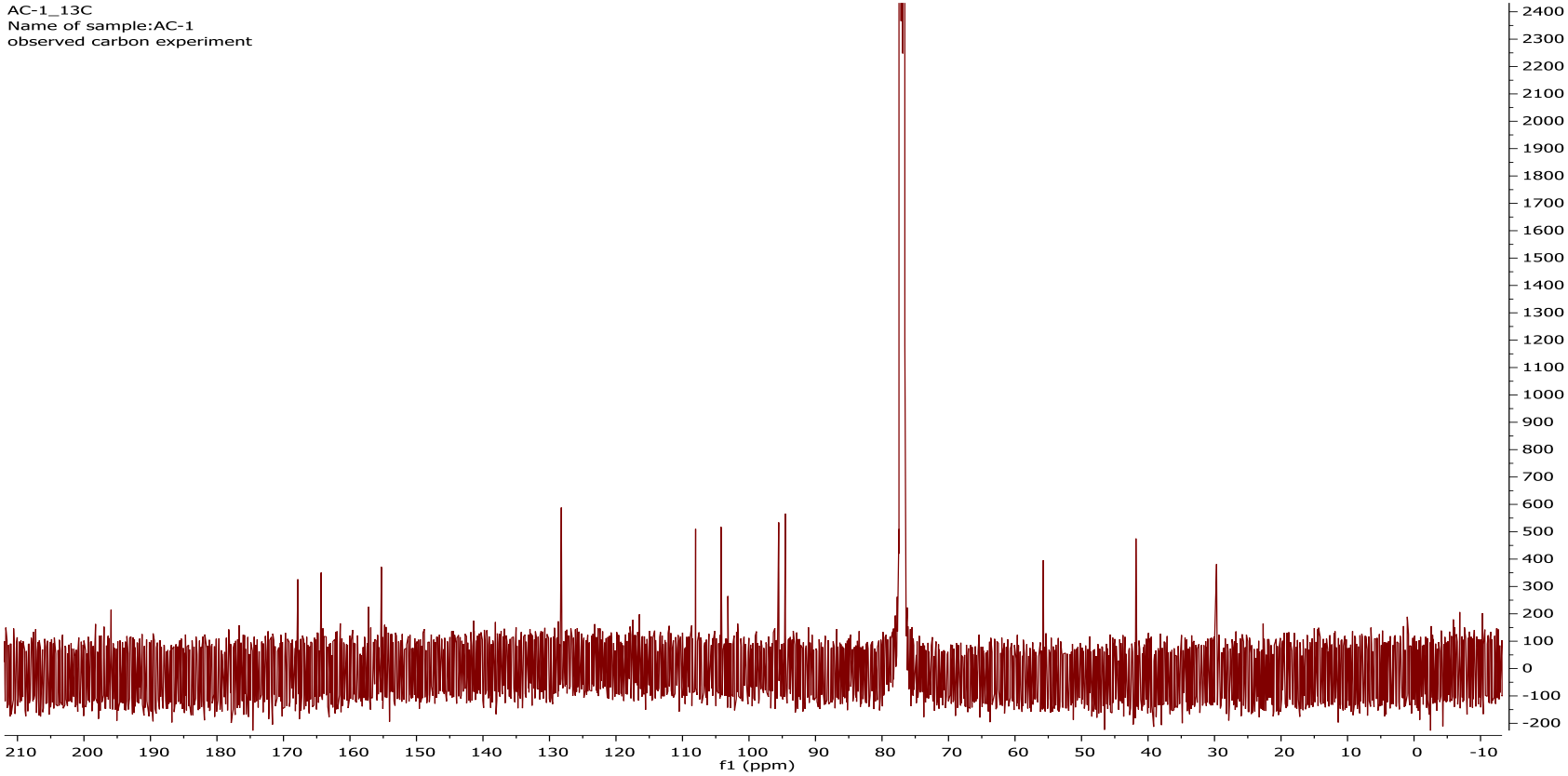

Figure A-5 ^{13}C NMR spectrum of homoeriodictyol (No.1)

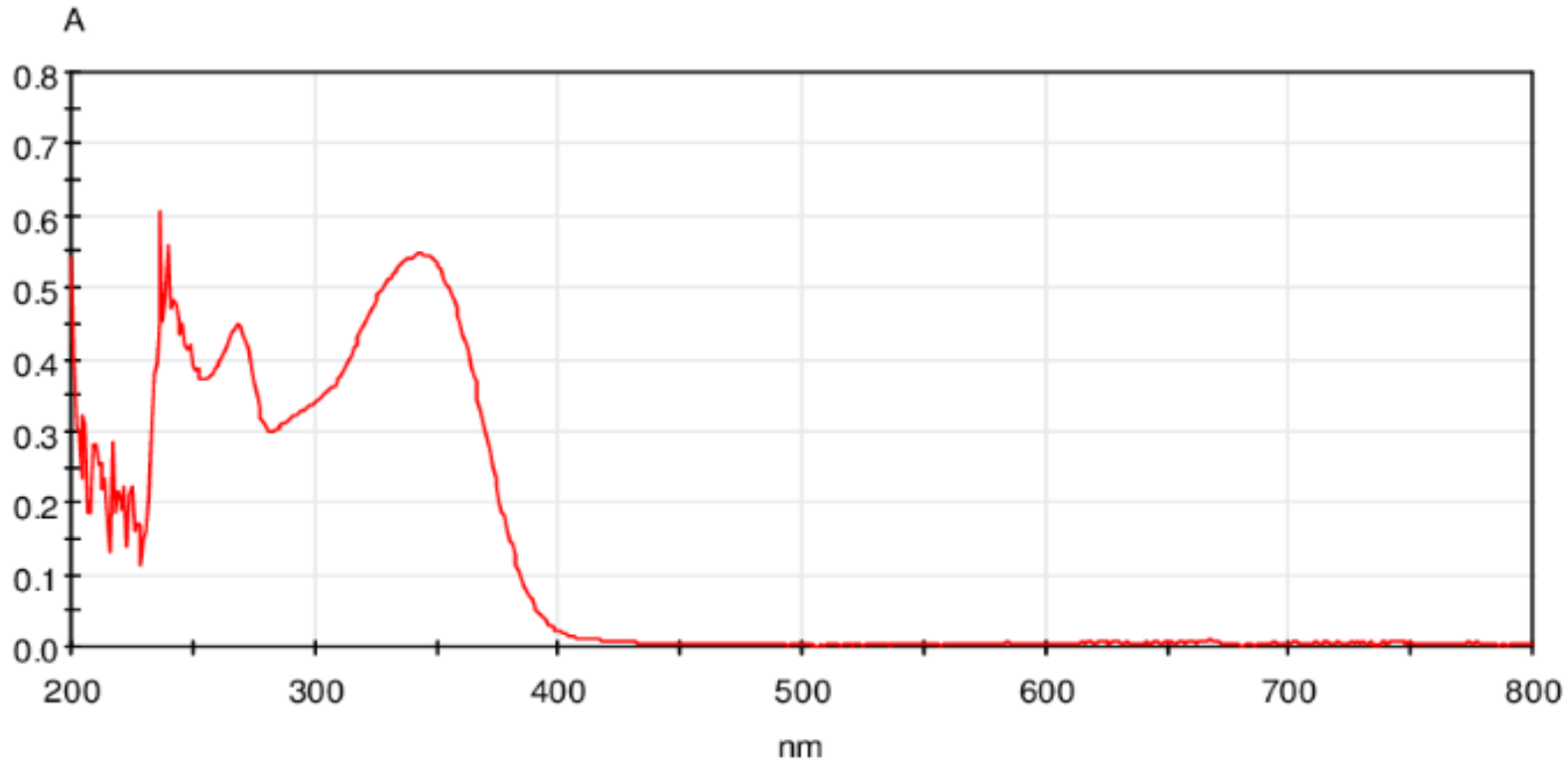

Figure B-1 UV-Visible spectrum of 3´-farnesyl apigenin (No.2)

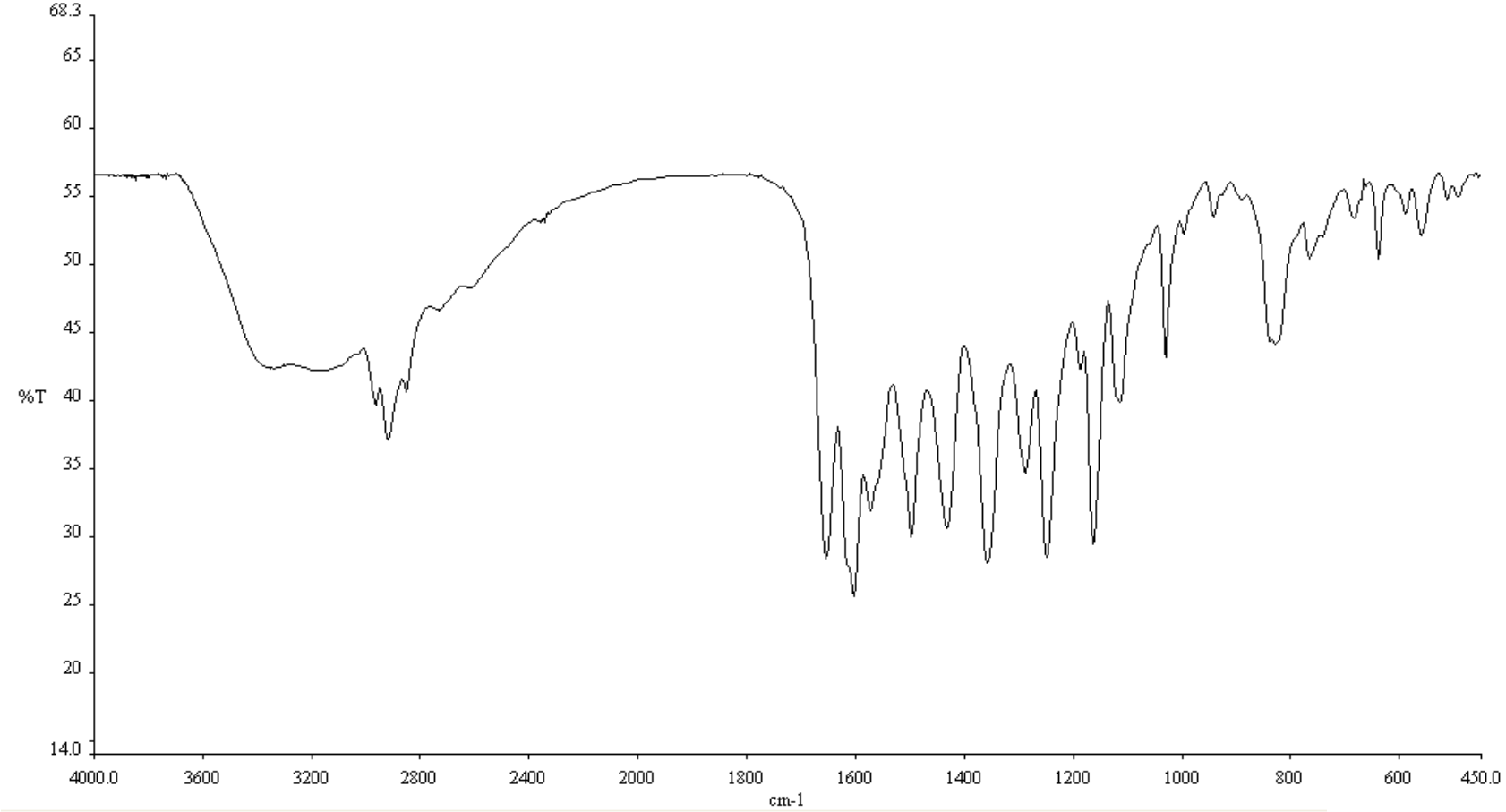

Figure B-2 IR spectrum of 3´-farnesyl apigenin (KBr disc) (No.2)

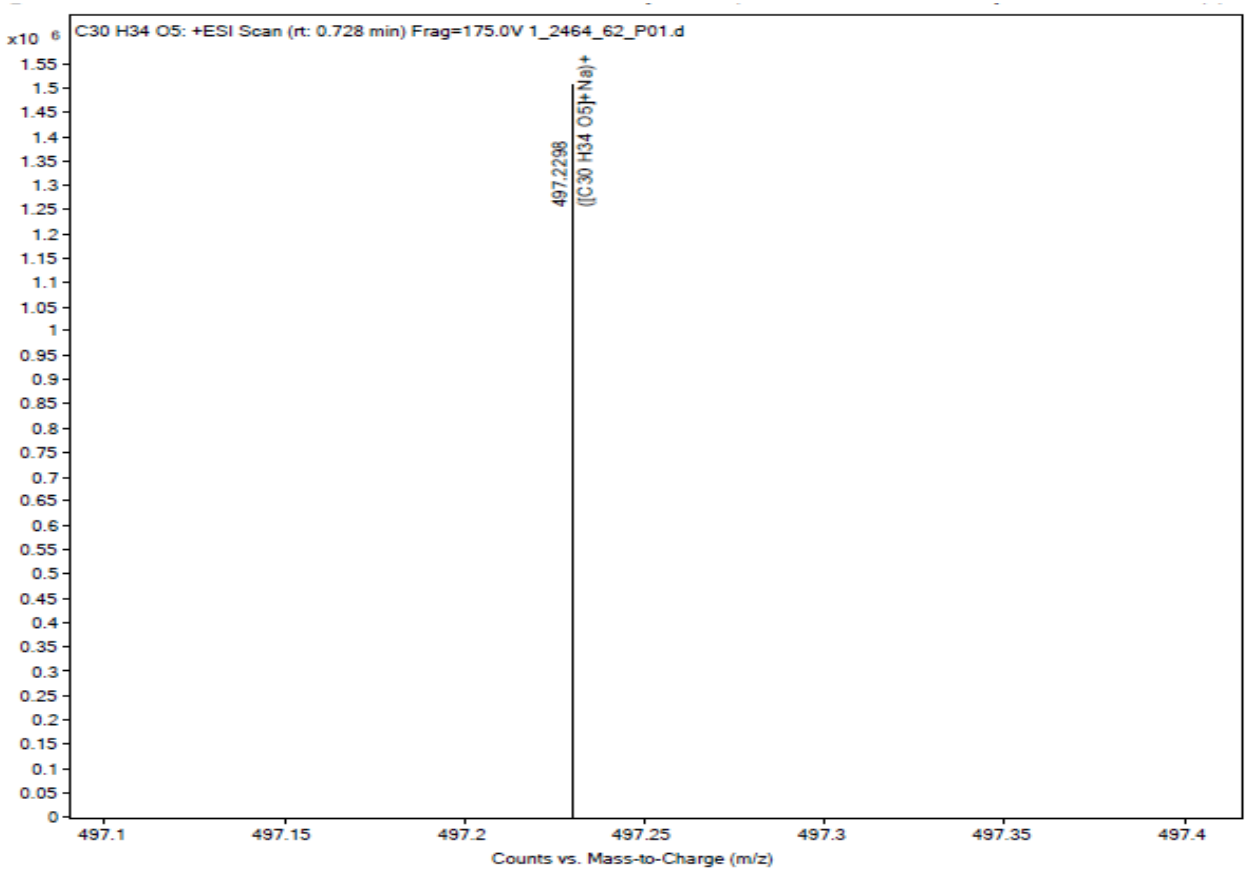

Figure B-3 HRESI mass spectrum of 3´-farnesyl apigenin (No.2)

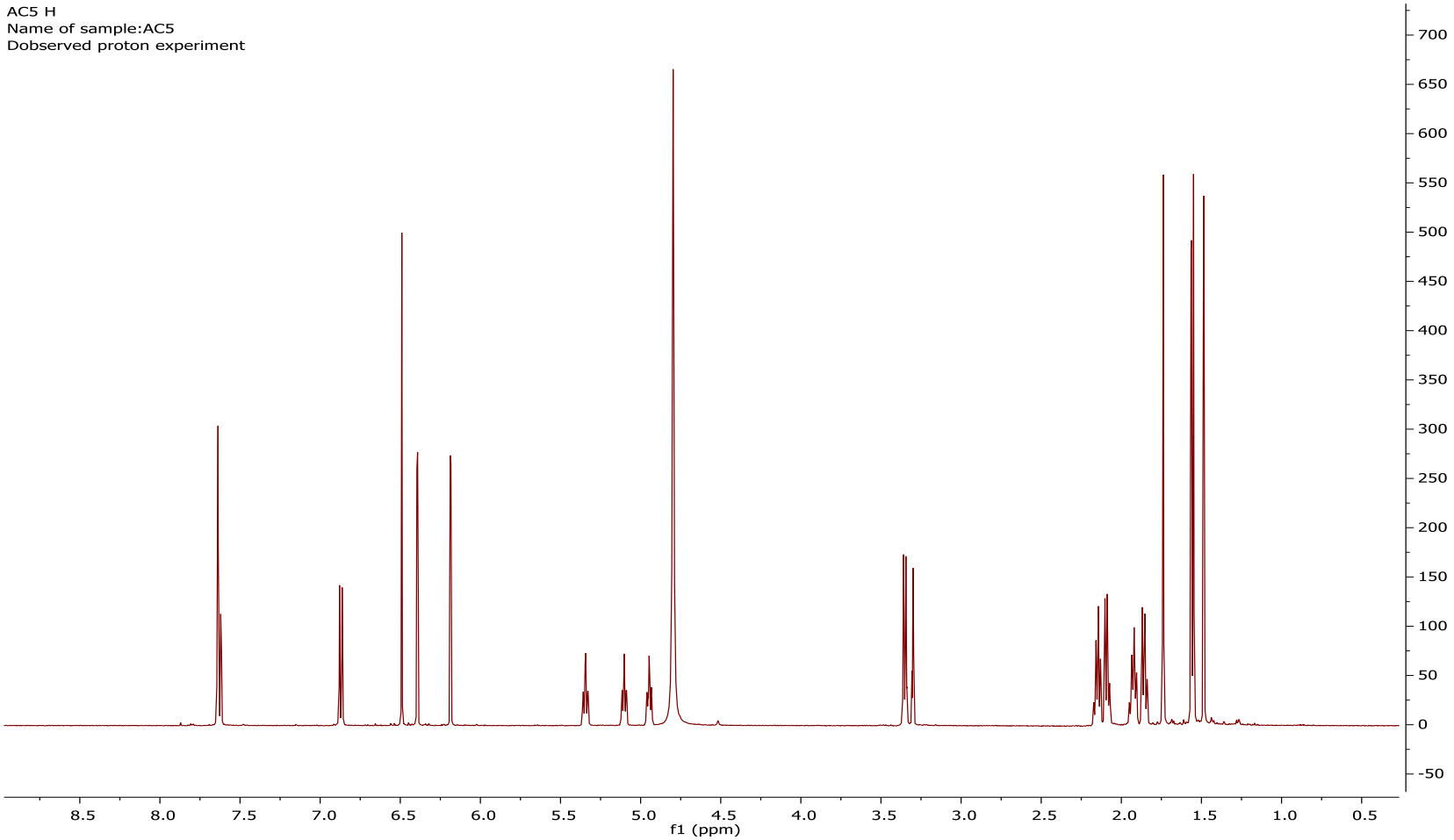

Figure B-4 ^{1}H NMR spectrum of 3´-farnesyl apigenin (No.2)

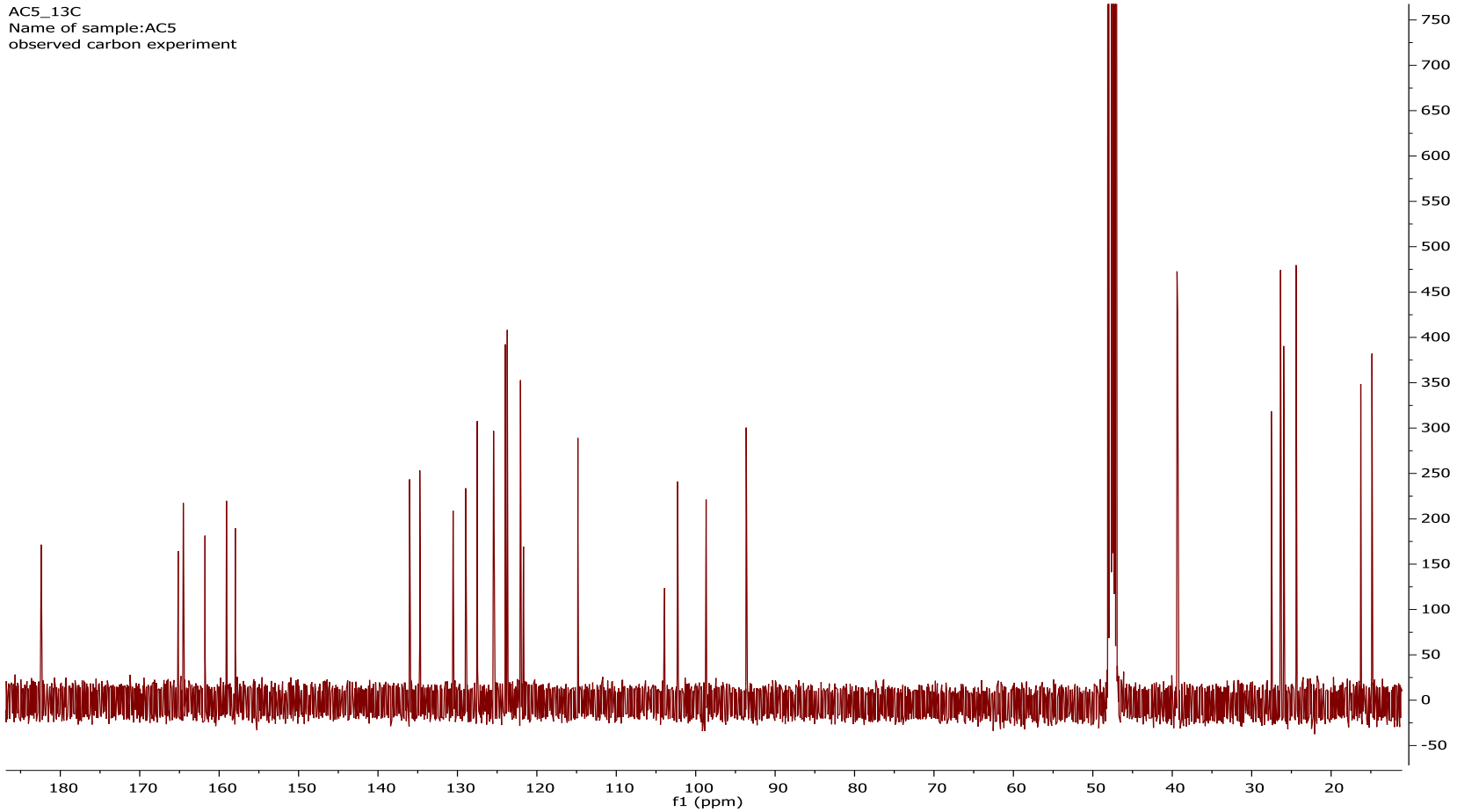

Figure B-5 ^{13}C NMR spectrum of 3´-farnesyl apigenin (No.2)

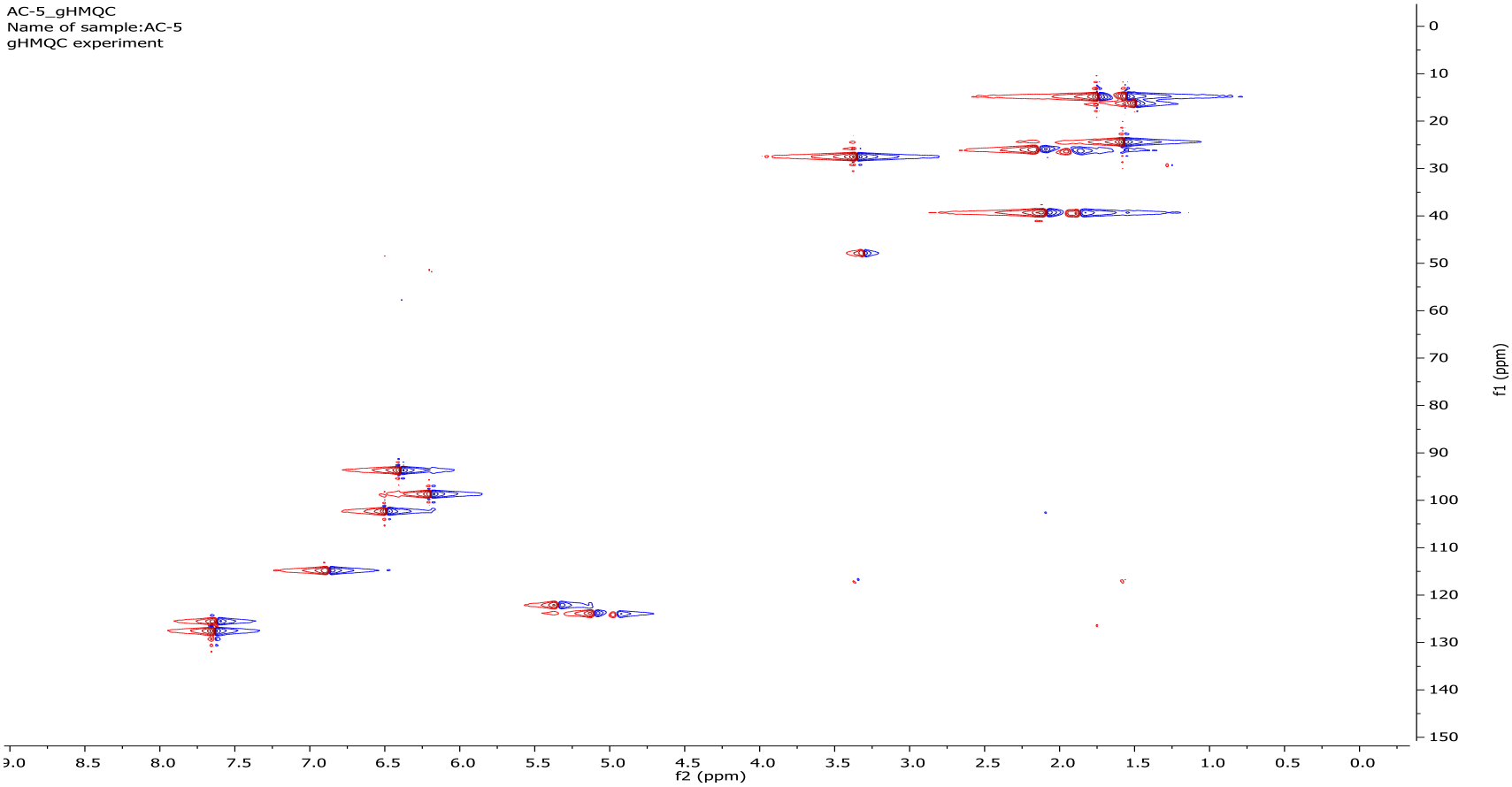

Figure B-6 HMQC spectrum of 3´-farnesyl apigenin (No.2)

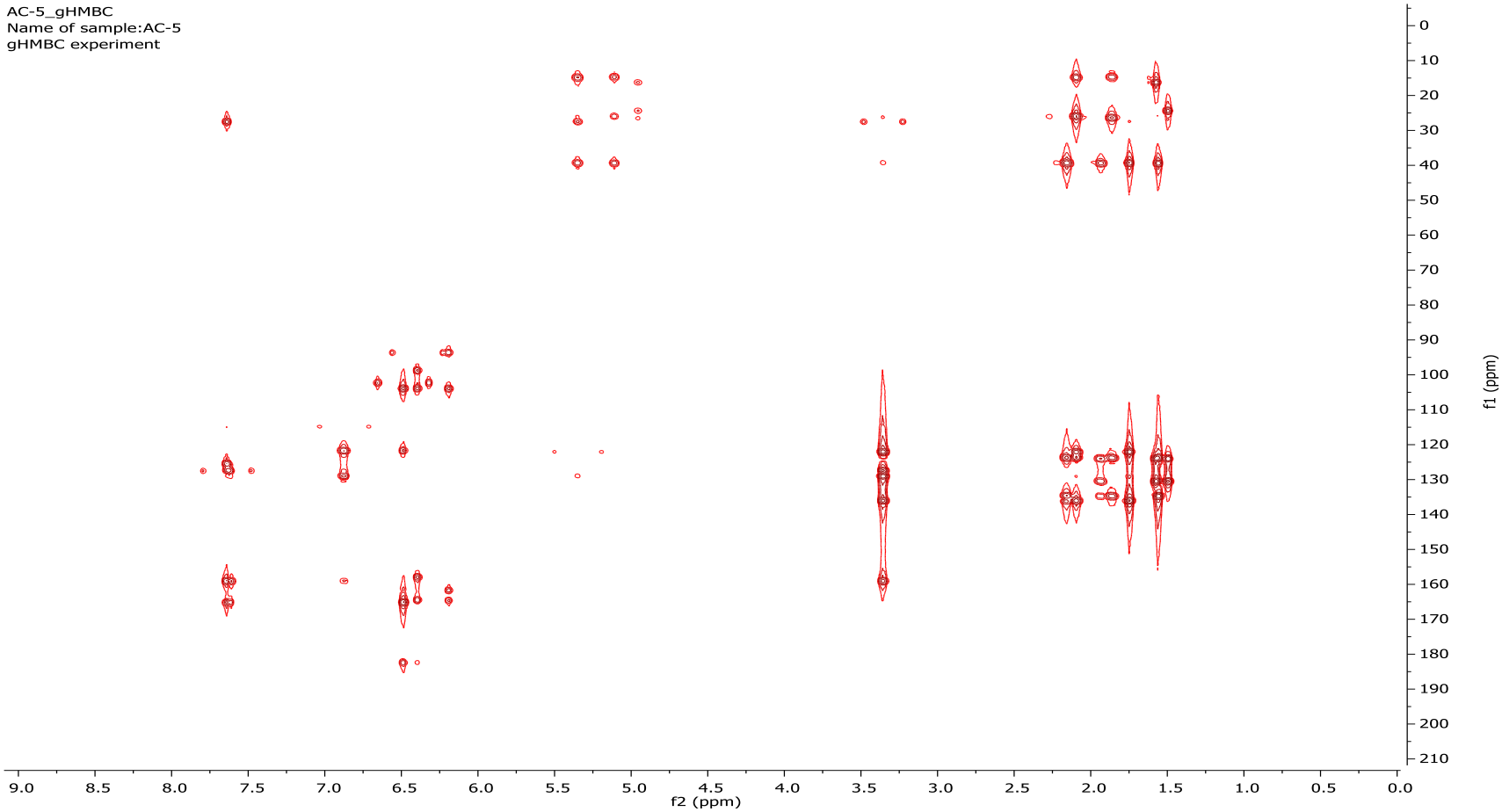

Figure B-7 HMBC spectrum of 3´-farnesyl apigenin (No.2)

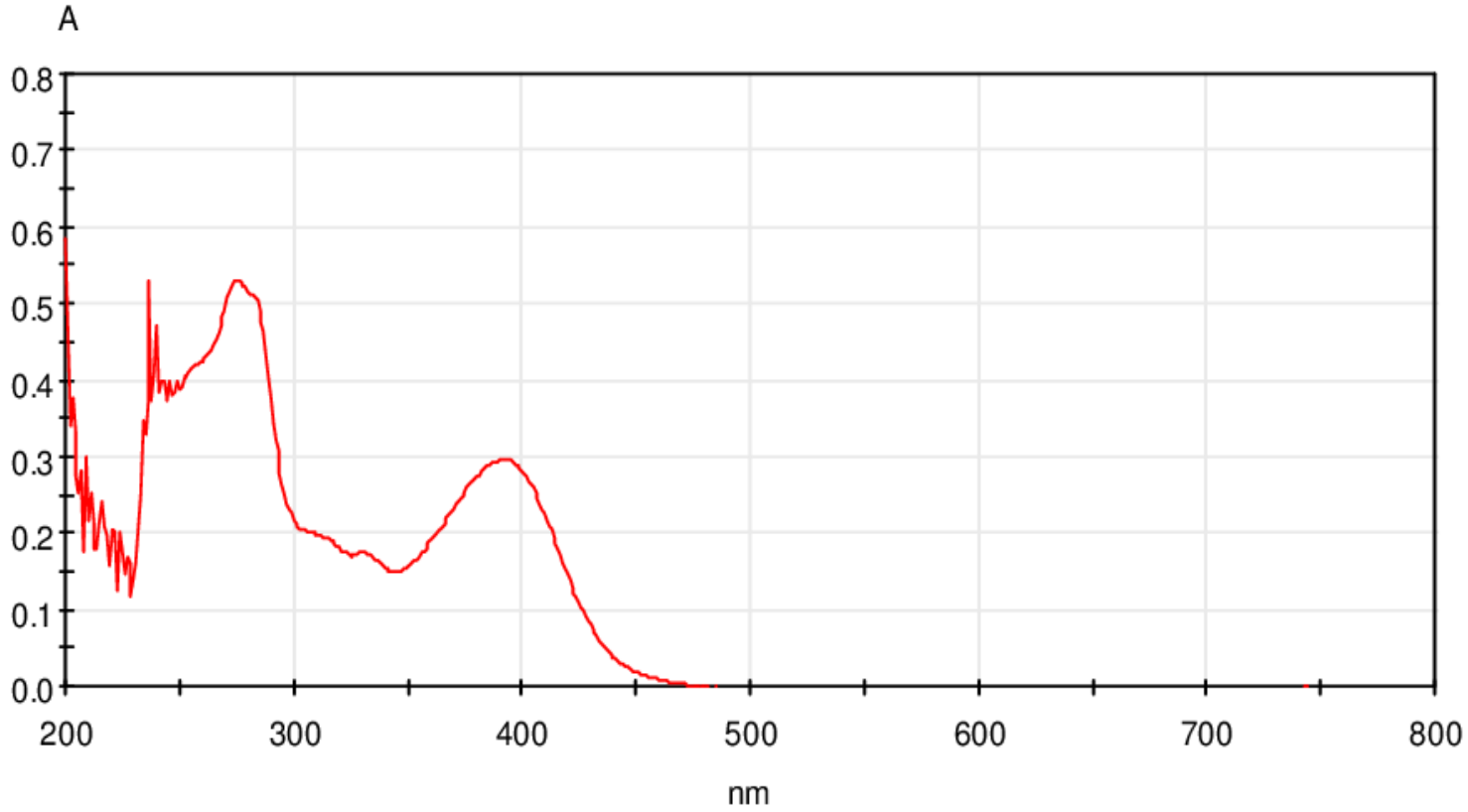

Figure C-1 UV-Visible spectrum of isocycloartobiloxanthone (No.3)

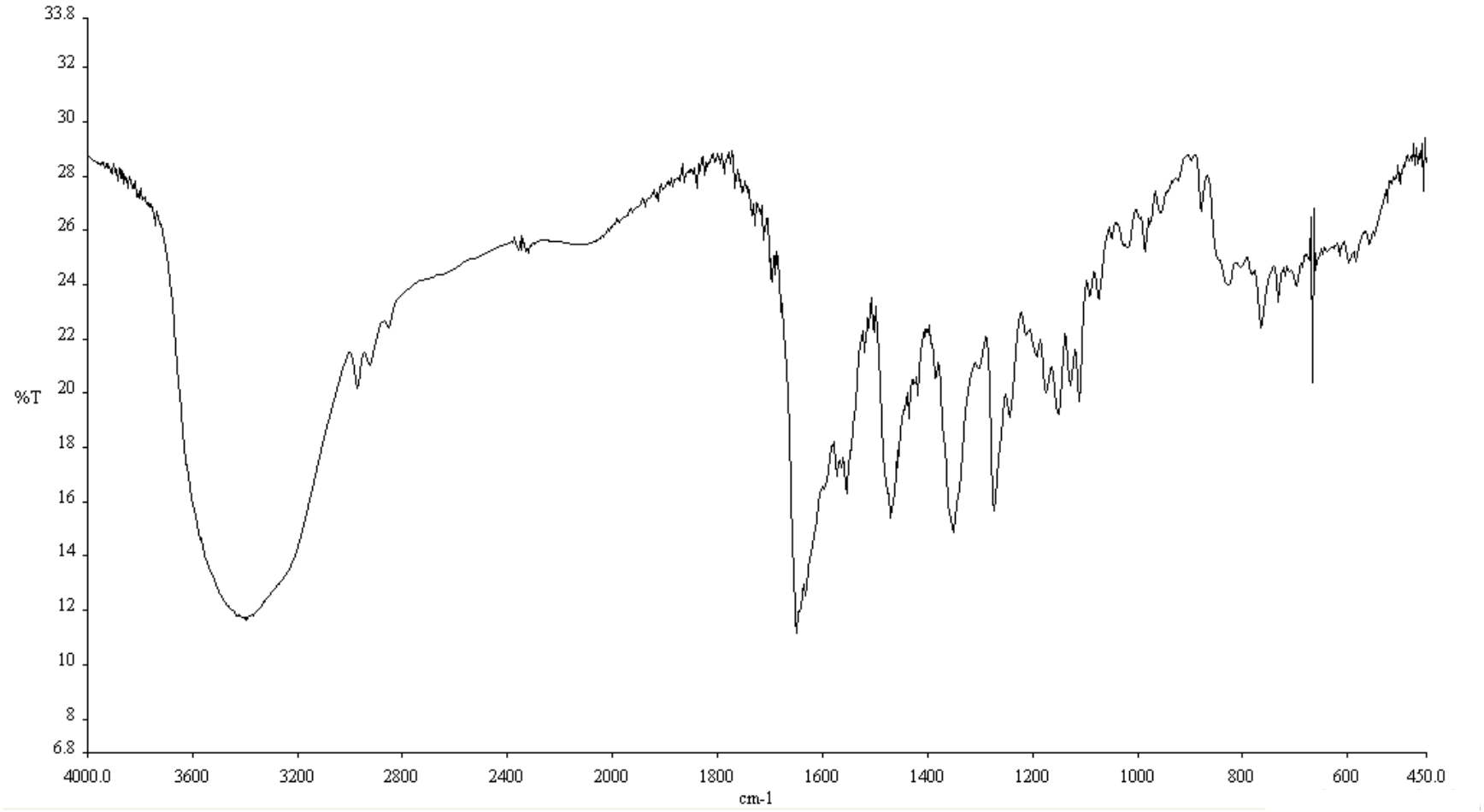

Figure C-2 IR spectrum of isocycloartobiloxanthone (KBr disc) (No.3)

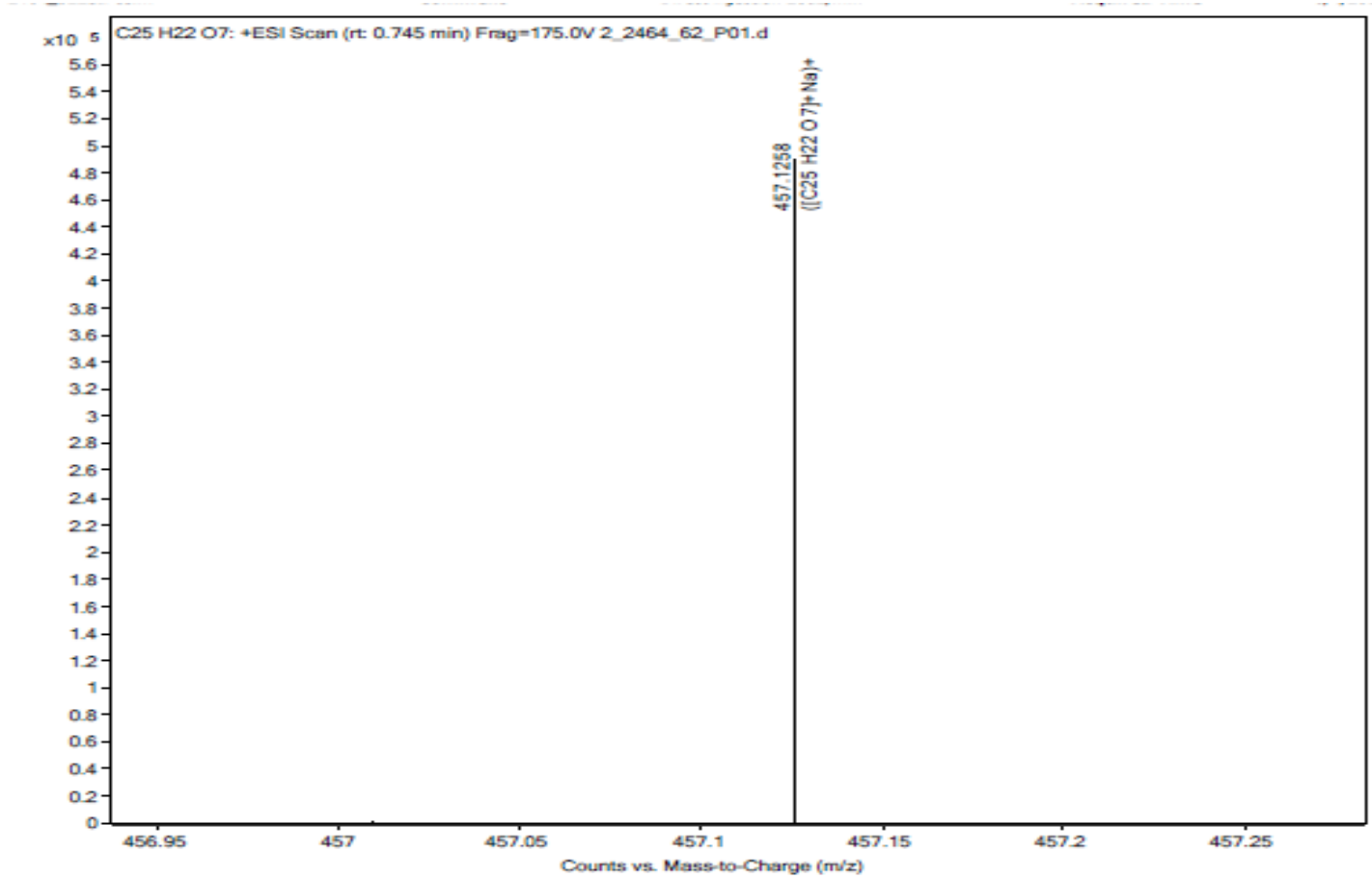

Figure C-3 HRESI mass spectrum of isocycloartobiloxanthone (No.3)

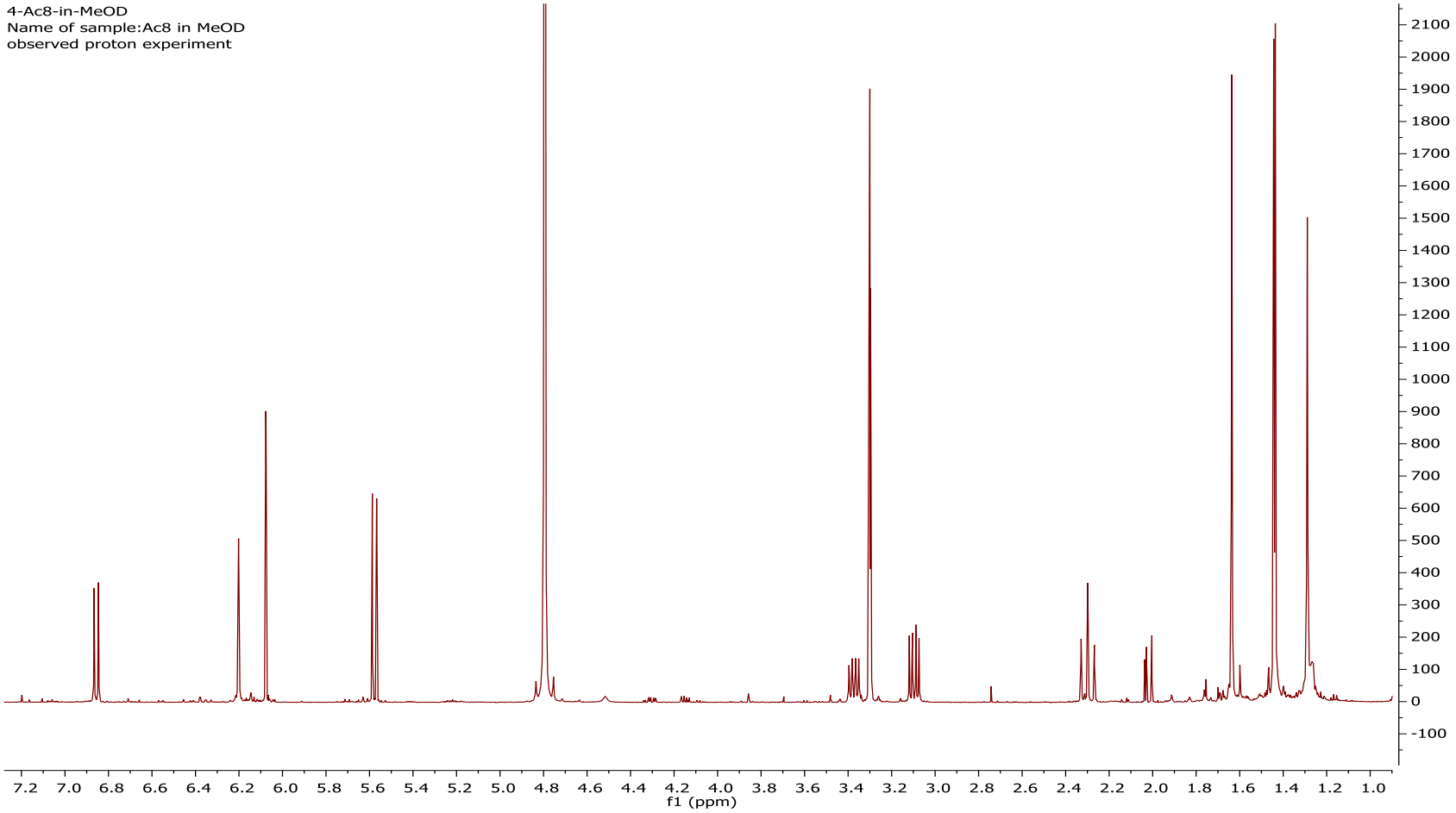

Figure C-4 ^{1}H NMR spectrum of isocycloartobiloxanthone (No.3)

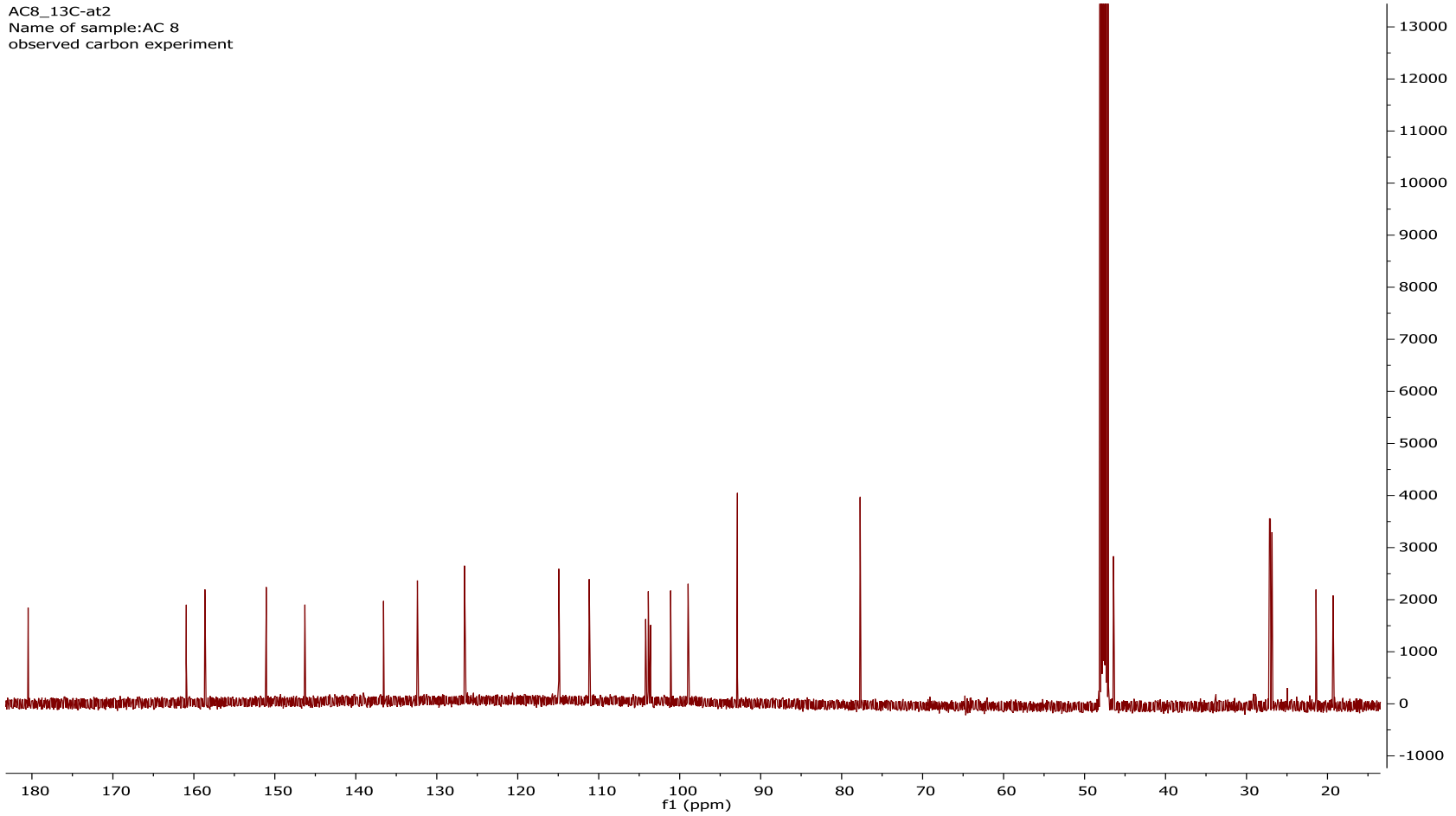

Figure C-5 ^{13}C NMR spectrum of isocycloartobiloxanthone (No.3)

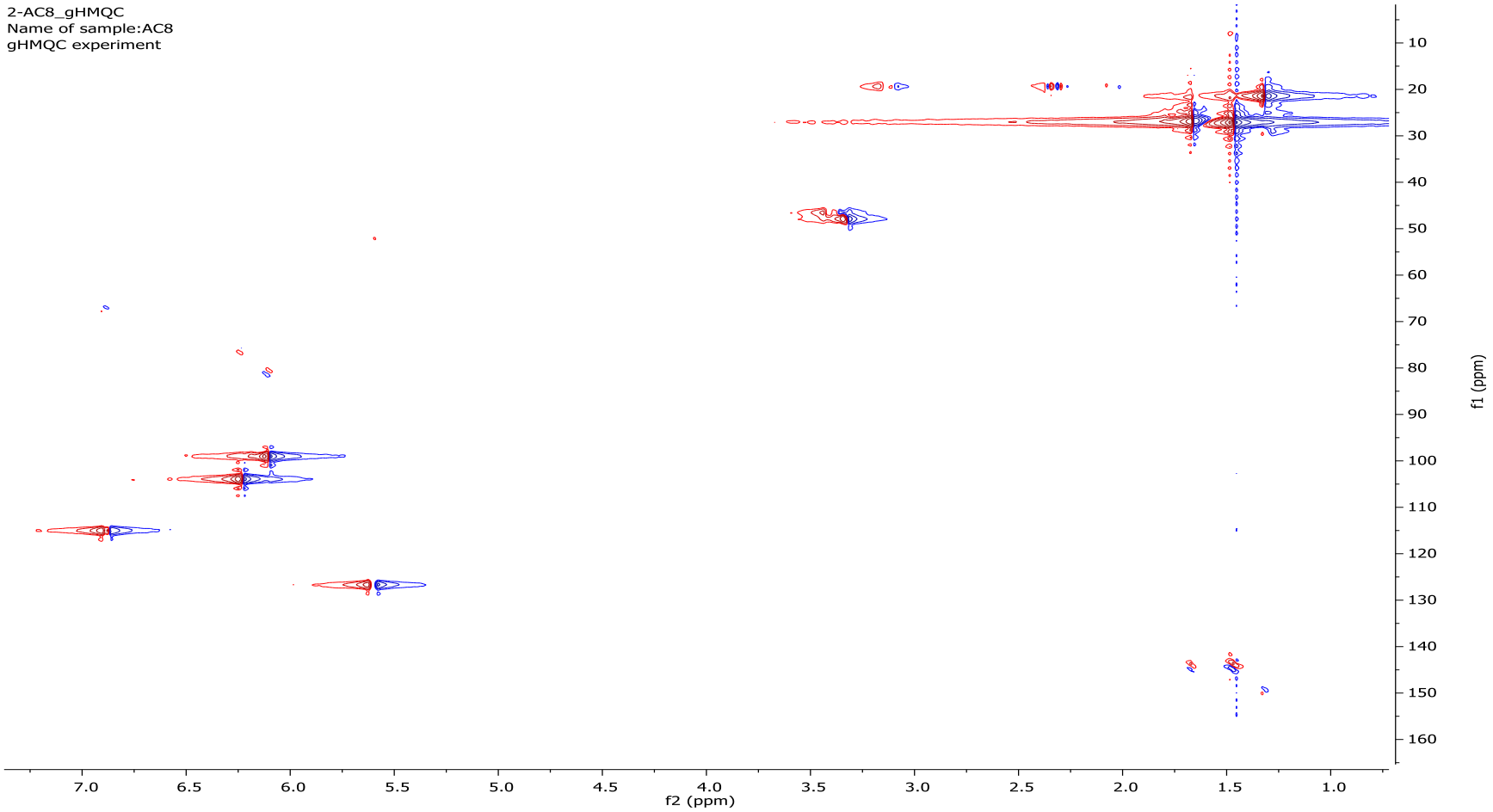

Figure C-6 HMQC spectrum of isocycloartobiloxanthone (No.3)

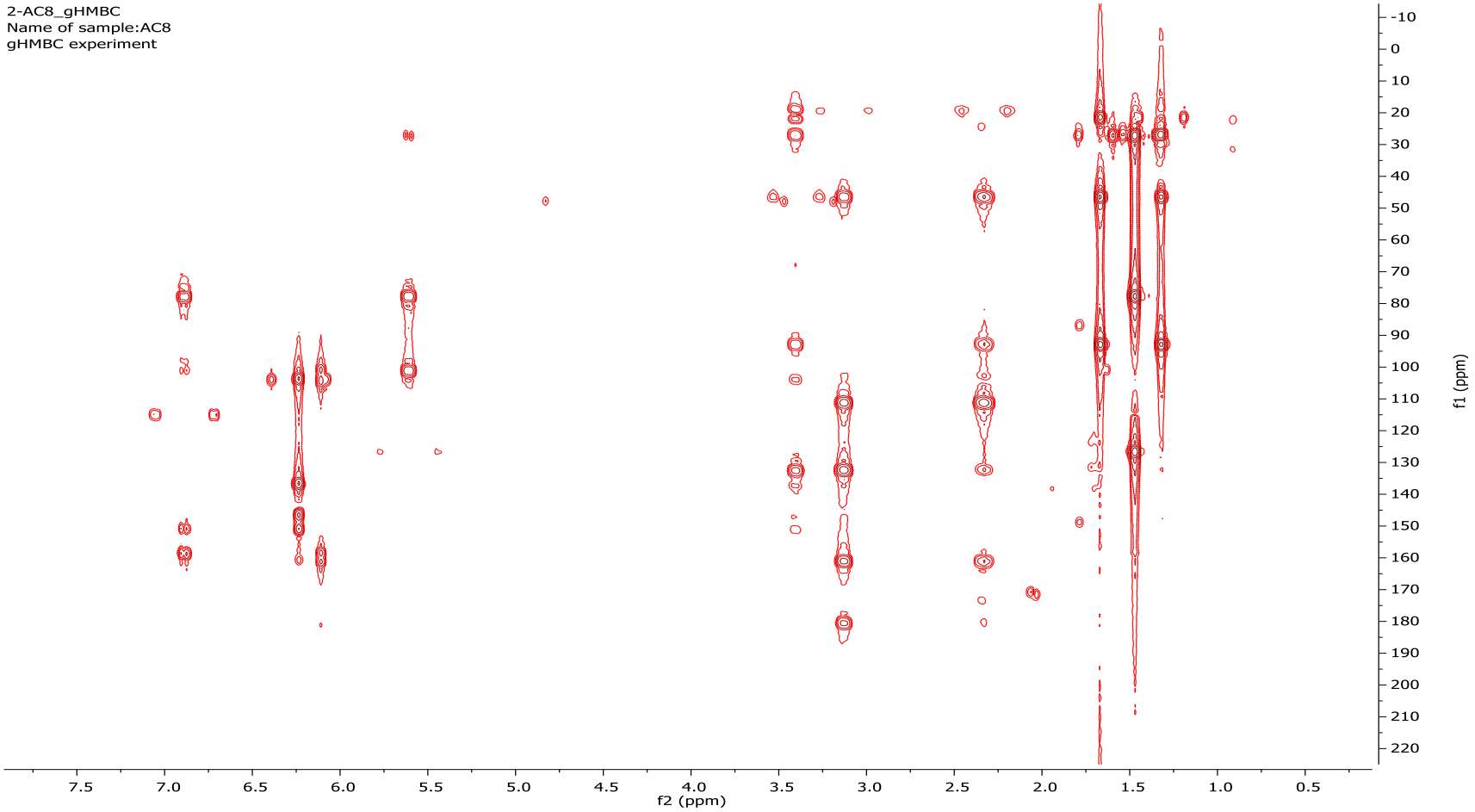

Figure C-7 HMBC spectrum of isocycloartobiloxanthone (No.3)

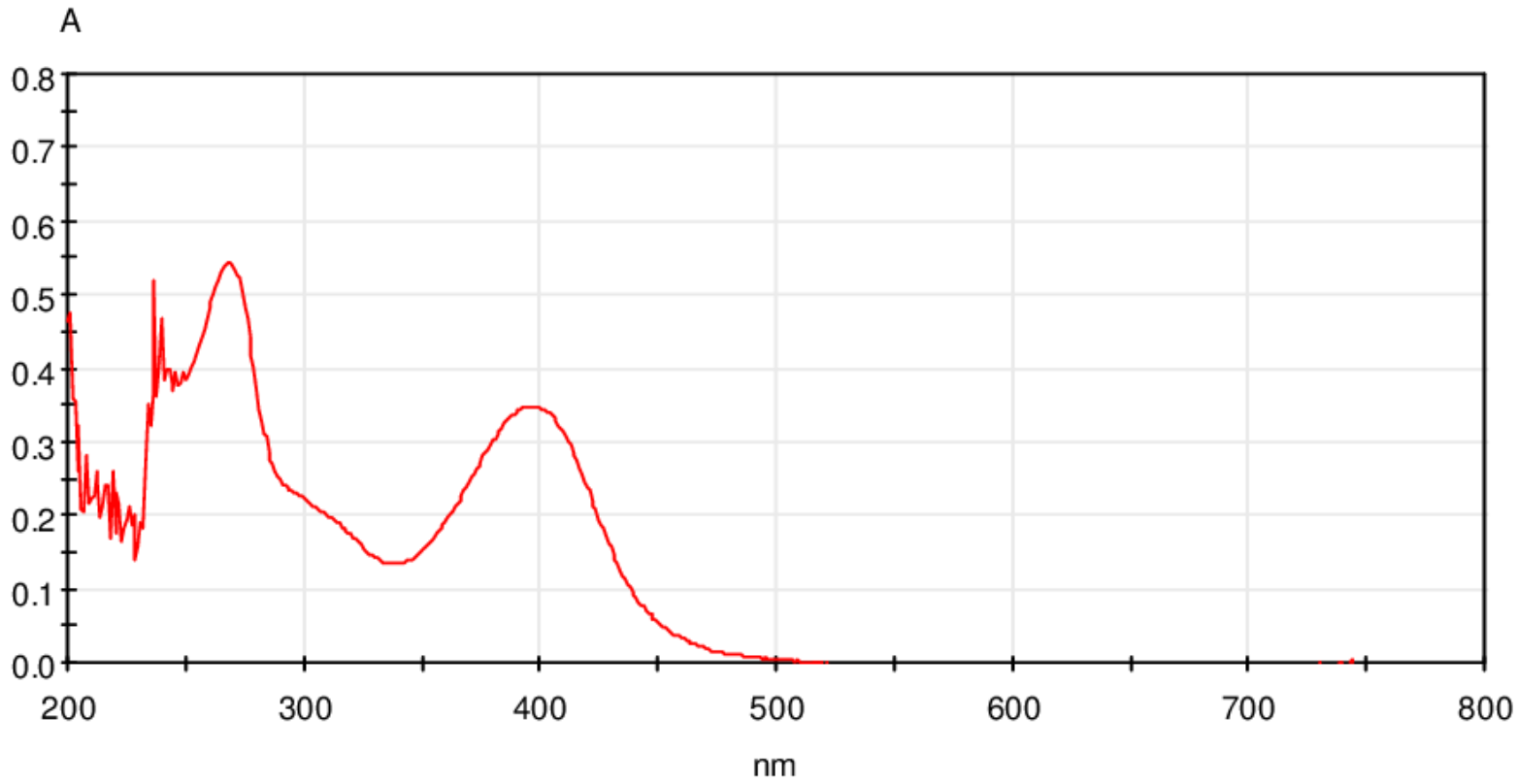

Figure D-1 UV-Visible spectrum of 3-(hydroxyprenyl) isoetin (No.4)

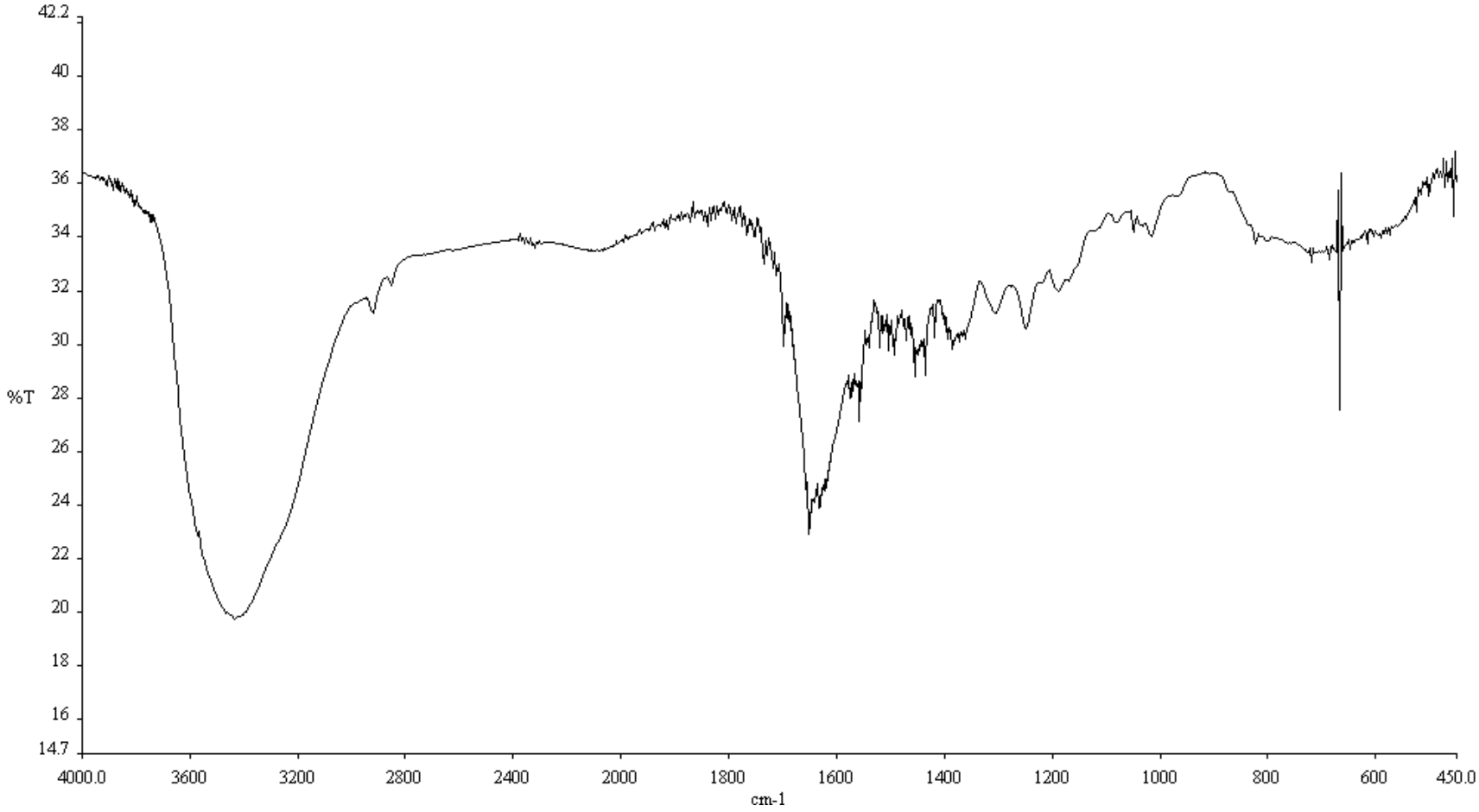

Figure D-2 IR spectrum of 3-(hydroxyprenyl) isoetin (KBr disc) (No.4)

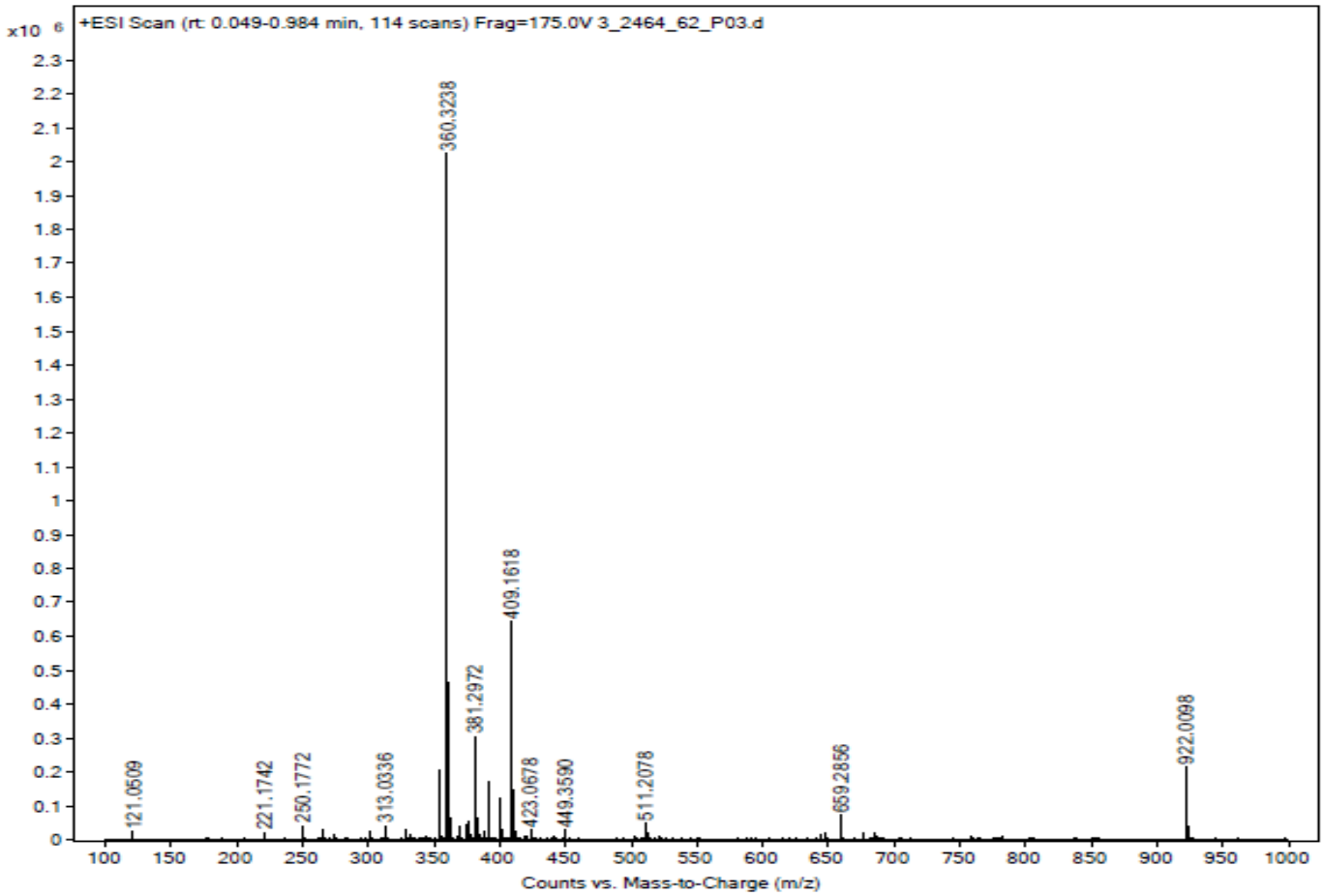

Figure D-3 ESI mass spectrum of 3-(hydroxyprenyl) isoetin (No.4)

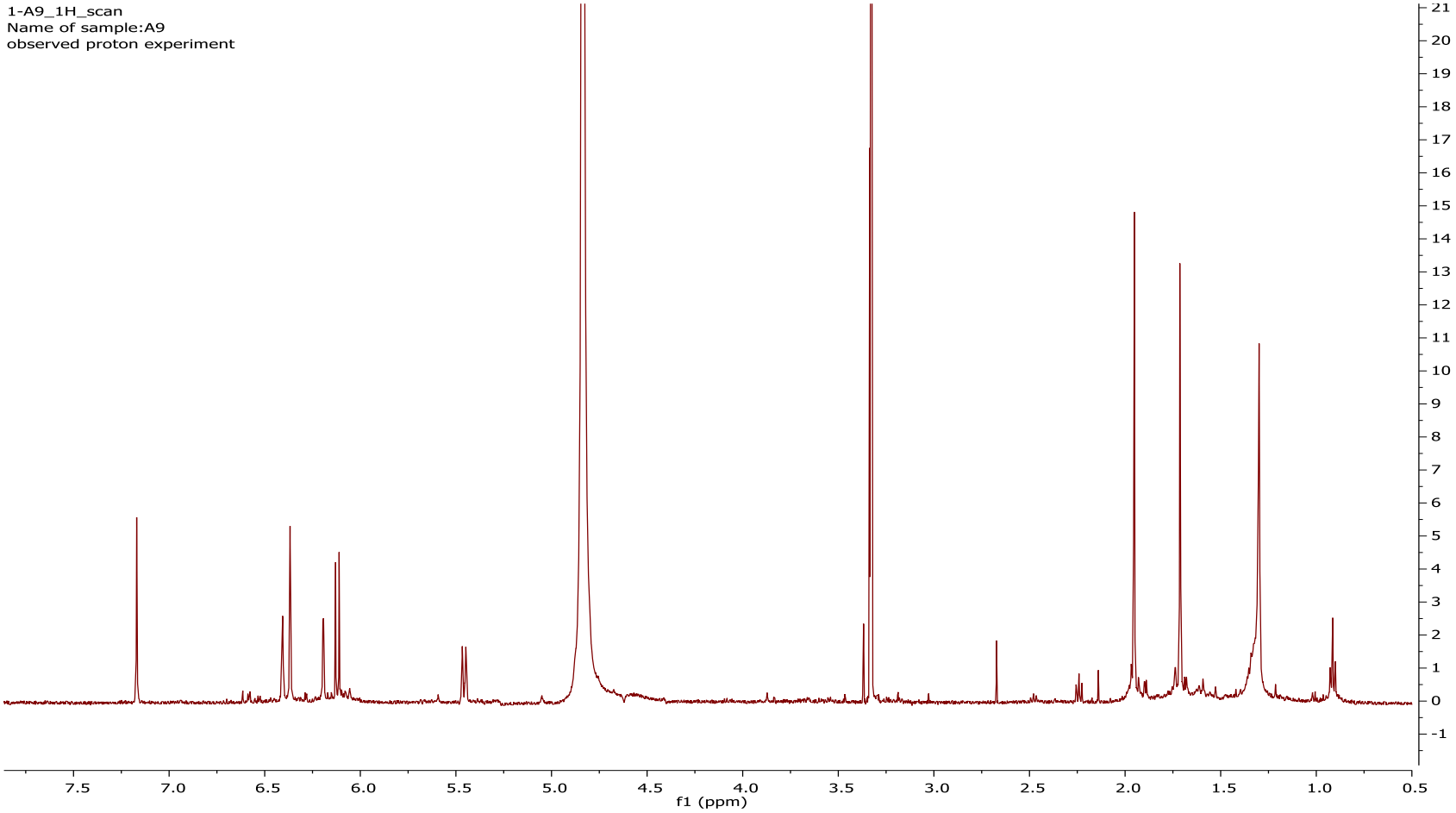

Figure D-4 ^{1}H NMR spectrum of 3-(hydroxyprenyl) isoetin (No.4)

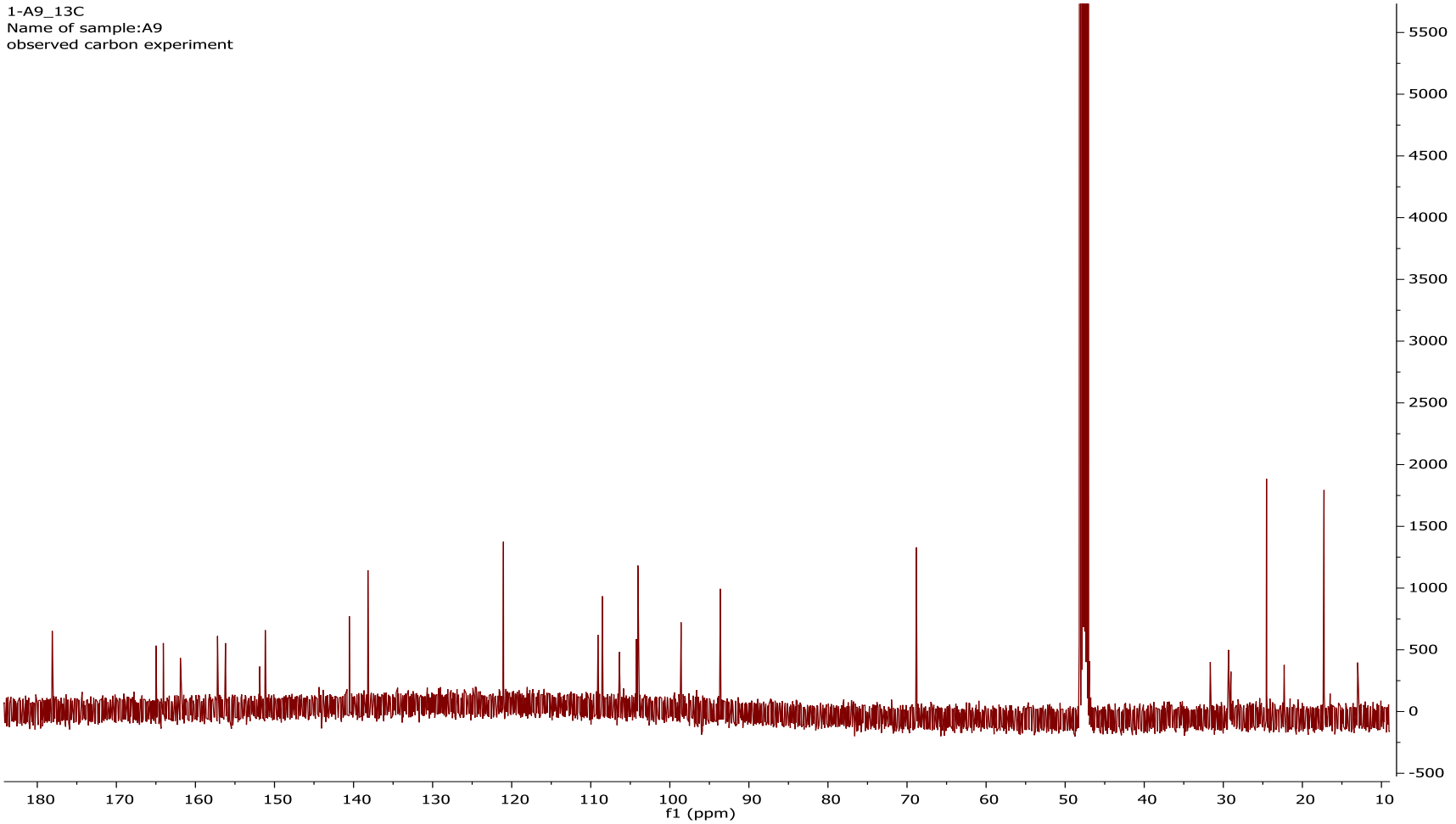

Figure D-5 ^{13}C NMR spectrum of 3-(hydroxyprenyl) isoetin (No.4)

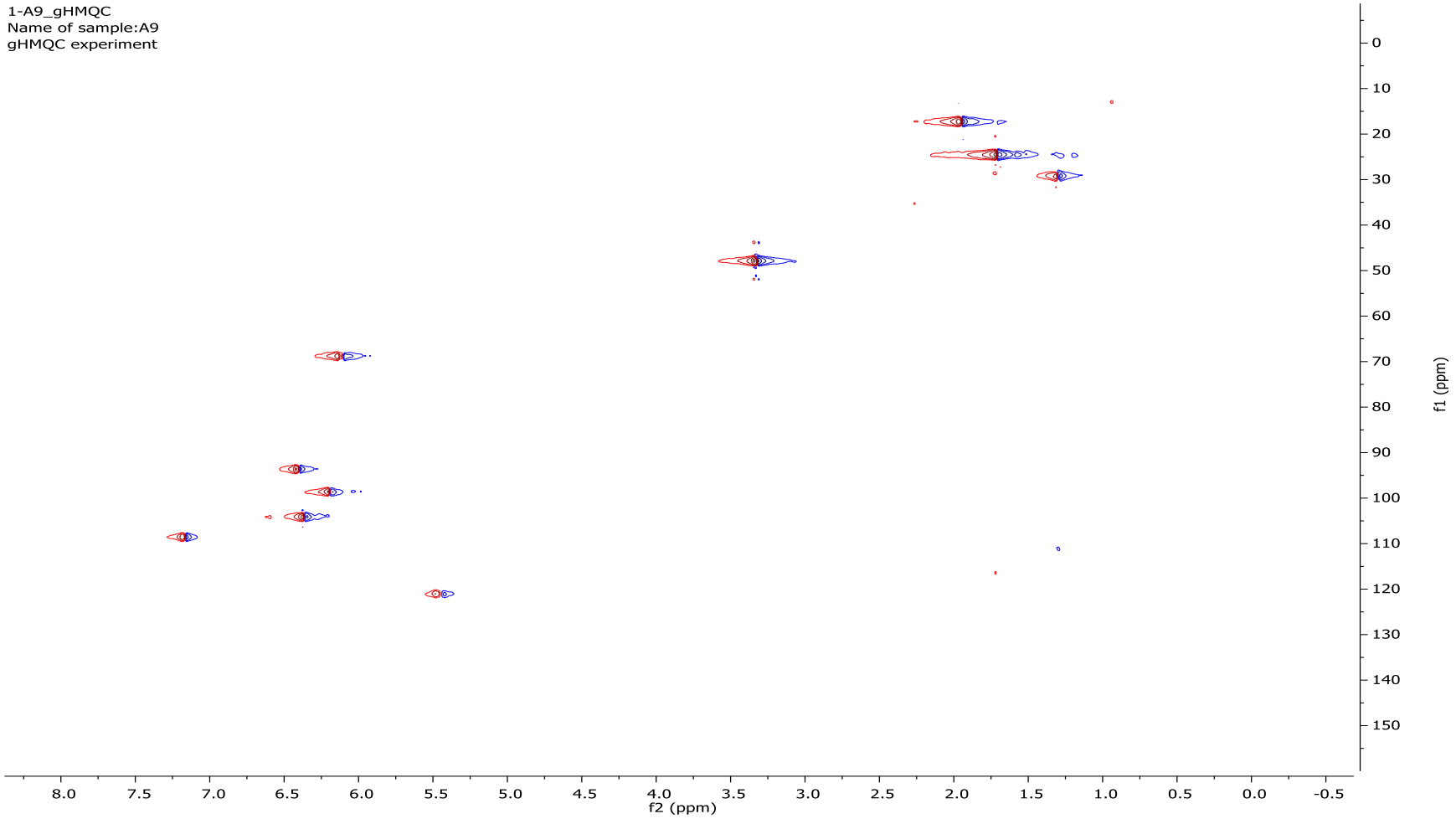

Figure D-6 HMQC spectrum of 3-(hydroxyprenyl) isoetin (No.4)

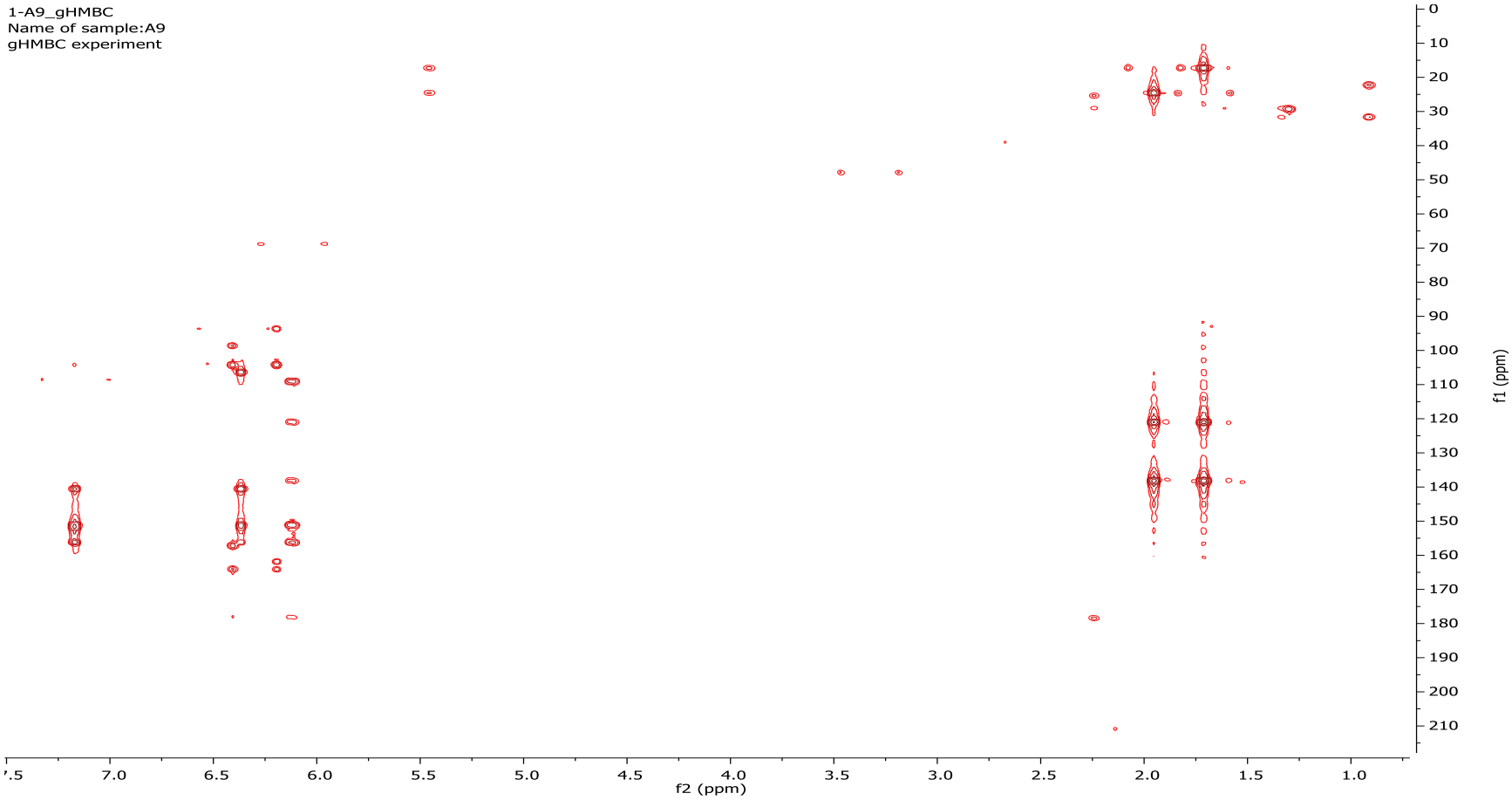

Figure D-7 HMBC spectrum of 3-(hydroxyprenyl) isoetin (No.4)

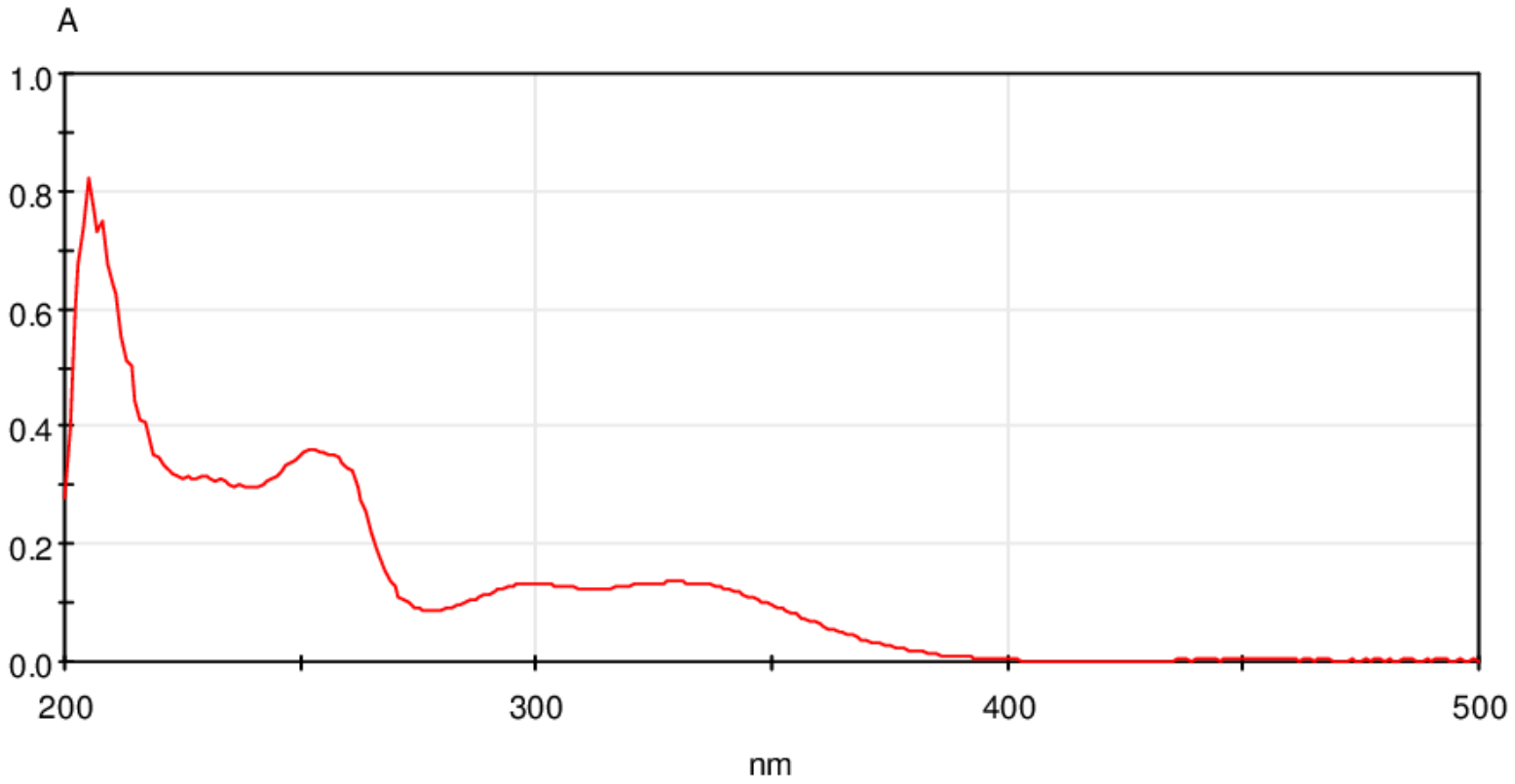

Figure E-1 UV-Visible spectrum of 3-prenyl-5,7,2´,5´-tetrahydroxy-4´-methoxyflavone (No.5)

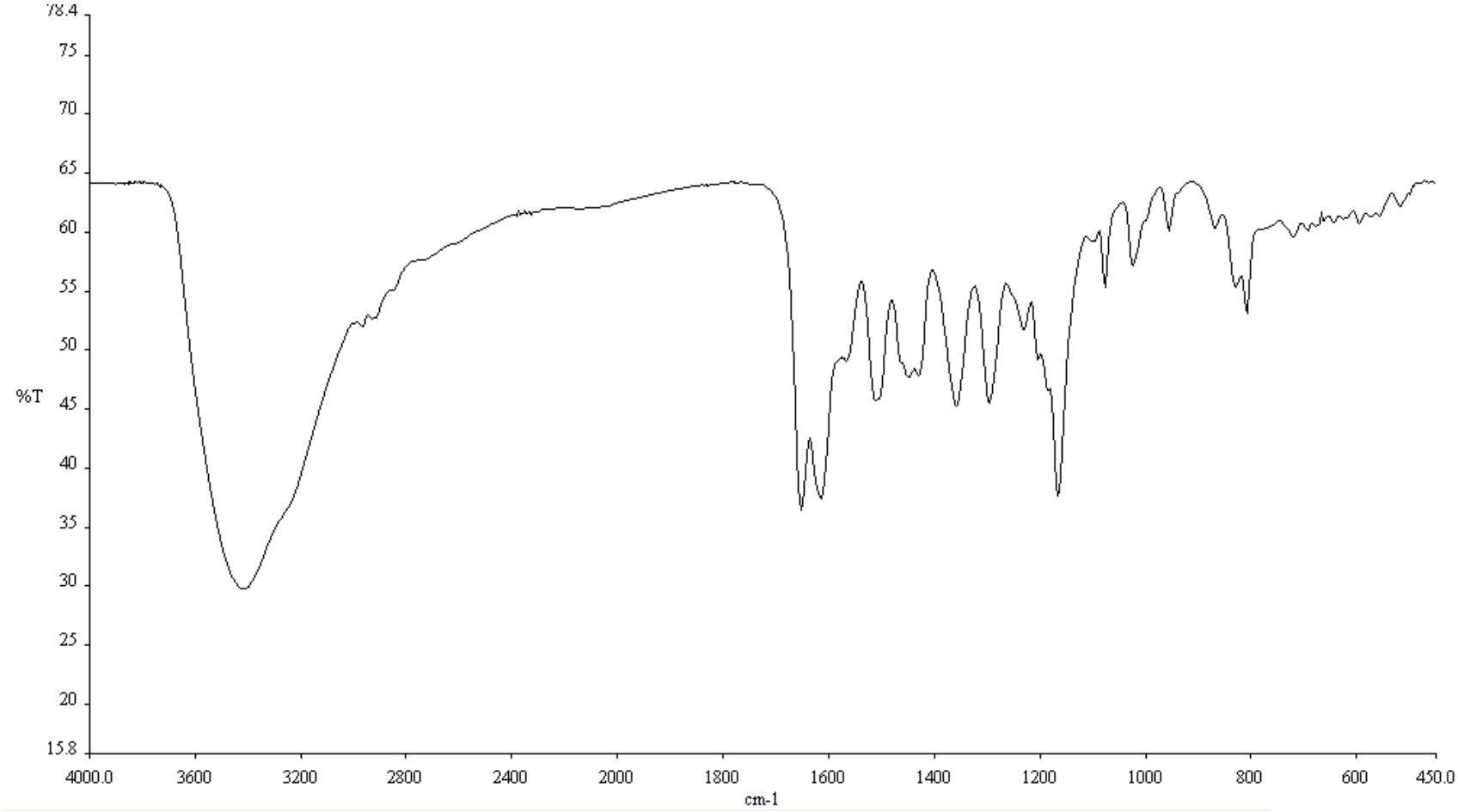

Figure E-2 IR spectrum of 3-prenyl-5,7,2´,5´-tetrahydroxy-4´-methoxyflavone (KBr disc) (No.5)

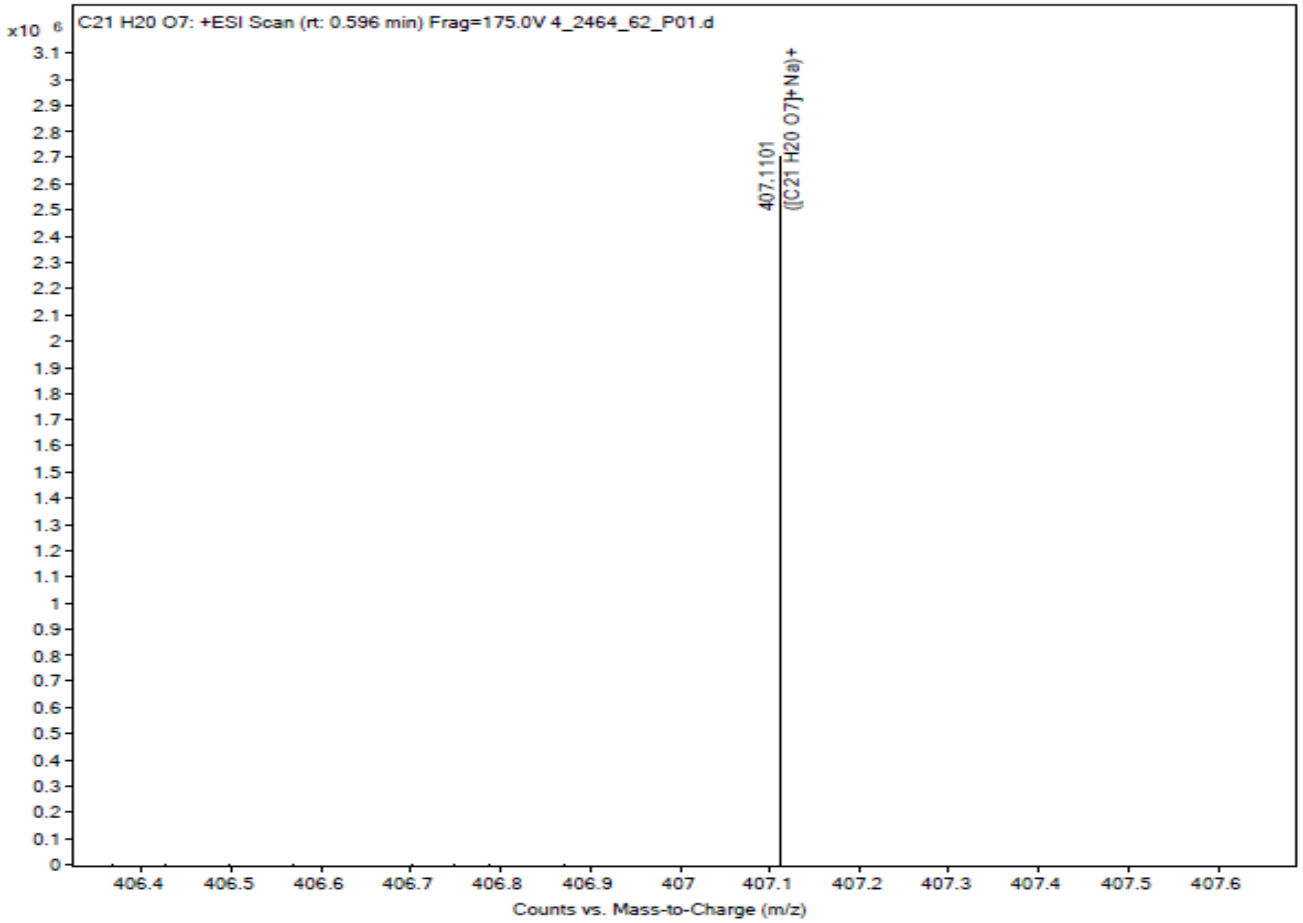

Figure E-3 HRESI mass spectrum of 3-prenyl-5,7,2´,5´-tetrahydroxy-4´-methoxyflavone (No.5)

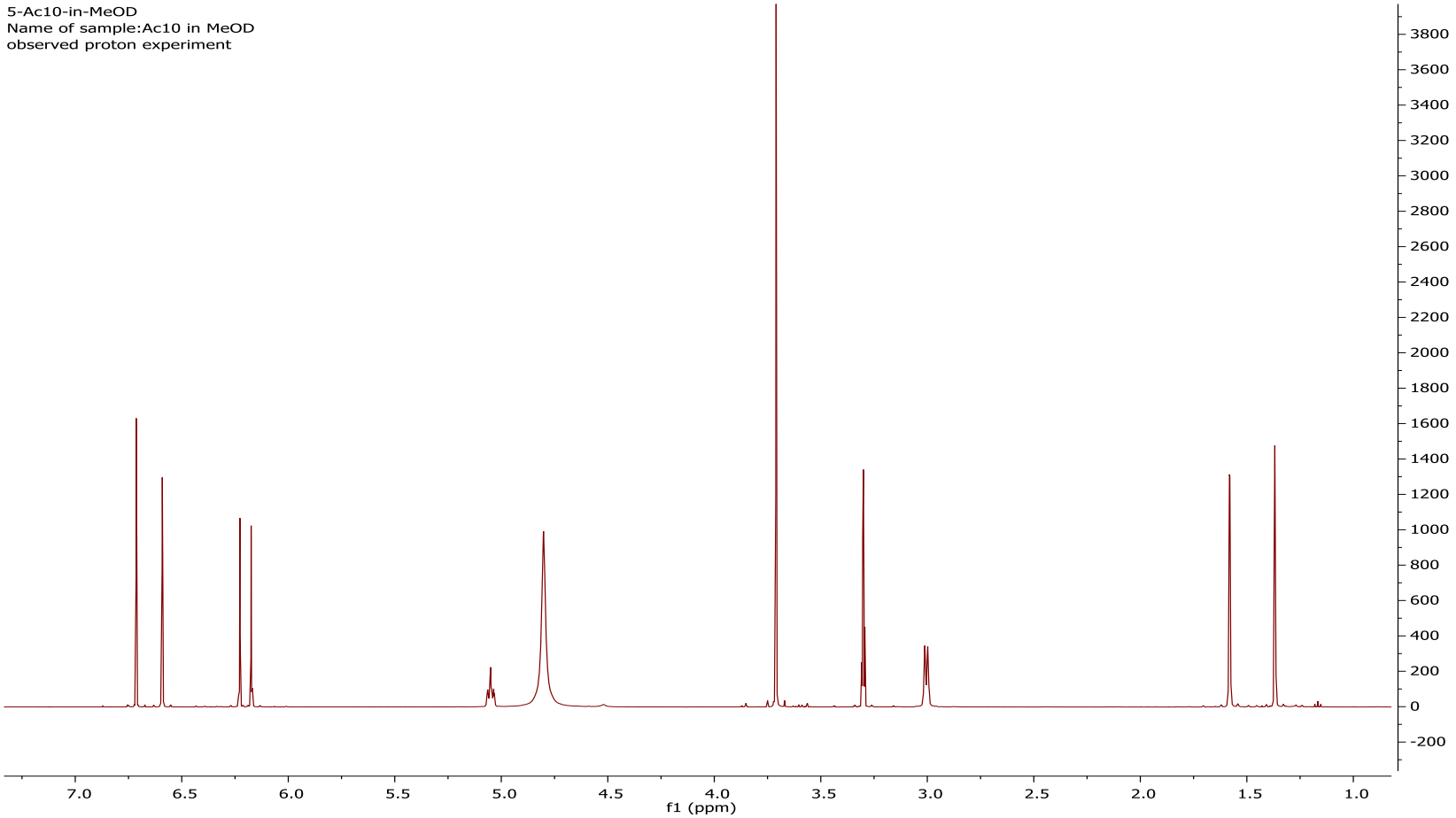

Figure E-4 ^{1}H NMR spectrum of 3-prenyl-5,7,2´,5´-tetrahydroxy-4´-methoxyflavone (No.5)

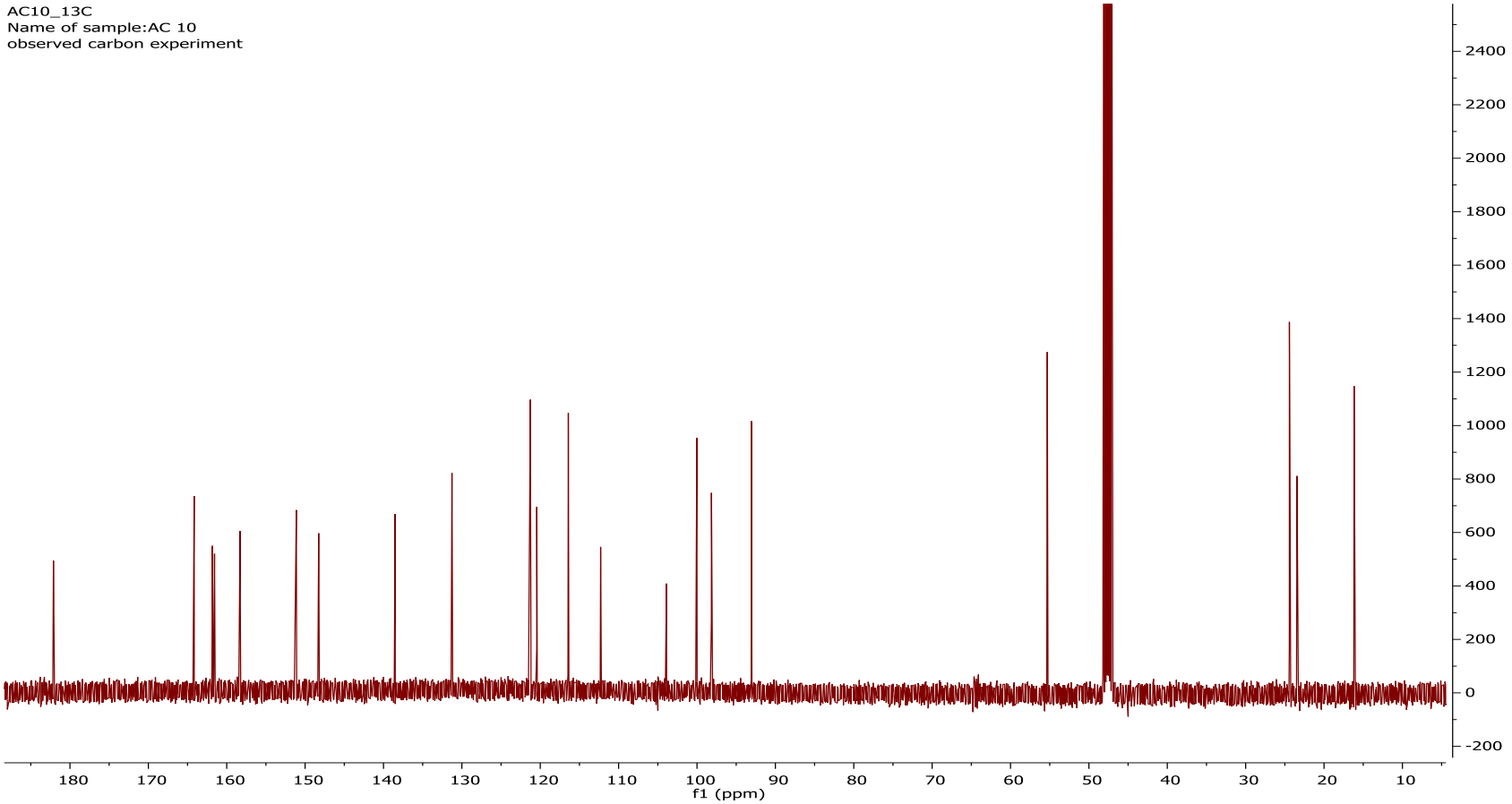

Figure E-5 ^{13}C NMR spectrum of 3-prenyl-5,7,2´,5´-tetrahydroxy-4´-methoxyflavone (No.5)

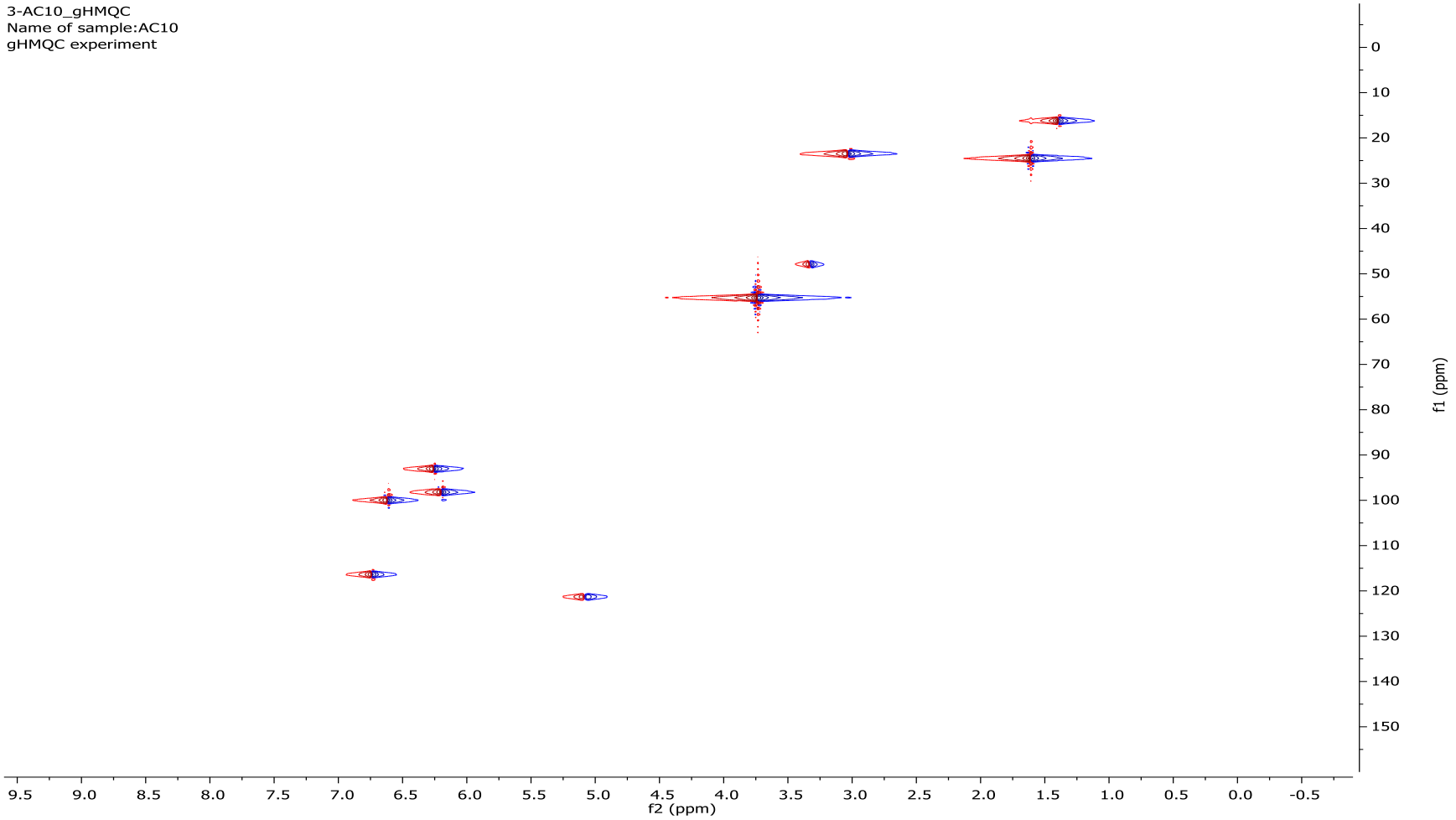

Figure E-6 HMQC spectrum of 3-prenyl-5,7,2´,5´-tetrahydroxy-4´-methoxyflavone (No.5)

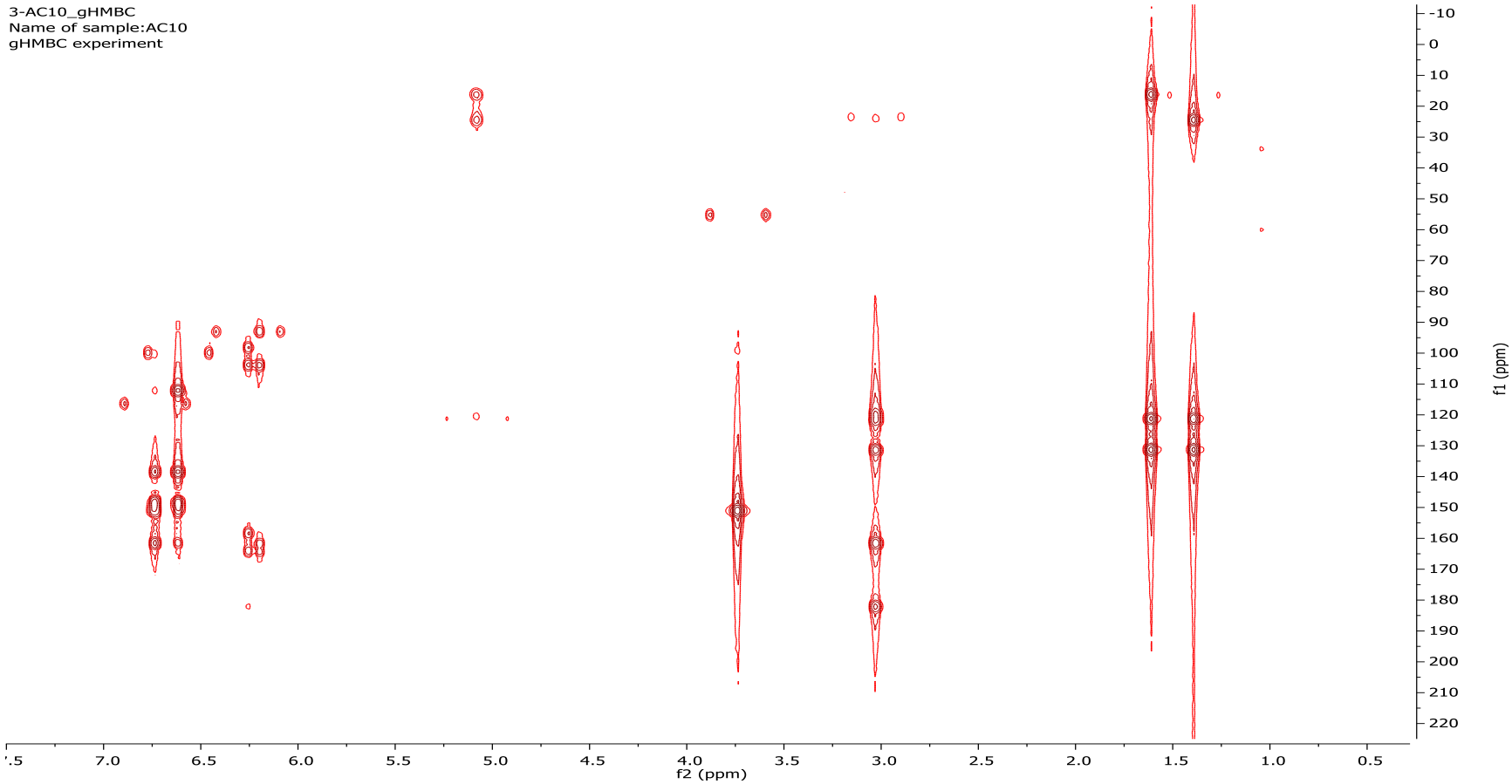

Figure E-7 HMBC spectrum of 3-prenyl-5,7,2´,5´-tetrahydroxy-4´-methoxyflavone (No.5)

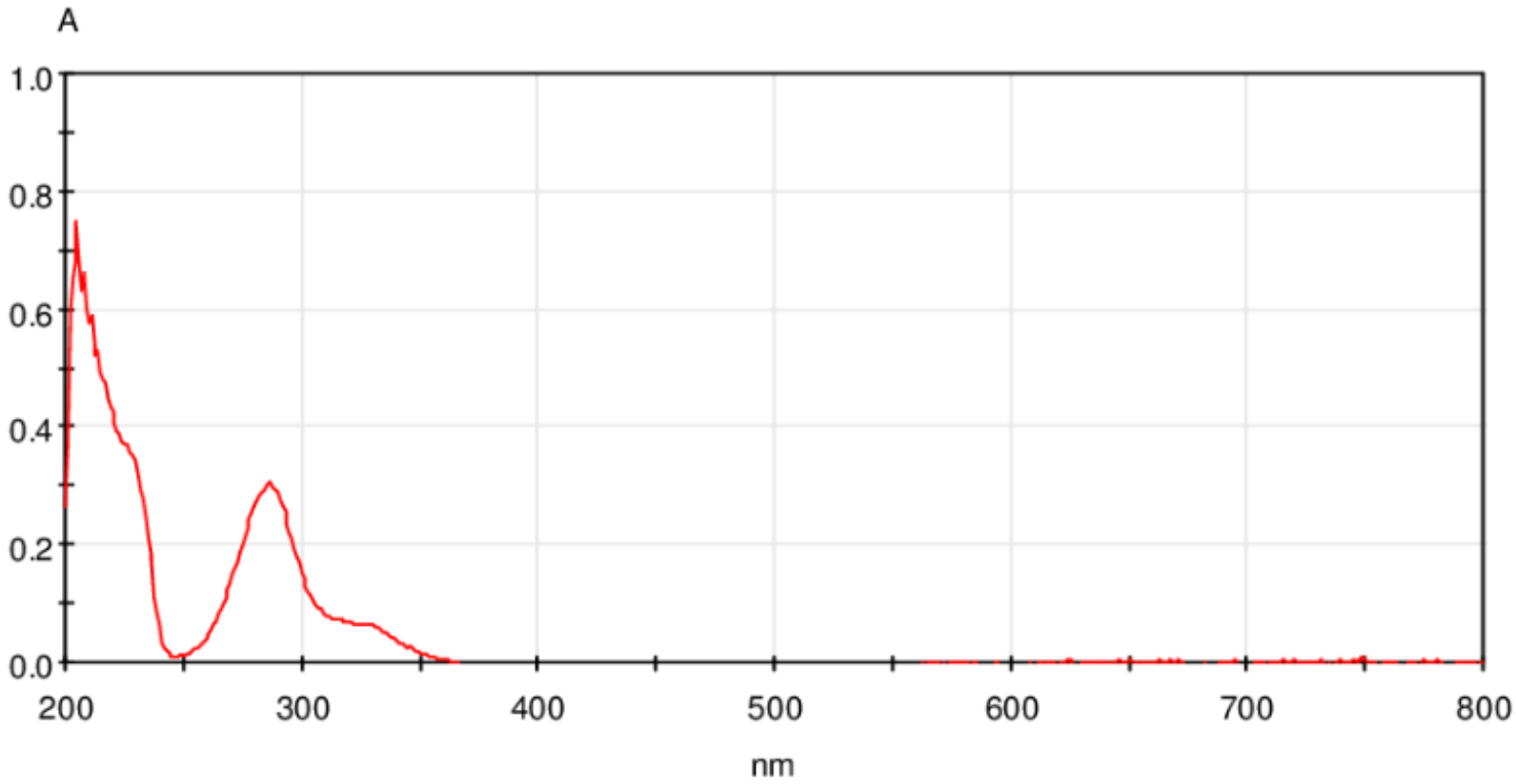

Figure F-1 UV-Visible spectrum of artocarpanone (No.6)

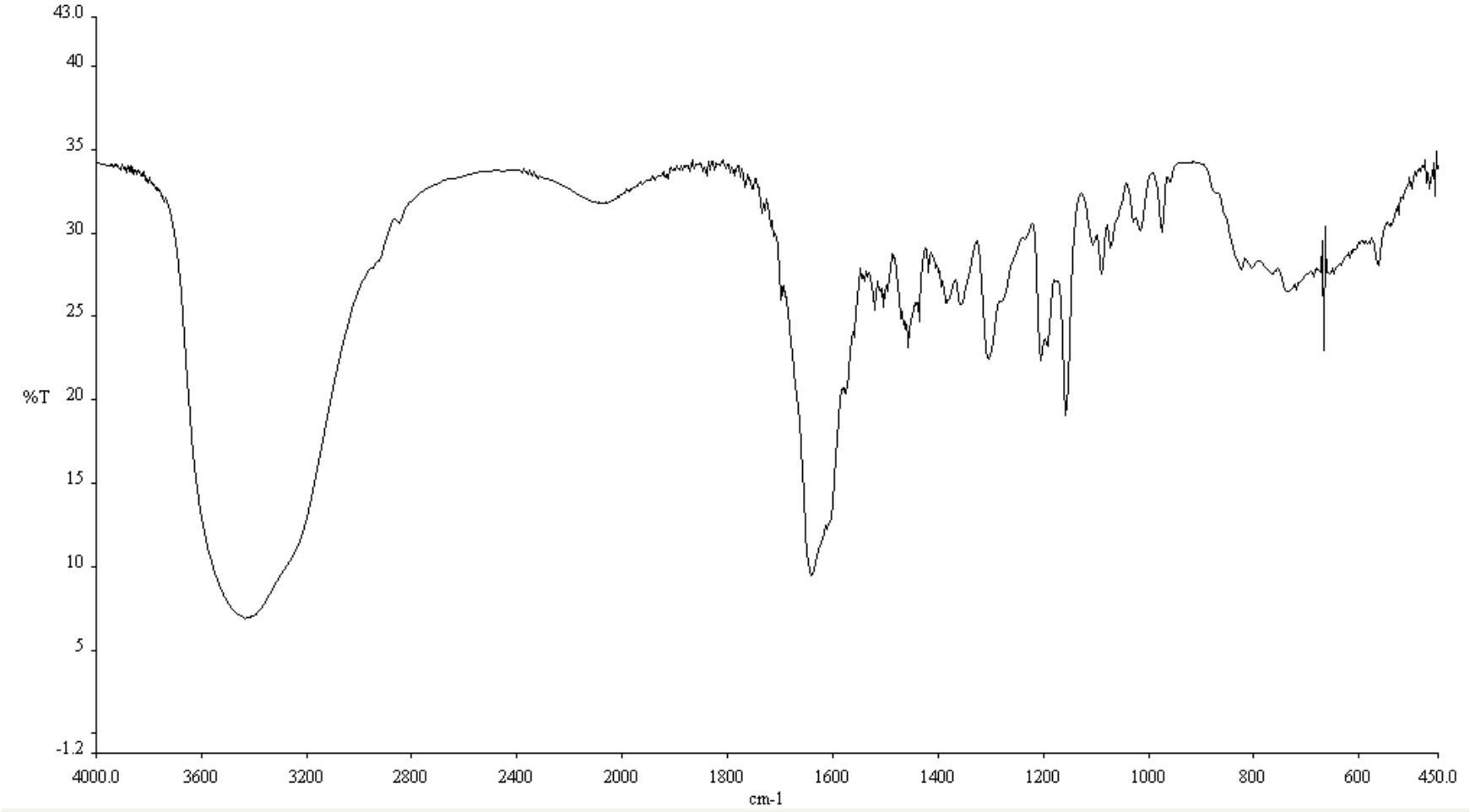

Figure F-2 IR spectrum of artocarpanone (KBr disc) (No.6)

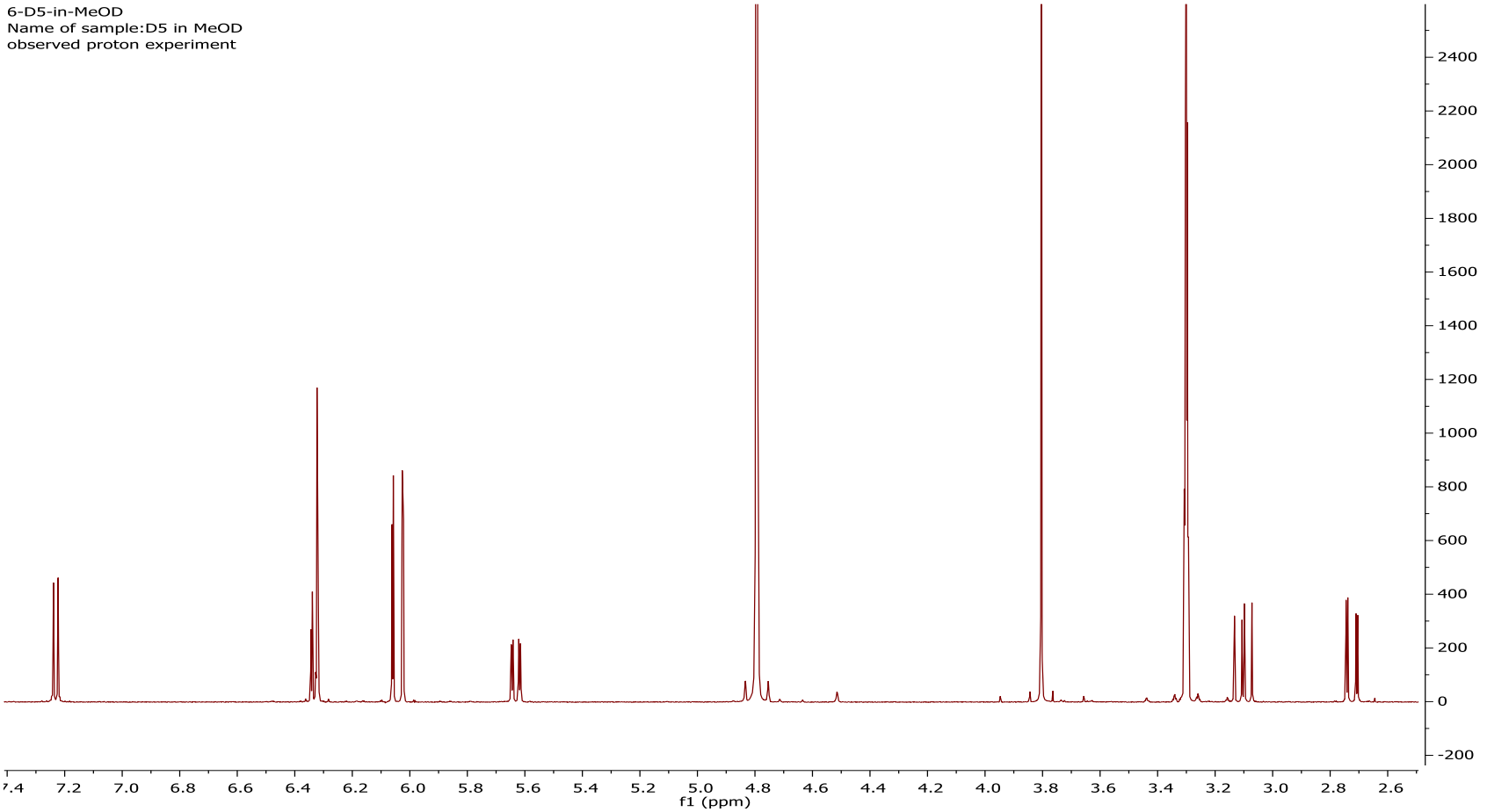

Figure F-4 ^{1}H NMR spectrum of artocarpanone (No.6)

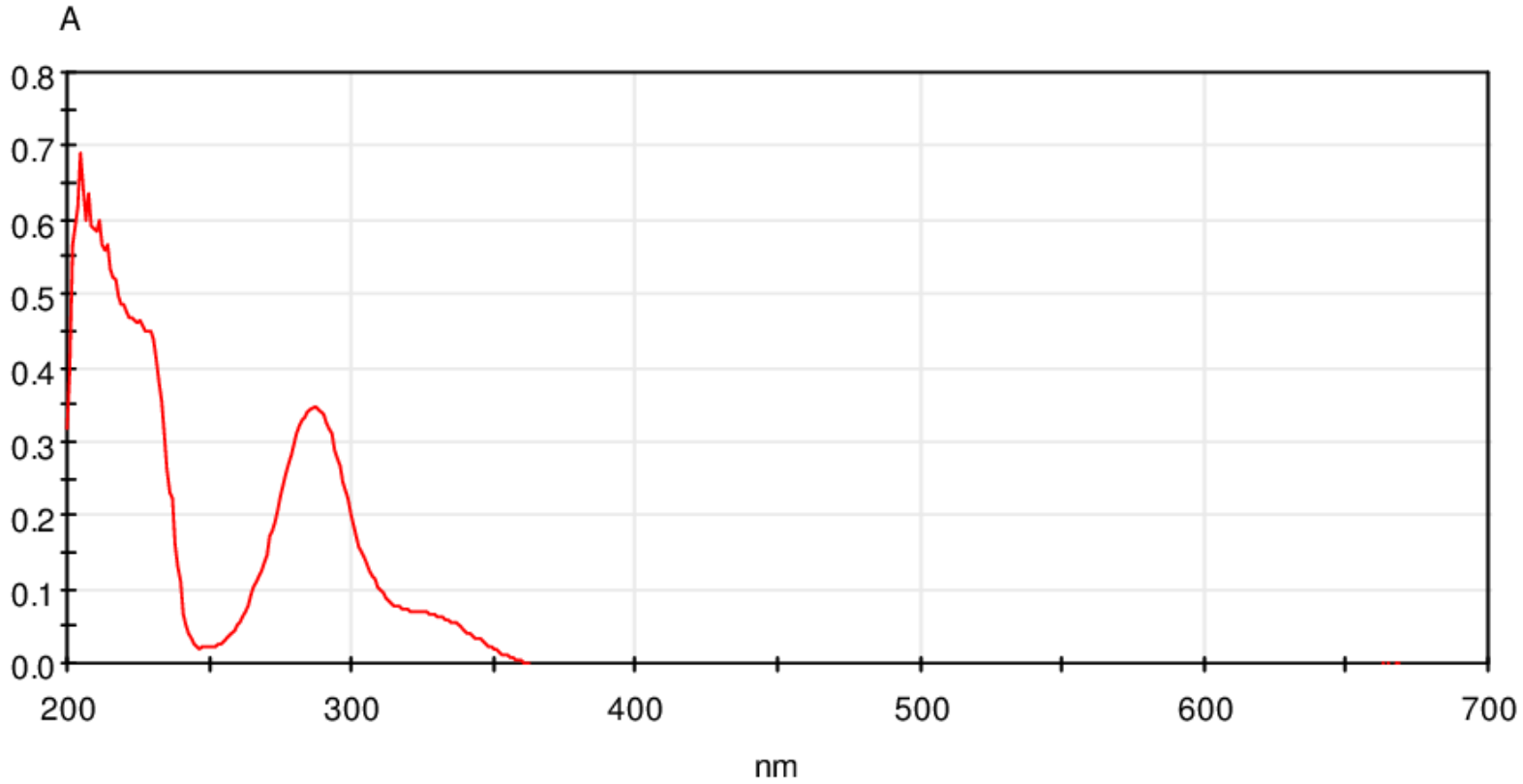

Figure G-1 UV-Visible spectrum of naringenin (No.7)

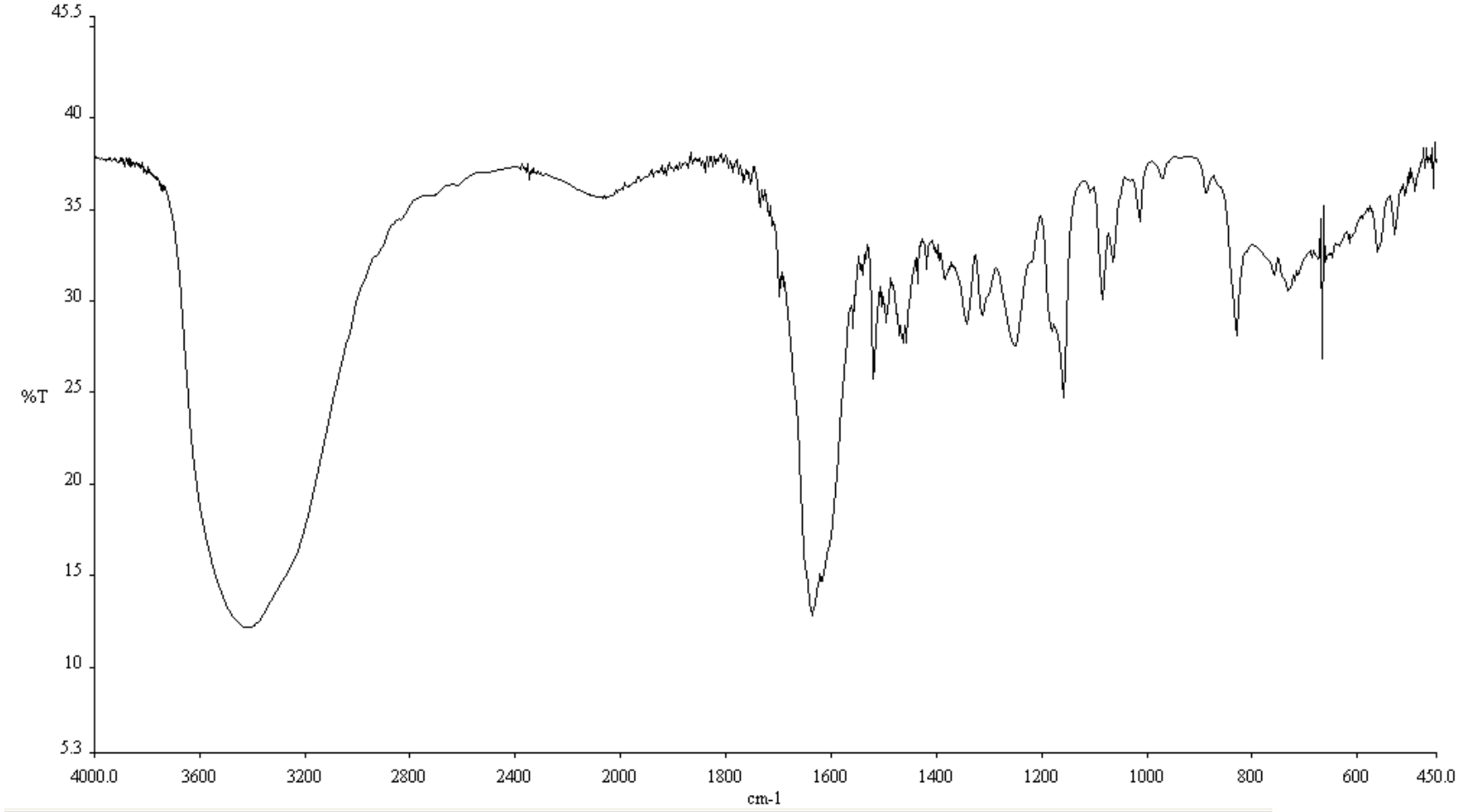

Figure G-2 IR spectrum of naringenin (KBr disc) (No.7)

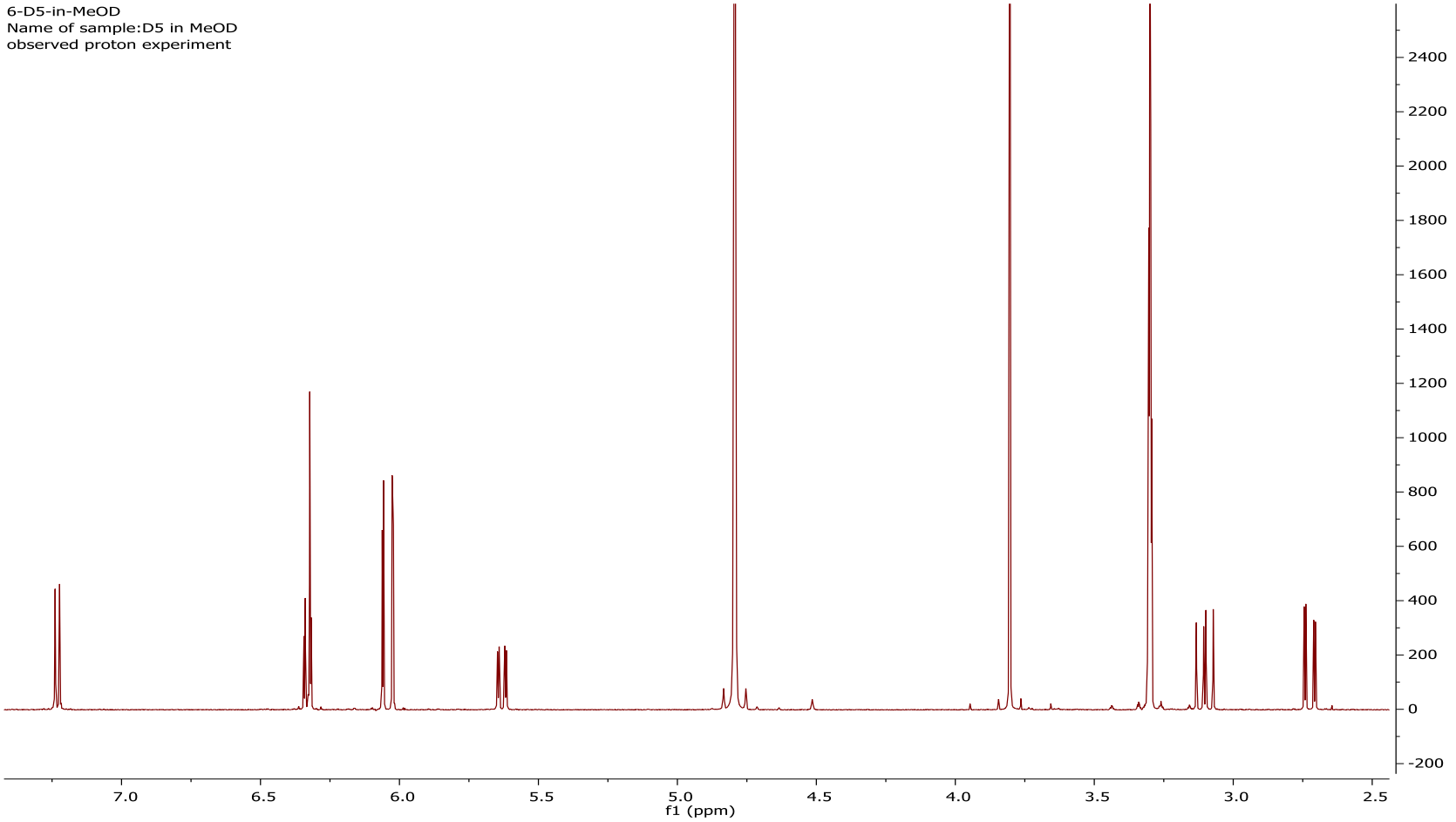

Figure G-4 ^{1}H NMR spectrum of naringenin (No.7)

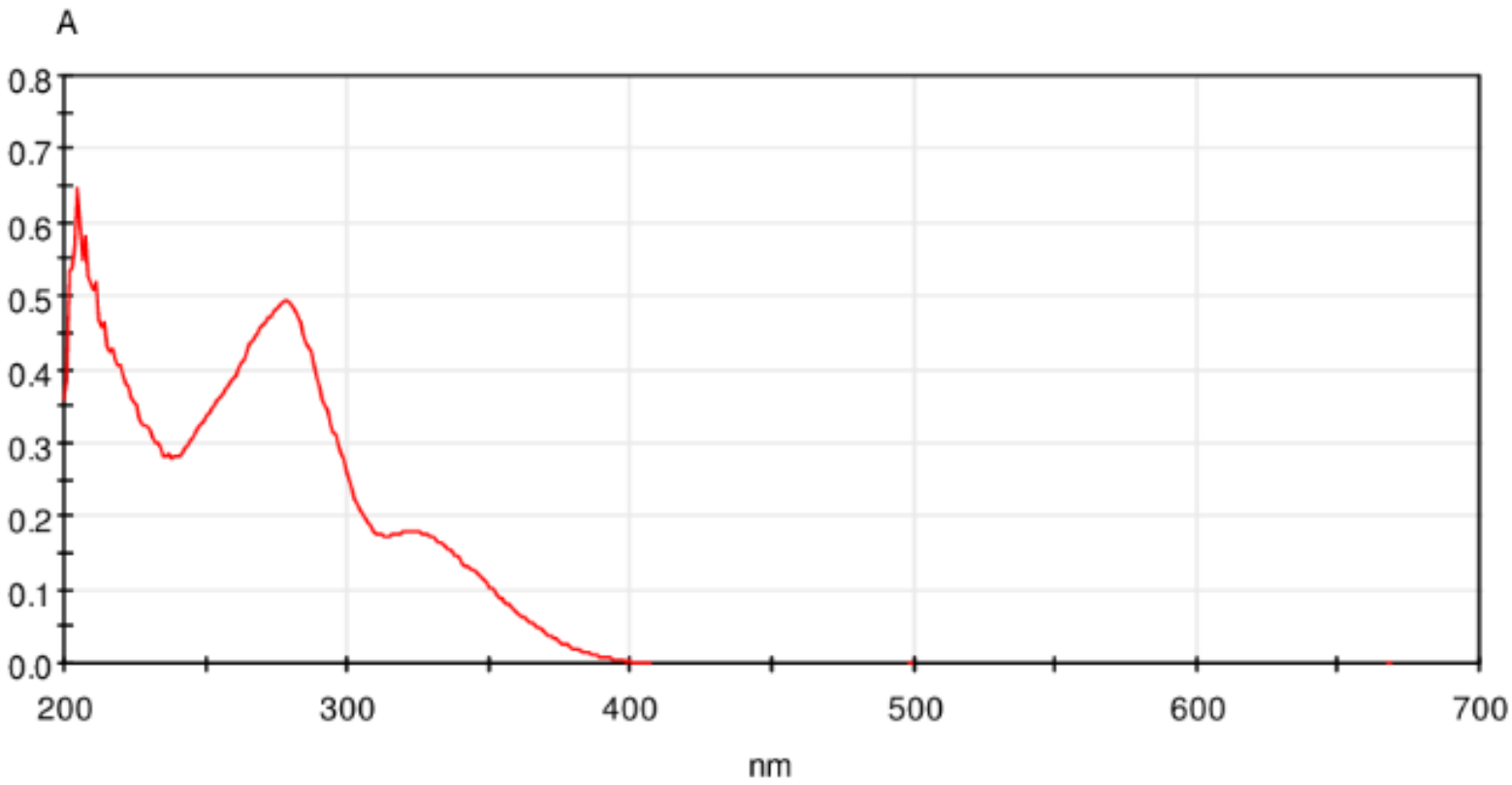

Figure H-1 UV-Visible spectrum of artocarpin (No.8)

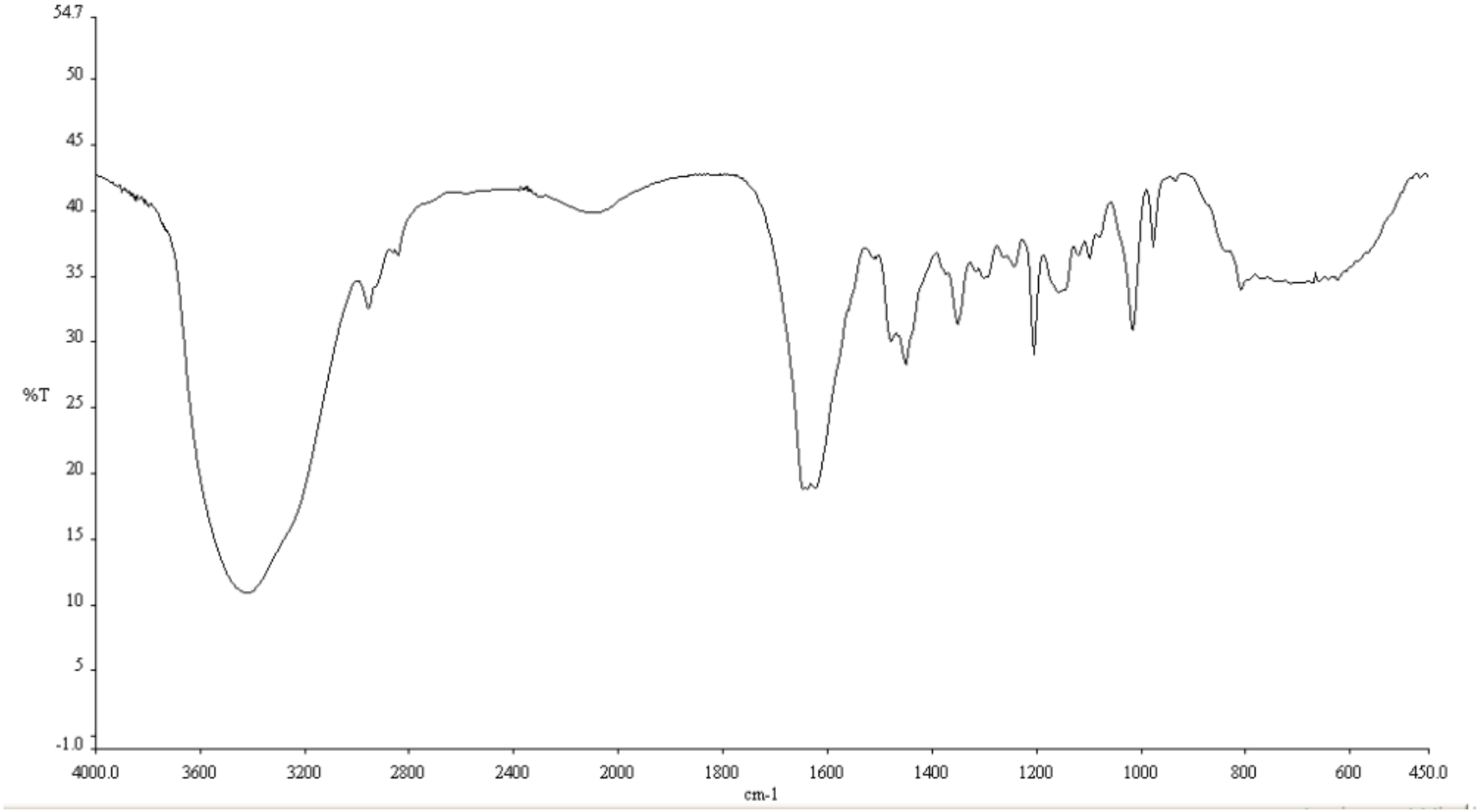

Figure H-2 IR spectrum of artocarpin (KBr disc) (No.8)

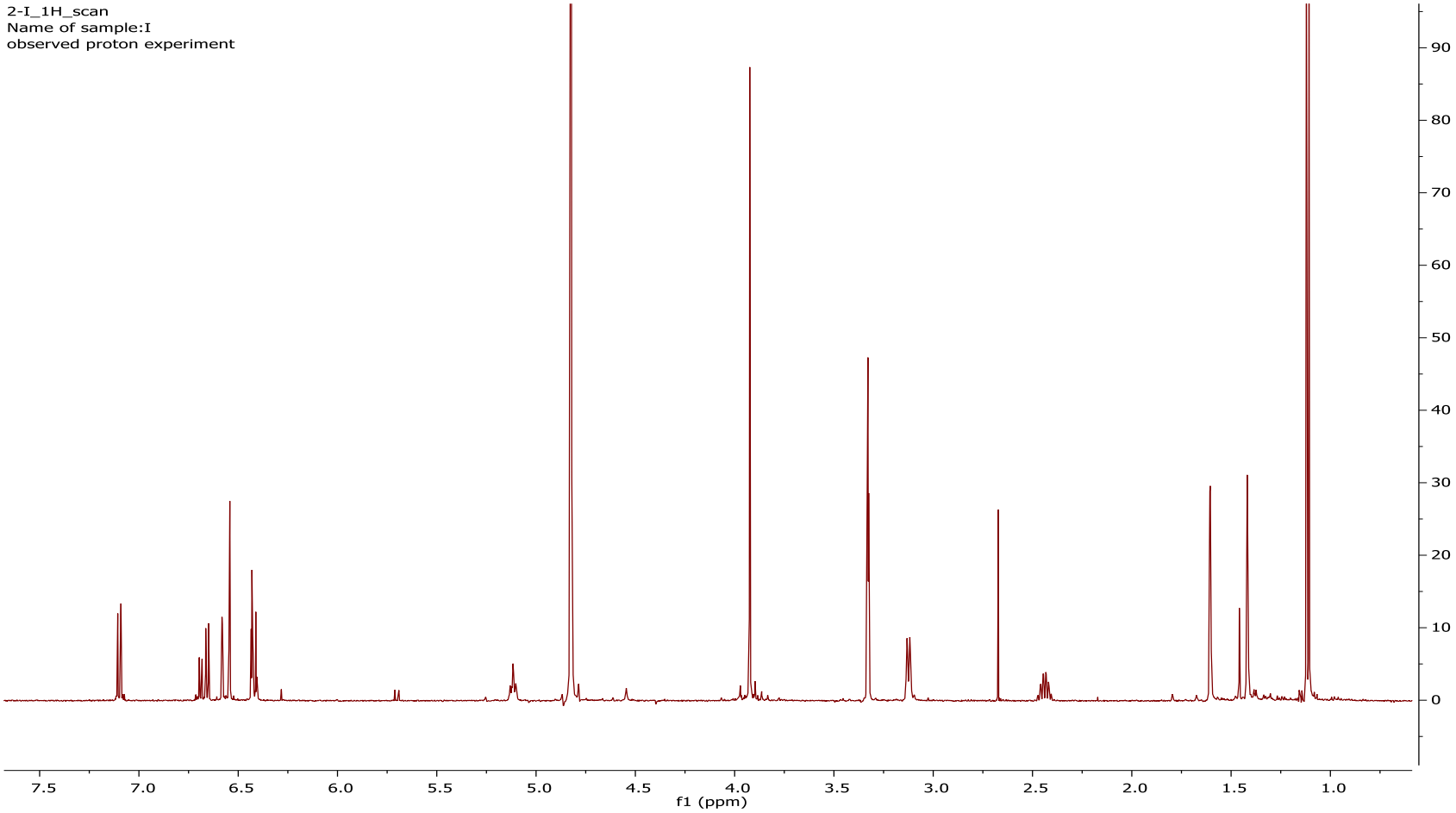

Figure H-4 ^{1}H NMR spectrum of artocarpin (No.8)

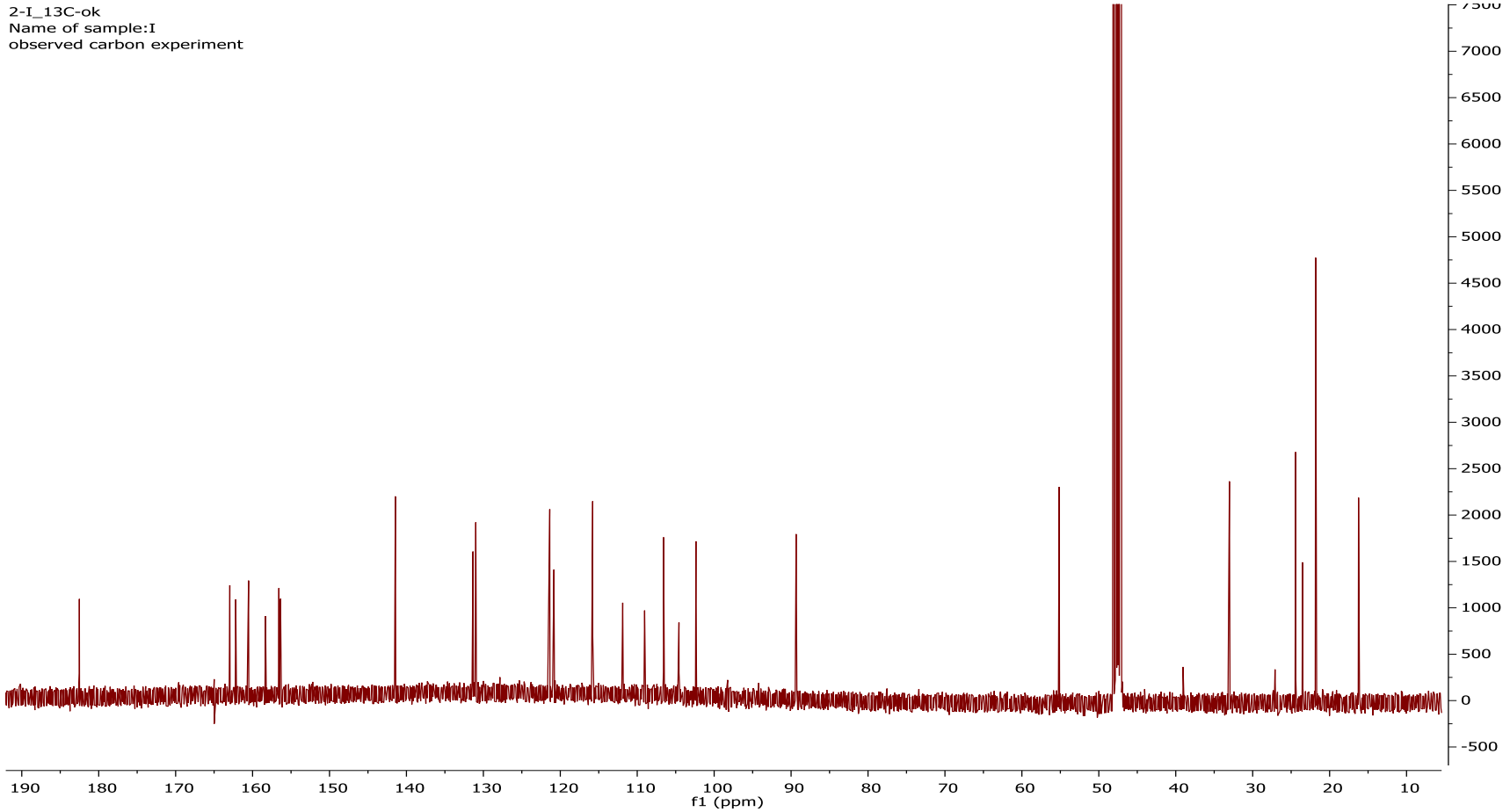

Figure H-5 ^{13}C NMR spectrum of artocarpin (No.8)

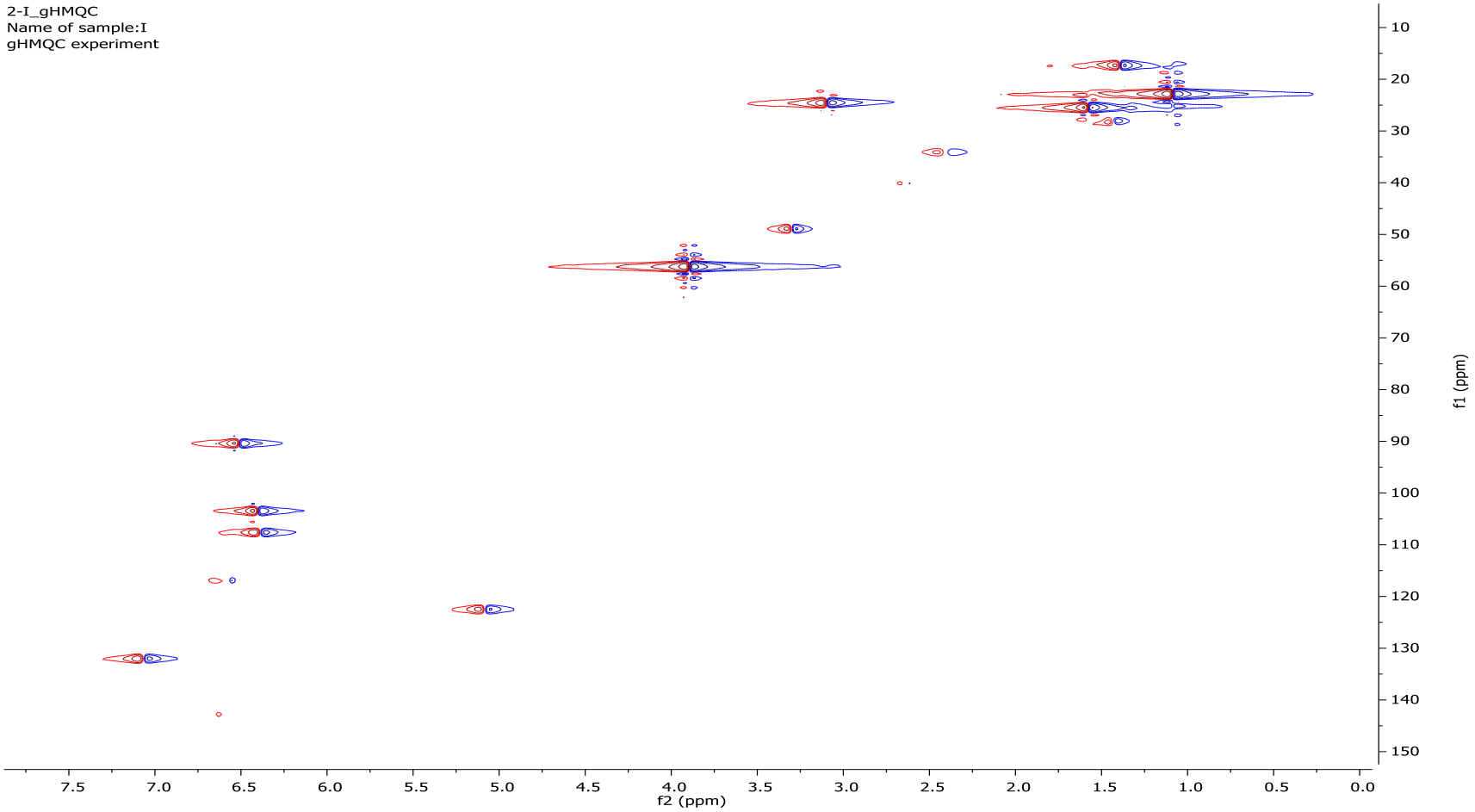

Figure H-6 HMQC spectrum of artocarpin (No.8)

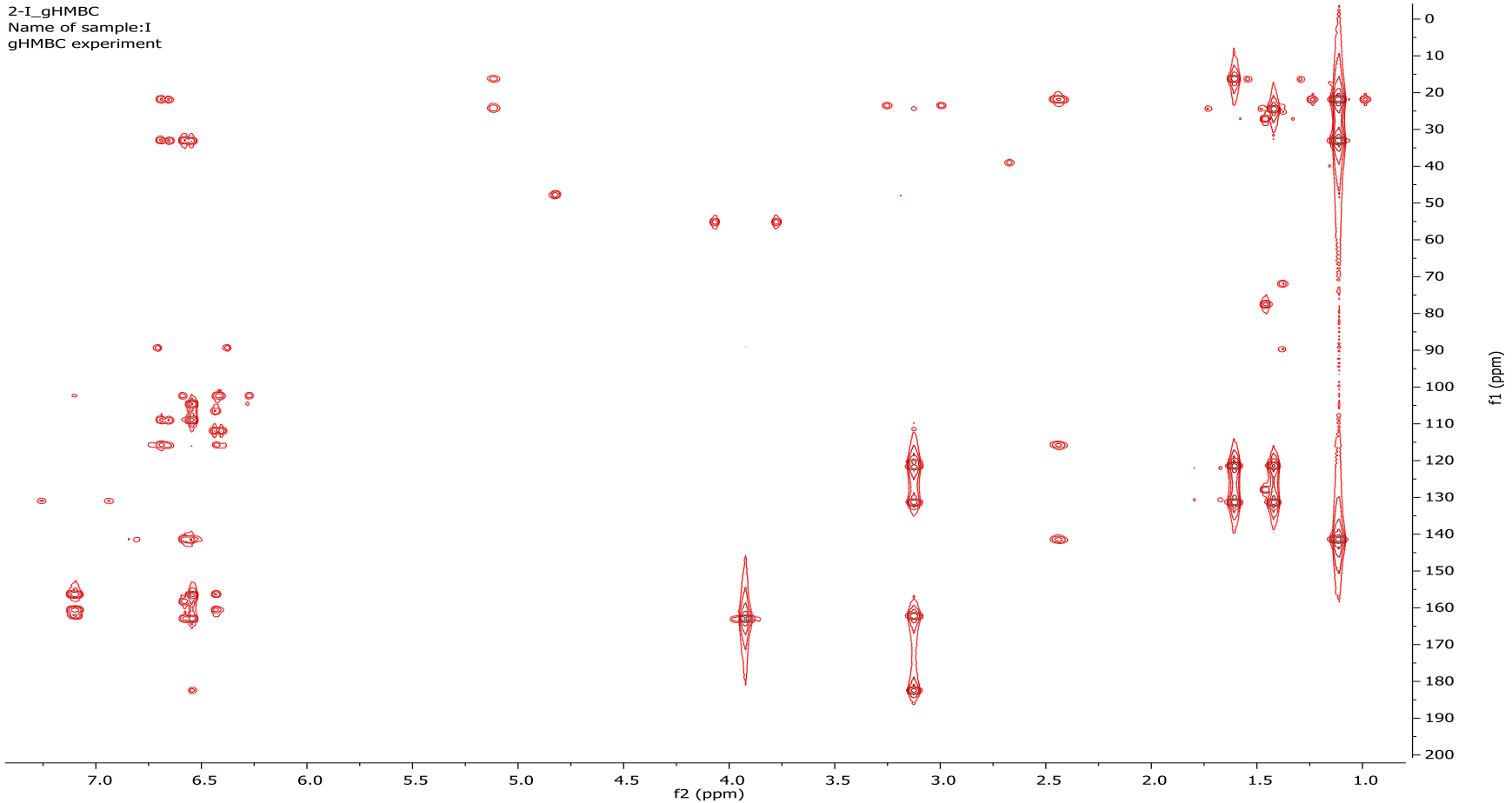

Figure H-7 HMBC spectrum of artocarpin (No.8)

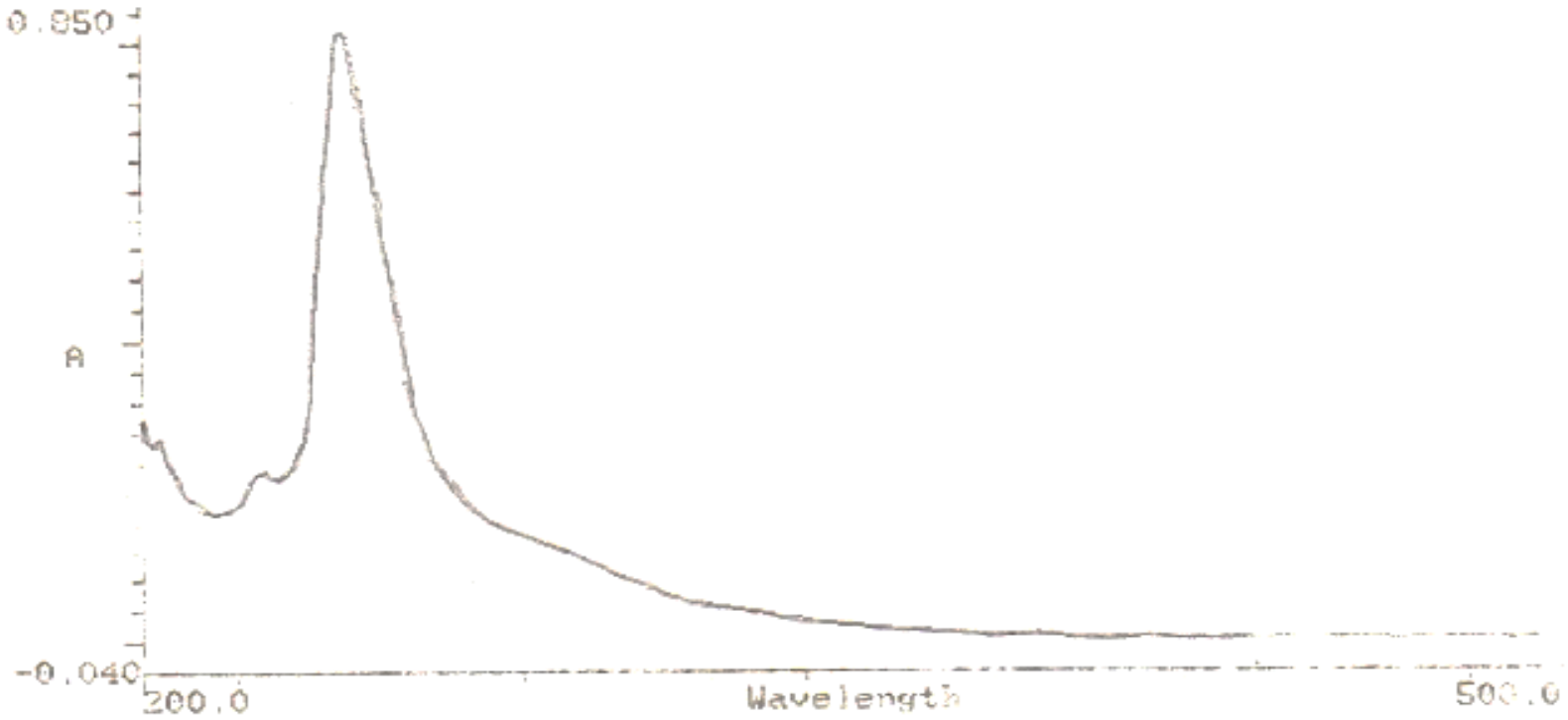

Figure I-1 UV-Visible spectrum of mixture of *β*-sitosterol and stigmasterol (No.9)

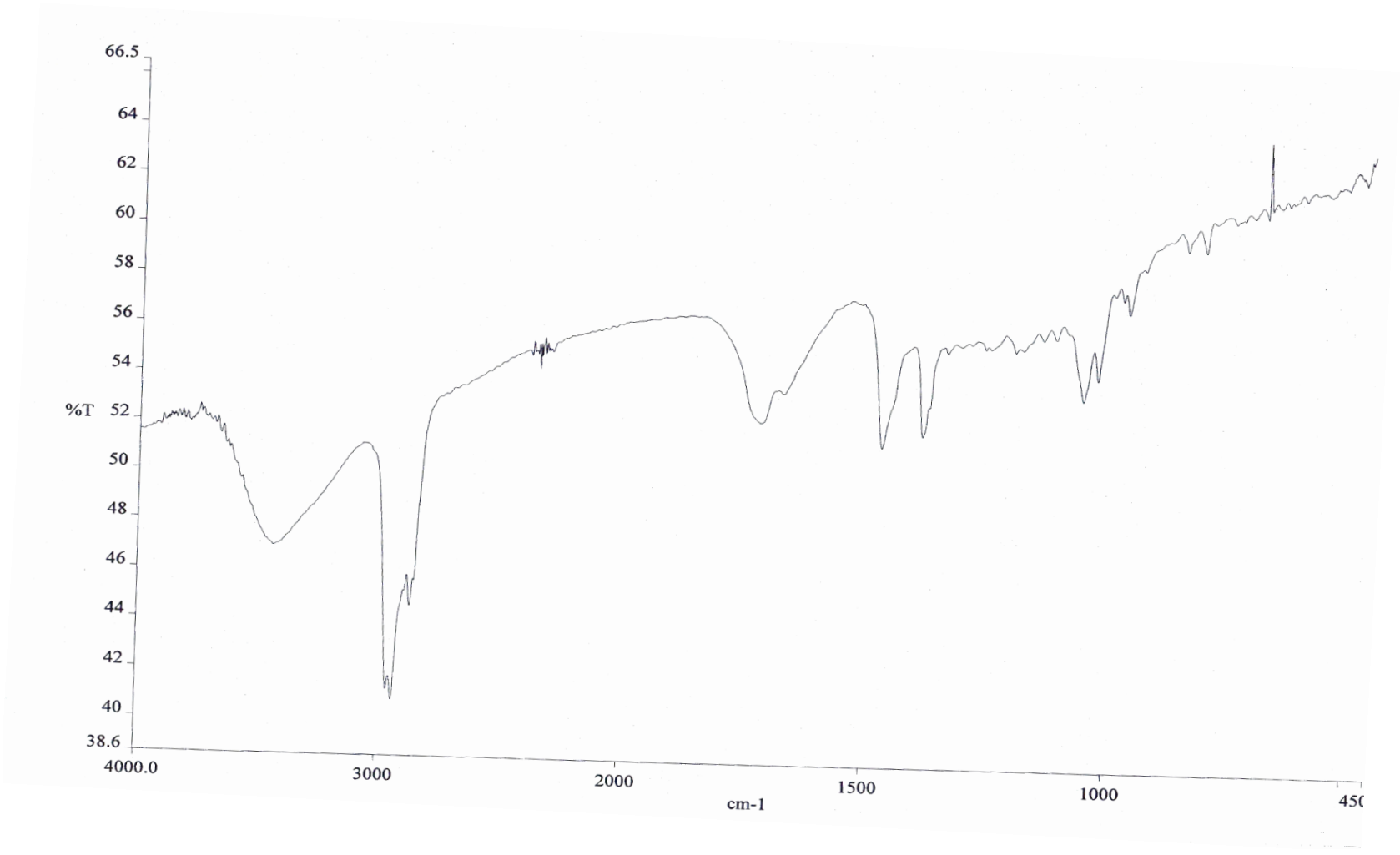

Figure I-2 IR spectrum of mixture of β-sitosterol and stigmasterol (KBr disc) (No.9)

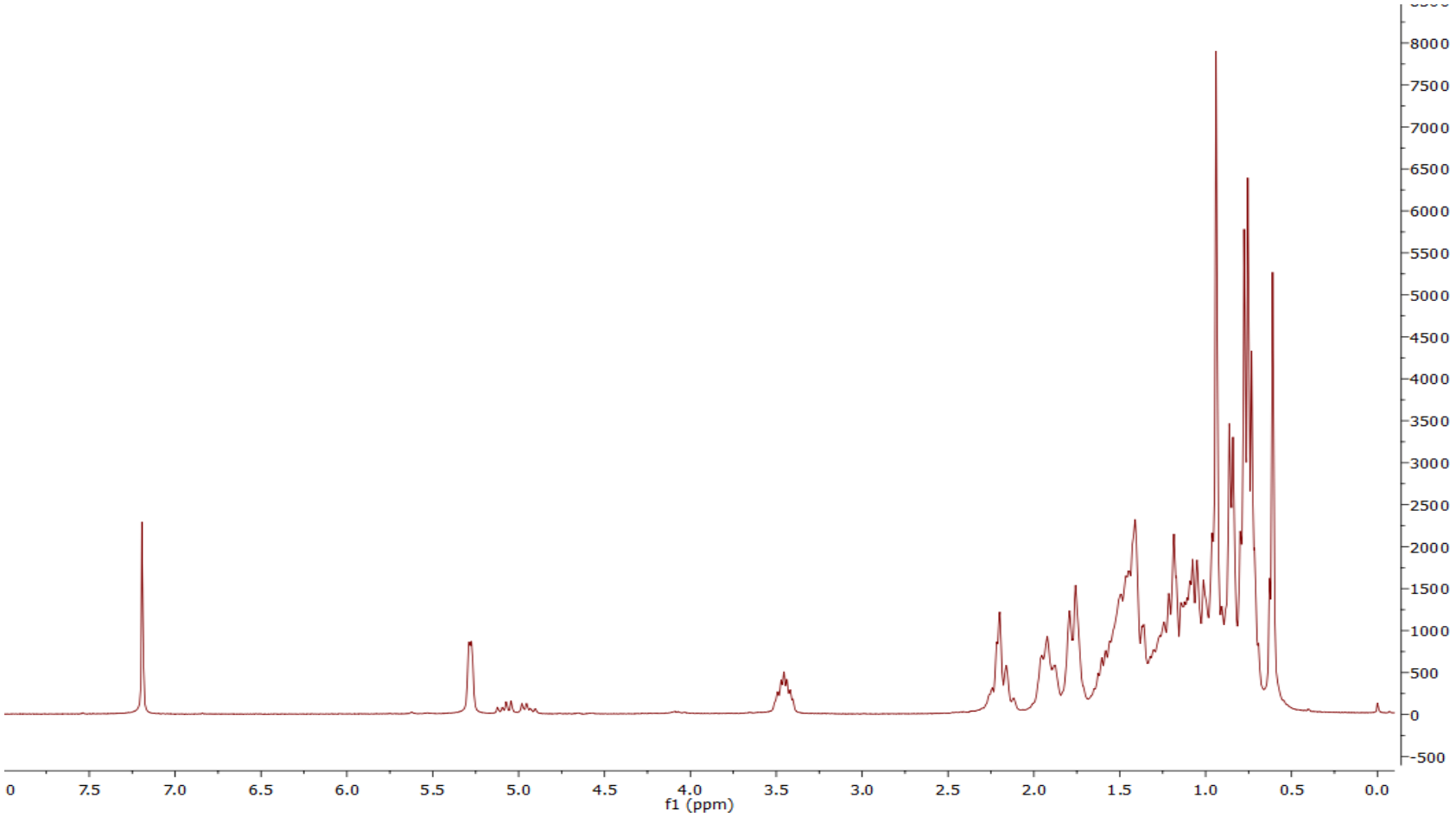

Figure I-4 ^{1}H NMR spectrum of mixture of β-sitosterol and stigmasterol (No.9)

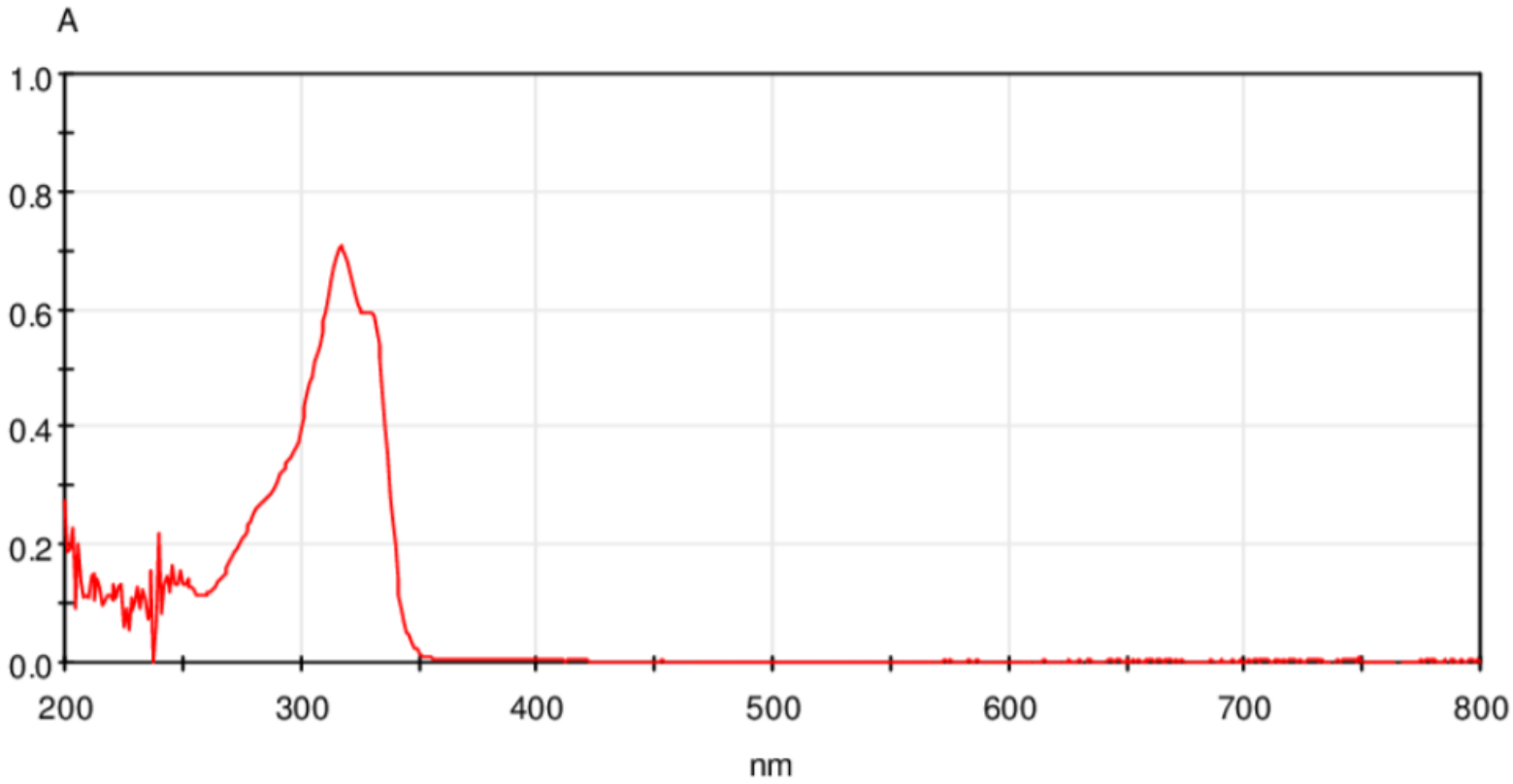

Figure J-1 UV-Visible spectrum of ω-hydroxymoracin C (No.10)

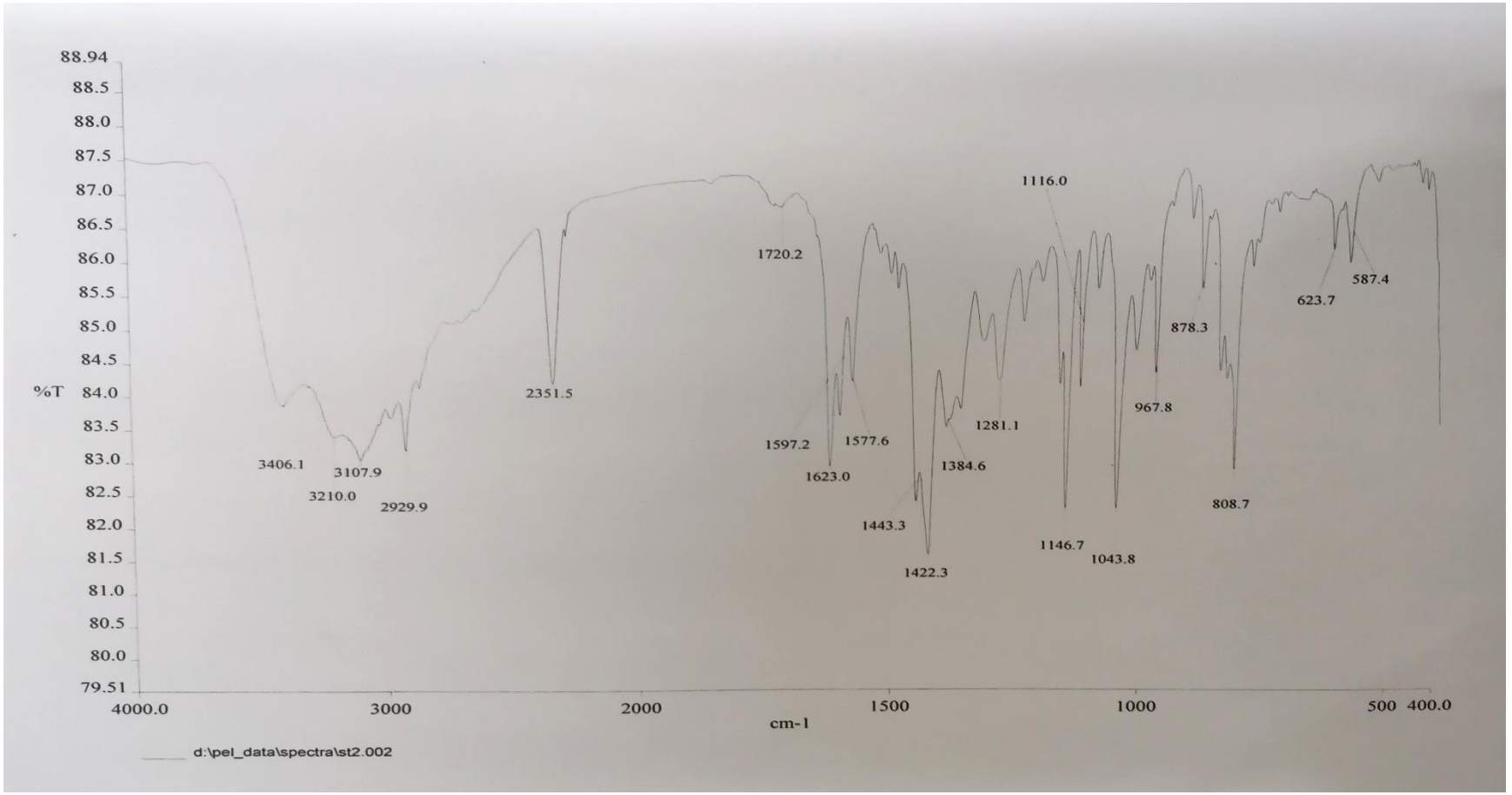

Figure J-2 IR spectrum of ω-hydroxymoracin C (KBr disc) (No.10)

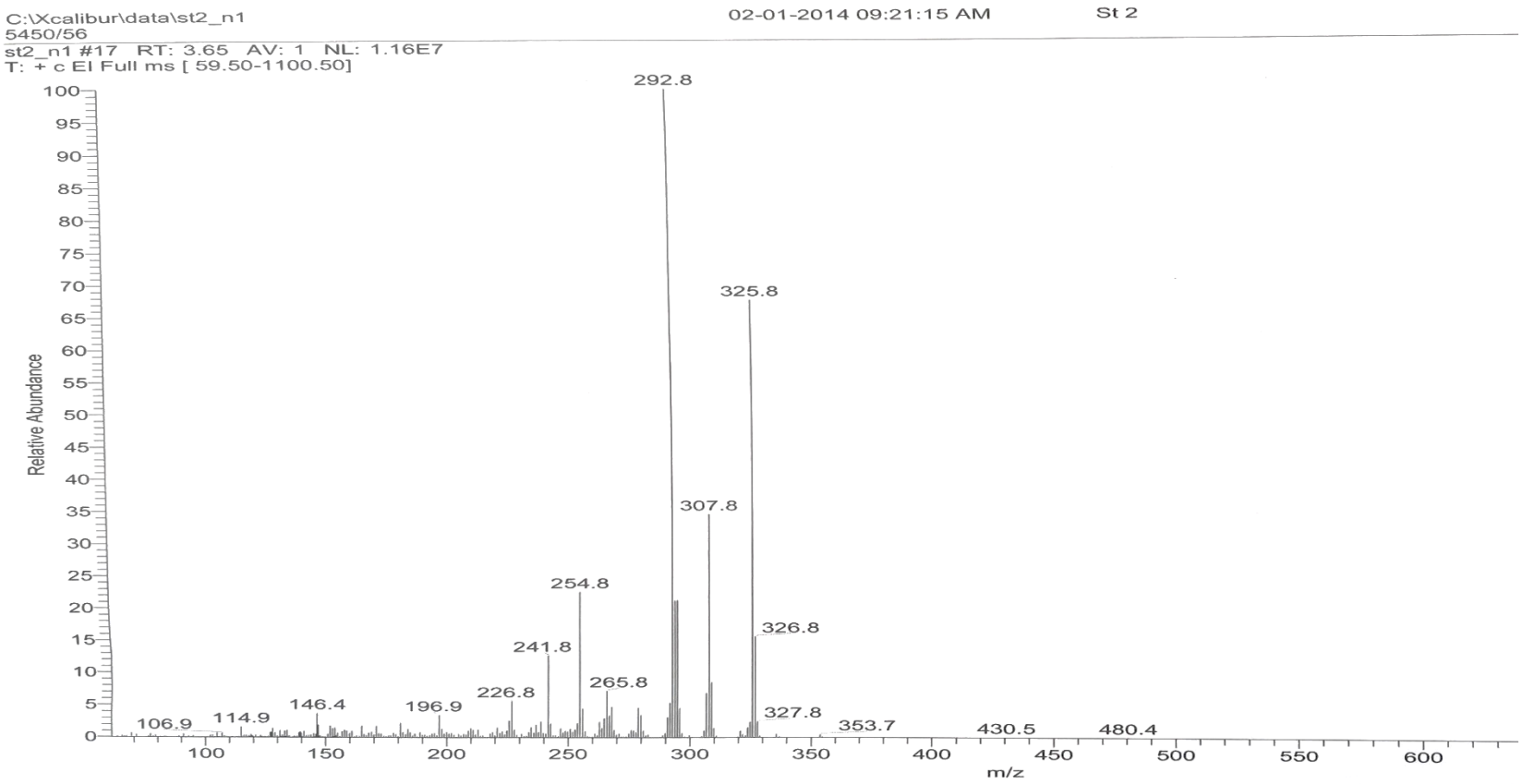

Figure J-3 EI mass spectrum of ω-hydroxymoracin C (No.10)

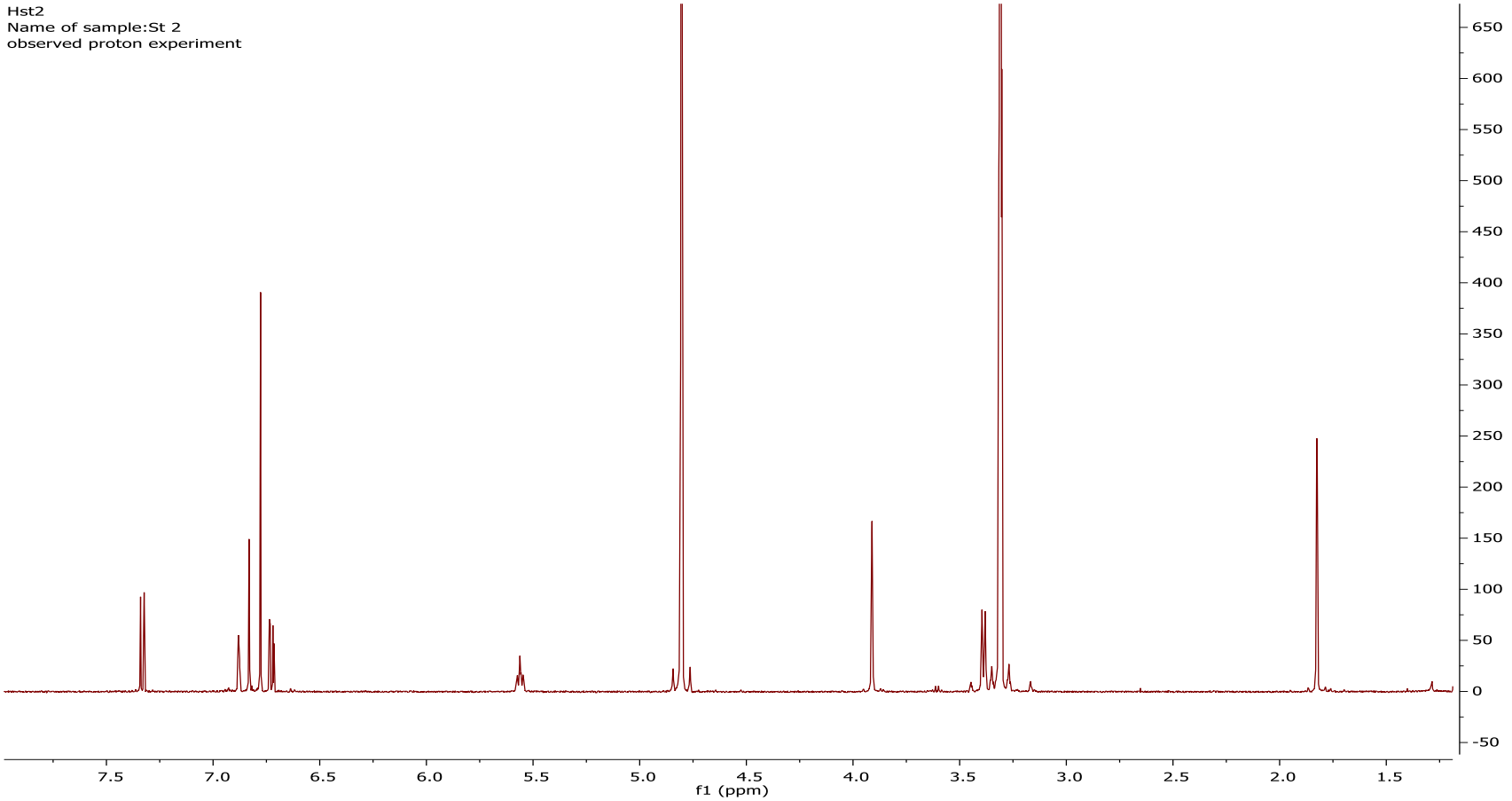

Figure J-4 ^{1}H NMR spectrum of ω-hydroxymoracin C (No.10)

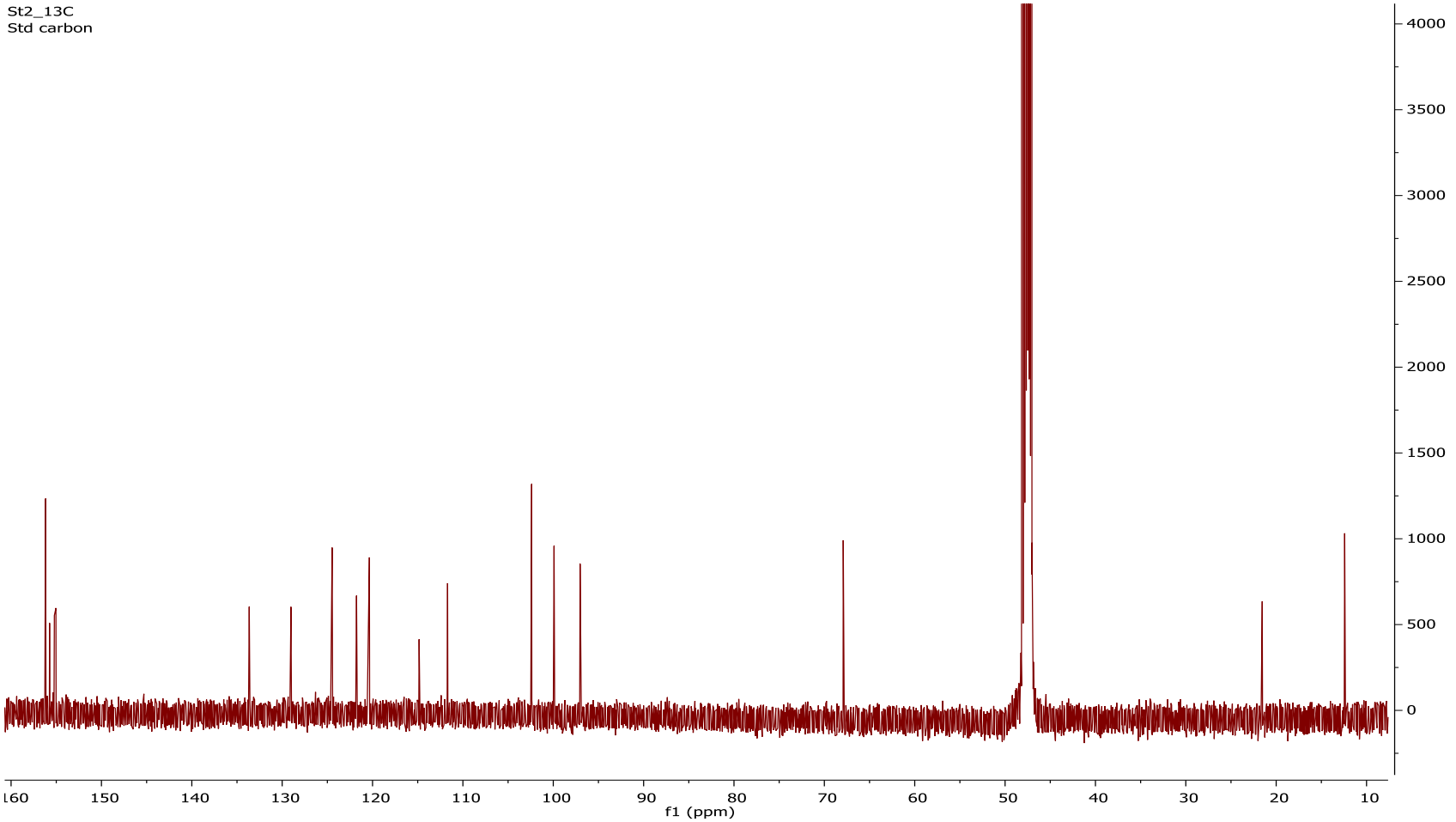

Figure J-5 ^{13}C NMR spectrum of ω-hydroxymoracin C (No.10)

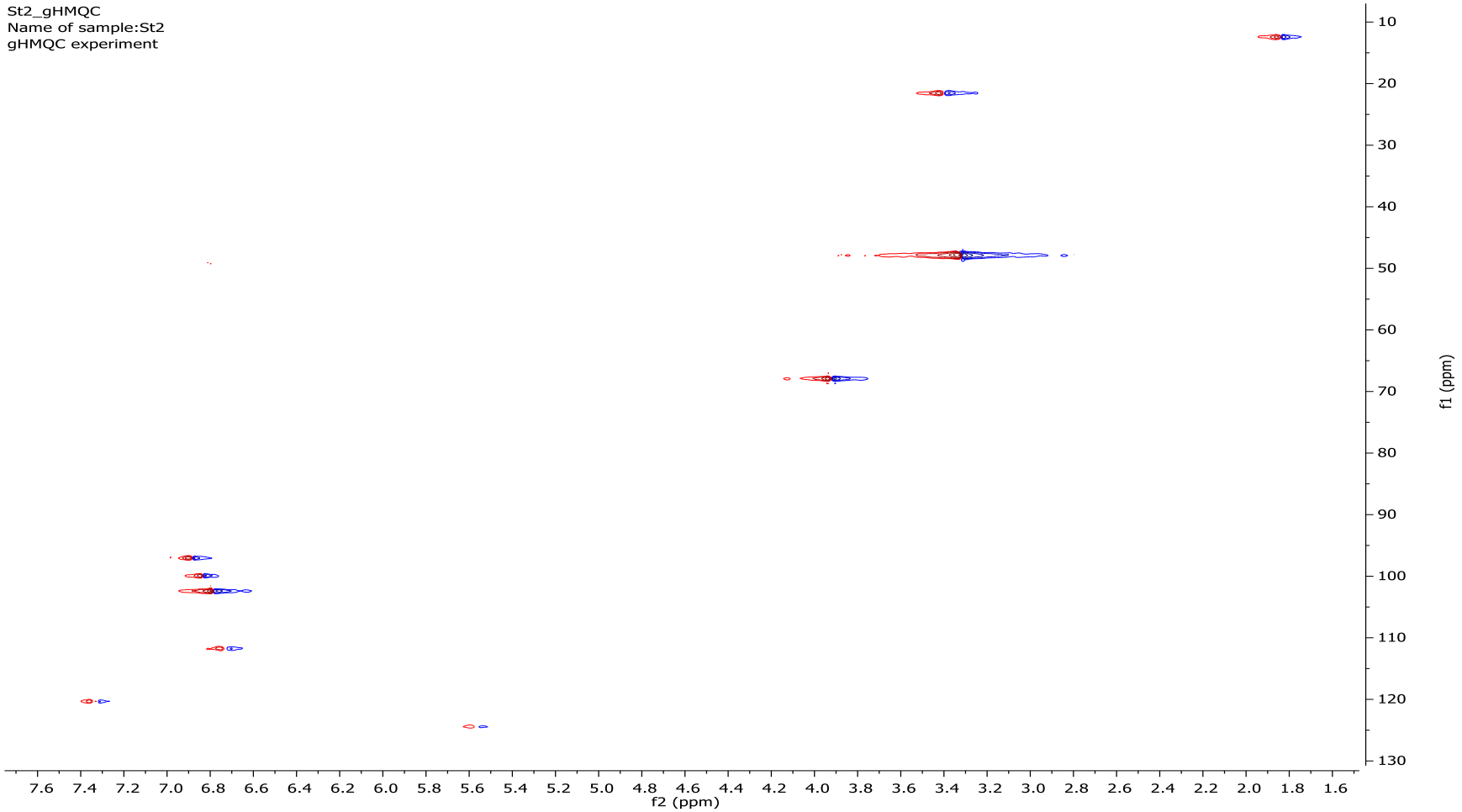

Figure J-6 HMQC spectrum of ω-hydroxymoracin C (No.10)

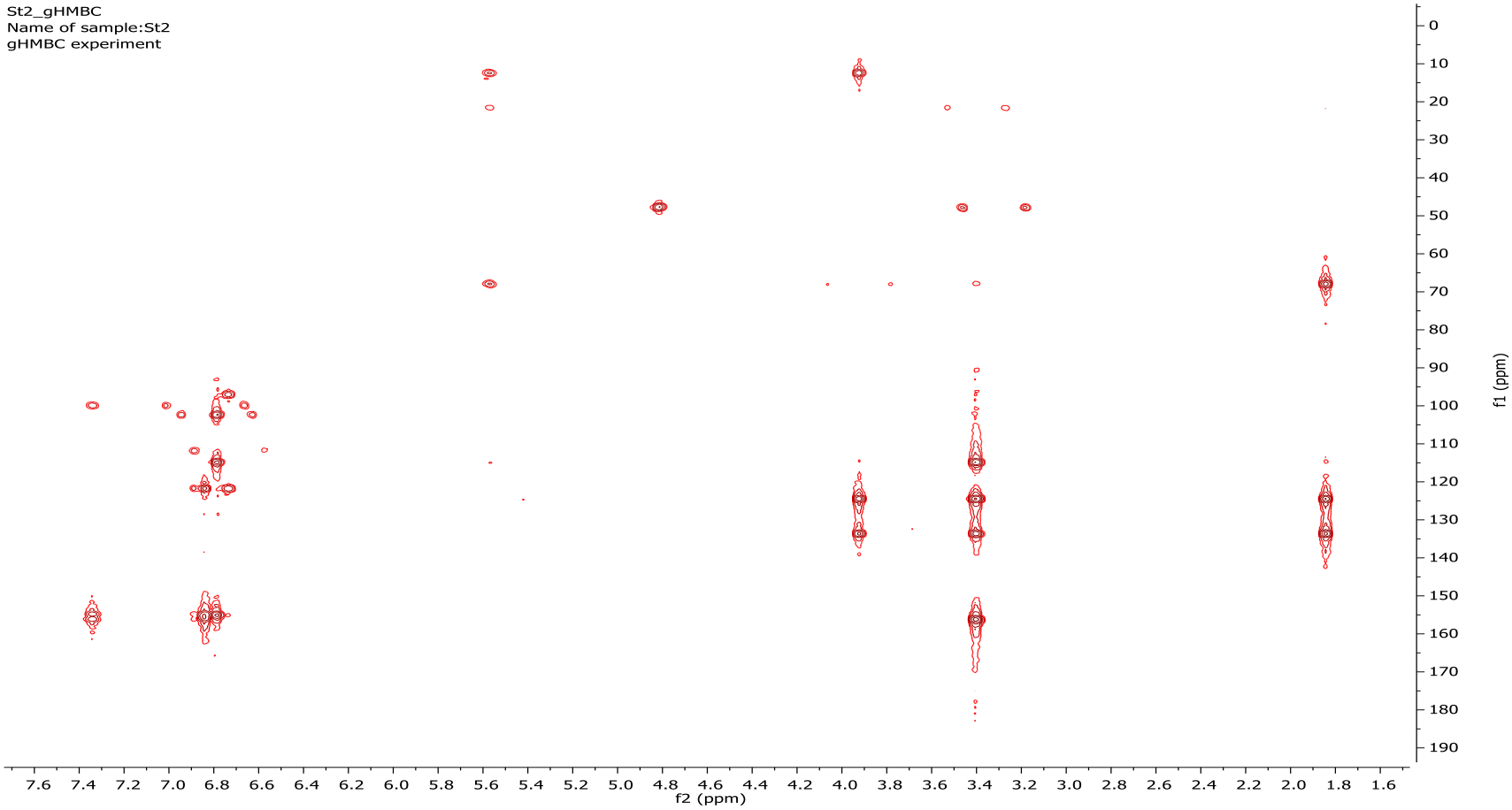

Figure J-7 HMBC spectrum of ω-hydroxymoracin C (No.10)

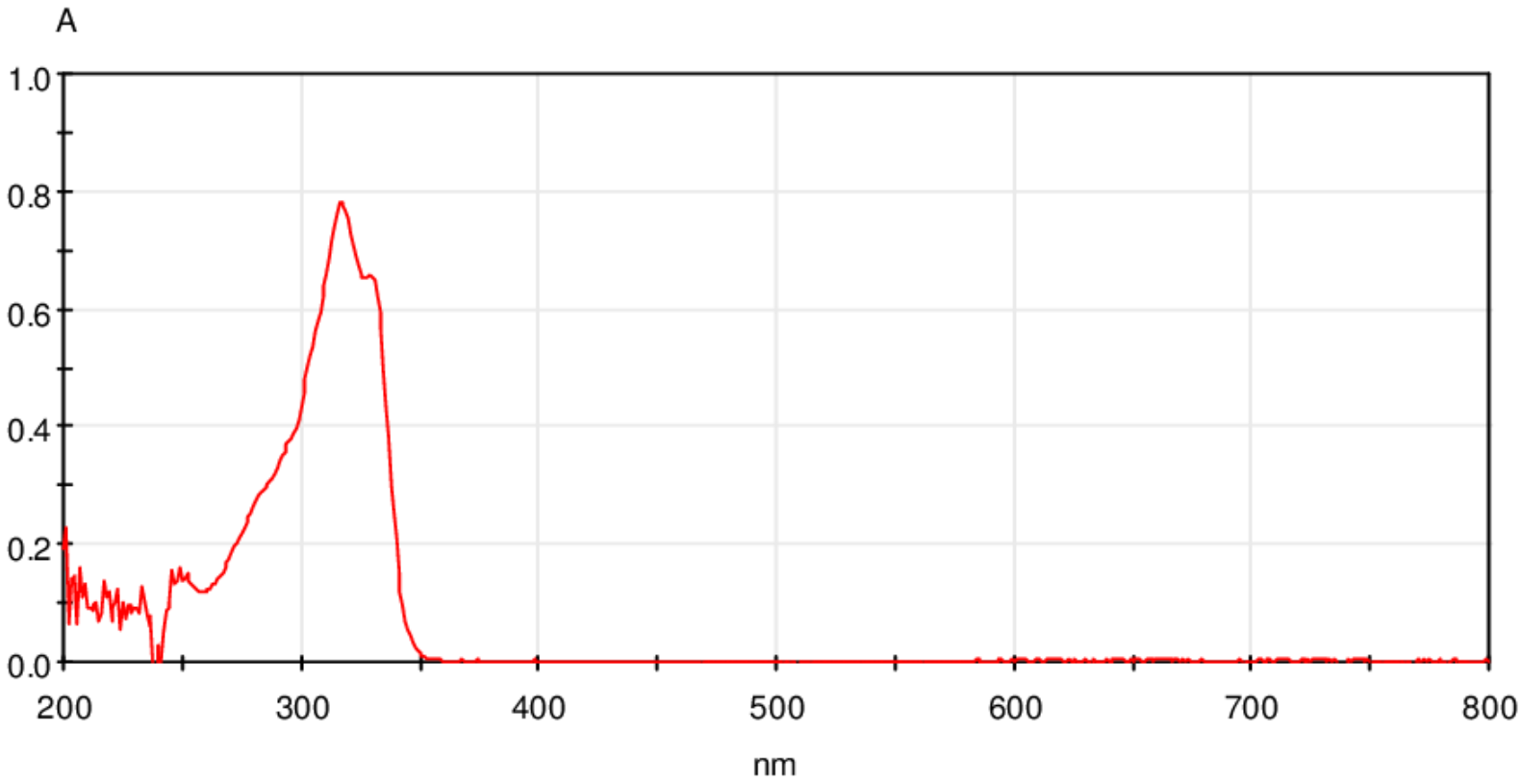

Figure K-1 UV-Visible spectrum of moracin M (No.11)

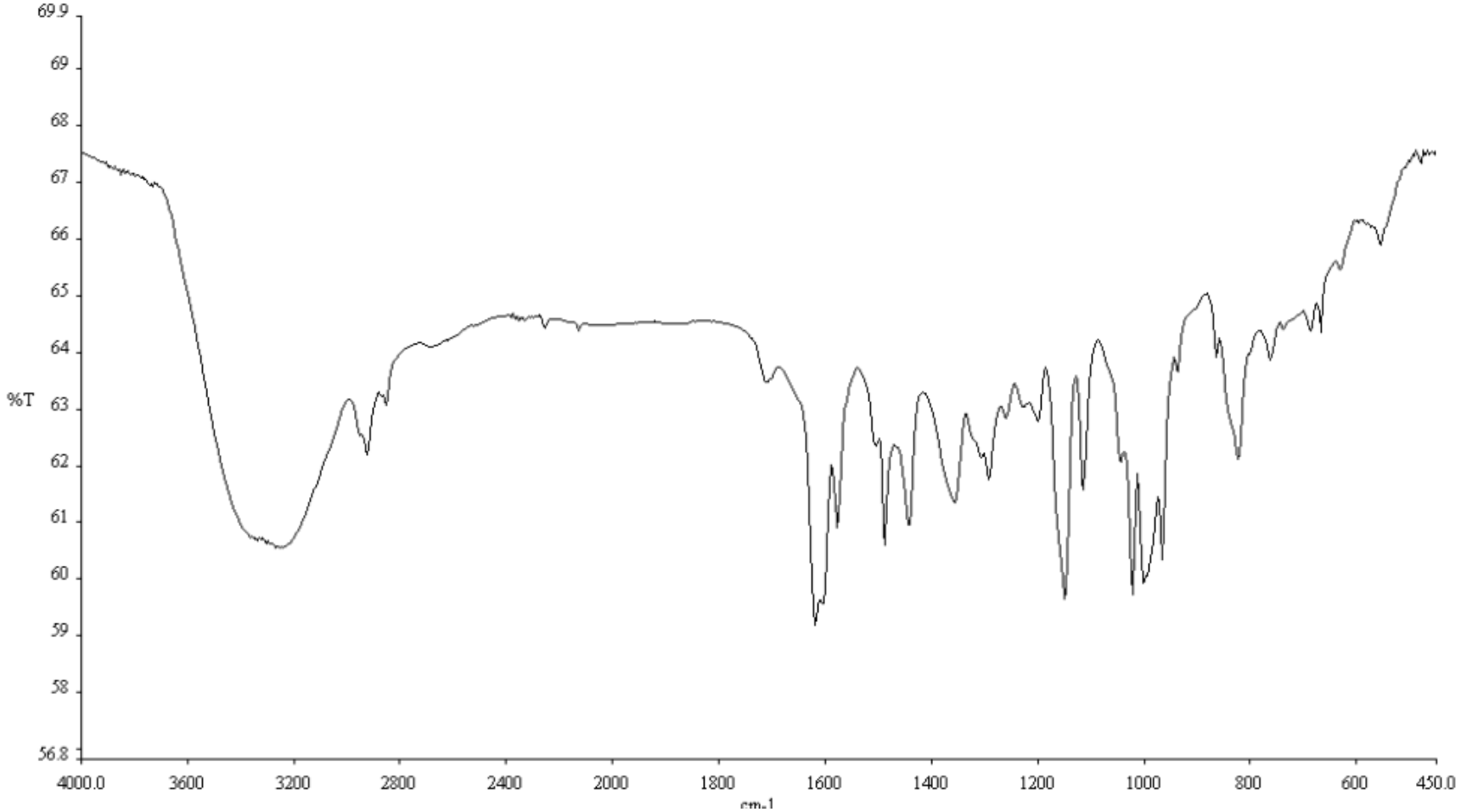

Figure K-2 IR spectrum of moracin M (KBr disc) (No.11)

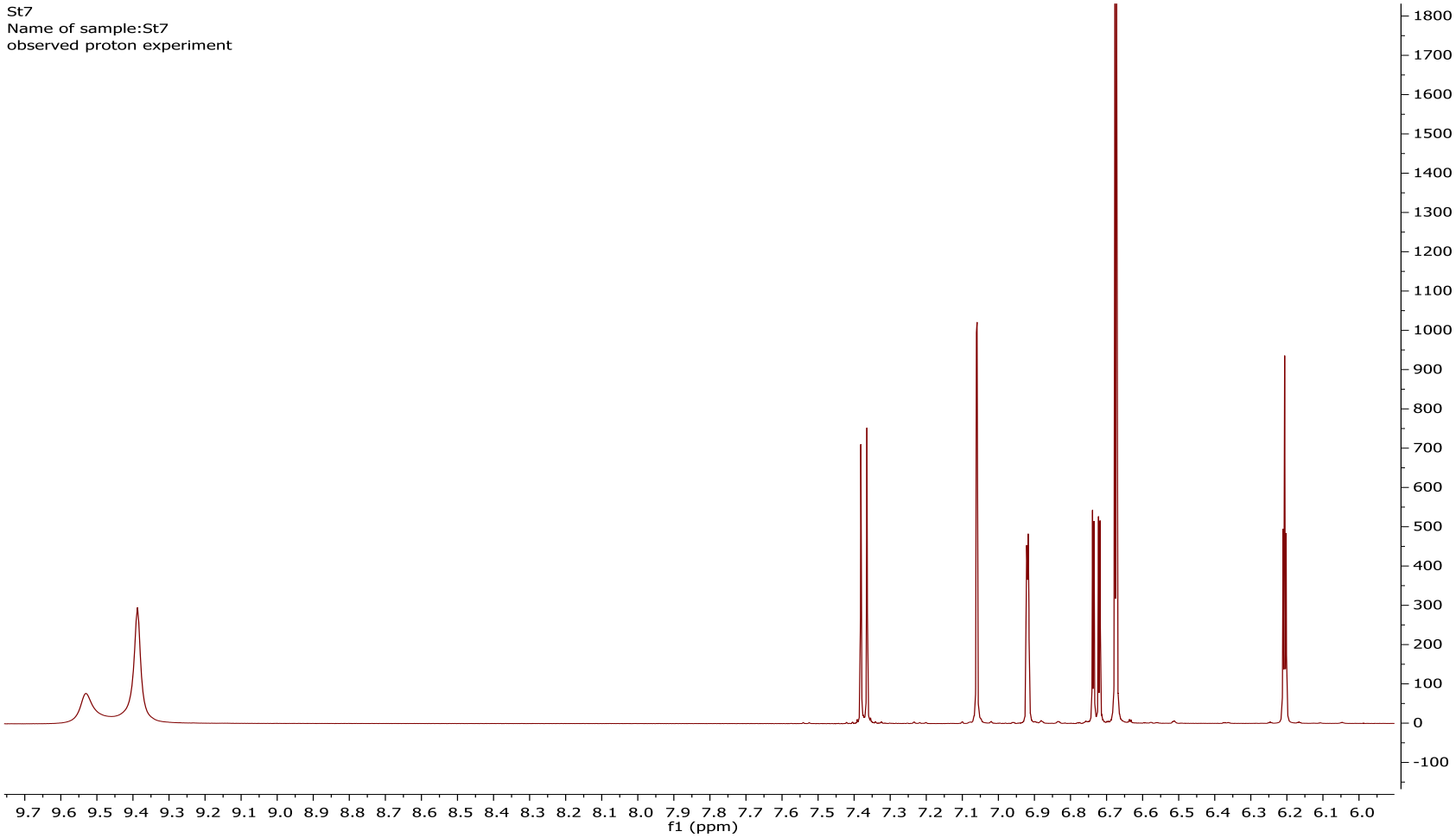

Figure K-4 ^{1}H NMR spectrum of moracin M (No.11)

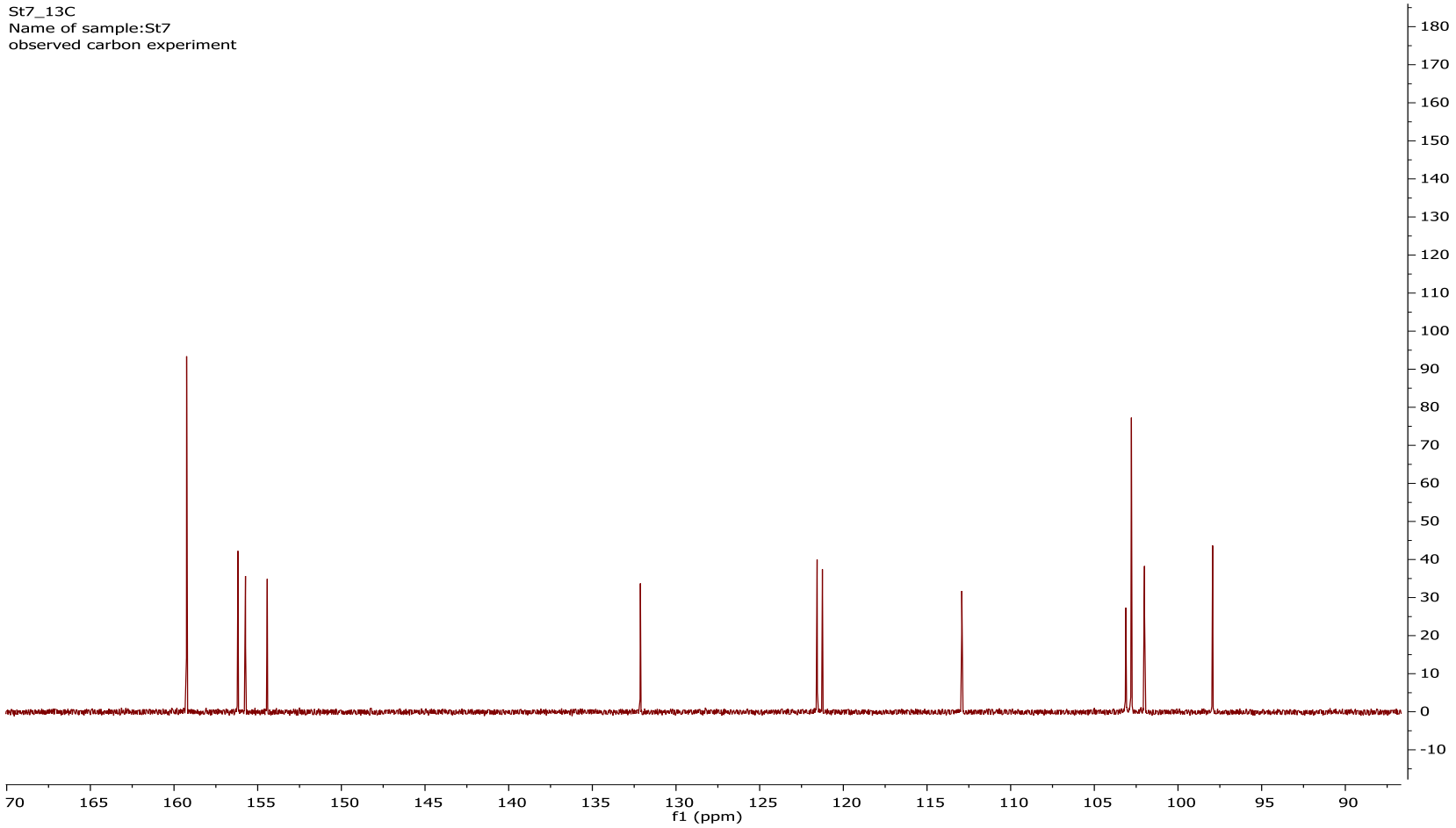

Figure K-5 ^{13}C NMR spectrum of moracin M (No.11)

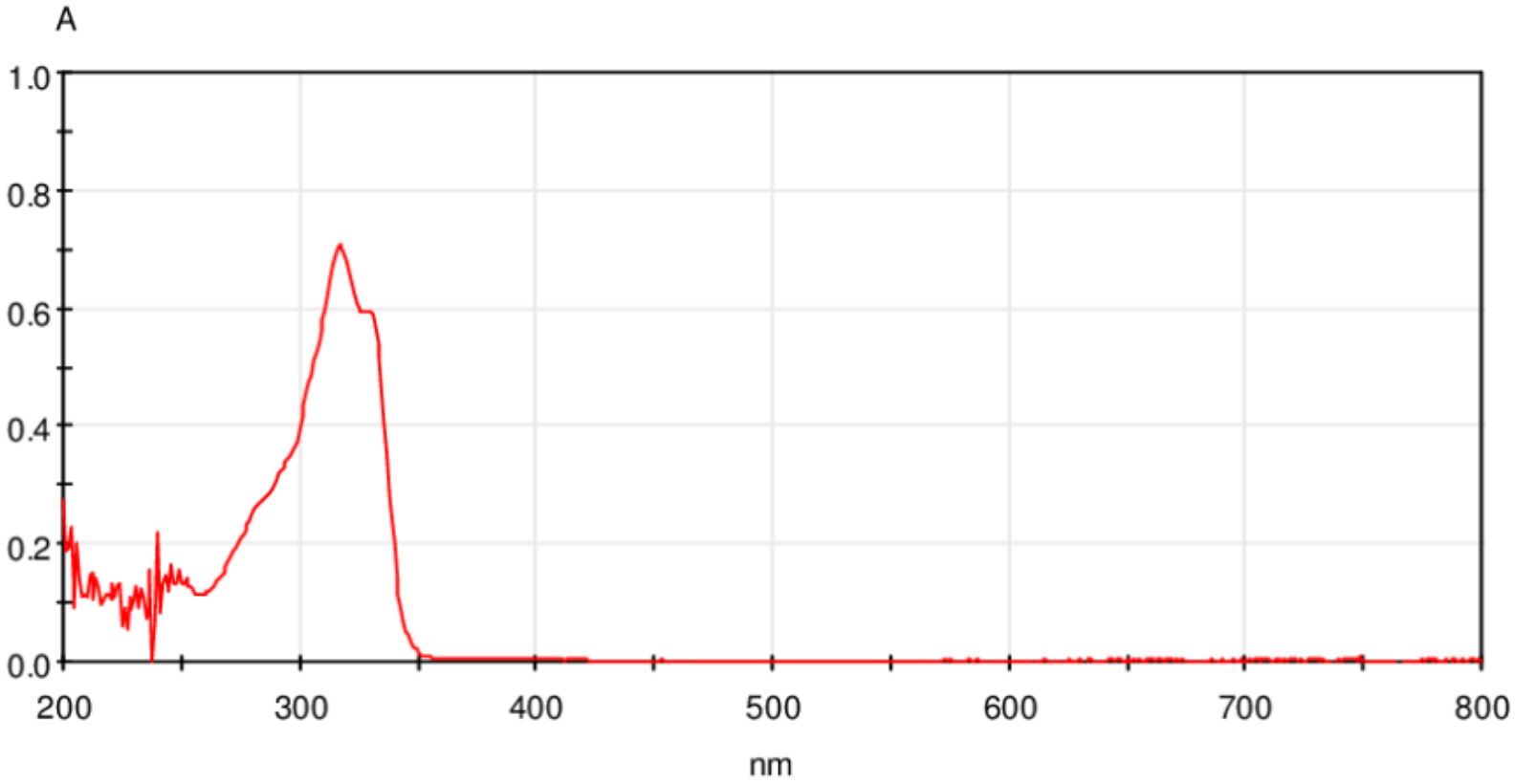

Figure L-1 UV-Visible spectrum of moracin C (No.12)

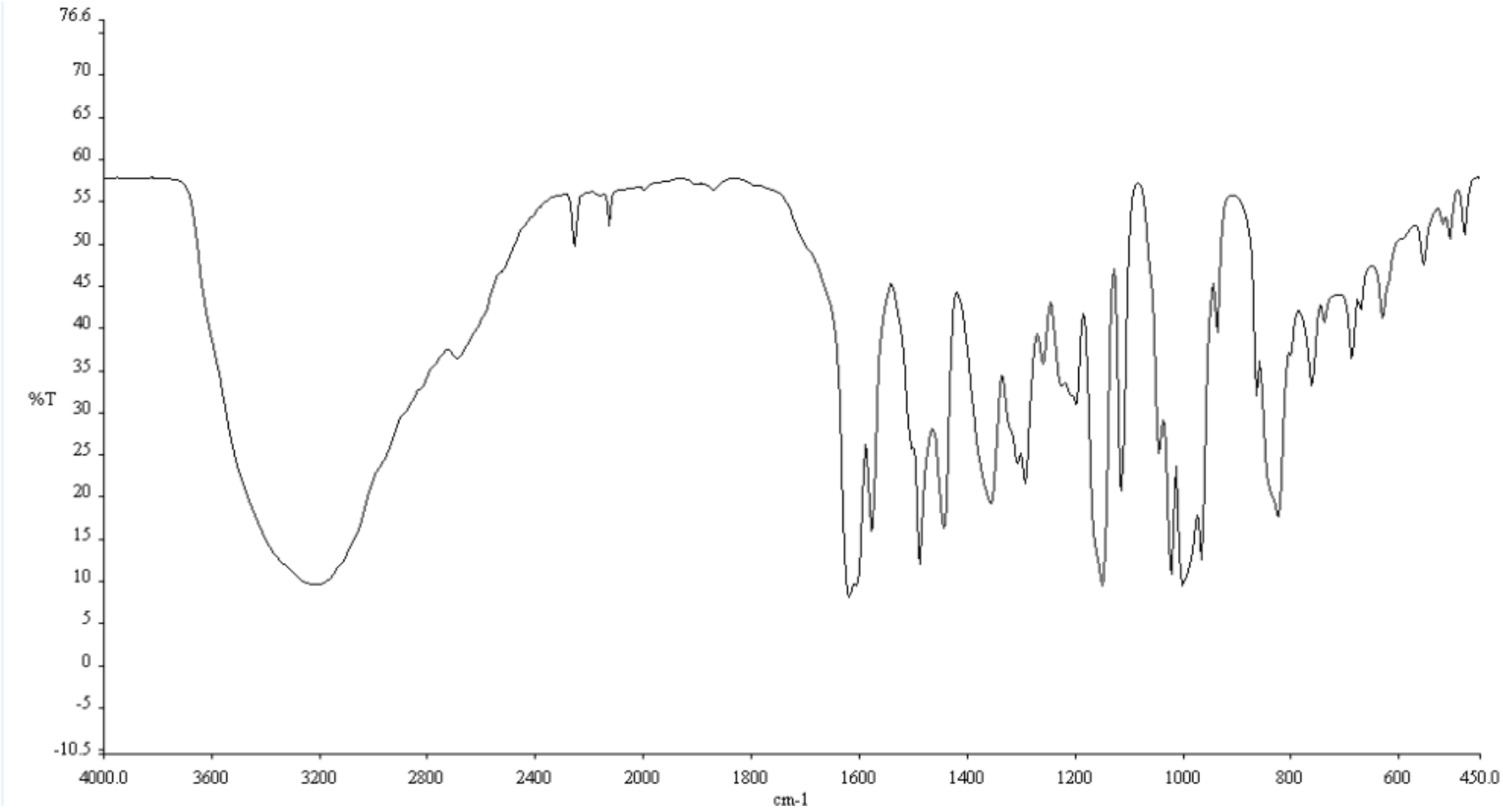

Figure L-2 IR spectrum of moracin C (KBr disc) (No.12)

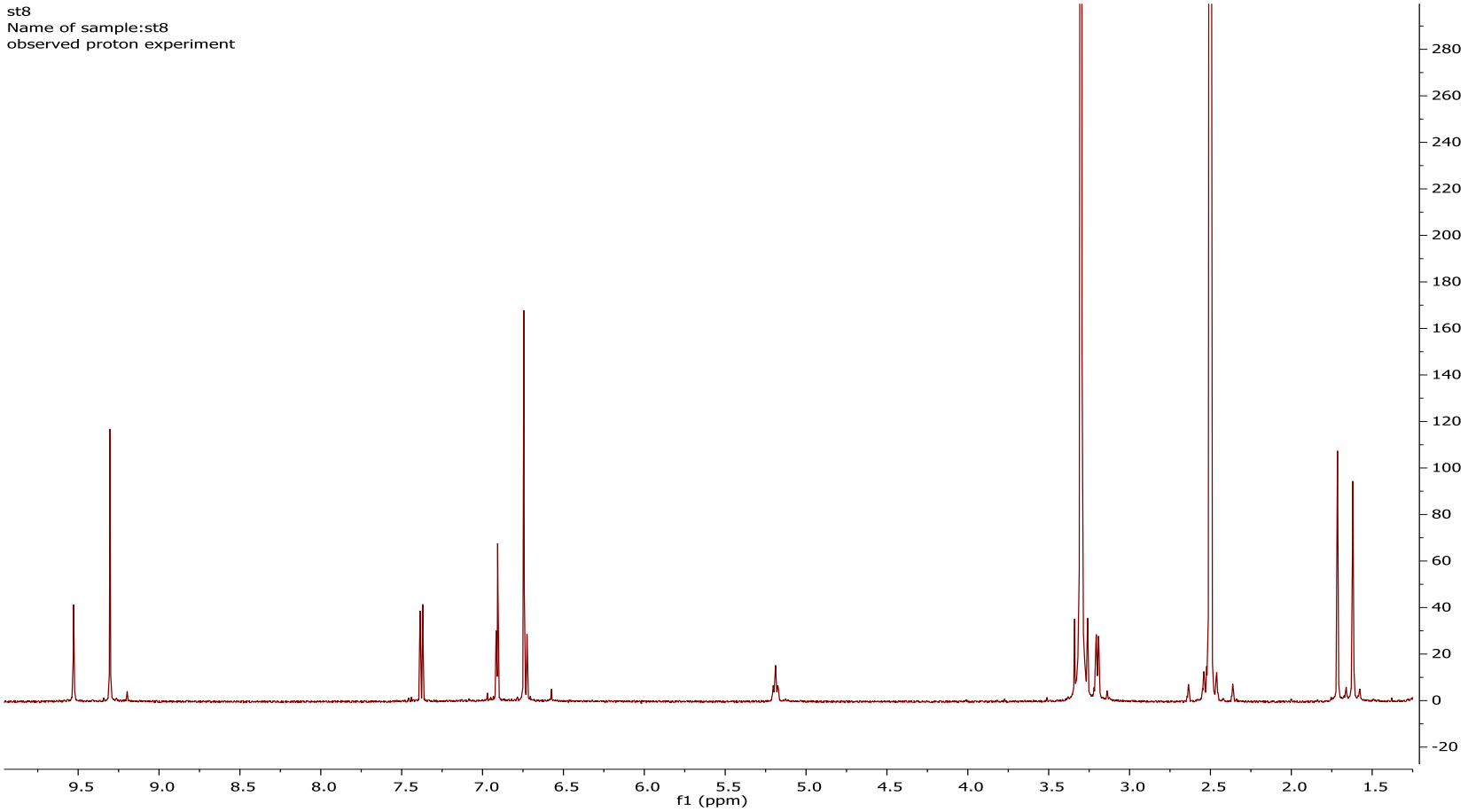

Figure L-4 ^{1}H NMR spectrum of moracin C (No.12)

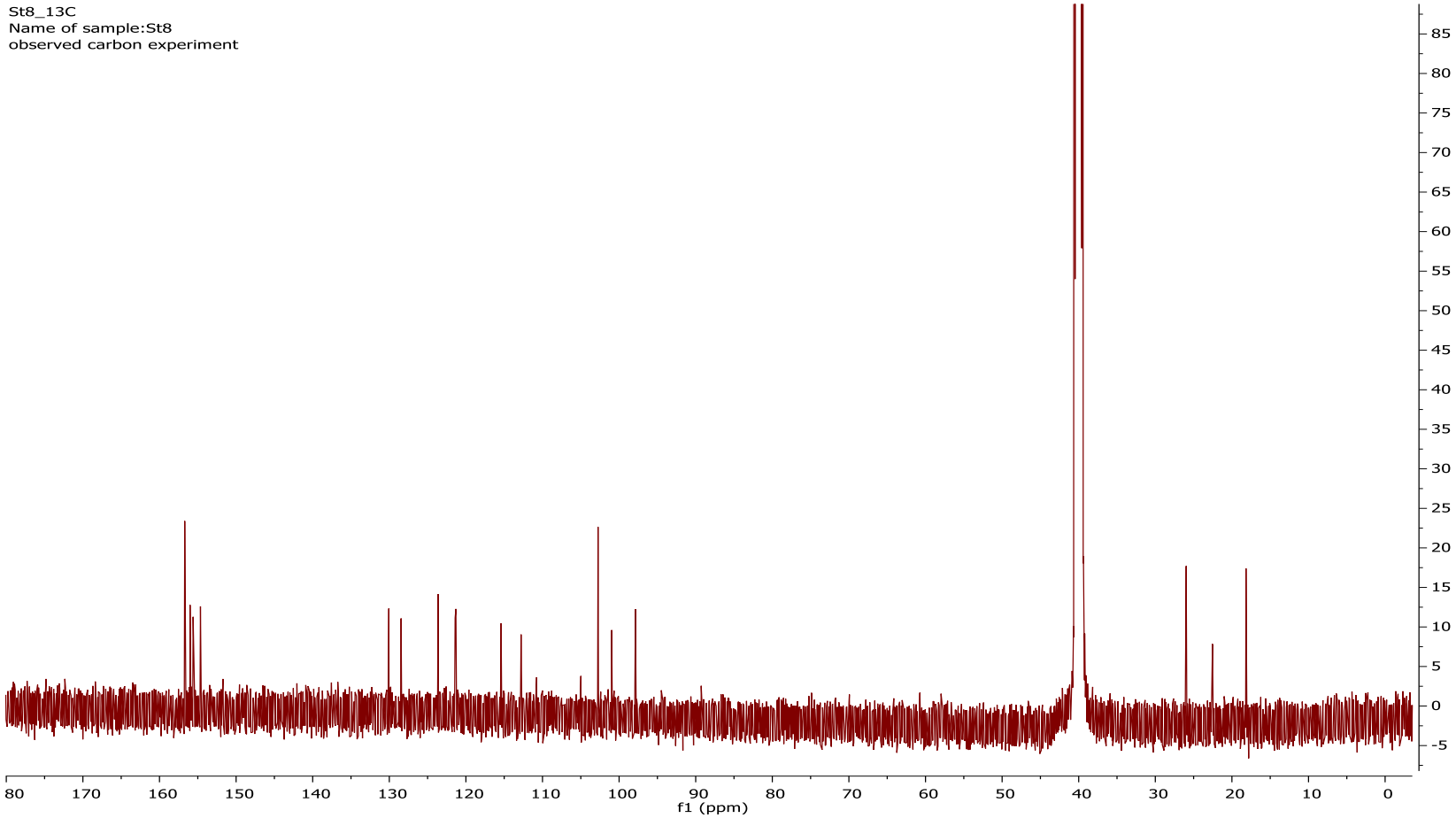

Figure L-5 ^{13}C NMR spectrum of moracin C (No.12)

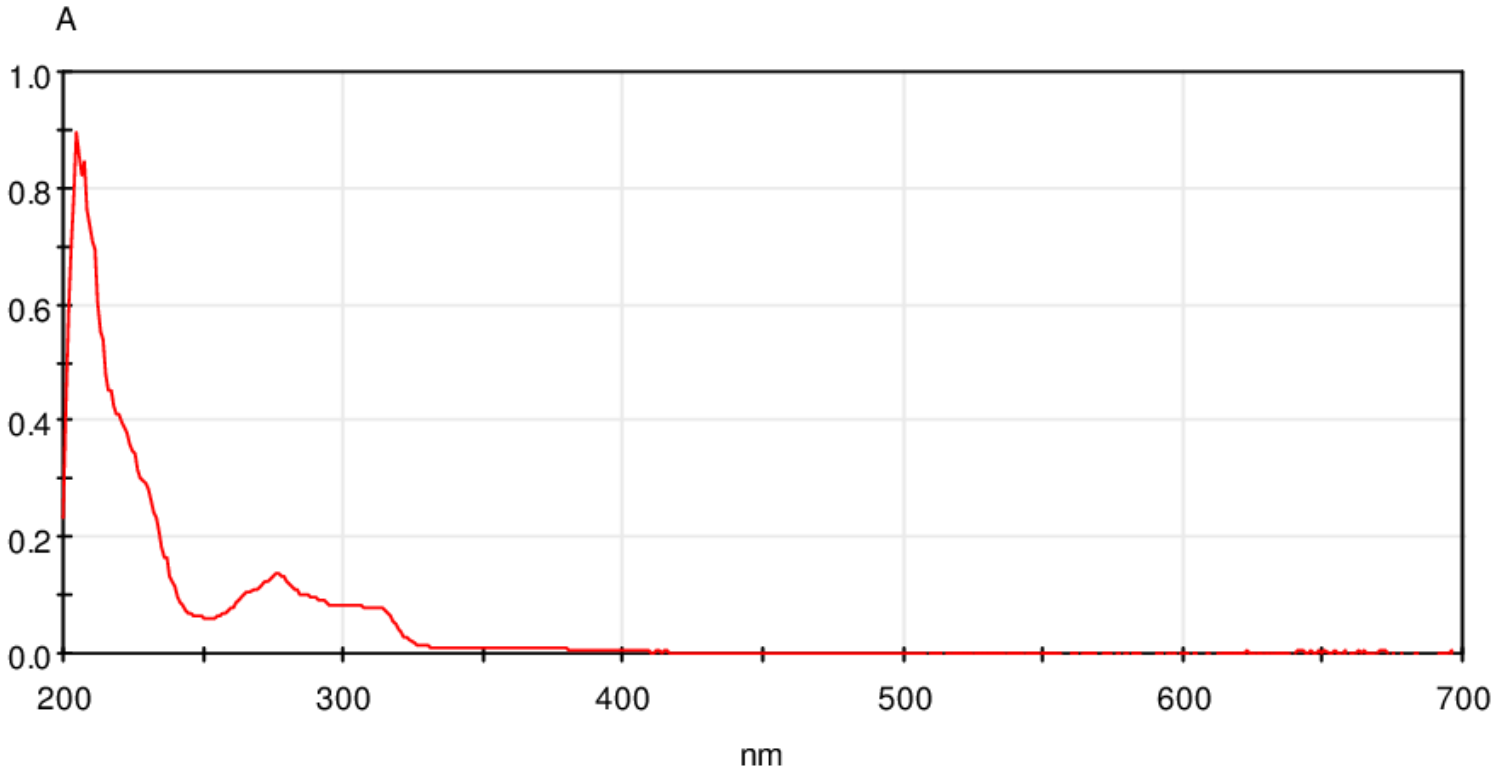

Figure M-1 UV-Visible spectrum of 3, 4, 3´, 5´-tetrahydroxybibenzyl (No.13)

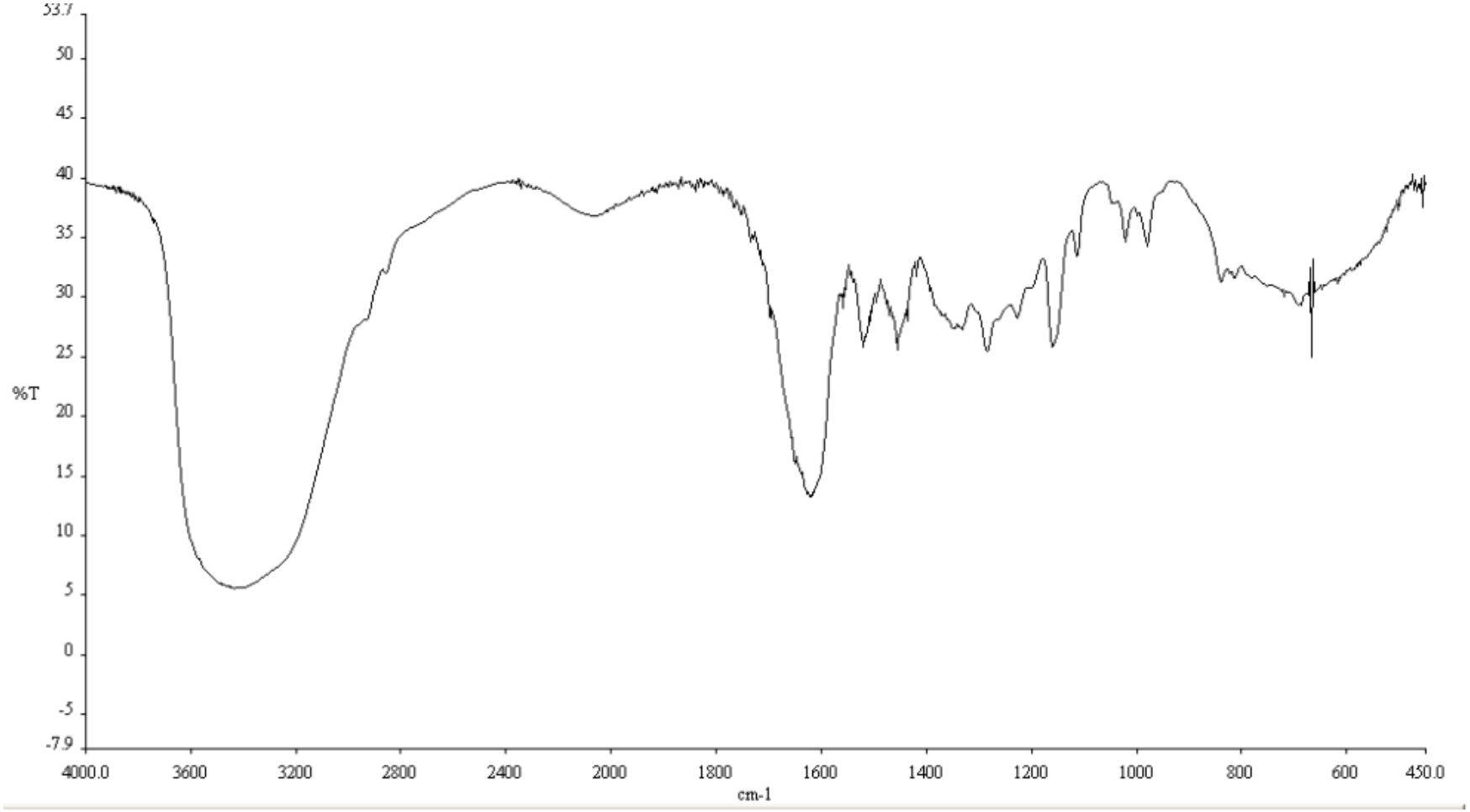

Figure M-2 IR spectrum of 3, 4, 3´, 5´-tetrahydroxybibenzyl (KBr disc) (No.13)

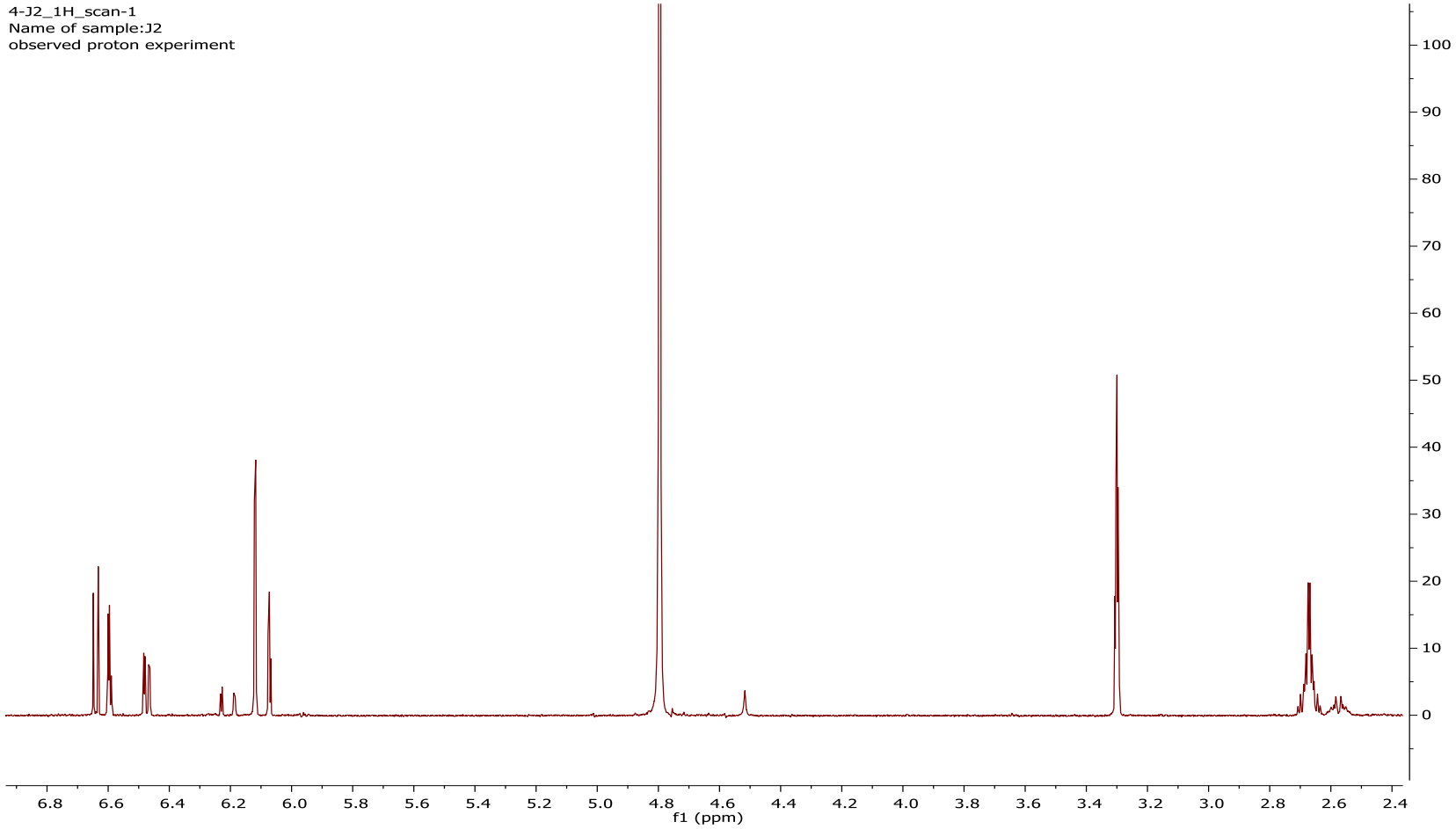

Figure M-4 ^{1}H NMR spectrum of 3, 4, 3´, 5´-tetrahydroxybibenzyl (No.13)

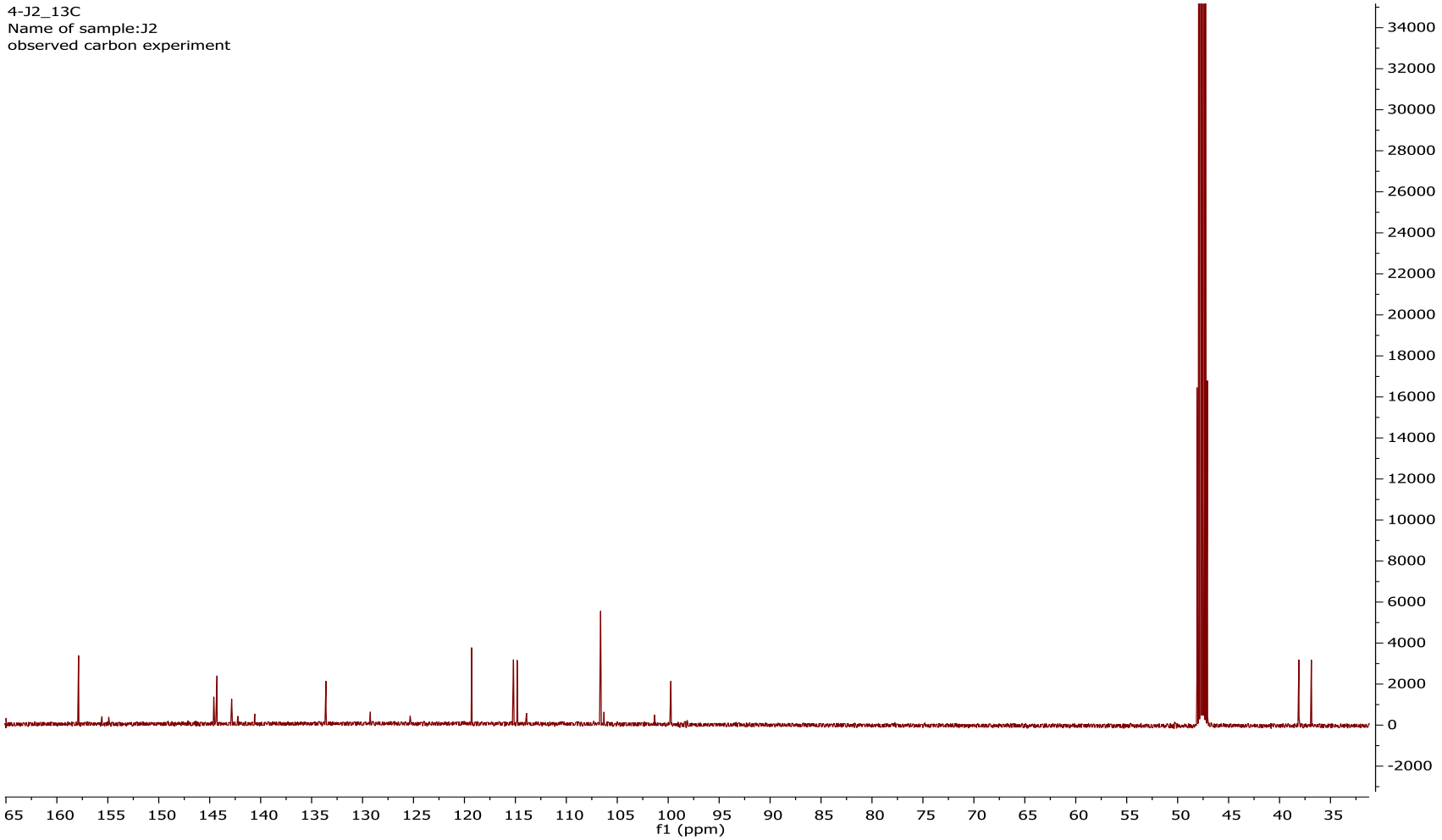

Figure M-5 ^{13}C NMR spectrum of 3, 4, 3′, 5′-tetrahydroxybibenzyl (No.13)

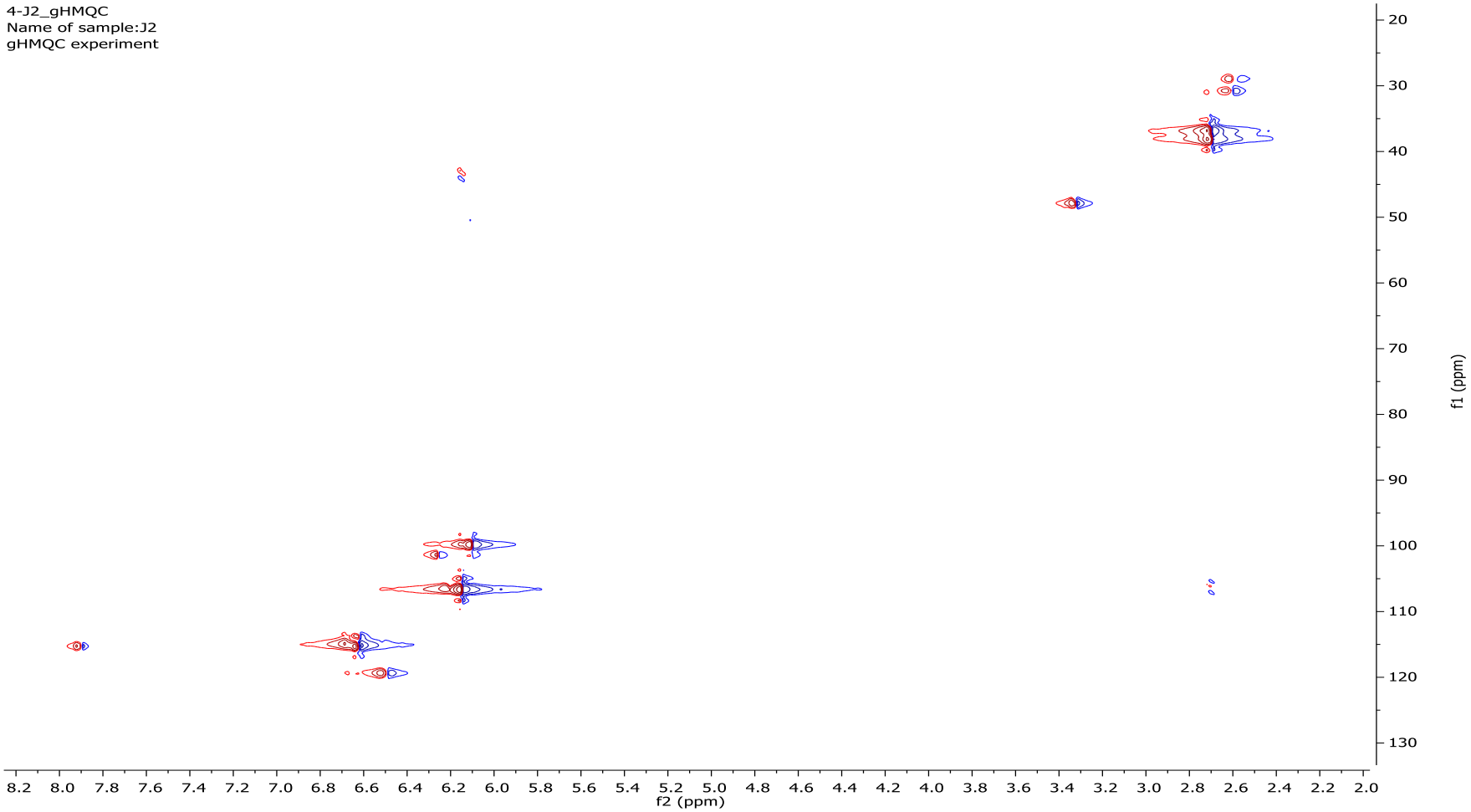

Figure M-6 HMQC spectrum of 3, 4, 3´, 5´-tetrahydroxybibenzyl (No.13)

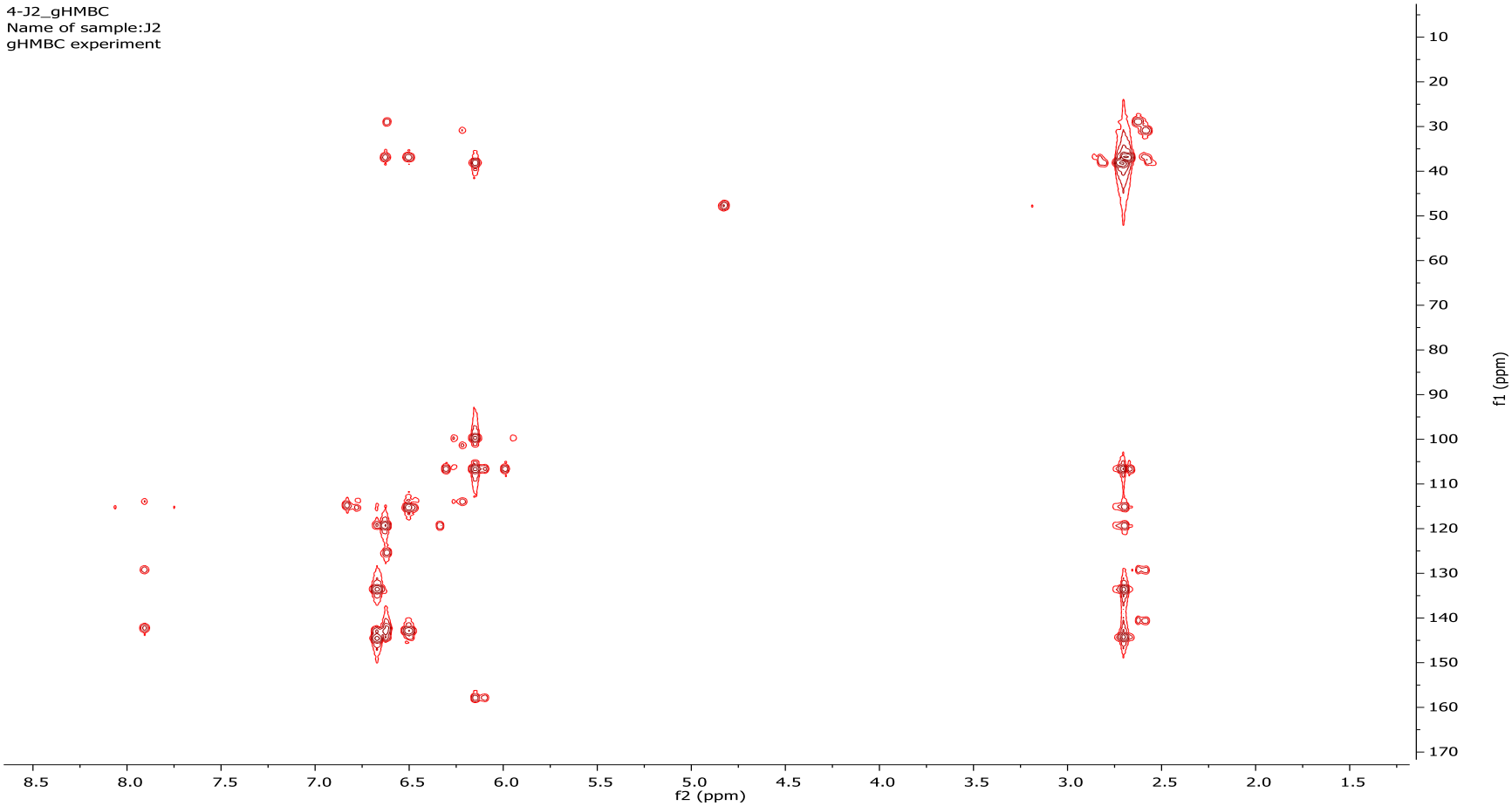

Figure M-7 HMBC spectrum of 3, 4, 3´, 5´-tetrahydroxybibenzyl (No.13)

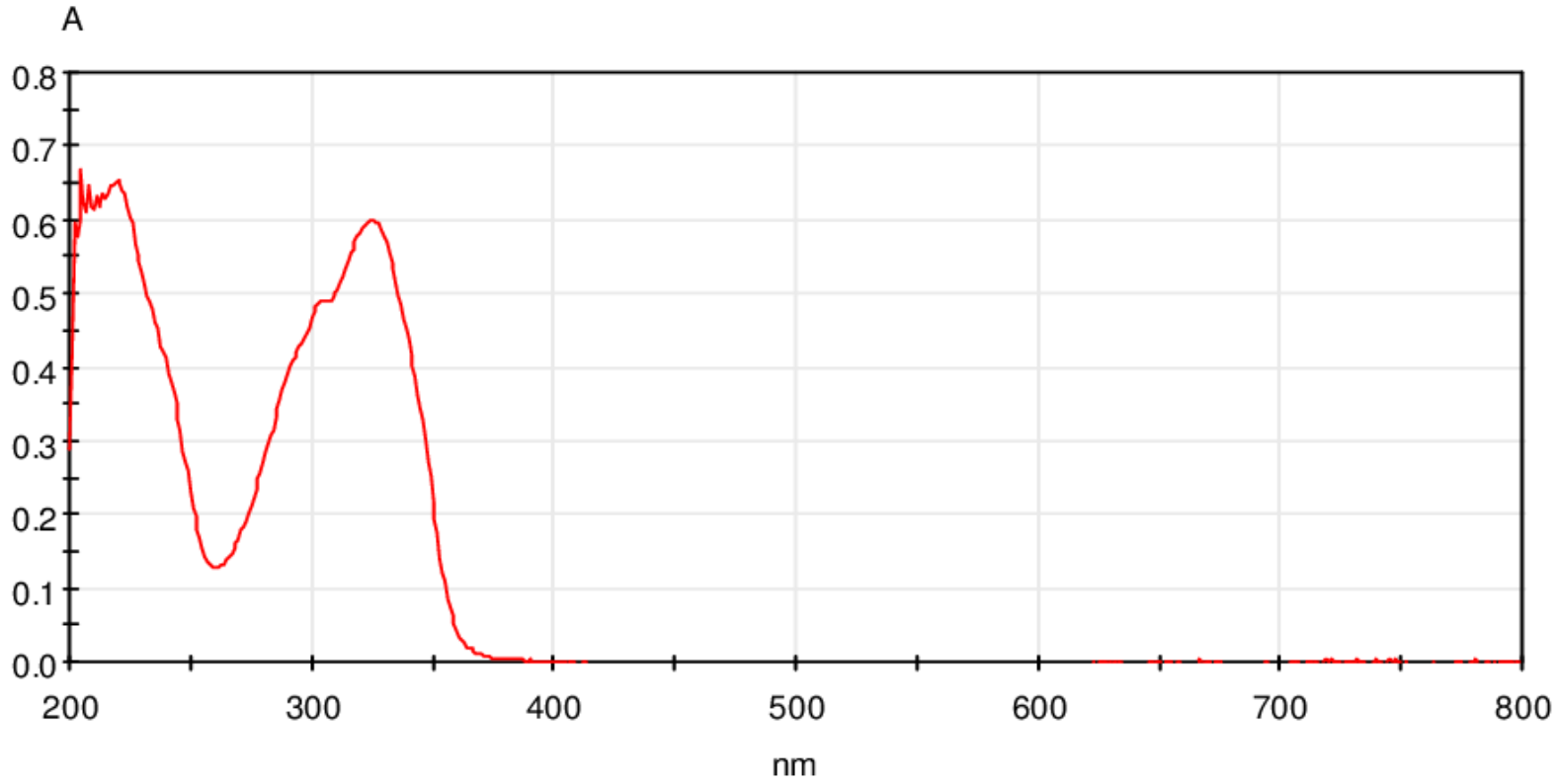

Figure N-1 UV-Visible spectrum of piceatanol (No.14)

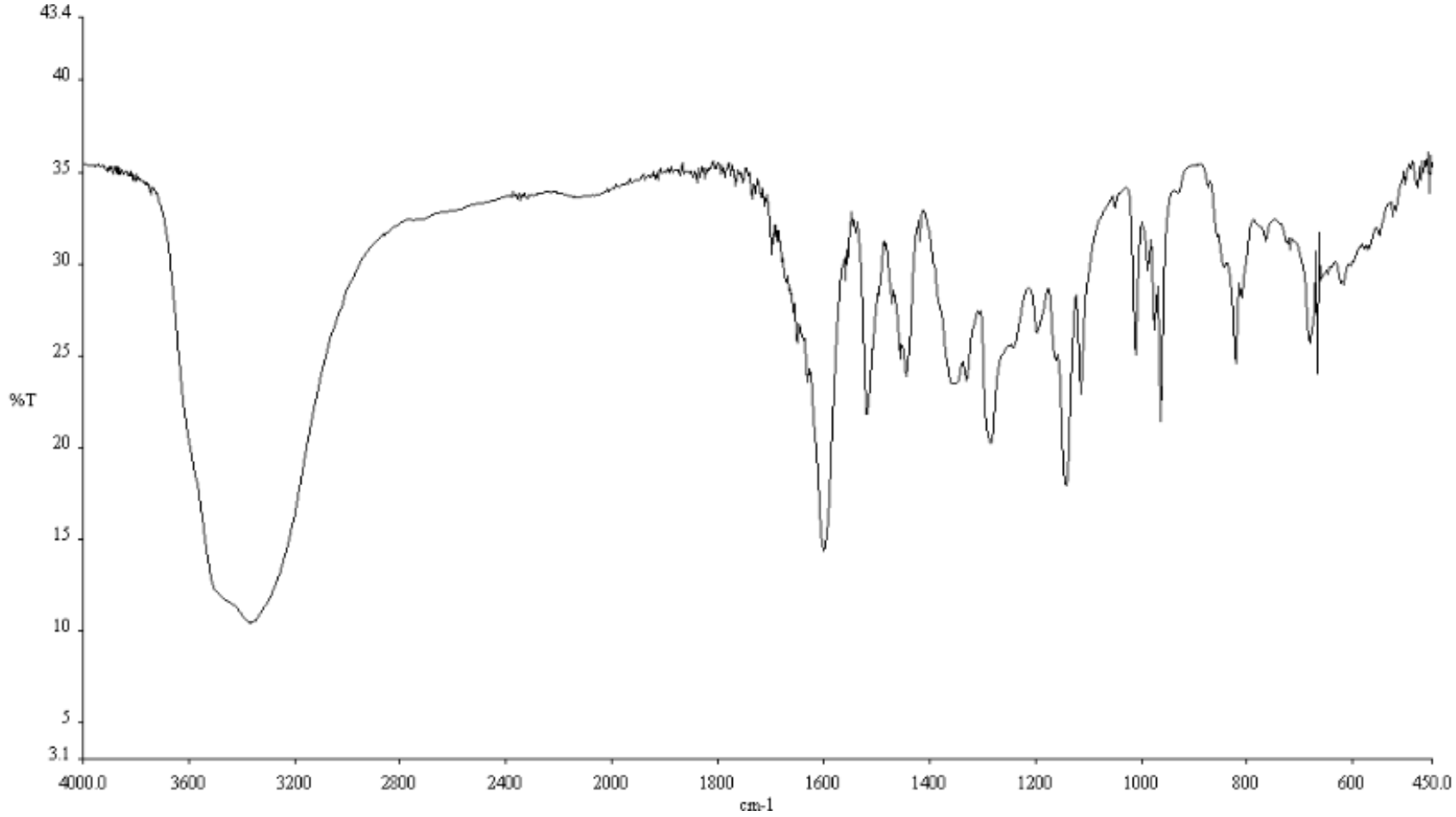

Figure N-2 IR spectrum of piceatanol (KBr disc) (No.14)

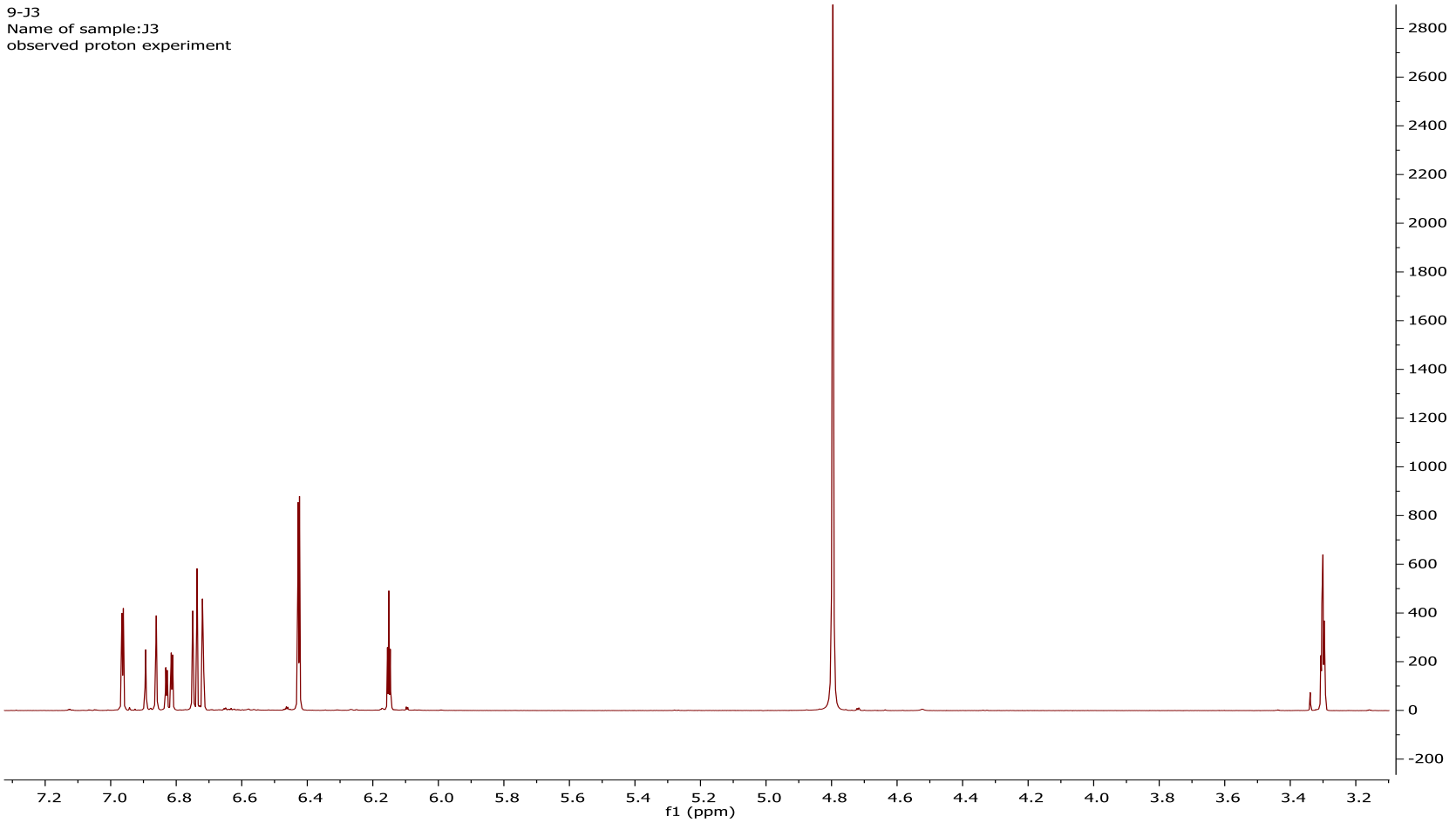

Figure N-4 ^{1}H NMR spectrum of piceatanol (No.14)

VITAE

Name Miss Kedsaraporn Parndaeng

Student ID 6210730009

Educational Attainment

Degree	Name of Institution	Year of Graduatio
Bachelor of Science (Biotechnology)	Prince of Songkla University	2002
Master degree of Pharmacy (Pharmaceutical Sciences)	Prince of Songkla University	2013

Scholarship Awards during Enrolment

1. PSU-Ph. D. Scholarship, Prince of Songkla University
2. Graduate School Dissertation Funding for Thesis, Prince of Songkla University
3. Scholarship for Support Exchange Student and International Credit Transferred Through ASEAN Community, Prince of Songkla University

List of Publication and Proceeding

1. Dej-adisai S., **Parndaeng K.**, Wattanapiromsakul C., Nuankaew W. and Kang T. H. 2019. Effects of selected moraceae plants on tyrosinase enzyme and melanin content. *Pharmacognosy Magazine* 15 (65): 708-714.
2. Dej-adisai S., **Parndaeng K.** and Wattanapiromsakul C. 2016. Determination of phytochemical compounds, and tyrosinase inhibitory and antibacterial activities of bioactive compounds from *Streblus ilicifolius* (S Vidal) Corner. *Tropical Journal of Pharmaceutical Research* 15: 497-506.